

(12)特許協力条約に基づいて公開された国際出願

(19) 世界知的所有権機関  
国際事務局(43) 国際公開日  
2002 年 9 月 19 日 (19.09.2002)

PCT

(10) 国際公開番号  
WO 02/073718 A1

(51) 国際特許分類: H01M 4/58, 4/02, 10/40

(21) 国際出願番号: PCT/JP02/02284

(22) 国際出願日: 2002 年 3 月 12 日 (12.03.2002)

(25) 国際出願の言語: 日本語

(26) 国際公開の言語: 日本語

(30) 優先権データ:

特願2001-071486 2001 年 3 月 14 日 (14.03.2001) JP

特願2001-080430 2001 年 3 月 21 日 (21.03.2001) JP

特願2001-080434 2001 年 3 月 21 日 (21.03.2001) JP

(71) 出願人 (米国を除く全ての指定国について): 株式会社  
ユアサコーポレーション (YUASA CORPORATION)  
[JP/JP]; 〒569-1115 大阪府 高槻市 古曽部町二丁目  
3 番 2 1 号 Osaka (JP).

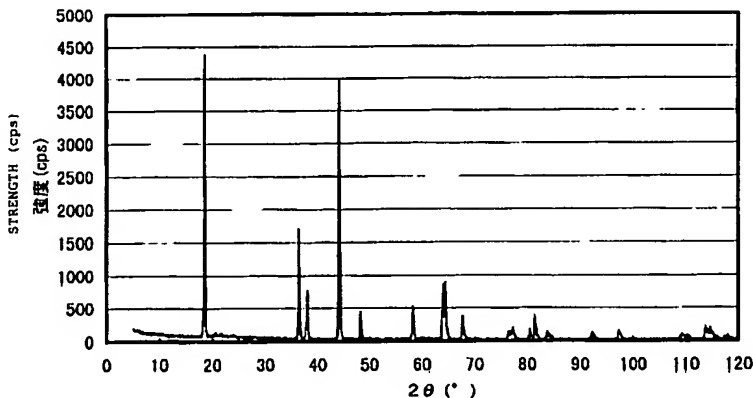
(72) 発明者; および

(75) 発明者/出願人 (米国についてのみ): 岡部 一弥 (OK-  
ABE, Kazuya) [JP/JP]; 〒569-1115 大阪府 高槻市 古曽  
部町二丁目 3 番 2 1 号 株式会社 ユアサ コーポレー  
ション内 Osaka (JP). 塩崎 竜二 (SHIOZAKI, Ryuji)  
[JP/JP]; 〒569-1115 大阪府 高槻市 古曽部町二丁目  
3 番 2 1 号 株式会社 ユアサ コーポレーション内 Os-  
aka (JP). 藤井 明博 (FUJII, Akihiro) [JP/JP]; 〒569-1115  
大阪府 高槻市 古曽部町二丁目 3 番 2 1 号 株式社 ユアサ コーポレーション内 Osaka (JP). 伊藤 明師  
(ITO, Akinori) [JP/JP]; 〒569-1115 大阪府 高槻市 古曽  
部町二丁目 3 番 2 1 号 株式会社 ユアサ コーポレー  
ション内 Osaka (JP). 油布 宏 (YUFU, Hiroshi) [JP/JP];  
〒569-1115 大阪府 高槻市 古曽部町二丁目 3 番 2 1 号  
株式会社 ユアサ コーポレーション内 Osaka (JP).(74) 代理人: 内藤 照雄 (NAITO, Teruo); 〒107-6029 東京都  
港区 赤坂一丁目 1 2 番 3 2 号 アーク森ビル 2 9 階  
信栄特許事務所 Tokyo (JP).(81) 指定国 (国内): AE, AG, AL, AM, AT, AU, AZ, BA, BB,  
BG, BR, BY, BZ, CA, CII, CN, CO, CR, CU, CZ, DE, DK,  
DM, DZ, EC, EE, ES, FI, GB, GD, GE, GH, GM, HR, HU,  
ID, IL, IN, IS, JP, KE, KG, KP, KR, KZ, LC, LK, LR, LS,  
LT, LU, LV, MA, MD, MG, MK, MN, MW, MX, MZ, NO,  
NZ, OM, PI, PL, PT, RO, RU, SD, SE, SG, SI, SK, SL,  
TJ, TM, TN, TR, TT, TZ, UA, UG, US, UZ, VN, YU, ZA,  
ZM, ZW.(84) 指定国 (広域): ARIPO 特許 (GH, GM, KE, LS, MW,  
MZ, SD, SL, SZ, TZ, UG, ZM, ZW), ユーラシア特許  
(AM, AZ, BY, KG, KZ, MD, RU, TJ, TM), ヨーロッパ特  
許 (AT, BE, CII, CY, DE, DK, ES, FI, FR, GB, GR, IE, IT,  
LU, MC, NL, PT, SE, TR), OAPI 特許 (BF, BJ, CF, CG,  
CI, CM, GA, GN, GQ, GW, ML, MR, NE, SN, TD, TG).添付公開書類:  
— 国際調査報告書

[続葉有]

(54) Title: POSITIVE ELECTRODE ACTIVE MATERIAL AND NONAQUEOUS ELECTROLYTE SECONDARY CELL COM-  
PRISING THE SAME

(54) 発明の名称: 正極活物質およびこれを用いた非水電解質二次電池

active material is characterized in that the specific surface of the Li-Mn-Ni composite oxide measured by the BET method is 0.3  
m<sup>2</sup>/g or above and 1.5 m<sup>2</sup>/g or below. The nonaqueous electrolyte secondary cell comprises such a positive electrode active material.

[続葉有]



2文字コード及び他の略語については、定期発行される各PCTガゼットの巻頭に掲載されている「コードと略語のガイダンスノート」を参照。

(57) 要約:

高率充放電性能及び充放電サイクル性能に優れる高エネルギー密度の非水電解質二次電池を得ることのできる正極活物質、および、高率充放電性能及び充放電サイクル性能に優れる高エネルギー密度の非水電解質二次電池を提供する。

Li-Mn-Ni系複合酸化物を主成分とする正極活物質であって、前記Li-Mn-Ni系複合酸化物のBET法による比表面積が $0.3\text{ m}^2/\text{g}$ 以上 $1.5\text{ m}^2/\text{g}$ 以下であることを特徴とする正極活物質およびこれを用いた非水電解質二次電池。

## 明 細 書

正極活物質およびこれを用いた非水電解質二次電池

## &lt;技術分野&gt;

本発明は、正極活物質およびこれを用いた非水電解質二次電池に関する。

## &lt;背景技術&gt;

リチウム二次電池等の非水電解質二次電池は高いエネルギー密度を示し、高電圧であることから小型携帯端末や移動体通信装置などへの電源として広く使用されている。リチウム二次電池用正極活物質には、リチウムの挿入・脱離の繰り返しによっても結晶構造が安定で、かつ電気化学的作動容量が大きいことが要求される。作動電圧が4 V付近のものとしては、層状構造のリチウムコバルト酸化物やリチウムニッケル酸化物、又はスピネル構造を持つリチウムマンガン酸化物等を基本構成とするリチウム含有遷移金属酸化物が知られている。

現在、4 V級の作動電位を有する非水電解質二次電池の正極活物質として、 $\text{LiCoO}_2$ 、 $\text{LiNiO}_2$ 、 $\text{LiMnO}_2$ 、 $\text{LiMn}_2\text{O}_4$  等のリチウムと遷移金属との複合酸化物が従来より知られている。なかでも、高エネルギー密度を期待できる $\alpha\text{-NaFeO}_2$ 構造を有する正極活物質の中で、 $\text{LiCoO}_2$ 等で表されるリチウムコバルト複合酸化物は民生用のリチウムイオン電池などに広く用いられているが、コバルトが希少金属であり、価格が高いといった問題があった。また、 $\text{LiNiO}_2$ 等で表されるリチウムニッケル複合酸化物は高温での安定性に欠けるため、安全性の確保が難しいことなどから実用化には至っていない。また、 $\text{LiMn}_2\text{O}_4$ 等で表されるスピネル構造を有するリチウムマンガン酸化物は、安価で、安全性にも優れた正極活物質であるが、リチウムコバルト複合酸化物に比べて重量当たりのエネルギー密度が70%程度にとどまり、一部で実用化はされているものの、広く民生用途で使用されるには至っていない。

一方、 $\text{LiMnO}_2$ は、原理的に高い容量が期待でき、安全性にも優れるため、広く検討されてきた。前記 $\text{LiMnO}_2$ は、ジグザグ層状構造である $\beta\text{-NaMn}$

$O_2$ 型の斜方晶系構造、及び、層状岩塩構造である $\alpha-NaFeO_2$ 型の単斜晶系構造が知られている。

前記斜方晶形構造の $LiMnO_2$ は、前記 $LiMn_2O_4$ よりも高い容量を期待できるが、充放電を繰り返すと、徐々にスピネル相への転位が生じることから、充放電サイクルに対する安定性に劣るといった問題点があった。また、前記単斜晶構造の $LiMnO_2$ は、高率充放電性能が充分でなく、充放電サイクルに伴う容量低下も大きいことが、例えば、Chiang, Y-M.; Sadoway, D.R.; Jang, Y-I.; Huang, B.; Wang, H. High Capacity, Temperature-Stable Lithium Aluminium Manganese Oxide Cathodes for Rechargeable Batteries. Electrochem. Solid-State Lett. 2(3), 1999, 107-110. に報告されている。

これらの問題を解決するため、特開2001-23617号公報では、 $LiMnO_2$ のMnをAl、Fe、Co、Ni、Mg又はCrで $1-y$  ( $0.5 \leq y \leq 1$ ) 量置換し、且つ、正極と負極との間に $60 \sim 100^\circ\text{C}$ にて $4.0\text{V} \sim 4.8\text{V}$ の電圧を印可して結晶構造の変化を加速し、高率充放電特性を改善する技術が開示されている。しかしながら、これらの技術を用いてもなお、高率充放電特性は十分ではなかった。

更に、前記リチウムマンガ氧化物は、その使用に当たって克服すべき技術課題が多い。特に高温時におけるサイクル性能や保存性能が劣るといった問題があった。

また、 $LiNiO_2$ のNiの一部をMnで置換した構造として、空間群 $R\bar{3}/m$ の結晶構造を有する $LiNi_{1-\alpha}Mn_{\alpha}O_2$ を考えたとき、MnによるNiサイトへの置換を確実にするためには、 $800^\circ\text{C}$ 以上の焼成が必要である。ところが、このような高温においては、結晶中のLiが入るべきサイトにNiやMnが入り込んで結晶構造を乱してしまい、容量やサイクル性能が低下してしまうという問題点があった。特開平8-171910号公報では、前記 $\alpha$ の値を $0.05 \sim 0.30$ とし、 $600^\circ\text{C} \sim 800^\circ\text{C}$ で焼成する技術を開示しているが、これらの技術を用いてもなお、サイクル性能は十分ではなかった。

上記の問題を解決手段として $LiNiO_2$ のNiの一部をMnとCoで置換した $LiMn_{\alpha}Ni_{\beta}Co_{\gamma}O_2$ の電気化学特性に係わる技術についても公知となって



いる。例えば、特許第3244314号報には、 $a$ 、 $b$ 、 $c$ について  $0.02 \leq a \leq 0.5$ 、 $0.02 \leq b/(b+c) \leq 0.9$ 、 $b > 0.34$ 、 $a+b+c=1$  の領域に関するLi複合酸化物の報告がなされている。しかしながら、本発明者らの検討によれば依然として充電時の熱的安定性に劣るといった問題を有している。この理由は定かではないが、該報告におけるLi複合酸化物の作製法が固体同士の機械的混合を経由するためであって、後工程の焼成時においても金属元素の拡散が不完全で、局所的な相分離が生じる結果、熱安定性に劣る結果となっているものと推定される。また原料を過度に粉碎することによって得られるLi複合酸化物の粒子が微細となり、これを正極として電池として用いた場合、正極が電解液と広く接触するために電解液の酸化分解などの副反応が起こり、経時劣化が起こりやすくなるといった問題も有している。

同様に、 $\text{LiMn}_a\text{Ni}_b\text{Co}_c\text{O}_2$  組成のうち、Yoshinari Makimura, Naoaki Yabuuchi, Tsutomu Ohzuku, Yukinori Kayama, Isao Tanaka, and Hirohiko Adachi, Lithium Insertion Material of  $\text{LiCo}_{1/3}\text{Ni}_{1/3}\text{Mn}_{1/3}\text{O}_2$  for Advanced Batteries; (II) Synthesis and Characterization as a Possible Alternative to  $\text{LiCoO}_2$ , The 42th Battery Symposium in Japan, 2I18, 2I19(2001)には  $\text{LiCo}_{0.33}\text{Ni}_{0.33}\text{Mn}_{0.33}\text{O}_2$  組成に関する報告がなされている。このLi複合酸化物は、MnとNiとCoの水溶液にアルカリを添加して沈殿させた共沈化合物と、Li化合物とを混合後、熱処理することで作製される。

しかしながら、該報告には得られたLi複合酸化物に関する物性の規定がなされていないといった問題があった。この種のLi複合酸化物の格子体積は、充電によって収縮し、放電によって拡大するため、放電時における活物質へのLiの取込速度は、充電時におけるLiの引抜速度に比べて著しく小さい。従って、活物質と電解液との接触界面状態といった、正極へのLiの取込速度に強い影響を与える因子に対して最大限の注意を払わなければ、十分な放電性能を持った電池を得ることができない。従って、本活物質を正極に用いた電池を実用化するにあたっては、前記因子を決定する活物質の物性を規定することは必須の要件である。

なお、空間群の表記について、本来「R3m」の数字「3」上にバー（横線）

を付して表記すべきところ、本明細書内においては便宜上「R 3/m」との表記をもって同一の意味を表すものとした。

本発明は、上記問題点を解決するためになされたものであって、高率充放電性能及び充放電サイクル性能に優れ、高い安全性を有する高エネルギー密度の非水電解質二次電池を得ることのできる正極活物質、および、高率充放電性能及び充放電サイクル性能に優れる高エネルギー密度の非水電解質二次電池を提供することを目的とする。

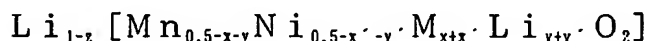
#### <発明の開示>

上記の課題を解決するために、本発明者らは鋭意検討の結果、特定の構造を有する正極活物質の物性を特定のものとすることにより、驚くべきことに、優れた電池特性を備える非水電解質二次電池が得られることを見出し、本発明に至った。すなわち、本発明の技術的構成およびその作用効果は以下の通りである。ただし、作用機構については推定を含んでおり、その作用機構の正否は、本発明を制限するものではない。

(1) Li-Mn-Ni系複合酸化物を主成分とする正極活物質であって、前記Li-Mn-Ni系複合酸化物のBET法による比表面積が $0.3\text{ m}^2/\text{g}$ 以上 $1.5\text{ m}^2/\text{g}$ 以下であることを特徴とする正極活物質。

(2) 前記Li-Mn-Ni系複合酸化物が、 $\text{LiMn}_{0.5}\text{Ni}_{0.5}\text{O}_2$ で表される複合酸化物であることを特徴とする前記(1)に記載の正極活物質。

(3) 前記Li-Mn-Ni系複合酸化物が、 $\text{LiMn}_{0.5}\text{Ni}_{0.5}\text{O}_2$ で表される複合酸化物を構成するMn及びNiの一部が異種元素で置換され、次の一般式；



(但し、Mは前記異種元素；

$$x = 0.001 \sim 0.1 \quad ; \quad x' = 0.001 \sim 0.1 \quad ;$$

$$y = 0 \sim 0.1 \quad ; \quad y' = 0 \sim 0.1 \quad ;$$

$$x + x' + y + y' \leq 0.4 \quad ; \quad 0 \leq z \leq 1)$$

で示される組成の複合酸化物であることを特徴とする前記（１）に記載の正極活物質。

（４） 前記Li-Mn-Ni系複合酸化物が、 $\text{LiMn}_{0.5}\text{Ni}_{0.5}\text{O}_2$ で表される複合酸化物を構成するMn及びNiの一部が異種元素で置換され、次の一般式；  
 $\text{Li}_{1-z} [\text{Mn}_{0.5-x-y}\text{Ni}_{0.5-x'-y'}\text{M}_{x+x'}\text{Li}_{y+y'}\text{O}_2]$

（但し、Mは前記異種元素；

$$x = 0.01 \sim 0.1 \quad ; \quad x' = 0.01 \sim 0.1 \quad ;$$

$$y = 0 \sim 0.1 \quad ; \quad y' = 0 \sim 0.1 \quad ;$$

$$x + x' + y + y' \leq 0.2 \quad ; \quad 0 \leq z \leq 1)$$

で示される組成の複合酸化物であることを特徴とする前記（１）に記載の正極活物質。

（５） 前記異種元素MがB, Mg, Al, Ti, V, Cr, Fe, Co, Cu及びZnから構成される群から選ばれる１種以上であることを特徴とする前記（３）または（４）に記載の正極活物質。

（６） 前記Li-Mn-Ni系複合酸化物が、 $\text{LiMn}_{0.5}\text{Ni}_{0.5}\text{O}_2$ で表される複合酸化物を構成するMn及びNiの一部が、異種元素並びにホウ素で置換され、次の一般式；

$$\text{Li}_{1-t} [\text{Mn}_{0.5-r-s-w}\text{Ni}_{0.5-r'-s'-w'}\text{B}_{w+w'}\text{M}'_{r+r'}\text{Li}_{s+s'}\text{O}_2]$$

（但し、M'は前記異種元素；

$$r = 0.001 \sim 0.1 \quad ; \quad r' = 0.001 \sim 0.1 \quad ;$$

$$s = 0 \sim 0.1 \quad ; \quad s' = 0 \sim 0.1 \quad ;$$

$$r + r' + s + s' + w + w' \leq 0.4 \quad ;$$

$$w + w' = 0.0005 \sim 0.01 \quad ; \quad 0 \leq t \leq 1)$$

で示される組成の複合酸化物であることを特徴とする前記（１）に記載の正極活物質。

（７） 前記Li-Mn-Ni系複合酸化物が、 $\text{LiMn}_{0.5}\text{Ni}_{0.5}\text{O}_2$ で表される複合酸化物を構成するMn及びNiの一部が、異種元素並びにホウ素で置換され、次の一般式；

$$\text{Li}_{1-t} [\text{Mn}_{0.5-r-s-w}\text{Ni}_{0.5-r'-s'-w'}\text{B}_{w+w'}\text{M}'_{r+r'}\text{Li}_{s+s'}\text{O}_2]$$

(但し、 $M'$  は前記異種元素 ;

$$r = 0.01 \sim 0.1 \quad ; \quad r' = 0.01 \sim 0.1 \quad ;$$

$$s = 0 \sim 0.1 \quad ; \quad s' = 0 \sim 0.1 \quad ;$$

$$r + r' + s + s' + w + w' \leq 0.2 \quad ;$$

$$w + w' = 0.0005 \sim 0.01 \quad ; \quad 0 \leq t \leq 1)$$

で示される組成の複合酸化物であることを特徴とする前記(1)に記載の正極活物質。

(8) 前記異種元素 $M'$  が  $Mg$ ,  $Al$ ,  $Ti$ ,  $V$ ,  $Cr$ ,  $Fe$ ,  $Co$ ,  $Cu$  及び  $Zn$  から構成される群から選ばれる1種以上であることを特徴とする前記(6)または(7)に記載の正極活物質。

(9) 前記  $Li-Mn-Ni$  系複合酸化物が、 $Li[Mn_cNi_dCo_eLi_aM''_b]O_2$  ( $M''$  は  $Mn$ ,  $Ni$ ,  $Co$ ,  $Li$  以外の元素、 $d \leq c + e + a + b$ ,  $c + d + e + a + b = 1$ ,  $0 \leq a \leq 0.05$ ,  $0 \leq b \leq 0.05$ ,  $0.2 \leq c \leq 0.5$ ,  $0.02 \leq e \leq 0.4$ ) で表される複合酸化物であることを特徴とする前記(1)に記載の正極活物質。

(10) 前記 $M''$  が、 $B$ ,  $Mg$ ,  $Al$ ,  $Ti$ ,  $V$ ,  $Cr$ ,  $Fe$ ,  $Cu$  及び  $Zn$  からなる群から選ばれる少なくとも1種の元素であることを特徴とする前記(9)に記載の正極活物質。

(11) 前記  $Li-Mn-Ni$  系複合酸化物が、 $CuK\alpha$  線を使用した粉末エックス線回折図の  $2\theta = 18.6 \pm 1^\circ$ ,  $36.6 \pm 1^\circ$ ,  $37.8 \pm 1^\circ$ ,  $38.2 \pm 1^\circ$ ,  $44.3 \pm 1^\circ$ ,  $48.4 \pm 1^\circ$ ,  $58.4 \pm 1^\circ$ ,  $64.2 \pm 1^\circ$ ,  $64.8 \pm 1^\circ$ ,  $68.8 \pm 1^\circ$  にピークを有する層状結晶構造であることを特徴とする前記(1)～(10)のいずれかに記載の正極活物質。

(12) 前記  $Li-Mn-Ni$  系複合酸化物は、 $CuK\alpha$  線を使用した粉末エックス線回折図の、 $2\theta = 18.6 \pm 1^\circ$  における回折ピークに対する  $2\theta = 44.1 \pm 1^\circ$  における回折ピークの相対強度比が0.6以上1.1以下であることを特徴とする前記(1)～(11)のいずれかに記載の正極活物質。

(13) 前記  $Li-Mn-Ni$  系複合酸化物は、 $CuK\alpha$  線を使用した粉末エックス線回折図の、 $2\theta = 18.6 \pm 1^\circ$  における回折ピークの半値幅が0.1

3°以上0.20°以下であり、かつ、 $2\theta = 44.1 \pm 1^\circ$ における回折ピークの半値幅が0.10°以上0.17°以下であることを特徴とする前記(1)～(12)のいずれかに記載の正極活物質。

(14) 前記Li-Mn-Ni系複合酸化物の粒径が3μm以上20μm以下である前記(1)～(13)のいずれかに記載の正極活物質。

(15) 前記(1)～(14)のいずれかに記載の正極活物質を用いた非水電解質二次電池。

本発明者らは、高容量が期待できるLiMnO<sub>2</sub>に着目し、次に、Mnを置換する元素として、Mnに対して固溶が容易で、4V付近を中心とした作動電位を示すことが期待できるNiを選択した。その結果、置換量を50%としたLiMn<sub>0.5</sub>Ni<sub>0.5</sub>O<sub>2</sub>では、従来のリチウムイオン電池との互換性に優れた4.3V～3.0Vという作動電位が得られること、及び、140mAh/gという高い放電容量が得られることを確認した。しかしながら、充放電サイクル性能については充分ではなかった。これは、充放電の繰り返しに伴って、正極活物質からMnが溶出し、これが電極界面抵抗の増加を導いているためと推察された。

そこで、本発明者らは、種々の物性を有するLiMn<sub>0.5</sub>Ni<sub>0.5</sub>O<sub>2</sub>、および、LiMn<sub>0.5</sub>Ni<sub>0.5</sub>O<sub>2</sub>を構成する元素のうちNi及びMnの一部を他の異種元素で置換したもの（以下、これらをまとめて、Li-Mn-Ni系複合酸化物ともいう）について、充放電サイクル性能との関係を鋭意検討したところ、比表面積の値を特定の範囲とすることにより、驚くべきことに、極めて安定した充放電サイクル性能が得られることがわかった。即ち、前記比表面積の値を1.5m<sup>2</sup>/g以下とすることにより、優れた充放電サイクル性能が得られることがわかった。

この作用効果については、必ずしも明らかではないが、比表面積が減少したことで、正極活物質であるLi-Mn-Ni系複合酸化物が電解質に触れる面積が減少したため、電解液の酸化分解が抑制されたことに加え、前記正極活物質の粒子表面にわずかに吸着した水分が比表面積の減少に伴い減少したため、水分に起因する電池内でのフッ酸(HF)の発生量を低下させ、これらの酸によるMnの溶解反応が起こりにくくなったものと考えられる。

さらに、前記比表面積の値を  $0.3 \text{ m}^2/\text{g}$  以上とすることにより、 $2 \text{ It}$  (0.5時間率) といった高率放電を行っても、高い放電容量を維持することが認められた。

また、本発明者らは、 $\text{Li-Mn-Ni}$ 系複合酸化物の中でも、 $\text{LiMn}_{0.5}\text{Ni}_{0.5}\text{O}_2$ を構成する元素のうち、 $\text{Ni}$ 及び $\text{Mn}$ の一部を他の異種元素で置換したものについて鋭意検討したところ、驚くべきことに、前記異種原子の種類を特定のものとすることで、高率放電特性をさらに大きく改善する効果があることを見出した。

この作用効果については必ずしも明らかではないが、前記異種元素の原子半径、即ち大きさが、 $\text{Mn}$ 元素や $\text{Ni}$ 元素の原子半径と異なるため、正極活物質を構成している層状構造に影響し、 $\text{Li}$ イオンの移動経路へ影響を及ぼし、イオン伝導を良好にする効果をもたらしたものと考えられる。また、このため、 $\text{Mn}$ 、 $\text{Ni}$ 以外の異種元素は、その元素の原子半径、即ち大きさが異なることから、大きさの異なる元素の存在により、充放電に伴う活物質結晶の膨張収縮歪みを緩和したものと考えられる。

さらに、特に表面組成が密接に関係することについては、 $\text{Li}$ イオンの授受が、正極活物質粒子と電解液との界面において行われることと関係しているものと考えられる。

また、本発明者らは、 $\text{LiMn}_{0.5}\text{Ni}_{0.5}\text{O}_2$ を合成する際の焼成条件やさらに添加する $\text{Li}$ 、 $\text{Mn}$ 、 $\text{Ni}$ 以外の異種金属元素の種類と組成比率について鋭意検討を重ねたところ、同一組成の複合酸化物ながらも、焼成条件によって、得られる結晶の構造が大きく異なり、結晶の形態によっては充放電サイクル性能が大きく改善できることがわかった。具体的には、 $\text{Li-Mn-Ni}$ 系複合酸化物が $\text{Cu K}\alpha$ 線を使用した粉末エックス線回折の $2\theta = 18.6 \pm 1^\circ$ 、 $36.6 \pm 1^\circ$ 、 $37.8 \pm 1^\circ$ 、 $38.2 \pm 1^\circ$ 、 $44.3 \pm 1^\circ$ 、 $48.4 \pm 1^\circ$ 、 $58.4 \pm 1^\circ$ 、 $64.2 \pm 1^\circ$ 、 $64.8 \pm 1^\circ$ 、 $68.8 \pm 1^\circ$ にピークを有する層状結晶構造である場合、優れたサイクル性能が得られることを確認した。

この作用効果については必ずしも明らかではないが、前記粉末エックス線回折パターンを示す結晶は、歪みが少なく、結晶の構造自体が安定であるものと考え

られる。また、特に Co を添加した場合、更に構造を安定化させる効果があり、このため、前記結晶構造物からのリチウムの引き抜き反応が、より卑な電位で進行しやすくなった結果、充放電容量が向上したものと考えられる。

また、本発明者らは、焼成温度が 850℃ の場合と 1000℃ の場合とでは、同じ成分であっても結晶構造が大きく変わり、これに伴って充放電時の電位変化曲線の形状も大きく異なっていることがわかった。特に高率放電性能に対しては、前記焼成時の温度や焼成時間がわずかに変わるだけで、影響を与える。

本発明者らは、このような事実から、焼成条件は活物質の結晶構造に影響を与えているものと考え、焼成で得られた粉末について、Cu K $\alpha$  線を使用した粉末エックス線回折測定による回折図の  $2\theta = 18.6 \pm 1^\circ$  における回折ピークに対する  $2\theta = 44.1 \pm 1^\circ$  における回折ピークの相対強度に着目して鋭意検討した結果、驚くべきことに、前記相対強度が 1.1 以下であるリチウムマンガニッケル複合酸化物を正極活物質として用いた場合、高率放電特性が特に改善されることがわかった。

この作用効果については、必ずしも明らかではないが、前記相対強度が 1.1 以下であることにより、リチウムイオンの固体内の移動が特に容易になったものと考えられる。但し、前記相対強度が 0.6 より小さくなった場合には、結晶の発達が悪いために、リチウムイオンの固体内の移動が阻害され、充放電サイクル性能が低下する傾向となる。このため、前記相対強度を 0.6 以上 1.1 以下とした正極活物質を用いることによって、良好な高率放電性能と良好な充放電サイクル性能とを兼ね備えた非水電解質二次電池を提供することができる。

また、 $2\theta = 18.6 \pm 1^\circ$  と  $2\theta = 44.1 \pm 1^\circ$  における半値幅は本発明電池に用いる正極活物質結晶の成長性や結晶子径を反映し、半値幅が大きいほど結晶子径は小さくなる関係にあると考えられるが、驚くべきことに、 $2\theta = 18.6 \pm 1^\circ$  における回折ピークの半値幅が  $0.13^\circ \sim 0.20^\circ$  であり、かつ、 $44.1 \pm 1^\circ$  における回折ピークの半値幅が  $0.10^\circ \sim 0.17^\circ$  である場合、特に優れた高率放電特性と充放電サイクル性能が得られることが確認できた。

この作用効果については、必ずしも明らかではないが、 $2\theta = 18.6 \pm 1^\circ$

における回折ピークの半値幅が $0.20^{\circ}$ 以下であり、かつ、 $44.1 \pm 1^{\circ}$ における回折ピークの半値幅が $0.17^{\circ}$ 以下である場合には、結晶中のLiイオン移動が容易となり、高率放電特性については改善されるものの、結晶の安定性が悪くなるために、充放電サイクル性能が低下するものと考えられる。このため、 $2\theta = 18.6 \pm 1^{\circ}$ における回折ピークの半値幅が $0.13^{\circ}$ 以上であり、かつ、 $44.1 \pm 1^{\circ}$ における回折ピークの半値幅が $0.10^{\circ}$ 以上である場合、適度な結晶中のLiイオン移動と十分な結晶の安定性とが得られるため、優れた高率放電特性と充放電サイクル性能を合わせ持つことが可能になる。

#### <図面の簡単な説明>

図1は、本発明に用いた正極活物質のエックス線光電子分光法(XPS)による分析結果を示す図であり、図2は、実施例および比較例の電池の一部断面図であり、図3は、実施例1-1の正極活物質のエックス線回折図であり、図4は、実施例1-10の正極活物質のエックス線回折図であり、図5は、実施例4-1の正極活物質のエックス線回折図であり、図6は、実施例1-1の電池の放電性能を示す図であり、図7は、実施例1-10の電池の放電性能を示す図であり、図8は、実施例4-1の電池の放電性能を示す図である。

なお、図中の符号、1は安全弁、2は蓋、3はレーザー溶接部、4は負極端子、5は正極端子、6はガasket、7は正極板、8はセパレータ、9は負極板、10は電槽である。

#### <発明を実施するための最良の形態>

以下に、本発明の実施の形態を例示するが、本発明は、以下の実施の形態に限定されるものではない。

本発明に係る正極活物質は、Li-Mn-Ni系複合酸化物を主成分とする正極活物質であって、前記Li-Mn-Ni系複合酸化物のBET法による比表面積(以下、単に比表面積ともいう)が $0.3 \text{ m}^2/\text{g}$ 以上 $1.5 \text{ m}^2/\text{g}$ 以下であることを特徴としている。前記したように、比表面積が $1.5 \text{ m}^2/\text{g}$ 以下である



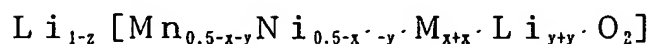
ことによって、充放電サイクル性能に優れた非水電解質二次電池（以下、単に電池ともいう）を得ることができ、比表面積が  $0.3 \text{ m}^2/\text{g}$  以上であることによって、高率充放電性能に優れた電池を得ることができる。

ここで、 $\text{Li}-\text{Mn}-\text{Ni}$  系複合酸化物とは、構成元素として、少なくとも、リチウム ( $\text{Li}$ )、マンガン ( $\text{Mn}$ )、ニッケル ( $\text{Ni}$ )、酸素 ( $\text{O}$ ) を有する複合酸化物のことをいう。

以下に、本発明における  $\text{Li}-\text{Mn}-\text{Ni}$  系複合酸化物の好適な形態を説明する。ただし、 $\text{Li}-\text{Mn}-\text{Ni}$  系複合酸化物は、以下に例示する形態に限定されない。

$\text{Li}-\text{Mn}-\text{Ni}$  系複合酸化物の第一実施形態は、 $\text{LiMn}_{0.5}\text{Ni}_{0.5}\text{O}_2$  で表わされる複合酸化物である。

$\text{Li}-\text{Mn}-\text{Ni}$  系複合酸化物の第二実施形態の 1 は、 $\text{LiMn}_{0.5}\text{Ni}_{0.5}\text{O}_2$  で表される複合酸化物を構成する  $\text{Mn}$  及び  $\text{Ni}$  の一部が異種元素で置換され、次の一般式；



（但し、 $\text{M}$  は前記異種元素；

$$x = 0.001 \sim 0.1 \quad ; \quad x' = 0.001 \sim 0.1 \quad ;$$

$$y = 0 \sim 0.1 \quad ; \quad y' = 0 \sim 0.1 \quad ;$$

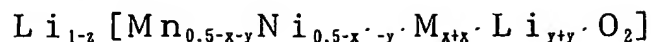
$$x + x' + y + y' \leq 0.4 \quad ; \quad 0 \leq z \leq 1)$$

で示される組成の複合酸化物である。

$x + x' + y + y' \leq 0.4$  であることによって、充放電の繰り返しによっても複合酸化物の結晶構造が安定であり、これにより、充放電サイクル性能に優れる。

$\text{Li}-\text{Mn}-\text{Ni}$  系複合酸化物の第二実施形態の 2 は、 $\text{LiMn}_{0.5}\text{Ni}_{0.5}\text{O}_2$  で表される複合酸化物を構成する  $\text{Mn}$  及び  $\text{Ni}$  の一部が異種元素で置換され、次

の一般式；



(但し、Mは前記異種元素；

$$x = 0.01 \sim 0.1 \quad ; \quad x' = 0.01 \sim 0.1 \quad ;$$

$$y = 0 \sim 0.1 \quad ; \quad y' = 0 \sim 0.1 \quad ;$$

$$x + x' + y + y' \leq 0.2 \quad ; \quad 0 \leq z \leq 1)$$

で示される組成の複合酸化物である。

$x + x' + y + y' \leq 0.2$ であることによって、充放電の繰り返しによっても複合酸化物の結晶構造が特に安定であり、これにより、より充放電サイクル性能に優れる。

前記異種元素Mは、Mn、Ni及びLi以外の元素で、Mnと置換しうる元素が好ましい。例えば、B, Be, V, C, Si, P, Sc, Cu, Zn, Ga, Ge, As, Se, Sr, Mo, Pd, Ag, Cd, In, Sn, Sb, Te, Ba, Ta, W, Pb, Bi, Co, Fe, Cr, Ni, Ti, Zr, Nb, Y, Al, Na, K, Mg, Ca, Cs, La, Ce, Nd, Sm, Eu, Tb等が挙げられる。

なかでも、B, Mg, Al, Ti, V, Cr, Fe, Co, Cu及びZnのいずれかを用いると、高率放電性能に特に顕著な効果が得られるため、さらに好ましい。

ここで、Mnの置換量を示すx、yは、 $0 < x + y \leq 0.2$ であり、Niの置換量を示すx'、y'は、 $0 < x' + y' \leq 0.2$ である。これは、Mnの置換量x+yとNiの置換量x'+y'を増やすと、可逆的に使用可能なリチウム量が減少するためである。

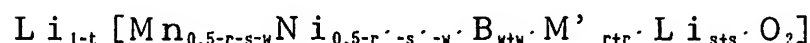
zは、可逆的に使用可能なリチウム量を示し、Mn及びNiに対する異種元素の量が多いほど小さくなる。

ここで、式中、 $\text{Li}_{y+y'}$ で示される部分のリチウムについては、前記式における組成比を示すものであり、 $\text{LiMn}_{0.5}\text{Ni}_{0.5}\text{O}_2$ の基本骨格中におけるリチウム元素の配置状態を示すものではなく、前記基本骨格を構成する元素の一部と置換し

ているか否かを示すものでもない。

高率放電性能は、 $0 < x' + y' \leq 0.2$ 、且つ、 $0 < x + y \leq 0.2$ の範囲内であれば、Mn及びNiに対する異種元素の量が多いほど向上し、 $x$ 、 $x'$ は、それぞれ0.001以上が好ましく、それぞれ0.01以上が特に好ましい。

Li-Mn-Ni系複合酸化物の第三実施形態の1は、 $\text{LiMn}_{0.5}\text{Ni}_{0.5}\text{O}_2$ で表される複合酸化物を構成するMn及びNiの一部が異種元素並びにホウ素で置換され、次の一般式；



(但し、M' は前記異種元素 ；

$$r = 0.001 \sim 0.1 \quad ; \quad r' = 0.001 \sim 0.1 \quad ;$$

$$s = 0 \sim 0.1 \quad ; \quad s' = 0 \sim 0.1 \quad ;$$

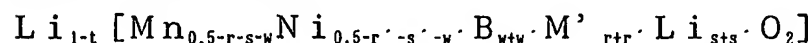
$$r + r' + s + s' + w + w' \leq 0.4 \quad ;$$

$$w + w' = 0.0005 \sim 0.01 \quad ; \quad 0 \leq t \leq 1)$$

で示される組成の複合酸化物である。

$r + r' + s + s' + w + w' \leq 0.4$ であることによって、充放電の繰り返しによっても複合酸化物の結晶構造が安定であり、これにより、充放電サイクル性能に優れる。

Li-Mn-Ni系複合酸化物の第三実施形態の2は、 $\text{LiMn}_{0.5}\text{Ni}_{0.5}\text{O}_2$ で表される複合酸化物を構成するMn及びNiの一部が異種元素並びにホウ素で置換され、次の一般式；



(但し、M' は前記異種元素 ；

$$r = 0.01 \sim 0.1 \quad ; \quad r' = 0.01 \sim 0.1 \quad ;$$

$$s = 0 \sim 0.1 \quad ; \quad s' = 0 \sim 0.1 \quad ;$$

$$r + r' + s + s' + w + w' \leq 0.2 \quad ;$$

$$w + w' = 0.0005 \sim 0.01 \quad ; \quad 0 \leq t \leq 1)$$

で示される組成の複合酸化物である。

$r + r' + s + s' + w + w' \leq 0.2$  であることによって、充放電の繰り返しによっても複合酸化物の結晶構造が特に安定であり、これにより、より充放電サイクル性能に優れる。

なお、本明細書においては、ホウ素を含んだ正極活物質の組成表現として、  
 $Li_{1-t} [Mn_{0.5-r-s-w} Ni_{0.5-r'-s'-w'} B_{w+w'} M'_{r+r'} Li_{s+s'} O_2]$   
 のように、ホウ素を置換された異種元素として表記しているが、前記ホウ素は電池の充放電によって溶解して負極上に析出することがわかっている。にもかかわらず、前記ホウ素は前記高率放電特性を改善する効果があることから、異種元素にホウ素を用いた正極活物質自身が電池内でホウ素を溶出することで、該正極活物質の結晶粒子表面に活性な面を形成する効果があり、これによって高率放電特性を改善する効果があるものと考えられる。

ここで、粒子表面の元素組成を定量する方法のひとつにエックス線光電子分光法 (XPS) により粒子をエッチングしながら測る方法がある。一例として、毎秒  $0.07 \text{ nm}$  の速度で粒子表面をエッチングした時の B の濃度変化を示した (図 1 参照)。その結果、本例◆印の試料における粒子の場合、表面から  $400$  秒、すなわち、 $28 \text{ nm}$  程度までにはほとんどの B が集積しているのがわかる。

異種元素  $M'$  は、Mn、Ni 及び Li 以外の元素で、Mn と置換しうる元素が好ましい。例えば、Be, V, C, Si, P, Sc, Cu, Zn, Ga, Ge, As, Se, Sr, Mo, Pd, Ag, Cd, In, Sn, Sb, Te, Ba, Ta, W, Pb, Bi, Co, Fe, Cr, Ni, Ti, Zr, Nb, Y, Al, Na, K, Mg, Ca, Cs, La, Ce, Nd, Sm, Eu, Tb 等が挙げられる。

なかでも、Mg, Al, Ti, V, Cr, Fe, Co, Cu 及び Zn のいずれかを用いると、高率放電性能に特に顕著な効果が得られるため、さらに好ましい。

ここで、Mn の置換量を示す  $r, s, w$  は、 $0 < r + s + w \leq 0.2$  であり、Ni の置換量を示す  $r', s', w'$  は、 $0 < r' + s' + w' \leq 0.2$  である。

。これは、Mnの置換量 $r + s + w$ とNiの置換量 $r' + s' + w'$ を増やすと、可逆的に使用可能なリチウム量が減少するためである。

tは、可逆的に使用可能なリチウム量を示し、Mn及びNiに対する異種元素の量が多いほど小さくなる。

高率放電性能は、 $0 < r' + s' + w' \leq 0.2$ 、且つ、 $0 < r + s + w \leq 0.2$ の範囲内であれば、Mn及びNiに対する異種元素の量が多いほど向上し、 $r, r'$ は、それぞれ0.001以上が好ましく、それぞれ0.01以上が特に好ましい。

また、Li-Mn-Ni系複合酸化物の第二実施形態および第三実施形態において、前記Mn及びNiの一部をリチウムや異種元素で置換する方法としては、活物質の焼成原料にあらかじめ置換する元素を添加する方法や、 $\text{LiMn}_{0.5}\text{Ni}_{0.5}\text{O}_2$ を焼成した後にイオン交換等により異種元素を置換する方法等が挙げられるが、これらに限定されるものではない。

Li-Mn-Ni系複合酸化物の第四実施形態は、 $\text{Li}[\text{Mn}_d\text{Ni}_e\text{Co}_f\text{Li}_a\text{M}''_b]\text{O}_2$  ( $\text{M}''$ はMn、Ni、Co、Li以外の元素、 $d \leq c + e + a + b$ 、 $c + d + e + a + b = 1$ 、 $0 \leq a \leq 0.05$ 、 $0 \leq b \leq 0.05$ 、 $0.2 \leq c \leq 0.5$ 、 $0.02 \leq e \leq 0.4$ )で表される複合酸化物である。cが0.2を下回るとサイクル性能が悪くなる傾向となり、cが0.5を上回るとサイクル性能が低下する傾向となるばかりでなく、原料の焼成中に $\text{Li}_2\text{MnO}_3$ などの不純物が比較的低温から安定に生成しやすくなるので好ましくない。eが0.4を上回ると、充電時における熱安定性が低下する傾向となる。aが0.05を上回ると、放電容量が低下する傾向となる。bが0.05を上回ると、放電容量が低下する傾向となる。

さらに、高率充放電特性を改善するため、構成元素の組成比を意図的に変化させて検討した結果、驚くべきことに、特定の異種元素を添加した場合、高率放電特性をさらに大きく改善する効果があることを見いだした。

前記異種元素 $\text{M}''$ は、Mn、Ni及びLi以外の元素で、Mnと置換しうる元

素が好ましい。例えば、B, Be, V, C, Si, P, Sc, Cu, Zn, Ga, Ge, As, Se, Sr, Mo, Pd, Ag, Cd, In, Sn, Sb, Te, Ba, Ta, W, Pb, Bi, Fe, Cr, Ni, Ti, Zr, Nb, Y, Al, Na, K, Mg, Ca, Cs, La, Ce, Nd, Sm, Eu, Tb等が挙げられる。

なかでも、B, Mg, Al, Ti, V, Cr, Fe, Cu及びZnのいずれかを用いると、高率放電性能に特に顕著な効果が得られるため、さらに好ましい。

この作用効果については必ずしも明らかではないが、前記異種元素の大きさが、Mn元素やNi元素の大きさと異なるため、正極活物質を構成している層状構造に影響し、Liイオンの移動経路へ影響を及ぼし、イオン伝導を良好にする効果をもたらしたものと考えられる。

また、Mn、Ni以外の異種元素は、その元素の原子半径、即ち大きさが異なることから、原子半径の異なる元素の存在により、充放電に伴う活物質結晶の膨張収縮歪みを緩和したものと考えられる。

また、Li-Mn-Ni系複合酸化物の第四実施形態において、前記異種元素を前記複合酸化物に取り込む方法としては、焼成原料にあらかじめ置換する元素を添加する方法や、焼成した後にイオン交換等により異種元素を置換する方法等が挙げられるが、これらに限定されるものではない。

以上に、Li-Mn-Ni系複合酸化物の各実施形態を例示したが、Li-Mn-Ni系複合酸化物は、CuK $\alpha$ 線を使用した粉末エックス線回折図の $2\theta = 18.6 \pm 1^\circ$ 、 $36.6 \pm 1^\circ$ 、 $37.8 \pm 1^\circ$ 、 $38.2 \pm 1^\circ$ 、 $44.3 \pm 1^\circ$ 、 $48.4 \pm 1^\circ$ 、 $58.4 \pm 1^\circ$ 、 $64.2 \pm 1^\circ$ 、 $64.8 \pm 1^\circ$ 、 $68.8 \pm 1^\circ$ にピークを有しており、これにより優れたサイクル性能が得られる。

また、Li-Mn-Ni系複合酸化物は、前記したように、CuK $\alpha$ 線を使用した粉末エックス線回折図において、 $2\theta = 18.6 \pm 1^\circ$ と $2\theta = 44.1 \pm 1^\circ$ とに回折ピークを有し、 $2\theta = 18.6 \pm 1^\circ$ における回折ピークに対する

$2\theta = 44.1 \pm 1^\circ$  における回折ピークの相対強度比が  $0.6 \sim 1.1$  であるものが好ましく、また、 $2\theta = 18.6 \pm 1^\circ$  における回折ピークの半値幅が  $0.13^\circ \sim 0.20^\circ$  であり、 $2\theta = 44.1 \pm 1^\circ$  における回折ピークの半値幅が  $0.10^\circ \sim 0.17^\circ$  であるものが好ましい。

また、Li-Mn-Ni系複合酸化物の粒子径は小さいほど比表面積が増えるため出力特性は出やすくなるが、その他の性能、特に保存性能の低下を防ぐため、また電極作製時の塗工性を考慮して、平均粒径 ( $D_{50}$ ) =  $3 \mu\text{m} \sim 30 \mu\text{m}$  が好ましく、特に  $5 \mu\text{m} \sim 20 \mu\text{m}$  が好ましい。この範囲内であれば、電池の保存性能や充放電サイクル性能には大きく影響を与えるものではなく、特に制限されるものではない。これは、前記粒径は結晶の1次粒子の粒径を示すものでなく、2次粒子の粒径を示すものであるためである。参考までに、以下の実施例に用いた正極活物質の平均粒径は全て  $9 \sim 20 \mu\text{m}$  である。

次に、Li-Mn-Ni系複合酸化物の好適な製造方法を例示する。

Li-Mn-Ni系複合酸化物は、 $900^\circ\text{C}$ 以上の温度で焼成する熱履歴を有することが好ましい。より具体的には、「少なくともLi成分とMn成分とNi成分とを含有するLi-Mn-Ni系複合酸化物前駆体」を $900^\circ\text{C}$ 以上の温度で焼成してLi-Mn-Ni系複合酸化物を製造することが好ましい。ここで、焼成温度は、 $900^\circ\text{C} \sim 1100^\circ\text{C}$ が好ましく、 $950^\circ\text{C} \sim 1025^\circ\text{C}$ が特に好ましい。

焼成温度が $900^\circ\text{C}$ を下回ると、Li-Mn-Ni系複合酸化物の比表面積を  $1.5 \text{ m}^2/\text{g}$ 以下としにくく、サイクル性能が劣った電池が得られやすい。

一方、焼成温度が $1100^\circ\text{C}$ を上回ると、Liの揮発によって目標とする組成の複合酸化物が得られにくいなどの作製上の問題や、粒子の高密度化によって電池性能が低下するという問題が生じやすい。これは、 $1100^\circ\text{C}$ を上回ると、1次粒子成長速度が増加し、複合酸化物の結晶粒子が大きくなりすぎることに起因しているが、それに加えて、局所的にLi欠損量が増大して、構造的に不安定となっていることも原因ではないかと考えられる。

焼成時間は、3時間～50時間が好ましい。焼成時間が50時間を超えると、Li-Mn-Ni系複合酸化物の比表面積を $0.3\text{ m}^2/\text{g}$ 以上としにくく、高率充放電性能が劣った電池が得られやすい。焼成時間が3時間より少ないと、Li-Mn-Ni系複合酸化物の比表面積を $1.5\text{ m}^2/\text{g}$ 以下としにくく、サイクル性能が劣った電池が得られやすい。

以上に、焼成温度と焼成時間について好ましい範囲を記載したが、得られる複合酸化物の比表面積が、本発明で規定する範囲となるように適宜選択される。

Li-Mn-Ni複合酸化物前駆体は、「マンガン(Mn)化合物とニッケル(Ni)化合物とが水に溶解された水溶液、または、Mn化合物とNi化合物と“異種元素を有する化合物”(前記した異種元素M, M', M")を含有する化合物であり、以下、[M]化合物とも表記する)とが水に溶解された水溶液に、アルカリ化合物を添加して、Mn-Ni複合共沈物、または、Mn-Ni-[M]複合共沈物を沈殿させる共沈工程」を経由して好適に製造される。

ここで、Ni化合物としては、水酸化ニッケル、炭酸ニッケル、硫酸ニッケル、硝酸ニッケル等を、Mn化合物としては、酸化マンガン、炭酸マンガン、硫酸マンガン、硝酸マンガン等を好適に挙げることができる。

[M]化合物としては、異種元素がBである場合、ホウ酸等を、異種元素がVである場合、酸化バナジウム等を、異種元素がAlである場合、硝酸アルミニウム等を、異種元素がMgである場合、硝酸マグネシウム等を、異種元素がCoである場合、水酸化コバルト、炭酸コバルト、酸化コバルト、硫酸コバルト、硝酸コバルト等を、異種元素がCrである場合、硝酸クロム等を、異種元素がTiである場合、酸化チタン等を、異種元素がFeである場合、硫酸鉄、硝酸鉄等を、異種元素がCuである場合、硫酸銅、硝酸銅等を、異種元素がZnである場合、硫酸亜鉛、硝酸亜鉛等を、それぞれ挙げることができる。

アルカリ化合物としては、水酸化アンモニウム、水酸化ナトリウム等を挙げることができる。また、アルカリ化合物は、水溶液の形態として添加されるのが好ましい。



以上に説明した共沈工程を経由して得られたMn-Ni複合共沈物またはMn-Ni-[M]複合共沈物（以下、これらをまとめて、単に“複合共沈物”ともいう）とリチウム化合物との混合物をLi-Mn-Ni系複合酸化物前駆体とし、このLi-Mn-Ni系複合酸化物前駆体を前記した焼成条件に基づいて焼成することによって、Li-Mn-Ni系複合酸化物を好適に製造できる。

ここで、Li-Mn-Ni系複合酸化物前駆体は、複合共沈物とリチウム化合物の水溶液から水を蒸発させて乾燥させて得られた混合物を好適に例示できる。

Li化合物としては、水酸化リチウム、炭酸リチウム等を挙げることができる。

本発明の正極活物質は、主成分である前記したLi-Mn-Ni系複合酸化物に加え、他の化合物を混合して用いてもよく、例えば、他のリチウム含有遷移金属酸化物などの1種以上を混合して用いると、高いサイクル性能が得られることがある。

その他のリチウム含有遷移金属酸化物としては、一般式 $Li_xMX_2$ 、 $Li_xMn_yX_2$ （M、NはIからVIII族の金属、Xは酸素、硫黄などのカルコゲン化合物を示す。）であり、例えば $Li_yCo_{1-x}M_xO_2$ 、 $Li_yMn_{2-x}M_xO_4$ （Mは、IからVIII族の金属（例えば、Li、Ca、Cr、Ni、Fe、Coの1種類以上の元素）等が挙げられる。該リチウム含有遷移金属酸化物の異種元素置換量を示すx値については置換できる最大量まで有効であるが、好ましくは放電容量の点から $0 \leq x \leq 1$ である。また、リチウム量を示すy値についてはリチウムを可逆的に利用しうる最大量が有効であり、好ましくは放電容量の点から $0 \leq y \leq 1$ である。）が挙げられるが、これらに限定されるものではない。

さらに、他の化合物としては、CuO、Cu<sub>2</sub>O、Ag<sub>2</sub>O、CuS、CuSO<sub>4</sub>等のI族金属化合物、TiS<sub>2</sub>、SiO<sub>2</sub>、SnO等のIV族金属化合物、V<sub>2</sub>O<sub>5</sub>、V<sub>6</sub>O<sub>12</sub>、VO<sub>x</sub>、Nb<sub>2</sub>O<sub>5</sub>、Bi<sub>2</sub>O<sub>3</sub>、Sb<sub>2</sub>O<sub>3</sub>等のV族金属化合物、CrO<sub>3</sub>、Cr<sub>2</sub>O<sub>3</sub>、MoO<sub>3</sub>、MoS<sub>2</sub>、WO<sub>3</sub>、SeO<sub>2</sub>等のVI族金属化合物、MnO<sub>2</sub>、Mn<sub>2</sub>O<sub>3</sub>等のVII族金属化合物、Fe<sub>2</sub>O<sub>3</sub>、FeO、Fe<sub>3</sub>O<sub>4</sub>、Ni<sub>2</sub>O<sub>3</sub>、NiO、CoO<sub>3</sub>、CoO等のVIII族金属化合物等で表される、例えばリチウム-コバルト系複

合酸化物やリチウム－マンガン系複合酸化物等の金属化合物、さらに、ジスルフィド、ポリピロール、ポリアニリン、ポリパラフェニレン、ポリアセチレン、ポリアセン系材料等の導電性高分子化合物、擬グラファイト構造炭素質材料等が挙げられるが、これらに限定されるものではない。

正極活物質として、前記した  $\text{Li}-\text{Mn}-\text{Ni}$  系複合酸化物以外に、前掲の他の化合物を併用する場合、他の化合物の使用割合は、本発明の効果を損なわない程度であれば限定されるものではないが、その他の成分は全正極活物質中、通常 1 重量%～50 重量%、好ましくは 5 重量%～30 重量%である。

次に、本発明の非水電解質二次電池について説明する。本発明の非水電解質二次電池（以下、単に電池ともいう）は、本発明の正極活物質を用いた電池であり、一般的に、少なくとも、本発明の正極活物質を主要構成成分とする正極と、負極材料を主要構成成分とする負極と、電解質塩が非水溶媒に含有された非水電解質とから構成され、通常、正極と負極との間に、セパレータが設けられる。

非水電解質は、一般にリチウム電池等への使用が提案されているものが使用可能である。非水溶媒としては、プロピレンカーボネート、エチレンカーボネート、ブチレンカーボネート、クロロエチレンカーボネート、ビニレンカーボネート等の環状炭酸エステル類； $\gamma$ -ブチロラクトン、 $\gamma$ -バレロラクトン等の環状エステル類；ジメチルカーボネート、ジエチルカーボネート、エチルメチルカーボネート等の鎖状カーボネート類；ギ酸メチル、酢酸メチル、酪酸メチル等の鎖状エステル類；テトラヒドロフランまたはその誘導体；1, 3-ジオキサン、1, 4-ジオキサン、1, 2-ジメトキシエタン、1, 4-ジブトキシエタン、メチルジグリム等のエーテル類；アセトニトリル、ベンゾニトリル等のニトリル類；ジオキソランまたはその誘導体；エチレンスルフィド、スルホラン、スルトンまたはその誘導体等の単独またはそれら 2 種以上の混合物等を挙げることができるが、これらに限定されるものではない。

電解質塩としては、例えば、 $\text{LiClO}_4$ 、 $\text{LiBF}_4$ 、 $\text{LiAsF}_6$ 、 $\text{LiPF}_6$ 、 $\text{LiSCN}$ 、 $\text{LiBr}$ 、 $\text{LiI}$ 、 $\text{Li}_2\text{SO}_4$ 、 $\text{Li}_2\text{B}_{10}\text{Cl}_{10}$ 、 $\text{NaClO}_4$ 、 $\text{N}$

a I, NaSCN, NaBr, KClO<sub>4</sub>, KSCN等のリチウム (Li)、ナトリウム (Na) またはカリウム (K) の1種を含む無機イオン塩、LiCF<sub>3</sub>SO<sub>3</sub>, LiN(CF<sub>3</sub>SO<sub>2</sub>)<sub>2</sub>, LiN(C<sub>2</sub>F<sub>5</sub>SO<sub>2</sub>)<sub>2</sub>, LiN(CF<sub>3</sub>SO<sub>2</sub>)(C<sub>4</sub>F<sub>9</sub>SO<sub>2</sub>), LiC(CF<sub>3</sub>SO<sub>2</sub>)<sub>3</sub>, LiC(C<sub>2</sub>F<sub>5</sub>SO<sub>2</sub>)<sub>3</sub>, (CH<sub>3</sub>)<sub>4</sub>NBF<sub>4</sub>, (CH<sub>3</sub>)<sub>4</sub>NBr, (C<sub>2</sub>H<sub>5</sub>)<sub>4</sub>NClO<sub>4</sub>, (C<sub>2</sub>H<sub>5</sub>)<sub>4</sub>NI, (C<sub>3</sub>H<sub>7</sub>)<sub>4</sub>NBr, (n-C<sub>4</sub>H<sub>9</sub>)<sub>4</sub>NClO<sub>4</sub>, (n-C<sub>4</sub>H<sub>9</sub>)<sub>4</sub>NI, (C<sub>2</sub>H<sub>5</sub>)<sub>4</sub>N-maleate, (C<sub>2</sub>H<sub>5</sub>)<sub>4</sub>N-benzoate, (C<sub>2</sub>H<sub>5</sub>)<sub>4</sub>N-phthalate、ステアリルスルホン酸リチウム、オクチルスルホン酸リチウム、ドデシルベンゼンスルホン酸リチウム等の有機イオン塩等が挙げられ、これらのイオン性化合物を単独、あるいは2種類以上混合して用いることが可能である。

さらに、LiBF<sub>4</sub>とLiN(C<sub>2</sub>F<sub>5</sub>SO<sub>2</sub>)<sub>2</sub>のようなパーフルオロアルキル基を有するリチウム塩とを混合して用いることにより、さらに非水電解質の粘度を下げるので、低温特性をさらに高めることができ、より望ましい。

非水電解質における電解質塩の濃度としては、高い電池特性を有する電池を確実に得るために、0.1mol/l～5mol/lが好ましく、さらに好ましくは、1mol/l～2.5mol/lである。

本発明の電池の正極には本発明によるLi-Mn-Ni系複合酸化物で構成された電極が、負極にはグラファイトで構成された電極が好適に使用される。

正極は、本発明による複合酸化物を導電剤および結着剤、さらに必要に応じてフィラーと混練して正極合剤とした後、この正極合剤を集電体としての箔やラス板等に塗布、または圧着して50℃～250℃程度の温度で、2時間程度加熱処理することにより作製される。

負極材料としては、リチウム金属、リチウム合金（リチウム-アルミニウム、リチウム-鉛、リチウム-スズ、リチウム-アルミニウム-スズ、リチウム-ガリウム、およびウッド合金等のリチウム金属含有合金）の他、リチウムを吸蔵・放出可能な合金、炭素材料（例えばグラファイト、ハードカーボン、低温焼成炭素、非晶質カーボン等）等が挙げられる。これらの中でもグラファイトは、金属リチウムに極めて近い作動電位を有するので電解質塩としてリチウム塩を採用し

た場合に自己放電を少なくでき、かつ充放電における不可逆容量を少なくできるので、負極材料として好ましい。例えば、人造黒鉛、天然黒鉛が好ましい。特に、負極活物質粒子表面を不定形炭素等で修飾してあるグラファイトは、充電中のガス発生が少ないことから望ましい。

以下に、好適に用いることのできるグラファイトのエックス線回折等による分析結果を示す；

格子面間隔 ( $d_{002}$ ) 0.333~0.350 nm

a 軸方向の結晶子の大きさ  $L_a$  20 nm 以上

c 軸方向の結晶子の大きさ  $L_c$  20 nm 以上

真密度 2.00~2.25 g/cm<sup>3</sup>

また、グラファイトに、スズ酸化物、ケイ素酸化物等の金属酸化物、リン、ホウ素、アモルファスカーボン等を添加して改質を行うことも可能である。特に、グラファイトの表面を上記の方法によって改質することで、電解質の分解を抑制し電池特性を高めることが可能であり望ましい。さらに、グラファイトに対して、リチウム金属、リチウム-アルミニウム、リチウム-鉛、リチウム-スズ、リチウム-アルミニウム-スズ、リチウム-ガリウム、およびウッド合金等のリチウム金属含有合金等を併用することや、あらかじめ電気化学的に還元することによってリチウムが挿入されたグラファイト等も負極活物質として使用可能である。

正極活物質の粉体及び負極材料の粉体は、平均粒子サイズ100  $\mu$ m以下であることが望ましい。特に、正極活物質の粉体は、非水電解質電池の高出力特性を向上する目的で10  $\mu$ m以下であることが望ましい。粉体を所定の形状で得るためには粉碎機や分級機が用いられる。例えば、乳鉢、ボールミル、サンドミル、振動ボールミル、遊星ボールミル、ジェットミル、カウンタージェットミル、旋回気流型ジェットミルや篩等が用いられる。粉碎時には水、あるいはヘキサン等の有機溶剤を共存させた湿式粉碎を用いることもできる。分級方法としては、特に限定はなく、篩や風力分級機などが、乾式、湿式ともに必要に応じて用いられる。

以上、正極及び負極の主要構成成分である正極活物質および負極材料について詳述したが、前記正極及び負極には、前記主要構成成分の他に、導電剤、結着剤、増粘剤、フィラー等が、他の構成成分として含有されてもよい。

導電剤としては、電池性能に悪影響を及ぼさない電子伝導性材料であれば限定されないが、通常、天然黒鉛（鱗状黒鉛，鱗片状黒鉛，土状黒鉛等）、人造黒鉛、カーボンブラック、アセチレンブラック、ケッチェンブラック、カーボンウイスキー、炭素繊維、金属（銅，ニッケル，アルミニウム，銀，金等）粉、金属繊維、導電性セラミックス材料等の導電性材料を1種またはそれらの混合物として含ませることができる。

これらの中で、導電剤としては、電子伝導性及び塗工性の観点よりアセチレンブラックが望ましい。導電剤の添加量は、正極または負極の総重量に対して0.1重量%～50重量%が好ましく、特に0.5重量%～30重量%が好ましい。特にアセチレンブラックを0.1～0.5  $\mu\text{m}$ の超微粒子に粉碎して用いると必要炭素量を削減できるため望ましい。これらの混合方法は、物理的な混合であり、その理想とするところは均一混合である。そのため、V型混合機、S型混合機、掻き機、ボールミル、遊星ボールミルといったような粉体混合機を乾式、あるいは湿式で混合することが可能である。

前記結着剤としては、通常、ポリテトラフルオロエチレン（PTFE）、ポリフッ化ビニリデン（PVDF）、ポリエチレン、ポリプロピレン等の熱可塑性樹脂、エチレン-プロピレン-ジエンターポリマー（EPDM）、スルホン化EPDM、スチレンブタジエンゴム（SBR）、フッ素ゴム等のゴム弾性を有するポリマーを1種または2種以上の混合物として用いることができる。結着剤の添加量は、正極または負極の総重量に対して1～50重量%が好ましく、特に2～30重量%が好ましい。

前記増粘剤としては、通常、カルボキシメチルセルロース、メチルセルロース等の多糖類等を1種または2種以上の混合物として用いることができる。また、

多糖類の様にリチウムと反応する官能基を有する増粘剤は、例えばメチル化する等してその官能基を失活させておくことが望ましい。増粘剤の添加量は、正極または負極の総重量に対して0.5～10重量%が好ましく、特に1～2重量%が好ましい。

フィラーとしては、電池性能に悪影響を及ぼさない材料であれば何でも良い。通常、ポリプロピレン、ポリエチレン等のオレフィン系ポリマー、無定形シリカ、アルミナ、ゼオライト、ガラス、炭素等が用いられる。フィラーの添加量は、正極または負極の総重量に対して添加量は30重量%以下が好ましい。

正極および負極は、前記正極活物質あるいは負極材料に、必要に応じて導電剤や結着剤を加え、N-メチルピロリドン、トルエン等の有機溶媒に混合させた後、得られた混合液を下記に詳述する集電体の上に塗布し、乾燥することによって、好適に作製される。前記塗布方法については、例えば、アプリケーションロールなどのローラーコーティング、スクリーンコーティング、ドクターブレード方式、スピンコーティング、バーコート等の手段を用いて任意の厚さおよび任意の形状に塗布することが望ましいが、これらに限定されるものではない。

集電体としては、構成された電池において悪影響を及ぼさない電子伝導体であれば何でもよい。例えば、正極用集電体としては、アルミニウム、チタン、ステンレス鋼、ニッケル、焼成炭素、導電性高分子、導電性ガラス等の他に、接着性、導電性および耐酸化性向上の目的で、アルミニウムや銅等の表面をカーボン、ニッケル、チタンや銀等で処理した物を用いることができる。負極用集電体としては、銅、ニッケル、鉄、ステンレス鋼、チタン、アルミニウム、焼成炭素、導電性高分子、導電性ガラス、Al-Cd合金等の他に、接着性、導電性、耐還元性の目的で、銅等の表面をカーボン、ニッケル、チタンや銀等で処理した物を用いることができる。これらの材料については表面を酸化処理することも可能である。

集電体の形状については、フォイル状の他、フィルム状、シート状、ネット状、パンチ又はエキスパンドされた物、ラス体、多孔質体、発砲体、繊維群の形成

体等が用いられる。厚さの限定は特にはないが、 $1 \sim 500 \mu\text{m}$ のものが用いられる。これらの集電体の中で、正極用としては、耐酸化性に優れているアルミニウム箔が、負極用としては、耐還元性および電子伝導性に優れ、安価な銅箔、ニッケル箔、鉄箔、およびそれらの一部を含む合金箔を使用することが好ましい。さらに、粗面表面粗さが $0.2 \mu\text{m Ra}$ 以上の箔であることが好ましく、これにより正極活物質または負極活物質と集電体との密着性は優れたものとなる。よって、このような粗面を有することから、電解箔を使用するのが好ましい。特に、ハナ付き処理を施した電解箔は最も好ましい。さらに、これらの箔に両面塗工する場合、箔の表面粗さが同じ、またはほぼ等しいことが望まれる。

セパレータとしては、優れた高率放電特性を示す多孔膜や不織布等を、単独あるいは併用することが好ましい。セパレータを構成する材料としては、例えばポリエチレン、ポリプロピレン等に代表されるポリオレフィン系樹脂、ポリエチレンテレフタレート、ポリブチレンテレフタレート等に代表されるポリエステル系樹脂、ポリフッ化ビニリデン、フッ化ビニリデンーヘキサフルオロプロピレン共重合体、フッ化ビニリデンーパーフルオロビニルエーテル共重合体、フッ化ビニリデンーテトラフルオロエチレン共重合体、フッ化ビニリデンートリフルオロエチレン共重合体、フッ化ビニリデンーフルオロエチレン共重合体、フッ化ビニリデンーヘキサフルオロアセトン共重合体、フッ化ビニリデンーエチレン共重合体、フッ化ビニリデンープロピレン共重合体、フッ化ビニリデンートリフルオロプロピレン共重合体、フッ化ビニリデンーテトラフルオロエチレンーヘキサフルオロプロピレン共重合体、フッ化ビニリデンーエチレンーテトラフルオロエチレン共重合体等を挙げることができる。

セパレータの空孔率は強度の観点から98体積%以下が好ましい。また、充放電特性の観点から空孔率は20体積%以上が好ましい。

また、セパレータは、例えばアクリロニトリル、エチレンオキシド、プロピレンオキシド、メチルメタアクリレート、ビニルアセテート、ビニルピロリドン、ポリフッ化ビニリデン等のポリマーと電解質とで構成されるポリマーゲルを用いてもよい。

本発明の非水電解質を上記のようにゲル状態で用いると、漏液を防止する効果がある点で好ましい。

さらに、セバレータは、上述したような多孔膜や不織布等とポリマーゲルを併用して用いると、電解質の保液性が向上するため望ましい。即ち、ポリエチレン微孔膜の表面及び微孔壁面に厚さ数 $\mu\text{m}$ 以下の親溶媒性ポリマーを被覆したフィルムを形成し、前記フィルムの微孔内に電解質を保持させることで、前記親溶媒性ポリマーがゲル化する。

前記親溶媒性ポリマーとしては、ポリフッ化ビニリデンの他、エチレンオキシド基やエステル基等を有するアクリレートモノマー、エポキシモノマー、イソシアナート基を有するモノマー等が架橋したポリマー等が挙げられる。該モノマーは、ラジカル開始剤を併用して加熱や紫外線（UV）を用いたり、電子線（EB）等の活性光線等を用いて架橋反応を行わせることが可能である。

前記親溶媒性ポリマーには、強度や物性制御の目的で、架橋体の形成を妨害しない範囲の物性調整剤を配合して使用することができる。前記物性調整剤の例としては、無機フィラー類 {酸化ケイ素、酸化チタン、酸化アルミニウム、酸化マグネシウム、酸化ジルコニウム、酸化亜鉛、酸化鉄などの金属酸化物、炭酸カルシウム、炭酸マグネシウムなどの金属炭酸塩}、ポリマー類 {ポリフッ化ビニリデン、フッ化ビニリデン／ヘキサフルオロプロピレン共重合体、ポリアクリロニトリル、ポリメチルメタクリレート等} 等が挙げられる。前記物性調整剤の添加量は、架橋性モノマーに対して通常50重量%以下、好ましくは20重量%以下である。

前記アクリレートモノマーについて例示すると、二官能以上の不飽和モノマーが好適に挙げられ、より具体例には、2官能（メタ）アクリレート {エチレングリコールジ（メタ）アクリレート、プロピレングリコールジ（メタ）アクリレート、アジピン酸・ジネオペンチルグリコールエステルジ（メタ）アクリレート、重合度2以上のポリエチレングリコールジ（メタ）アクリレート、重合度2以上のポリプロピレングリコールジ（メタ）アクリレート、ポリオキシエチレン／ポリオキシプロピレン共重合体のジ（メタ）アクリレート、ブタンジオールジ（メタ）アクリレート、ヘキサメチレングリコールジ（メタ）アクリレート等}、3官



能(メタ)アクリレート {トリメチロールプロパントリ(メタ)アクリレート、グリセリントリ(メタ)アクリレート、グリセリンのエチレンオキシド付加物のトリ(メタ)アクリレート、グリセリンのプロピレンオキシド付加物のトリ(メタ)アクリレート、グリセリンのエチレンオキシド、プロピレンオキシド付加物のトリ(メタ)アクリレート等}、4官能以上の多官能(メタ)アクリレート {ペンタエリスリトールテトラ(メタ)アクリレート、ジグリセリンヘキサ(メタ)アクリレート等} が挙げられる。これらのモノマーを単独もしくは、併用して用いることができる。

前記アクリレートモノマーには、物性調整等の目的で1官能モノマーを添加することもできる。前記一官能モノマーの例としては、不飽和カルボン酸 {アクリル酸、メタクリル酸、クロトン酸、けい皮酸、ビニル安息香酸、マレイン酸、フマル酸、イタコン酸、シトラコン酸、メサコン酸、メチレンマロン酸、アコニット酸等}、不飽和スルホン酸 {スチレンスルホン酸、アクリルアミド-2-メチルプロパンスルホン酸等} またはそれらの塩 (Li塩、Na塩、K塩、アンモニウム塩、テトラアルキルアンモニウム塩等)、またこれらの不飽和カルボン酸をC1~C18の脂肪族または脂環式アルコール、アルキレン(C2~C4)グリコール、ポリアルキレン(C2~C4)グリコール等で部分的にエステル化したもの(メチルマレート、モノヒドロキシエチルマレート、など)、およびアンモニア、1級または2級アミンで部分的にアミド化したもの(マレイン酸モノアミド、N-メチルマレイン酸モノアミド、N,N-ジエチルマレイン酸モノアミドなど)、(メタ)アクリル酸エステル [C1~C18の脂肪族(メチル、エチル、プロピル、ブチル、2-エチルヘキシル、ステアリル等)アルコールと(メタ)アクリル酸とのエステル、またはアルキレン(C2~C4)グリコール(エチレングリコール、プロピレングリコール、1,4-ブタンジオール等)およびポリアルキレン(C2~C4)グリコール(ポリエチレングリコール、ポリプロピレングリコール)と(メタ)アクリル酸とのエステル]; (メタ)アクリルアミドまたはN-置換(メタ)アクリルアミド [(メタ)アクリルアミド、N-メチル(メタ)アクリルアミド、N-メチロール(メタ)アクリルアミド等]; ビニルエステルまたはアリルエステル [酢酸ビニル、酢酸アリル等]; ビニルエーテルまたはアリル

エーテル [ブチルビニルエーテル、ドデシルアリルエーテル等]; 不飽和ニトリル化合物 [(メタ) アクリロニトリル、クロトンニトリル等]; 不飽和アルコール [(メタ) アリルアルコール等]; 不飽和アミン [(メタ) アリルアミン、ジメチルアミノエチル(メタ)アクリレート、ジエチルアミノエチル(メタ)アクリレート等]; 複素環含有モノマー [N-ビニルピロリドン、ビニルピリジン等]; オレフィン系脂肪族炭化水素 [エチレン、プロピレン、ブチレン、イソブチレン、ペンテン、(C6~C50)  $\alpha$ -オレフィン等]; オレフィン系脂環式炭化水素 [シクロペンテン、シクロヘキセン、シクロヘプテン、ノルボルネン等]; オレフィン系芳香族炭化水素 [スチレン、 $\alpha$ -メチルスチレン、スチルベン等]; 不飽和イミド [マレイミド等]; ハロゲン含有モノマー [塩化ビニル、塩化ビニリデン、フッ化ビニリデン、ヘキサフルオロプロピレン等] 等が挙げられる。

前記エポキシモノマーについて例示すると、グリシジルエーテル類 {ビスフェノールAジグリシジルエーテル、ビスフェノールFジグリシジルエーテル、臭素化ビスフェノールAジグリシジルエーテル、フェノールノボラックグリシジルエーテル、クレゾールノボラックグリシジルエーテル等}、グリシジルエステル類 {ヘキサヒドロフタル酸グリシジルエステル、ダイマー酸グリシジルエステル等}、グリシジルアミン類 {トリグリシジルイソシアヌレート、テトラグリシジルジアミノフェニルメタン等}、線状脂肪族エポキシイド類 {エポキシ化ポリブタジエン、エポキシ化大豆油等}、脂環族エポキシイド類 {3, 4エポキシ-6メチルシクロヘキシルメチルカルボキシレート、3, 4エポキシシクロヘキシルメチルカルボキシレート等} 等が挙げられる。これらのエポキシ樹脂は、単独もしくは硬化剤を添加して硬化させて使用することができる。

前記硬化剤の例としては、脂肪族ポリアミン類 {ジエチレントリアミン、トリエチレンテトラミン、3, 9-(3-アミノプロピル)-2, 4, 8, 10-テトロオキサスピロ[5, 5]ウンデカン等}、芳香族ポリアミン類 {メタキシレンジアミン、ジアミノフェニルメタン等}、ポリアミド類 {ダイマー酸ポリアミド等}、酸無水物類 {無水フタル酸、テトラヒドロメチル無水フタル酸、ヘキサヒドロ無水フタル酸、無水トリメリット酸、無水メチルナジック酸}、フェノール類 {フェノールノボラック等}、ポリメルカプタン {ポリサルファイド等}、第三アミン

類 {トリス (ジメチルアミノメチル) フェノール、2-エチル-4-メチルイミダゾール等}、ルイス酸錯体 {三フッ化ホウ素・エチルアミン錯体等} 等が挙げられる。

前記イソシアナート基を有するモノマーについて例示すると、トルエンジイソシアナート、ジフェニルメタンジイソシアナート、1, 6-ヘキサメチレンジイソシアナート、2, 2, 4 (2, 2, 4) -トリメチル-ヘキサメチレンジイソシアナート、p-フェニレンジイソシアナート、4, 4'-ジシクロヘキシルメタンジイソシアナート、3, 3'-ジメチルジフェニル 4, 4'-ジイソシアナート、ジアニシジンジイソシアナート、m-キシレンジイソシアナート、トリメチルキシレンジイソシアナート、イソフォロンジイソシアナート、1, 5-ナフタレンジイソシアナート、trans-1, 4-シクロヘキシルジイソシアナート、リジンジイソシアナート等が挙げられる。

前記イソシアナート基を有するモノマーを架橋するにあたって、ポリオール類およびポリアミン類 [2 官能化合物 {水、エチレングリコール、プロピレングリコール、ジエチレングリコール、ジプロピレングリコール等}、3 官能化合物 {グリセリン、トリメチロールプロパン、1, 2, 6-ヘキサントリオール、トリエタノールアミン等}、4 官能化合物 {ペンタエリスリトール、エチレンジアミン、トリレンジアミン、ジフェニルメタンジアミン、テトラメチロールシクロヘキサン、メチルグルコシド等}、5 官能化合物 {2, 2, 6, 6-テトラキス (ヒドロキシメチル) シクロヘキサノール、ジエチレントリアミンなど}、6 官能化合物 {ソルビトール、マンニトール、ズルシトール等}、8 官能化合物 {スクロース等}]、およびポリエーテルポリオール類 {前記ポリオールまたはポリアミンのプロピレンオキサイドおよび/またはエチレンオキサイド付加物}、ポリエステルポリオール [前記ポリオールと多塩基酸 {アジピン酸、o, m, p-フタル酸、コハク酸、アゼライン酸、セバシン酸、リシノール酸} との縮合物、ポリカプロラクトンポリオール {ポリε-カプロラクトン等}、ヒドロキシカルボン酸の重縮合物等] 等、活性水素を有する化合物を併用することができる。

前記架橋反応にあたって、触媒を併用することができる。前記触媒について例示すると、有機スズ化合物類、トリアルキルホスフィン類、アミン類 [モノアミ

ン類 {N, N-ジメチルシクロヘキシルアミン、トリエチルアミン等}、環状モノアミン類 {ピリジン、N-メチルモルホリン等}、ジアミン類 {N, N, N', N'-テトラメチルエチレンジアミン、N, N, N', N'-テトラメチル1, 3-ブタンジアミン等}、トリアミン類 {N, N, N', N'-ペンタメチルジエレントリアミン等}、ヘキサミン類 {N, N, N', N'-テトラ(3-ジメチルアミノプロピル)-メタンジアミン等}、環状ポリアミン類 {ジアザビシクロオクタン(DABCO)、N, N'-ジメチルピペラジン、1, 2-ジメチルイミダゾール、1, 8-ジアザビシクロ(5, 4, 0)ウンデセン-7(DBU)等}等、およびそれらの塩類等が挙げられる。

本発明に係る非水電解質二次電池は、電解質を、例えば、セパレータと正極と負極とを積層する前または積層した後に注液し、最終的に、外装材で封止することによって好適に作製される。また、正極と負極とがセパレータを介して積層された発電要素を巻回してなる非水電解質電池においては、電解質は、前記巻回の前後に発電要素に注液されるのが好ましい。注液法としては、常圧で注液することも可能であるが、真空含浸方法や加圧含浸方法も使用可能である。

非水電解質二次電池の外装体の材料としては、ニッケルメッキした鉄やステンレススチール、アルミニウム、金属樹脂複合フィルム等が一例として挙げられる。例えば、金属箔を樹脂フィルムで挟み込んだ構成の金属樹脂複合フィルムが好ましい。前記金属箔の具体例としては、アルミニウム、鉄、ニッケル、銅、ステンレス鋼、チタン、金、銀等、ピンホールのない箔であれば限定されないが、好ましくは軽量且つ安価なアルミニウム箔が好ましい。また、電池外部側の樹脂フィルムとしては、ポリエチレンテレフタレートフィルム、ナイロンフィルム等の突き刺し強度に優れた樹脂フィルムを、電池内部側の樹脂フィルムとしては、ポリエチレンフィルム、ナイロンフィルム等の、熱融着可能であり、かつ耐溶剤性を有するフィルムが好ましい。

非水電解質二次電池の構成については特に限定されるものではなく、正極、負極および単層又は複層のセパレータを有するコイン電池やボタン電池、さらに、正極、負極およびロール状のセパレータを有する円筒型電池、角型電池、扁平型

電池等が一例として挙げられる。

### <実施例>

次に、前記した各実施形態における実施例および比較例を挙げて本発明を具体的に説明するが、本発明は、以下の実施例によって限定されるものではない。

#### [第一実施形態]

##### (実施例 1 - 1)

硝酸マンガン及び硝酸ニッケルを、Mn : Ni の原子比が 1 : 1 の割合で含む水溶液に水酸化ナトリウム水溶液を加えて共沈させ、150℃で加熱、乾燥し、マンガン-ニッケル共沈化合物を得た。水酸化リチウム水溶液に前記マンガン-ニッケル共沈化合物を添加し、攪拌後溶媒を蒸発させて乾燥した後、1000℃で12時間、酸素雰囲気下で焼成した後、粒子を分級して $D_{50} = 9 \mu\text{m}$ の粉末とした。BET法により測定した比表面積は $1.0 \text{ m}^2/\text{g}$ であった。

該粉末のCuK $\alpha$ 線によるエックス線回折測定の結果、 $2\theta = 18.58^\circ$ 、 $36.38^\circ$ 、 $37.68^\circ$ 、 $38.02^\circ$ 、 $44.10^\circ$ 、 $48.24^\circ$ 、 $58.22^\circ$ 、 $63.92^\circ$ 、 $64.10^\circ$ 、 $64.4^\circ$ 及び $67.68^\circ$ 付近にそれぞれ回折ピークが認められ、完全に一致しているわけではないが空間群R3/mに属する層状構造と思われる結晶性の高い単相が合成できていることがわかった。該粉末のエックス線回折図を図3に示す。元素分析の結果、該粉末の組成は $\text{LiMn}_{0.5}\text{Ni}_{0.5}\text{O}_2$ であることがわかった。該粉末を粉末Aとする。

該粉末Aを正極活物質として用い、次のようにして図2に示す容量約15Ahの角形非水電解質電池を作製した。

正極活物質である粉末A、導電剤であるアセチレンブラック及び結着剤であるポリフッ化ビニリデン(PVDF)を重量比85 : 10 : 5で混合し、溶剤としてN-メチルピロリドンを加え、混練分散し正極塗布液を調製した。なお、前記ポリフッ化ビニリデンは固形分が溶解分散された溶解液を用い、固形分として重量換算した。前記正極塗布液を厚さ $20 \mu\text{m}$ のアルミ箔集電体の両面に塗布し、全体の厚さを $230 \mu\text{m}$ に調整し、 $6.3 \text{ mAh}/\text{cm}^2$ の容量を持つ正極シー

トを作製した。前記正極シートを幅 61 mm、高さ 107 mm の形状に裁断して、シートの末端に厚さ 20  $\mu$ m、幅 10 mm のアルミニウムリード板を取り付け、正極板 7 とした。

人造黒鉛（粒径 6  $\mu$ m）を負極材料として用い、結着剤であるポリフッ化ビニリデン（PVDF）を前記負極材料に対して 10 重量% 加え、溶剤として N-メチルピロリドンを加え、混練分散し、負極塗布液を調製した。なお、前記ポリフッ化ビニリデンは固形分が溶解分散された溶解液を用い、固形分として重量換算した。前記負極塗布液を厚さ 10  $\mu$ m の銅箔集電体の両面に塗布し、全体の厚さを 180  $\mu$ m に調整し、7 mAh/cm<sup>2</sup> の容量を持つ負極シートを作製した。前記負極シートを幅 65 mm、高さ 111 mm の形状に裁断して、シートの末端に厚さ 10  $\mu$ m、幅 10 mm の銅リード板を取り付け、負極板 9 とした。

前記正極板 7 及び負極板 9 を 150 °C で 12 時間減圧乾燥した。次に、セパレータ 8 として、幅 65 mm、高さ 111 mm の袋形状に裁断したポリエチレン製微多孔膜の袋に前記正極板を挿入し、セパレータ 8 付き正極板 7、負極板 9 の順でこれらを交互に積層し、40 枚のセパレータ 8 付き正極板 7 及び 41 枚の負極板 9 からなる極群を得た。

前記極群をポリエチレン樹脂からなる絶縁フィルムに包み込み、アルミニウム製の角形電槽 10 に収納し、安全弁 1 を有するアルミニウム製の蓋 2 に取り付けられた正極端子 5 及び負極端子 4 に、正極板 7 及び負極板 9 のリード板をそれぞれボルトによって接続した。なお、端子 5、4 はポリプロピレン樹脂からなるガasket 6 を用いて前記蓋 2 との間を絶縁してある。

前記蓋 2 と電槽 10 とをレーザー溶接部 3 においてレーザー溶接し、前記電槽 10 の中に、エチレンカーボネートとジエチルカーボネートとの体積比 1 : 1 の混合溶剤に LiPF<sub>6</sub> を 1 mol/l 溶解した電解液を 65 g 注入し、封口した後、25 °C において、1.5 A、4.2 V、15 時間の定電流定電圧充電を行い、1.5 A、終止電圧 3 V の定電流放電を行った。このようにして、横 70 mm、高さ 130 mm（端子込み高さ 136 mm）、幅 22 mm の角形リチウム電池を得た。この電池を実施例 1-1 の電池とする。

## (実施例 1-2)

硝酸マンガン及び硝酸ニッケルを、Mn : Ni の原子比が 1 : 1 の割合で含む水溶液に水酸化ナトリウム水溶液を加えて共沈させ、150℃で加熱、乾燥し、マンガン-ニッケル共沈化合物を得た。水酸化リチウム水溶液に前記マンガン-ニッケル共沈化合物を添加し、攪拌後溶媒を蒸発させて乾燥した後、1000℃で12時間、酸素雰囲気下で焼成した後、粒子を分級して $D_{50} = 20 \mu\text{m}$ の粉末とした。BET法により測定した比表面積は $1.0 \text{ m}^2/\text{g}$ であった。

該粉末のCuK $\alpha$ 線によるエックス線回折測定の結果、粉末Aと同様な層状構造とみられる結晶性の高い単相が合成できていることがわかった。元素分析の結果、該粉末の組成は $\text{LiMn}_{0.5}\text{Ni}_{0.5}\text{O}_2$ であることがわかった。該粉末を正極活物質として用いたこと以外は（実施例1-1）と同様にして図2に示す容量約15Ahの角形リチウム電池を作製した。この電池を実施例1-2の電池とする。

## (実施例 1-3)

硝酸マンガン及び硝酸ニッケルを、Mn : Ni の原子比が 1 : 1 の割合で含む水溶液に水酸化ナトリウム水溶液を加えて共沈させ、150℃で加熱、乾燥し、マンガン-ニッケル共沈化合物を得た。水酸化リチウム水溶液に前記マンガン-ニッケル共沈化合物を添加し、攪拌後溶媒を蒸発させて乾燥した後、1030℃で12時間、酸素雰囲気下で焼成した後、粒子を分級して $D_{50} = 20 \mu\text{m}$ の粉末とした。BET法により測定した比表面積は $0.9 \text{ m}^2/\text{g}$ であった。

該粉末のCuK $\alpha$ 線によるエックス線回折測定の結果、粉末Aと同様な層状構造とみられる結晶性の高い単相が合成できていることがわかった。元素分析の結果、該粉末の組成は $\text{LiMn}_{0.5}\text{Ni}_{0.5}\text{O}_2$ であることがわかった。該粉末を正極活物質として用いたこと以外は（実施例1-1）と同様にして図2に示す容量約15Ahの角形リチウム電池を作製した。この電池を実施例1-3の電池とする。

## (実施例 1-4)

硝酸マンガン及び硝酸ニッケルを、Mn : Ni の原子比が 1 : 1 の割合で含む水溶液に水酸化ナトリウム水溶液を加えて共沈させ、150℃で加熱、乾燥し、

マンガン–ニッケル共沈化合物を得た。水酸化リチウム水溶液に前記マンガン–ニッケル共沈化合物を添加し、攪拌後溶媒を蒸発させて乾燥した後、 $1060^{\circ}\text{C}$ で12時間、酸素雰囲気下で焼成した後、粒子を分級して $D_{50}=20\mu\text{m}$ の粉末とした。BET法により測定した比表面積は $0.9\text{m}^2/\text{g}$ であった。

該粉末のCuK $\alpha$ 線によるエックス線回折測定の結果、粉末Aと同様な層状構造とみられる結晶性の高い単相が合成できていることがわかった。元素分析の結果、該粉末の組成は $\text{LiMn}_{0.5}\text{Ni}_{0.5}\text{O}_2$ であることがわかった。該粉末を正極活物質として用いたこと以外は（実施例1–1）と同様にして図2に示す容量約15Ahの角形リチウム電池を作製した。この電池を実施例1–4の電池とする。

#### （実施例1–5）

硝酸マンガン及び硝酸ニッケルを、Mn：Niの原子比が1：1の割合で含む水溶液に水酸化ナトリウム水溶液を加えて共沈させ、 $150^{\circ}\text{C}$ で加熱、乾燥し、マンガン–ニッケル共沈化合物を得た。水酸化リチウム水溶液に前記マンガン–ニッケル共沈化合物を添加し、攪拌後溶媒を蒸発させて乾燥した後、 $1000^{\circ}\text{C}$ で12時間、酸素雰囲気下で焼成した後、粒子を分級して $D_{50}=20\mu\text{m}$ の粉末とした。BET法により測定した比表面積は $0.9\text{m}^2/\text{g}$ であった。

該粉末のCuK $\alpha$ 線によるエックス線回折測定の結果、粉末Aと同様な層状構造とみられる結晶性の高い単相が合成できていることがわかった。元素分析の結果、該粉末の組成は $\text{LiMn}_{0.5}\text{Ni}_{0.5}\text{O}_2$ であることがわかった。該粉末を正極活物質として用いたこと以外は（実施例1–1）と同様にして図2に示す容量約15Ahの角形リチウム電池を作製した。この電池を実施例1–5の電池とする。

#### （実施例1–6）

硝酸マンガン及び硝酸ニッケルを、Mn：Niの原子比が1：1の割合で含む水溶液に水酸化ナトリウム水溶液を加えて共沈させ、 $150^{\circ}\text{C}$ で加熱、乾燥し、マンガン–ニッケル共沈化合物を得た。水酸化リチウム水溶液に前記マンガン–ニッケル共沈化合物を添加し、攪拌後溶媒を蒸発させて乾燥した後、 $950^{\circ}\text{C}$ で12時間、酸素雰囲気下で焼成した後、粒子を分級して $D_{50}=20\mu\text{m}$ の粉末と



した。BET法により測定した比表面積は $0.9 \text{ m}^2/\text{g}$ であった。

該粉末のCuK $\alpha$ 線によるエックス線回折測定の結果、粉末Aと同様な層状構造とみられる結晶性の高い単相が合成できていることがわかった。元素分析の結果、該粉末の組成は $\text{LiMn}_{0.5}\text{Ni}_{0.5}\text{O}_2$ であることがわかった。該粉末を正極活物質として用いたこと以外は（実施例1-1）と同様にして図2に示す容量約15Ahの角形リチウム電池を作製した。この電池を実施例1-6の電池とする。

#### （実施例1-7）

硝酸マンガン及び硝酸ニッケルを、Mn：Niの原子比が1：1の割合で含む水溶液に水酸化ナトリウム水溶液を加えて共沈させ、 $150^\circ\text{C}$ で加熱、乾燥し、マンガン-ニッケル共沈化合物を得た。水酸化リチウム水溶液に前記マンガン-ニッケル共沈化合物を添加し、攪拌後溶媒を蒸発させて乾燥した後、 $960^\circ\text{C}$ で12時間、酸素雰囲気下で焼成した後、粒子を分級して $D_{50}=20 \mu\text{m}$ の粉末とした。BET法により測定した比表面積は $0.9 \text{ m}^2/\text{g}$ であった。

該粉末のCuK $\alpha$ 線によるエックス線回折測定の結果、粉末Aと同様な層状構造とみられる結晶性の高い単相が合成できていることがわかった。元素分析の結果、該粉末の組成は $\text{LiMn}_{0.5}\text{Ni}_{0.5}\text{O}_2$ であることがわかった。該粉末を正極活物質として用いたこと以外は（実施例1-1）と同様にして図2に示す容量約15Ahの角形リチウム電池を作製した。この電池を実施例1-7の電池とする。

#### （実施例1-8）

硝酸マンガン及び硝酸ニッケルを、Mn：Niの原子比が1：1の割合で含む水溶液に水酸化ナトリウム水溶液を加えて共沈させ、 $150^\circ\text{C}$ で加熱、乾燥し、マンガン-ニッケル共沈化合物を得た。水酸化リチウム水溶液に前記マンガン-ニッケル共沈化合物を添加し、攪拌後溶媒を蒸発させて乾燥した後、 $980^\circ\text{C}$ で12時間、酸素雰囲気下で焼成した後、粒子を分級して $D_{50}=20 \mu\text{m}$ の粉末とした。BET法により測定した比表面積は $0.9 \text{ m}^2/\text{g}$ であった。

該粉末のCuK $\alpha$ 線によるエックス線回折測定の結果、粉末Aと同様な層状構造とみられる結晶性の高い単相が合成できていることがわかった。元素分析の結

果、該粉末の組成は  $\text{LiMn}_{0.5}\text{Ni}_{0.5}\text{O}_2$  であることがわかった。該粉末を正極活物質として用いたこと以外は実施例（1－1）と同様にして図2に示す容量約15Ahの角形リチウム電池を作製した。この電池を実施例1－8の電池とする。

（実施例1－9）

硝酸マンガン及び硝酸ニッケルを、Mn：Niの原子比が1：1の割合で含む水溶液に水酸化ナトリウム水溶液を加えて共沈させ、150℃で加熱、乾燥して、マンガン－ニッケル共沈化合物を得た。水酸化リチウム水溶液に前記マンガン－ニッケル共沈化合物を添加し、攪拌後溶媒を蒸発させて乾燥した後、1000℃で5時間、酸素雰囲気下で焼成した後、粒子を分級して  $D_{50}=20\mu\text{m}$  の粉末とした。BET法により測定した比表面積は  $0.3\text{m}^2/\text{g}$  であった。

該粉末のCuK $\alpha$ 線によるエックス線回折測定の結果、粉末Aと同様な層状構造とみられる結晶性の高い単相が合成できていることがわかった。元素分析の結果、該粉末の組成は  $\text{LiMn}_{0.5}\text{Ni}_{0.5}\text{O}_2$  であることがわかった。

該粉末を正極活物質として用いたこと以外は（実施例1－1）と同様にして図2に示す容量約15Ahの角形リチウム電池を作製した。この電池を実施例1－9の電池とする。

（実施例1－10）

硝酸マンガン及び硝酸ニッケルを、Mn：Niの原子比が1：1の割合で含む水溶液に水酸化ナトリウム水溶液を加えて共沈させ、150℃で加熱、乾燥して、マンガン－ニッケル共沈化合物を得た。水酸化リチウム水溶液に前記マンガン－ニッケル共沈化合物を添加し、攪拌後溶媒を蒸発させて乾燥した後、1000℃で5時間、酸素雰囲気下で焼成した後、粒子を分級して  $D_{50}=9\mu\text{m}$  の粉末とした。BET法により測定した比表面積は  $0.3\text{m}^2/\text{g}$  であった。

該粉末のCuK $\alpha$ 線によるエックス線回折測定の結果、粉末Aと同様な層状構造とみられる結晶性の高い単相が合成できていることがわかった。該粉末のエックス線回折図を図4に示す。元素分析の結果、該粉末の組成は  $\text{LiMn}_{0.5}\text{Ni}_{0.5}\text{O}_2$  であることがわかった。該粉末を正極活物質として用いたこと以外は（実施例

1-1)と同様にして図2に示す容量約15Ahの角形リチウム電池を作製した。この電池を実施例1-10の電池とする。

(実施例1-11)

硝酸マンガン及び硝酸ニッケルを、Mn:Niの原子比が1:1の割合で含む水溶液に水酸化ナトリウム水溶液を加えて共沈させ、150℃で加熱、乾燥して、マンガン-ニッケル共沈化合物を得た。水酸化リチウム水溶液に前記マンガン-ニッケル共沈化合物を添加し、攪拌後溶媒を蒸発させて乾燥した後、1000℃で20時間、酸素雰囲気下で焼成した後、粒子を分級して $D_{50}=5\mu\text{m}$ の粉末とした。BET法により測定した比表面積は $1.5\text{m}^2/\text{g}$ であった。該粉末のCuK $\alpha$ 線によるエックス線回折測定の結果、粉末Aと同様な層状構造とみられる結晶性の高い単相が合成できていることがわかった。元素分析の結果、該粉末の組成は $\text{LiMn}_{0.5}\text{Ni}_{0.5}\text{O}_2$ であることがわかった。該粉末を正極活物質として用いたこと以外は実施例(1-1)と同様にして図2に示す容量約15Ahの角形リチウム電池を作製した。この電池を実施例1-11の電池とする。

(比較例1-1)

硝酸マンガン及び硝酸ニッケルを、Mn:Niの原子比が1.9:0.1の割合で含む水溶液に水酸化ナトリウム水溶液を加えて共沈させ、150℃で加熱、乾燥して、マンガン-ニッケル共沈化合物を得た。水酸化リチウム水溶液に前記マンガン-ニッケル共沈化合物を添加し、攪拌後溶媒を蒸発させて乾燥した後、950℃で3時間、酸素雰囲気下で本焼成した後、粒子を分級して $D_{50}=20\mu\text{m}$ の粉末とした。BET法により測定した比表面積は $0.6\text{m}^2/\text{g}$ であった。

該粉末のCuK $\alpha$ 線によるエックス線回折測定の結果、 $2\theta=18$ 度、37度、39度、45度、61度、65度、67度に回折ピークが認められ、空間群C2/mに属する層状岩塩型の結晶が合成できていることがわかった。元素分析の結果、該粉末の組成は $\text{LiMn}_{0.95}\text{Ni}_{0.05}\text{O}_2$ であることがわかった。該粉末を正極活物質として用いたこと以外は実施例(1-1)と同様にして図2に示す容量約15Ahの角形リチウム電池を作製した。この電池を比較例1-1の電池とす

る。

(比較例 1-2)

硝酸マンガンを含む水溶液に水酸化ナトリウム水溶液を加えて沈殿させ、150℃で加熱、乾燥して、マンガン化合物を得た。水酸化リチウム水溶液に前記マンガン化合物を添加し、攪拌後溶媒を蒸発させて乾燥した後、850℃で3時間、酸素雰囲気下で本焼成した後、粒子を分級して $D_{50}=10\mu\text{m}$ の粉末とした。BET法により測定した比表面積は $0.4\text{ m}^2/\text{g}$ であった。前記粉末のCuK $\alpha$ 線によるエックス線回折測定の結果、スピネル構造を有する結晶が合成できていることがわかった。元素分析の結果、該粉末の組成は $\text{Li}_{1.05}\text{Mn}_{1.95}\text{O}_4$ であることがわかった。該粉末を正極活物質として用いたこと以外は(実施例1-1)と同様にして図2に示す容量約15Ahの角形リチウム電池を作製した。この電池を比較例1-2の電池とする。

(比較例 1-3)

硝酸マンガン及び硝酸ニッケルを、Mn:Niの原子比が1:1の割合で含む水溶液に水酸化ナトリウム水溶液を加えて共沈させ、150℃で加熱、乾燥して、マンガン-ニッケル共沈化合物を得た。水酸化リチウム水溶液に前記マンガン-ニッケル共沈化合物を添加し、攪拌後溶媒を蒸発させて乾燥した後、1000℃で3時間、酸素雰囲気下で焼成した後、粒子を分級して $D_{50}=3\mu\text{m}$ の粉末とした。BET法により測定した比表面積は $2.0\text{ m}^2/\text{g}$ であった。

該粉末のCuK $\alpha$ 線によるエックス線回折測定の結果、粉末Aと同様な層状構造とみられる結晶性の高い単相が合成できていることがわかった。元素分析の結果、該粉末の組成は $\text{LiMn}_{0.5}\text{Ni}_{0.5}\text{O}_2$ であることがわかった。該粉末を正極活物質として用いたこと以外は(実施例1-1)と同様にして図2に示す容量約15Ahの角形リチウム電池を作製した。この電池を比較例1-3の電池とする。

(比較例 1-4)

硝酸マンガン及び硝酸ニッケルを、Mn:Niの原子比が1:1の割合で含む

水溶液に水酸化ナトリウム水溶液を加えて共沈させ、 $150^{\circ}\text{C}$ で加熱、乾燥して、マンガン-ニッケル共沈化合物を得た。水酸化リチウム水溶液に前記マンガン-ニッケル共沈化合物を添加し、攪拌後溶媒を蒸発させて乾燥した後、 $800^{\circ}\text{C}$ で15時間、酸素雰囲気下で焼成した後、粒子を分級して $D_{50}=5\mu\text{m}$ の粉末とした。BET法により測定した比表面積は $2.0\text{m}^2/\text{g}$ であった。該粉末のCu K $\alpha$ 線によるエックス線回折測定の結果、粉末Aと同様な層状構造とみられる結晶性の高い単相が合成できていることがわかった。元素分析の結果、該粉末の組成は $\text{LiMn}_{0.5}\text{Ni}_{0.5}\text{O}_2$ であることがわかった。該粉末を正極活物質として用いたこと以外は（実施例1-1）と同様にして図2に示す容量約15Ahの角形リチウム電池を作製した。この電池を比較例1-4の電池とする。

（比較例1-5）

硝酸マンガン及び硝酸ニッケルを、Mn：Niの原子比が1：1の割合で含む水溶液に水酸化ナトリウム水溶液を加えて共沈させ、 $150^{\circ}\text{C}$ で加熱、乾燥して、マンガン-ニッケル共沈化合物を得た。水酸化リチウム水溶液に前記マンガン-ニッケル共沈化合物を添加し、攪拌後溶媒を蒸発させて乾燥した後、 $1000^{\circ}\text{C}$ で24時間、酸素雰囲気下で焼成した後、粒子を分級して $D_{50}=5\mu\text{m}$ の粉末とした。BET法により測定した比表面積は $0.2\text{m}^2/\text{g}$ であった。該粉末のCu K $\alpha$ 線によるエックス線回折測定の結果、粉末Aと同様な層状構造とみられる結晶性の高い単相が合成できていることがわかった。元素分析の結果、該粉末の組成は $\text{LiMn}_{0.5}\text{Ni}_{0.5}\text{O}_2$ であることがわかった。

該粉末を正極活物質として用いたこと以外は（実施例1-1）と同様にして図2に示す設計容量15Ahの角形リチウム電池を作製した。この電池を比較例1-5の電池とする。

（比較例1-6）

硝酸マンガン及び硝酸ニッケルを、Mn：Niの原子比が1：1の割合で含む水溶液に水酸化ナトリウム水溶液を加えて共沈させ、 $150^{\circ}\text{C}$ で加熱、乾燥して、マンガン-ニッケル共沈化合物を得た。水酸化リチウム水溶液に前記マンガン

ーニッケル共沈化合物を添加し、攪拌後溶媒を蒸発させて乾燥した後、 $1100^{\circ}\text{C}$ で24時間、酸素雰囲気下で焼成した後、粒子を分級して $D_{50}=30\mu\text{m}$ の粉末とした。BET法により測定した比表面積は $0.2\text{m}^2/\text{g}$ であった。該粉末のCuK $\alpha$ 線によるエックス線回折測定の結果、粉末Aと同様な層状構造とみられる結晶性の高い単相が合成できていることがわかった。元素分析の結果、該粉末の組成は $\text{LiMn}_{0.5}\text{Ni}_{0.5}\text{O}_2$ であることがわかった。該粉末を正極活物質として用いたこと以外は（実施例1-1）と同様にして図2に示す容量約15Ahの角形リチウム電池を作製した。この電池を比較例1-6の電池とする。

### [第二実施形態]

#### （実施例2-1）

硝酸マンガン、硝酸ニッケルを、Mn：Niの原子比が0.95：0.95の割合で含む水溶液に水酸化ナトリウム水溶液を加えて共沈させ、 $150^{\circ}\text{C}$ で加熱、乾燥して、マンガンーニッケル共沈化合物を得た。水酸化リチウムに前記マンガンーニッケル共沈化合物とホウ酸を、元素比Li：Mn：Ni：Bが2：0.95：0.95：0.10となるように添加し、 $1000^{\circ}\text{C}$ で12時間、酸素雰囲気下で焼成した後、粒子を分級して $D_{50}=9\mu\text{m}$ の粉末とした。BET法により測定した比表面積は $0.9\text{m}^2/\text{g}$ であった。該粉末のCuK $\alpha$ 線によるエックス線回折測定の結果、粉末Aと同様な層状構造とみられる結晶性の高い単相が合成できていることがわかった。元素分析の結果、該粉末の組成は $\text{LiMn}_{0.475}\text{Ni}_{0.475}\text{B}_{0.05}\text{O}_2$ であることがわかった。該粉末を正極活物質として用いたこと以外は（実施例1-1）と同様にして図2に示す容量約15Ahの角形リチウム電池を作製した。この電池を実施例2-1の電池とする。

#### （実施例2-2）

硝酸マンガン、硝酸ニッケル及び酸化バナジウムを、Mn：Ni：Vの原子比が0.95：0.95：0.1の割合で含む水溶液に水酸化ナトリウム水溶液を加えて共沈させ、 $150^{\circ}\text{C}$ で加熱、乾燥して、マンガンーニッケルーバナジウム共沈化合物を得た。水酸化リチウム水溶液に前記マンガンーニッケルーバナジウ

ム共沈化合物を添加し、攪拌後溶媒を蒸発させて乾燥した後、 $1000^{\circ}\text{C}$ で12時間、酸素雰囲気下で本焼成した後、粒子を分級して $D_{50}=9\mu\text{m}$ の粉末とした。BET法により測定した比表面積は $0.9\text{m}^2/\text{g}$ であった。該粉末のCuK $\alpha$ 線によるエックス線回折測定の結果、粉末Aと同様な層状構造とみられる結晶性の高い単相が合成できていることがわかった。元素分析の結果、該粉末の組成は $\text{LiMn}_{0.475}\text{Ni}_{0.475}\text{V}_{0.05}\text{O}_2$ であることがわかった。該粉末を正極活物質として用いたこと以外は（実施例1-1）と同様にして図2に示す容量約15Ahの角形リチウム電池を作製した。この電池を実施例2-2の電池とする。

#### （実施例2-3）

硝酸マンガン、硝酸ニッケル及び硝酸アルミニウムを、Mn : Ni : Alの原子比が0.95 : 0.95 : 0.1の割合で含む水溶液に水酸化ナトリウム水溶液を加えて共沈させ、 $150^{\circ}\text{C}$ で加熱、乾燥して、マンガン-ニッケル-アルミニウム共沈化合物を得た。水酸化リチウム水溶液に前記マンガン-ニッケル-アルミニウム共沈化合物を添加し、攪拌後溶媒を蒸発させて乾燥した後、 $1000^{\circ}\text{C}$ で12時間、酸素雰囲気下で本焼成した後、粒子を分級して $D_{50}=9\mu\text{m}$ の粉末とした。BET法により測定した比表面積は $0.9\text{m}^2/\text{g}$ であった。該粉末のCuK $\alpha$ 線によるエックス線回折測定の結果、粉末Aと同様な層状構造とみられる結晶性の高い単相が合成できていることがわかった。元素分析の結果、該粉末の組成は $\text{LiMn}_{0.475}\text{Ni}_{0.475}\text{Al}_{0.05}\text{O}_2$ であることがわかった。該粉末を正極活物質として用いたこと以外は（実施例1-1）と同様にして図2に示す容量約15Ahの角形リチウム電池を作製した。この電池を実施例2-3の電池とする。

#### （実施例2-4）

硝酸マンガン、硝酸ニッケル及び硝酸マグネシウムを、Mn : Ni : Mgの原子比が0.95 : 0.95 : 0.1の割合で含む水溶液に水酸化ナトリウム水溶液を加えて共沈させ、 $150^{\circ}\text{C}$ で加熱、乾燥して、マンガン-ニッケル-マグネシウム共沈化合物を得た。水酸化リチウム水溶液に前記マンガン-ニッケル-マグネシウム共沈化合物を添加し、攪拌後溶媒を蒸発させて乾燥した後、 $1000$

℃で12時間、酸素雰囲気下で本焼成した後、粒子を分級して $D_{50}=9\mu\text{m}$ の粉末とした。BET法により測定した比表面積は $0.9\text{m}^2/\text{g}$ であった。該粉末のCuK $\alpha$ 線によるエックス線回折測定の結果、粉末Aと同様な層状構造とみられる結晶性の高い単相が合成できていることがわかった。元素分析の結果、該粉末の組成は $\text{LiMn}_{0.475}\text{Ni}_{0.475}\text{Mg}_{0.05}\text{O}_2$ であることがわかった。該粉末を正極活物質として用いたこと以外は（実施例1-1）と同様にして図2に示す容量約15Ahの角形リチウム電池を作製した。この電池を実施例2-4の電池とする。

（実施例2-5）

硝酸マンガン、硝酸ニッケル及び硝酸コバルトを、Mn：Ni：Coの原子比が0.95：0.95：0.1の割合で含む水溶液に水酸化ナトリウム水溶液を加えて共沈させ、150℃で加熱、乾燥して、マンガン-ニッケル-コバルト共沈化合物を得た。水酸化リチウム水溶液に前記マンガン-ニッケル-コバルト共沈化合物を添加し、攪拌後溶媒を蒸発させて乾燥した後、1000℃で12時間、酸素雰囲気下で本焼成した後、粒子を分級して $D_{50}=9\mu\text{m}$ の粉末とした。BET法により測定した比表面積は $0.9\text{m}^2/\text{g}$ であった。該粉末のCuK $\alpha$ 線によるエックス線回折測定の結果、粉末Aと同様な層状構造とみられる結晶性の高い単相が合成できていることがわかった。元素分析の結果、該粉末の組成は $\text{LiMn}_{0.475}\text{Ni}_{0.475}\text{Co}_{0.05}\text{O}_2$ であることがわかった。この粉末を粉末を正極活物質として用いたこと以外は（実施例1-1）と同様にして図2に示す容量約15Ahの角形リチウム電池を作製した。この電池を実施例2-5の電池とする。

（実施例2-6）

硝酸マンガン、硝酸ニッケル及び硝酸クロムを、Mn：Ni：Crの原子比が0.95：0.95：0.1の割合で含む水溶液に水酸化ナトリウム水溶液を加えて共沈させ、150℃で加熱、乾燥して、マンガン-ニッケル-クロム共沈化合物を得た。水酸化リチウム水溶液に前記マンガン-ニッケル-マグネシウム共沈化合物を添加し、攪拌後溶媒を蒸発させて乾燥した後、1000℃で12時間、酸素雰囲気下で本焼成した後、粒子を分級して $D_{50}=9\mu\text{m}$ の粉末とした。B



E T法により測定した比表面積は  $0.9 \text{ m}^2/\text{g}$  であった。該粉末の  $\text{Cu K } \alpha$  線によるエックス線回折測定の結果、粉末Aと同様な層状構造とみられる結晶性の高い単相が合成できていることがわかった。元素分析の結果、該粉末の組成は  $\text{Li Mn}_{0.475} \text{Ni}_{0.475} \text{Cr}_{0.05} \text{O}_2$  であることがわかった。この粉末を粉末を正極活物質として用いたこと以外は（実施例1-1）と同様にして図2に示す容量約15 Ahの角形リチウム電池を作製した。この電池を実施例2-6の電池とする。

（実施例2-7）

硝酸マンガン、硝酸ニッケル及び酸化チタンを、 $\text{Mn} : \text{Ni} : \text{Ti}$ の原子比が  $0.95 : 0.95 : 0.1$ の割合で含む水溶液に水酸化ナトリウム水溶液を加えて共沈させ、 $150^\circ\text{C}$ で加熱、乾燥して、マンガン-ニッケル-チタン共沈化合物を得た。水酸化リチウム水溶液に前記マンガン-ニッケル-チタン共沈化合物を添加し、攪拌後溶媒を蒸発させて乾燥した後、 $1000^\circ\text{C}$ で12時間、酸素雰囲気下で本焼成した後、粒子を分級して  $D_{50} = 9 \mu\text{m}$ の粉末とした。BET法により測定した比表面積は  $0.9 \text{ m}^2/\text{g}$  であった。該粉末の  $\text{Cu K } \alpha$  線によるエックス線回折測定の結果、粉末Aと同様な層状構造とみられる結晶性の高い単相が合成できていることがわかった。元素分析の結果、該粉末の組成は  $\text{Li Mn}_{0.475} \text{Ni}_{0.475} \text{Ti}_{0.05} \text{O}_2$  であることがわかった。この粉末を粉末を正極活物質として用いたこと以外は（実施例1-1）と同様にして図2に示す容量約15 Ahの角形リチウム電池を作製した。この電池を実施例2-7の電池とする。

（実施例2-8）

硝酸マンガン、硝酸ニッケル及び硫酸鉄を、 $\text{Mn} : \text{Ni} : \text{Fe}$ の原子比が  $0.95 : 0.95 : 0.1$ の割合で含む水溶液に水酸化ナトリウム水溶液を加えて共沈させ、 $150^\circ\text{C}$ で加熱、乾燥して、マンガン-ニッケル-鉄共沈化合物を得た。水酸化リチウム水溶液に前記マンガン-ニッケル-鉄共沈化合物を添加し、攪拌後溶媒を蒸発させて乾燥した後、 $1000^\circ\text{C}$ で12時間、酸素雰囲気下で本焼成した後、粒子を分級して  $D_{50} = 9 \mu\text{m}$ の粉末とした。BET法により測定した比表面積は  $0.9 \text{ m}^2/\text{g}$  であった。該粉末の  $\text{Cu K } \alpha$  線によるエックス線回折

測定の結果、粉末Aと同様な層状構造とみられる結晶性の高い単相が合成できていることがわかった。元素分析の結果、該粉末の組成は $\text{LiMn}_{0.475}\text{Ni}_{0.475}\text{Fe}_{0.05}\text{O}_2$ であることがわかった。この粉末を粉末を正極活物質として用いたこと以外は（実施例1-1）と同様にして図2に示す容量約15Ahの角形リチウム電池を作製した。この電池を実施例2-8の電池とする。

（実施例2-9）

硝酸マンガン、硝酸ニッケル及び硫酸銅を、 $\text{Mn}:\text{Ni}:\text{Cu}$ の原子比が0.95:0.95:0.1の割合で含む水溶液に水酸化ナトリウム水溶液を加えて共沈させ、150℃で加熱、乾燥して、マンガン-ニッケル-銅共沈化合物を得た。水酸化リチウム水溶液に前記マンガン-ニッケル-銅共沈化合物を添加し、攪拌後溶媒を蒸発させて乾燥した後、1000℃で12時間、酸素雰囲気下で本焼成した後、粒子を分級して $D_{50}=9\mu\text{m}$ の粉末とした。BET法により測定した比表面積は $0.9\text{m}^2/\text{g}$ であった。該粉末の $\text{CuK}\alpha$ 線によるエックス線回折測定の結果、粉末Aと同様な層状構造とみられる結晶性の高い単相が合成できていることがわかった。元素分析の結果、該粉末の組成は $\text{LiMn}_{0.475}\text{Ni}_{0.475}\text{Cu}_{0.05}\text{O}_2$ であることがわかった。この粉末を粉末を正極活物質として用いたこと以外は（実施例1-1）と同様にして図2に示す容量約15Ahの角形リチウム電池を作製した。この電池を実施例2-9の電池とする。

（実施例2-10）

硝酸マンガン、硝酸ニッケル及び硫酸亜鉛を、 $\text{Mn}:\text{Ni}:\text{Zn}$ の原子比が0.95:0.95:0.1の割合で含む水溶液に水酸化ナトリウム水溶液を加えて共沈させ、150℃で加熱、乾燥して、マンガン-ニッケル-亜鉛共沈化合物を得た。水酸化リチウム水溶液に前記マンガン-ニッケル-亜鉛共沈化合物を添加し、攪拌後溶媒を蒸発させて乾燥した後、1000℃で12時間、酸素雰囲気下で本焼成した後、粒子を分級して $D_{50}=9\mu\text{m}$ の粉末とした。BET法により測定した比表面積は $0.9\text{m}^2/\text{g}$ であった。該粉末の $\text{CuK}\alpha$ 線によるエックス線回折測定の結果、粉末Aと同様な層状構造とみられる結晶性の高い単相が合成

できていることがわかった。元素分析の結果、該粉末の組成は  $\text{LiMn}_{0.475}\text{Ni}_{0.475}\text{Zn}_{0.05}\text{O}_2$  であることがわかった。この粉末を粉末を正極活物質として用いたこと以外は（実施例 1-1）と同様にして図 2 に示す容量約 15 Ah の角形リチウム電池を作製した。この電池を実施例 2-10 の電池とする。

（比較例 2-1）

硝酸マンガン、硝酸ニッケル及び硝酸マグネシウムを、 $\text{Mn}:\text{Ni}:\text{Mg}$  の原子比が 0.95 : 0.95 : 0.1 の割合で含む水溶液に水酸化ナトリウム水溶液を加えて共沈させ、150℃で加熱、乾燥して、マンガン-ニッケル-マグネシウム共沈化合物を得た。水酸化リチウム水溶液に前記マンガン-ニッケル-マグネシウム共沈化合物を添加し、攪拌後溶媒を蒸発させて乾燥した後、1000℃で12時間、酸素雰囲気下で本焼成した後、粒子を分級して  $D_{50}=15\mu\text{m}$  の粉末とした。BET法により測定した比表面積は  $0.2\text{m}^2/\text{g}$  であった。該粉末の  $\text{CuK}\alpha$  線によるエックス線回折測定の結果、粉末 A と同様な層状構造とみられる結晶性の高い単相が合成できていることがわかった。元素分析の結果、該粉末の組成は  $\text{LiMn}_{0.475}\text{Ni}_{0.475}\text{Mg}_{0.05}\text{O}_2$  であることがわかった。該粉末を正極活物質として用いたこと以外は（実施例 1-1）と同様にして図 2 に示す容量約 15 Ah の角形リチウム電池を作製した。この電池を比較例 2-1 の電池とする。

（比較例 2-2）

硝酸マンガン、硝酸ニッケル及び硝酸マグネシウムを、 $\text{Mn}:\text{Ni}:\text{Mg}$  の原子比が 0.95 : 0.95 : 0.1 の割合で含む水溶液に水酸化ナトリウム水溶液を加えて共沈させ、150℃で加熱、乾燥して、マンガン-ニッケル-マグネシウム共沈化合物を得た。水酸化リチウム水溶液に前記マンガン-ニッケル-マグネシウム共沈化合物を添加し、攪拌後溶媒を蒸発させて乾燥した後、1000℃で12時間、酸素雰囲気下で本焼成した後、粒子を分級して  $D_{50}=6\mu\text{m}$  の粉末とした。BET法により測定した比表面積は  $1.9\text{m}^2/\text{g}$  であった。該粉末の  $\text{CuK}\alpha$  線によるエックス線回折測定の結果、粉末 A と同様な層状構造とみられ

る結晶性の高い単相が合成できていることがわかった。元素分析の結果、該粉末の組成は $\text{LiMn}_{0.475}\text{Ni}_{0.475}\text{Mg}_{0.05}\text{O}_2$ であることがわかった。該粉末を正極活物質として用いたこと以外は（実施例 1-1）と同様にして図 2 に示す容量約 15 Ah の角形リチウム電池を作製した。この電池を比較例 2-2 の電池とする。

### [第三実施形態]

#### （実施例 3-1）

硝酸マンガン、硝酸ニッケルを、 $\text{Mn}:\text{Ni}$  の原子比が 0.95 : 0.95 の割合で含む水溶液に水酸化ナトリウム水溶液を加えて共沈させ、150℃で加熱、乾燥して、マンガン-ニッケル共沈化合物を得た。水酸化リチウムに前記マンガン-ニッケル共沈化合物とホウ酸を元素比  $\text{Li}:\text{Mn}:\text{Ni}:\text{B}$  が 2.00 : 0.95 : 0.95 : 0.1 となるように添加し、1000℃で12時間、酸素雰囲気下で焼成した後、粒子を分級して $D_{50}=9\mu\text{m}$ の粉末とした。BET法により測定した比表面積は $1.0\text{m}^2/\text{g}$ であった。該粉末の $\text{CuK}\alpha$ 線によるエックス線回折測定の結果、粉末Aと同様な層状構造とみられる結晶性の高い単相が合成できていることがわかった。該粉末を粉末Bとする。元素分析の結果、該粉末Bの組成は $\text{LiMn}_{0.475}\text{Ni}_{0.475}\text{B}_{0.05}\text{O}_2$ であることがわかった。

深さ方向分析ではB（ホウ素）は表面に偏析しているのが観測された（図1参照）。該粉末Bを正極活物質として用いたこと以外は（実施例 1-1）と同様にして図2に示す容量約15 Ahの角形リチウム電池を作製した。この電池を実施例 3-1の電池とする。

#### （実施例 3-2）

硝酸マンガン、硝酸ニッケル、酸化バナジウムを、 $\text{Mn}:\text{Ni}:\text{V}$  の原子比が 0.95 : 0.948 : 0.1 の割合で含む水溶液に水酸化ナトリウム水溶液を加えて共沈させ、150℃で加熱、乾燥して、マンガン-ニッケル-バナジウム共沈化合物を得た。水酸化リチウムに前記マンガン-ニッケル-バナジウム共沈化合物とホウ酸を元素比  $\text{Li}:\text{Mn}:\text{Ni}:\text{V}:\text{B}$  が 2 : 0.95 : 0.948 : 0.1 : 0.002 となるように添加し、1000℃で12時間、酸素雰囲気

下で本焼成した後、粒子を分級して $D_{50} = 9 \mu\text{m}$ の粉末とした。BET法により測定した比表面積は $1.0 \text{ m}^2/\text{g}$ であった。該粉末のCuK $\alpha$ 線によるエックス線回折測定の結果、粉末Aと同様な層状構造とみられる結晶性の高い単相が合成できていることがわかった。元素分析の結果、該粉末の組成は $\text{LiMn}_{0.475}\text{Ni}_{0.474}\text{V}_{0.05}\text{B}_{0.001}\text{O}_2$ であることがわかった。

該粉末を正極活物質として用いたこと以外は（実施例1-1）と同様にして図2に示す容量約15 Ahの角形リチウム電池を作製した。この電池を実施例3-2の電池とする。

### （実施例3-3）

硝酸マンガン、硝酸ニッケル、硝酸アルミニウムを、Mn : Ni : Alの原子比が0.95 : 0.948 : 0.1の割合で含む水溶液に水酸化ナトリウム水溶液を加えて共沈させ、150℃で加熱、乾燥して、マンガン-ニッケル-アルミニウム共沈化合物を得た。水酸化リチウムに前記マンガン-ニッケル-アルミニウム共沈化合物とホウ酸を元素比Li : Mn : Ni : Al : Bが2 : 0.95 : 0.948 : 0.1 : 0.002となるように添加し、1000℃で12時間、酸素雰囲気下で本焼成した後、粒子を分級して $D_{50} = 9 \mu\text{m}$ の粉末とした。BET法により測定した比表面積は $1.0 \text{ m}^2/\text{g}$ であった。該粉末のCuK $\alpha$ 線によるエックス線回折測定の結果、粉末Aと同様な層状構造とみられる結晶性の高い単相が合成できていることがわかった。元素分析の結果、該粉末の組成は $\text{LiMn}_{0.475}\text{Ni}_{0.474}\text{Al}_{0.05}\text{B}_{0.001}\text{O}_2$ であることがわかった。該粉末を粉末とする。

該粉末を正極活物質として用いたこと以外は（実施例1-1）と同様にして図2に示す容量約15 Ahの角形リチウム電池を作製した。この電池を実施例3-3の電池とする。

### （実施例3-4）

硝酸マンガン、硝酸ニッケル、硝酸マグネシウムを、Mn : Ni : Mgの原子比が0.95 : 0.948 : 0.1の割合で含む水溶液に水酸化ナトリウム水溶液を加えて共沈させ、150℃で加熱、乾燥して、マンガン-ニッケル-マグネ

シウム共沈化合物を得た。水酸化リチウム水溶液にマンガン－ニッケル－マグネシウム共沈化合物とホウ酸を元素比  $\text{Li} : \text{Mn} : \text{Ni} : \text{Mg} : \text{B}$  が  $2 : 0.95 : 0.948 : 0.1 : 0.002$  となるように添加し、 $1000^\circ\text{C}$  で 12 時間、酸素雰囲気下で本焼成した後、粒子を分級して  $D_{50} = 9 \mu\text{m}$  の粉末とした。BET 法により測定した比表面積は  $1.0 \text{ m}^2/\text{g}$  であった。該粉末の  $\text{Cu K}\alpha$  線によるエックス線回折測定の結果、粉末 A と同様な層状構造とみられる結晶性の高い単相が合成できていることがわかった。元素分析の結果、該粉末の組成は  $\text{Li Mn}_{0.475} \text{Ni}_{0.474} \text{Mg}_{0.05} \text{B}_{0.001} \text{O}_2$  であることがわかった。

該粉末を正極活物質として用いたこと以外は（実施例 1－1）と同様にして図 2 に示す容量約 15 Ah の角形リチウム電池を作製した。この電池を実施例 3－4 の電池とする。

#### （実施例 3－5）

硝酸マンガン、硝酸ニッケル、硝酸コバルトを、 $\text{Mn} : \text{Ni} : \text{Co}$  の原子比が  $0.95 : 0.948 : 0.1$  の割合で含む水溶液に水酸化ナトリウム水溶液を加えて共沈させ、 $150^\circ\text{C}$  で加熱、乾燥して、マンガン－ニッケル－コバルト共沈化合物を得た。水酸化リチウム水溶液に前記マンガン－ニッケル－コバルト共沈化合物とホウ酸を元素比  $\text{Li} : \text{Mn} : \text{Ni} : \text{Co} : \text{B}$  が  $2 : 0.95 : 0.948 : 0.1 : 0.002$  となるように添加し、 $1000^\circ\text{C}$  で 12 時間、酸素雰囲気下で本焼成した後、粒子を分級して  $D_{50} = 9 \mu\text{m}$  の粉末とした。BET 法により測定した比表面積は  $1.0 \text{ m}^2/\text{g}$  であった。該粉末の  $\text{Cu K}\alpha$  線によるエックス線回折測定の結果、粉末 A と同様な層状構造とみられる結晶性の高い単相が合成できていることがわかった。元素分析の結果、該粉末の組成は  $\text{Li Mn}_{0.475} \text{Ni}_{0.474} \text{Co}_{0.05} \text{B}_{0.001} \text{O}_2$  であることがわかった。

該粉末を正極活物質として用いたこと以外は（実施例 1－1）と同様にして図 2 に示す容量約 15 Ah の角形リチウム電池を作製した。この電池を実施例 3－5 の電池とする。

#### （実施例 3－6）

硝酸マンガン、硝酸ニッケル、硝酸クロムを、 $Mn : Ni : Cr$ の原子比が $0.95 : 0.948 : 0.1$ の割合で含む水溶液に水酸化ナトリウム水溶液を加えて共沈させ、 $150^{\circ}C$ で加熱、乾燥して、マンガン－ニッケル－クロム共沈化合物を得た。水酸化リチウム水溶液に前記マンガン－ニッケル－クロム共沈化合物とホウ酸を元素比 $Li : Mn : Ni : Cr : B$ が $2 : 0.95 : 0.948 : 0.1 : 0.002$ となるように添加し、 $1000^{\circ}C$ で12時間、酸素雰囲気下で本焼成した後、粒子を分級して $D_{50} = 9 \mu m$ の粉末とした。BET法により測定した比表面積は $1.0 m^2/g$ であった。該粉末の $Cu K \alpha$ 線によるエックス線回折測定の結果、粉末Aと同様な層状構造とみられる結晶性の高い単相が合成できていることがわかった。元素分析の結果、該粉末の組成は $Li Mn_{0.475} Ni_{0.474} Cr_{0.05} B_{0.001} O_2$ であることがわかった。

該粉末を正極活物質として用いたこと以外は（実施例1－1）と同様にして図2に示す容量約15 Ahの角形リチウム電池を作製した。この電池を実施例3－6の電池とする。

#### （実施例3－7）

硝酸マンガン、硝酸ニッケル、酸化チタンを、 $Mn : Ni : Ti$ の原子比が $0.95 : 0.948 : 0.1$ の割合で含む水溶液に水酸化ナトリウム水溶液を加えて共沈させ、 $150^{\circ}C$ で加熱、乾燥して、マンガン－ニッケル－チタン共沈化合物を得た。水酸化リチウム水溶液に前記マンガン－ニッケル－チタン共沈化合物とホウ酸を元素比 $Li : Mn : Ni : Ti : B$ が $2 : 0.95 : 0.948 : 0.1 : 0.002$ となるように添加し、 $1000^{\circ}C$ で12時間、酸素雰囲気下で本焼成した後、粒子を分級して $D_{50} = 9 \mu m$ の粉末とした。BET法により測定した比表面積は $1.0 m^2/g$ であった。該粉末の $Cu K \alpha$ 線によるエックス線回折測定の結果、粉末Aと同様な層状構造とみられる結晶性の高い単相が合成できていることがわかった。元素分析の結果、該粉末の組成は $Li Mn_{0.475} Ni_{0.474} Ti_{0.05} B_{0.001} O_2$ であることがわかった。

該粉末を正極活物質として用いたこと以外は（実施例1－1）と同様にして図2に示す容量約15 Ahの角形リチウム電池を作製した。この電池を実施例3－

7の電池とする。

(実施例3-8)

硝酸マンガン、硝酸ニッケル、硫酸鉄を、 $\text{Mn}:\text{Ni}:\text{Fe}$ の原子比が $0.95:0.948:0.1$ の割合で含む水溶液に水酸化ナトリウム水溶液を加えて共沈させ、 $150^{\circ}\text{C}$ で加熱、乾燥して、マンガン-ニッケル-鉄共沈化合物を得た。水酸化リチウム水溶液に前記マンガン-ニッケル-鉄共沈化合物とホウ酸を元素比 $\text{Li}:\text{Mn}:\text{Ni}:\text{Fe}:\text{B}$ が $2:0.95:0.948:0.1:0.002$ となるように添加し、 $1000^{\circ}\text{C}$ で12時間、酸素雰囲気下で本焼成した後、粒子を分級して $D_{50}=9\mu\text{m}$ の粉末とした。BET法により測定した比表面積は $1.0\text{m}^2/\text{g}$ であった。該粉末の $\text{CuK}\alpha$ 線によるエックス線回折測定の結果、粉末Aと同様な層状構造とみられる結晶性の高い単相が合成できていることがわかった。元素分析の結果、該粉末の組成は $\text{LiMn}_{0.475}\text{Ni}_{0.474}\text{Fe}_{0.05}\text{B}_{0.001}\text{O}_2$ であることがわかった。

該粉末を正極活物質として用いたこと以外は（実施例1-1）と同様にして図2に示す容量約 $15\text{Ah}$ の角形リチウム電池を作製した。この電池を実施例3-8の電池とする。

(実施例3-9)

硝酸マンガン、硝酸ニッケル、硫酸銅を、 $\text{Mn}:\text{Ni}:\text{Cu}$ の原子比が $0.95:0.948:0.1$ の割合で含む水溶液に水酸化ナトリウム水溶液を加えて共沈させ、 $150^{\circ}\text{C}$ で加熱、乾燥して、マンガン-ニッケル-銅共沈化合物を得た。水酸化リチウム水溶液に前記マンガン-ニッケル-銅共沈化合物とホウ酸を元素比 $\text{Li}:\text{Mn}:\text{Ni}:\text{Cu}:\text{B}$ が $2:0.95:0.948:0.1:0.002$ となるように添加し、 $1000^{\circ}\text{C}$ で12時間、酸素雰囲気下で本焼成した後、粒子を分級して $D_{50}=9\mu\text{m}$ の粉末とした。BET法により測定した比表面積は $1.0\text{m}^2/\text{g}$ であった。該粉末の $\text{CuK}\alpha$ 線によるエックス線回折測定の結果、粉末Aと同様な層状構造とみられる結晶性の高い単相が合成できていることがわかった。元素分析の結果、該粉末の組成は $\text{LiMn}_{0.475}\text{Ni}_{0.474}\text{Cu}_{0.05}\text{B}_{0.001}\text{O}_2$



O<sub>2</sub>であることがわかった。

該粉末を正極活物質として用いたこと以外は（実施例 1－1）と同様にして図 2 に示す容量約 15 A h の角形リチウム電池を作製した。この電池を実施例 3－9 の電池とする。

#### （実施例 3－10）

硝酸マンガン、硝酸ニッケル、硫酸亜鉛を、Mn : Ni : Zn の原子比が 0.95 : 0.948 : 0.1 の割合で含む水溶液に水酸化ナトリウム水溶液を加えて共沈させ、150℃で加熱、乾燥して、マンガン－ニッケル－亜鉛共沈化合物を得た。水酸化リチウム水溶液に前記マンガン－ニッケル－亜鉛共沈化合物とホウ酸を元素比 Li : Mn : Ni : Zn : B が 2 : 0.95 : 0.948 : 0.1 : 0.002 となるように添加し、1000℃で 12 時間、酸素雰囲気下で本焼成した後、粒子を分級して D<sub>50</sub> = 10 μm の粉末とした。BET 法により測定した比表面積は 1.0 m<sup>2</sup>/g であった。該粉末の Cu K α 線によるエックス線回折測定の結果、粉末 A と同様な層状構造とみられる結晶性の高い単相が合成できていることがわかった。元素分析の結果、該粉末の組成は Li Mn<sub>0.475</sub> Ni<sub>0.474</sub> Zn<sub>0.05</sub> B<sub>0.001</sub> O<sub>2</sub> であることがわかった。

該粉末を正極活物質として用いたこと以外は（実施例 1－1）と同様にして図 2 に示す容量約 15 A h の角形リチウム電池を作製した。この電池を実施例 3－10 の電池とする。

#### （比較例 3－1）

硝酸マンガン、硝酸ニッケルを、Mn : Ni の原子比が 0.95 : 0.95 の割合で含む水溶液に水酸化ナトリウム水溶液を加えて共沈させ、150℃で加熱、乾燥して、マンガン－ニッケル共沈化合物を得た。水酸化リチウムに前記マンガン－ニッケル共沈化合物とホウ酸を元素比 Li : Mn : Ni : B が 2.00 : 0.95 : 0.95 : 0.1 となるように添加し、1000℃で 12 時間、酸素雰囲気下で焼成した後、粒子を分級して D<sub>50</sub> = 9 μm の粉末とした。BET 法により測定した比表面積は 0.2 m<sup>2</sup>/g であった。該粉末の Cu K α 線によるエッ

クス線回折測定の結果、粉末Aと同様な層状構造とみられる結晶性の高い単相が合成できていることがわかった。元素分析の結果、該粉末の組成は $\text{LiMn}_{0.475}\text{Ni}_{0.475}\text{B}_{0.05}\text{O}_2$ であることがわかった。

該粉末を正極活物質として用いたこと以外は（実施例1-1）と同様にして図2に示す容量約15Ahの角形リチウム電池を作製した。この電池を比較例3-1の電池とする。

#### （比較例3-2）

硝酸マンガン、硝酸ニッケルを、 $\text{Mn}:\text{Ni}$ の原子比が0.95:0.95の割合で含む水溶液に水酸化ナトリウム水溶液を加えて共沈させ、150℃で加熱、乾燥して、マンガン-ニッケル共沈化合物を得た。水酸化リチウムに前記マンガン-ニッケル共沈化合物とホウ酸を元素比 $\text{Li}:\text{Mn}:\text{Ni}:\text{B}$ が2.00:0.95:0.95:0.1となるように添加し、1000℃で12時間、酸素雰囲気下で焼成した後、粒子を分級して $D_{50}=4\mu\text{m}$ の粉末とした。BET法により測定した比表面積は $2.4\text{m}^2/\text{g}$ であった。該粉末のCuK $\alpha$ 線によるエックス線回折測定の結果、粉末Aと同様な層状構造とみられる結晶性の高い単相が合成できていることがわかった。元素分析の結果、該粉末の組成は $\text{LiMn}_{0.475}\text{Ni}_{0.475}\text{B}_{0.05}\text{O}_2$ であることがわかった。

該粉末を正極活物質として用いたこと以外は（実施例1-1）と同様にして図2に示す容量約15Ahの角形リチウム電池を作製した。この電池を比較例3-2の電池とする。

#### 〔第四実施形態〕

##### （実施例4-1）

硝酸マンガン、硝酸ニッケル及び硝酸コバルトを、 $\text{Mn}:\text{Ni}:\text{Co}$ の原子比が9:9:2の割合で含む水溶液に水酸化ナトリウム水溶液を加えて共沈させ、150℃で加熱、乾燥して、マンガン-ニッケル-コバルト共沈化合物を得た。水酸化リチウム水溶液に該共沈化合物を添加し、攪拌後溶媒を蒸発させて乾燥した後、1000℃で12時間、酸素雰囲気下で焼成した後、分級して $D_{50}=2.0$

$\mu\text{m}$ の粉末とした。BET法で測定した比表面積は $0.9\text{ m}^2/\text{g}$ であった。

該粉末のCuK $\alpha$ 線によるエックス線回折測定の結果、 $2\theta = 18.56^\circ$ 、 $36.56^\circ$ 、 $37.76^\circ$ 、 $38.24^\circ$ 、 $44.32^\circ$ 、 $48.4^\circ$ 、 $58.4^\circ$ 、 $64.16^\circ$ 、 $64.8^\circ$ 、 $68.8^\circ$ に回折ピークが認められ、空間群R3mに属する層状構造と思われる結晶性の高い単相が合成できていることがわかった。該粉末のエックス線回折図を図5に示す。元素分析の結果、該粉末の組成は $\text{LiMn}_{0.45}\text{Ni}_{0.45}\text{Co}_{0.1}\text{O}_2$ であることがわかった。該粉末を粉末Dとする。

該粉末Dを正極活物質として用いたこと以外は（実施例1-1）と同様にして図2に示す容量約15Ahの角形リチウム電池を作製した。この電池を実施例4-1の電池とする。

#### （実施例4-2）

硝酸マンガン、硝酸ニッケル及び硝酸コバルトを、Mn:Ni:Coの原子比が2:2:1の割合で含む水溶液に水酸化ナトリウム水溶液を加えて共沈させ、 $150^\circ\text{C}$ で加熱、乾燥し、マンガン-ニッケル-コバルト共沈化合物を得た。水酸化リチウム水溶液に該共沈化合物を添加し、攪拌後溶媒を蒸発させて乾燥した後、 $1000^\circ\text{C}$ で12時間、酸素雰囲気下で焼成した後、分級して $D_{50} = 20\mu\text{m}$ の粉末とした。BET法により測定した比表面積は $0.9\text{ m}^2/\text{g}$ であった。

該粉末のCuK $\alpha$ 線によるエックス線回折測定の結果、粉末Dと同様な層状構造とみられる結晶性の高い単相が合成できていることがわかった。元素分析の結果、該粉末の組成は $\text{LiMn}_{0.4}\text{Ni}_{0.4}\text{Co}_{0.2}\text{O}_2$ であることがわかった。該粉末を正極活物質として用いたこと以外は（実施例1-1）と同様にして図2に示す容量約15Ahの角形リチウム電池を作製した。この電池を実施例4-2の電池とする。

#### （実施例4-3）

硝酸マンガン、硝酸ニッケル及び硝酸コバルトを、Mn:Ni:Coの原子比が9:9:2の割合で含む水溶液に水酸化ナトリウム水溶液を加えて共沈させ、

150℃で加熱、乾燥し、マンガン–ニッケル–コバルト共沈化合物を得た。水酸化リチウム水溶液に該共沈化合物を添加し、攪拌後溶媒を蒸発させて乾燥した後、1000℃で5時間、酸素雰囲気下で焼成した後、分級して $D_{50}=20\mu\text{m}$ の粉末とした。BET法により測定した比表面積は $0.3\text{m}^2/\text{g}$ であった。

該粉末のCuK $\alpha$ 線によるエックス線回折測定の結果、粉末Dと同様な層状構造とみられる結晶性の高い単相が合成できていることがわかった。元素分析の結果、該粉末の組成は $\text{LiMn}_{0.45}\text{Ni}_{0.45}\text{Co}_{0.1}\text{O}_2$ であることがわかった。該粉末を正極活物質として用いたこと以外は（実施例1–1）と同様にして図2に示す容量約15Ahの角形リチウム電池を作製した。この電池を実施例4–3の電池とする。

#### （実施例4–4）

硝酸マンガン、硝酸ニッケル及び硝酸コバルトを、Mn：Ni：Coの原子比が9：9：2の割合で含む水溶液に水酸化ナトリウム水溶液を加えて共沈させ、150℃で加熱、乾燥し、マンガン–ニッケル–コバルト共沈化合物を得た。水酸化リチウム水溶液に該共沈化合物を添加し、攪拌後溶媒を蒸発させて乾燥した後、1000℃で20時間、酸素雰囲気下で焼成した後、分級して $D_{50}=5\mu\text{m}$ の粉末とした。BET法により測定した比表面積は $1.5\text{m}^2/\text{g}$ であった。

該粉末のCuK $\alpha$ 線によるエックス線回折測定の結果、粉末Dと同様な層状構造とみられる結晶性の高い単相が合成できていることがわかった。元素分析の結果、該粉末の組成は $\text{LiMn}_{0.45}\text{Ni}_{0.45}\text{Co}_{0.1}\text{O}_2$ であることがわかった。該粉末を正極活物質として用いたこと以外は（実施例1–1）と同様にして図2に示す容量約15Ahの角形リチウム電池を作製した。この電池を実施例4–4の電池とする。

#### （実施例4–5）

硝酸マンガン、硝酸ニッケル、硝酸コバルトを、Mn：Ni：Coの原子比が17：17：4の割合で含む水溶液に水酸化ナトリウム水溶液を加えて共沈させ、150℃で加熱、乾燥し、マンガン–ニッケル–コバルト共沈化合物を得た。

水酸化リチウムに該共沈化合物とホウ酸を元素比  $\text{Li} : \text{Mn} : \text{Ni} : \text{Co} : \text{B}$  が  $2 : 0.85 : 0.85 : 0.2 : 0.1$  となるように添加し、 $1000^\circ\text{C}$  で 12 時間、酸素雰囲気下で焼成した後、分級して  $D_{50} = 9 \mu\text{m}$  の粉末とした。BET 法により測定した比表面積は  $1.0 \text{ m}^2/\text{g}$  であった。

該粉末の  $\text{Cu K}\alpha$  線によるエックス線回折測定の結果、粉末 D と同様な層状構造とみられる結晶性の高い単相が合成できていることがわかった。元素分析の結果、該粉末の組成は  $\text{Li Mn}_{0.425} \text{Ni}_{0.425} \text{Co}_{0.1} \text{B}_{0.05} \text{O}_2$  であることがわかった。該粉末を正極活物質として用いたこと以外は（実施例 1-1）と同様にして図 2 に示す容量約 15 Ah の角形リチウム電池を作製した。この電池を実施例 4-5 の電池とする。

#### （実施例 4-6）

硝酸マンガン、硝酸ニッケル、硝酸コバルト及び酸化バナジウムを、 $\text{Mn} : \text{Ni} : \text{Co} : \text{V}$  の原子比が  $17 : 17 : 4 : 2$  の割合で含む水溶液に水酸化ナトリウム水溶液を加えて共沈させ、 $150^\circ\text{C}$  で加熱、乾燥し、マンガン-ニッケル-コバルト-バナジウム共沈化合物を得た。水酸化リチウム水溶液に該共沈化合物を添加し、攪拌後溶媒を蒸発させて乾燥した後、 $1000^\circ\text{C}$  で 12 時間、酸素雰囲気下で焼成した後、分級して  $D_{50} = 9 \mu\text{m}$  の粉末とした。BET 法により測定した比表面積は  $1.0 \text{ m}^2/\text{g}$  であった。

該粉末の  $\text{Cu K}\alpha$  線によるエックス線回折測定の結果、粉末 D と同様な層状構造とみられる結晶性の高い単相が合成できていることがわかった。元素分析の結果、該粉末の組成は  $\text{Li Mn}_{0.425} \text{Ni}_{0.425} \text{Co}_{0.1} \text{V}_{0.05} \text{O}_2$  であることがわかった。該粉末を正極活物質として用いたこと以外は（実施例 1-1）と同様にして図 2 に示す容量約 15 Ah の角形リチウム電池を作製した。この電池を実施例 4-6 の電池とする。

#### （実施例 4-7）

硝酸マンガン、硝酸ニッケル、硝酸コバルト及び硝酸アルミニウムを、 $\text{Mn} : \text{Ni} : \text{Co} : \text{Al}$  の原子比が  $17 : 17 : 4 : 2$  の割合で含む水溶液に水酸化ナ

トリウム水溶液を加えて共沈させ、150℃で加熱、乾燥し、マンガン–ニッケル–コバルト–アルミニウム共沈化合物を得た。水酸化リチウム水溶液に該共沈化合物を添加し、攪拌後溶媒を蒸発させて乾燥した後、1000℃で12時間、酸素雰囲気下で焼成した後、分級して $D_{50}=9\mu\text{m}$ の粉末とした。BET法により測定した比表面積は $1.0\text{ m}^2/\text{g}$ であった。

該粉末のCuK $\alpha$ 線によるエックス線回折測定の結果、粉末Dと同様な層状構造とみられる結晶性の高い単相が合成できていることがわかった。元素分析の結果、該粉末の組成は $\text{LiMn}_{0.425}\text{Ni}_{0.425}\text{Co}_{0.1}\text{Al}_{0.05}\text{O}_2$ であることがわかった。該粉末を正極活物質として用いたこと以外は（実施例1–1）と同様にして図2に示す容量約15Ahの角形リチウム電池を作製した。この電池を実施例4–7の電池とする。

#### （実施例4–8）

硝酸マンガン、硝酸ニッケル、硝酸コバルト及び硝酸マグネシウムを、Mn : Ni : Co : Mgの原子比が17 : 17 : 4 : 2の割合で含む水溶液に水酸化ナトリウム水溶液を加えて共沈させ、150℃で加熱、乾燥し、マンガン–ニッケル–コバルト–マグネシウム共沈化合物を得た。水酸化リチウム水溶液に該共沈化合物を添加し、攪拌後溶媒を蒸発させて乾燥した後、1000℃で12時間、酸素雰囲気下で焼成した後、分級して $D_{50}=9\mu\text{m}$ の粉末とした。BET法により測定した比表面積は $1.0\text{ m}^2/\text{g}$ であった。

該粉末のCuK $\alpha$ 線によるエックス線回折測定の結果、粉末Dと同様な層状構造とみられる結晶性の高い単相が合成できていることがわかった。元素分析の結果、該粉末の組成は $\text{LiMn}_{0.425}\text{Ni}_{0.425}\text{Co}_{0.1}\text{Mg}_{0.05}\text{O}_2$ であることがわかった。該粉末を正極活物質として用いたこと以外は（実施例1–1）と同様にして図2に示す容量約15Ahの角形リチウム電池を作製した。この電池を実施例4–8の電池とする。

#### （実施例4–9）

硝酸マンガン、硝酸ニッケル、硝酸コバルト及び硝酸クロムを、Mn : Ni :

Co : Cr の原子比が 17 : 17 : 4 : 2 の割合で含む水溶液に水酸化ナトリウム水溶液を加えて共沈させ、150℃で加熱、乾燥し、マンガン–ニッケル–コバルト–クロム共沈化合物を得た。水酸化リチウム水溶液に該共沈化合物を添加し、攪拌後溶媒を蒸発させて乾燥した後、1000℃で12時間、酸素雰囲気下で焼成した後、分級して $D_{50} = 9 \mu\text{m}$ の粉末とした。BET法により測定した比表面積は $1.0 \text{ m}^2/\text{g}$ であった。

該粉末のCuK $\alpha$ 線によるエックス線回折測定の結果、粉末Dと同様な層状構造とみられる結晶性の高い単相が合成できていることがわかった。元素分析の結果、該粉末の組成は $\text{LiMn}_{0.425}\text{Ni}_{0.425}\text{Co}_{0.1}\text{Cr}_{0.05}\text{O}_2$ であることがわかった。該粉末を正極活物質として用いたこと以外は（実施例1–1）と同様にして図2に示す容量約15Ahの角形リチウム電池を作製した。この電池を実施例4–9の電池とする。

#### （実施例4–10）

硝酸マンガン、硝酸ニッケル、硝酸コバルト及び酸化チタンを、Mn : Ni : Co : Ti の原子比が 17 : 17 : 4 : 2 の割合で含む水溶液に水酸化ナトリウム水溶液を加えて共沈させ、150℃で加熱、乾燥し、マンガン–ニッケル–コバルト–チタン共沈化合物を得た。水酸化リチウム水溶液に該共沈化合物を添加し、攪拌後溶媒を蒸発させて乾燥した後、1000℃で12時間、酸素雰囲気下で焼成した後、分級して $D_{50} = 9 \mu\text{m}$ の粉末とした。BET法により測定した比表面積は $1.0 \text{ m}^2/\text{g}$ であった。

該粉末のCuK $\alpha$ 線によるエックス線回折測定の結果、粉末Dと同様な層状構造とみられる結晶性の高い単相が合成できていることがわかった。元素分析の結果、該粉末の組成は $\text{LiMn}_{0.425}\text{Ni}_{0.425}\text{Co}_{0.1}\text{Ti}_{0.05}\text{O}_2$ であることがわかった。該粉末を正極活物質として用いたこと以外は（実施例1–1）と同様にして図2に示す容量約15Ahの角形リチウム電池を作製した。この電池を実施例4–10の電池とする。

#### （実施例4–11）

硝酸マンガン、硝酸ニッケル、硝酸コバルト及び硫酸鉄を、 $\text{Mn} : \text{Ni} : \text{Co} : \text{Fe}$ の原子比が $17 : 17 : 4 : 2$ の割合で含む水溶液に水酸化ナトリウム水溶液を加えて共沈させ、 $150^\circ\text{C}$ で加熱、乾燥し、マンガン－ニッケル－コバルト－鉄共沈化合物を得た。水酸化リチウム水溶液に該共沈化合物を添加し、攪拌後溶媒を蒸発させて乾燥した後、 $1000^\circ\text{C}$ で12時間、酸素雰囲気下で焼成した後、分級して $D_{50} = 9\ \mu\text{m}$ の粉末とした。BET法により測定した比表面積は $0.9\ \text{m}^2/\text{g}$ であった。

該粉末のCu K $\alpha$ 線によるエックス線回折測定の結果、粉末Dと同様な層状構造とみられる結晶性の高い単相が合成できていることがわかった。元素分析の結果、該粉末の組成は $\text{LiMn}_{0.425}\text{Ni}_{0.425}\text{Co}_{0.1}\text{Fe}_{0.05}\text{O}_2$ であることがわかった。該粉末を正極活物質として用いたこと以外は（実施例1－1）と同様にして図2に示す容量約15 Ahの角形リチウム電池を作製した。この電池を実施例4－11の電池とする。

#### （実施例4－12）

硝酸マンガン、硝酸ニッケル、硝酸コバルト及び硫酸銅を、 $\text{Mn} : \text{Ni} : \text{Co} : \text{Cu}$ の原子比が $17 : 17 : 4 : 2$ の割合で含む水溶液に水酸化ナトリウム水溶液を加えて共沈させ、 $150^\circ\text{C}$ で加熱、乾燥し、マンガン－ニッケル－コバルト－銅共沈化合物を得た。水酸化リチウム水溶液に該共沈化合物を添加し、攪拌後溶媒を蒸発させて乾燥した後、 $1000^\circ\text{C}$ で12時間、酸素雰囲気下で焼成した後、分級して $D_{50} = 9\ \mu\text{m}$ の粉末とした。BET法により測定した比表面積は $0.9\ \text{m}^2/\text{g}$ であった。

該粉末のCu K $\alpha$ 線によるエックス線回折測定の結果、粉末Dと同様な層状構造とみられる結晶性の高い単相が合成できていることがわかった。元素分析の結果、該粉末の組成は $\text{LiMn}_{0.425}\text{Ni}_{0.425}\text{Co}_{0.1}\text{Cu}_{0.05}\text{O}_2$ であることがわかった。該粉末を正極活物質として用いたこと以外は（実施例1－1）と同様にして図2に示す容量約15 Ahの角形リチウム電池を作製した。この電池を実施例4－12の電池とする。



## (実施例 4-13)

硝酸マンガン、硝酸ニッケル、硝酸コバルト及び硫酸亜鉛を、 $Mn : Ni : Co : Zn$ の原子比が $17 : 17 : 4 : 2$ の割合で含む水溶液に水酸化ナトリウム水溶液を加えて共沈させ、 $150^{\circ}C$ で加熱、乾燥し、マンガン-ニッケル-コバルト-亜鉛共沈化合物を得た。水酸化リチウム水溶液に該共沈化合物を添加し、攪拌後溶媒を蒸発させて乾燥した後、 $1000^{\circ}C$ で12時間、酸素雰囲気下で焼成した後、分級して $D_{50} = 9 \mu m$ の粉末とした。BET法により測定した比表面積は $0.9 m^2/g$ であった。

該粉末のCuK $\alpha$ 線によるエックス線回折測定の結果、粉末Dと同様な層状構造とみられる結晶性の高い単相が合成できていることがわかった。元素分析の結果、該粉末の組成は $LiMn_{0.425}Ni_{0.425}Co_{0.1}Zn_{0.05}O_2$ であることがわかった。該粉末を正極活物質として用いたこと以外は（実施例1-1）と同様にして図2に示す容量約15 Ahの角形リチウム電池を作製した。この電池を実施例4-13の電池とする。

## (比較例 4-1)

硝酸マンガン、硝酸ニッケル及び硝酸コバルトを、 $Mn : Ni : Co$ の原子比が $7 : 11 : 2$ の割合で含む水溶液に水酸化ナトリウム水溶液を加えて共沈させ、 $150^{\circ}C$ で加熱、乾燥し、マンガン-ニッケル-コバルト共沈化合物を得た。水酸化リチウム水溶液に該共沈化合物を添加し、攪拌後溶媒を蒸発させて乾燥した後、 $1000^{\circ}C$ で12時間、酸素雰囲気下で焼成した後、分級して $D_{50} = 20 \mu m$ の粉末とした。BET法により測定した比表面積は $1.0 m^2/g$ であった。

該粉末のCuK $\alpha$ 線によるエックス線回折測定の結果、粉末Dと同様な層状構造とみられる結晶性の高い単相が合成できていることがわかった。元素分析の結果、該粉末の組成は $LiMn_{0.35}Ni_{0.55}Co_{0.1}O_2$ であることがわかった。該粉末を正極活物質として用いたこと以外は（実施例1-1）と同様にして図2に示す容量約15 Ahの角形リチウム電池を作製した。この電池を比較例4-1の電池とする。

## (比較例 4-2)

硝酸マンガン、硝酸ニッケル及び硝酸コバルトを、 $Mn : Ni : Co$ の原子比が9 : 9 : 2の割合で含む水溶液に水酸化ナトリウム水溶液を加えて共沈させ、 $150^{\circ}C$ で加熱、乾燥し、マンガン-ニッケル-コバルト共沈化合物を得た。水酸化リチウム水溶液に該共沈化合物を添加し、攪拌後溶媒を蒸発させて乾燥した後、 $1000^{\circ}C$ で24時間、酸素雰囲気下で焼成した後、分級して $D_{50} = 5 \mu m$ の粉末とした。BET法により測定した比表面積は $0.3 m^2/g$ であった。

該粉末のCuK $\alpha$ 線によるエックス線回折測定の結果、粉末Dと同様な層状構造とみられる結晶性の高い単相が合成できていることがわかった。元素分析の結果、該粉末の組成は $LiMn_{0.45}Ni_{0.45}Co_{0.1}O_2$ であることがわかった。該粉末を正極活物質として用いたこと以外は（実施例1-1）と同様にして図2に示す容量約15Ahの角形リチウム電池を作製した。この電池を比較例4-2の電池とする。

## (比較例 4-3)

硝酸マンガン、硝酸ニッケル及び硝酸コバルトを、 $Mn : Ni : Co$ の原子比が9 : 9 : 2の割合で含む水溶液に水酸化ナトリウム水溶液を加えて共沈させ、 $150^{\circ}C$ で加熱、乾燥し、マンガン-ニッケル-コバルト共沈化合物を得た。水酸化リチウム水溶液に該共沈化合物を添加し、攪拌後溶媒を蒸発させて乾燥した後、 $1000^{\circ}C$ で3時間、酸素雰囲気下で焼成した後、分級して $D_{50} = 5 \mu m$ の粉末とした。BET法により測定した比表面積は $2.0 m^2/g$ であった。

該粉末のCuK $\alpha$ 線によるエックス線回折測定の結果、粉末Dと同様な層状構造とみられる結晶性の高い単相が合成できていることがわかった。元素分析の結果、該粉末の組成は $LiMn_{0.45}Ni_{0.45}Co_{0.1}O_2$ であることがわかった。該粉末を正極活物質として用いたこと以外は（実施例1-1）と同様にして図2に示す容量約15Ahの角形リチウム電池を作製した。この電池を比較例4-3の電池とする。

## (電池性能試験)

以上の本発明電池及び比較電池を用いて、温度  $25^{\circ}\text{C}$  で高率放電性能試験を行い、引き続き、充放電サイクル性能試験を行なった。

高率放電性能試験の条件は、充電は電流  $7.5\text{ A}$  ( $0.5\text{ I t}$ )、 $4.3\text{ V}$ 、3時間の定電流定電圧充電とし、放電は電流  $1.5\text{ A}$  ( $0.1\text{ I t}$ ) または  $30\text{ A}$  ( $2\text{ I t}$ )、終止電圧  $3.0\text{ V}$  の定電流放電とした。

充放電サイクル性能試験の条件は、充電は電流  $7.5\text{ A}$  ( $0.5\text{ I t}$ )、 $4.3\text{ V}$ 、3時間の定電流定電圧充電とし、放電は電流  $7.5\text{ A}$  ( $0.5\text{ I t}$ )、終止電圧  $3.0\text{ V}$  の定電流放電とした。充電後及び放電後には、それぞれ10分の休止モードを挿入した。

高率放電試験において、 $30\text{ A}$  の電流で放電したときの放電容量の、 $1.5\text{ A}$  の電流で放電したときの放電容量に対する比を高率放電性能値 (%) とした。充放電サイクル性能試験において、放電容量が、前記充放電サイクル性能試験を開始した初期の放電容量に対して80%にまで低下したときのサイクル数をサイクル寿命とした。これらの性能試験の結果を表1～表4に示す。表中、“半値幅  $18.6^{\circ}$ ” とは、 $2\theta = 18.6 \pm 1^{\circ}$  における回折ピークの半値幅を示し、“半値幅  $44.1^{\circ}$ ” とは、 $2\theta = 44.1 \pm 1^{\circ}$  における回折ピークの半値幅を示し、“ピーク強度比” とは、 $2\theta = 18.6 \pm 1^{\circ}$  における回折ピークに対する  $2\theta = 44.1 \pm 1^{\circ}$  における回折ピークの相対強度比を示す。

表1

電池	正極活物質				電池性能					
	組成	比表面積 ( $\text{g}/\text{m}^2$ )	平均粒径 ( $\mu\text{m}$ )	ピーク 強度比	半値幅 18.6°	半値幅 44.1°	1.5A放電容量 (mAh/g)	30A放電容量 (mAh/g)	高率放電性能値 (%)	サイクル 寿命
実施例1-1	$\text{LiMn}_{0.5}\text{Ni}_{0.5}\text{O}_2$	1.0	9	1.0	0.17	0.15	140	85	60.7	500
実施例1-2	$\text{LiMn}_{0.5}\text{Ni}_{0.5}\text{O}_2$	1.0	20	0.9	0.17	0.14	140	85	60.7	500
実施例1-3	$\text{LiMn}_{0.5}\text{Ni}_{0.5}\text{O}_2$	0.9	20	0.6	0.20	0.17	150	92	61.3	350
実施例1-4	$\text{LiMn}_{0.5}\text{Ni}_{0.5}\text{O}_2$	0.9	20	0.6	0.17	0.15	150	93	62.0	450
実施例1-5	$\text{LiMn}_{0.5}\text{Ni}_{0.5}\text{O}_2$	0.9	20	1.1	0.17	0.12	135	81	60.0	480
実施例1-6	$\text{LiMn}_{0.5}\text{Ni}_{0.5}\text{O}_2$	0.9	20	1.1	0.13	0.10	135	78	57.8	520
実施例1-7	$\text{LiMn}_{0.5}\text{Ni}_{0.5}\text{O}_2$	0.9	20	1.2	0.17	0.12	130	65	50.0	550
実施例1-8	$\text{LiMn}_{0.5}\text{Ni}_{0.5}\text{O}_2$	0.9	20	1.0	0.12	0.10	137	62	45.3	500
実施例1-9	$\text{LiMn}_{0.5}\text{Ni}_{0.5}\text{O}_2$	0.3	20	0.9	0.18	0.15	140	84	60.0	510
実施例1-10	$\text{LiMn}_{0.5}\text{Ni}_{0.5}\text{O}_2$	0.3	9	0.9	0.17	0.15	140	84	60.0	510
実施例1-11	$\text{LiMn}_{0.5}\text{Ni}_{0.5}\text{O}_2$	1.5	5	0.9	0.17	0.15	140	85	60.7	470
比較例1-1	$\text{LiMn}_{0.95}\text{Ni}_{0.05}\text{O}_2$	0.6	20	0.6	0.20	0.17	160	50	31.3	300
比較例1-2	$\text{Li}_{1.05}\text{Mn}_{1.95}\text{O}_4$	0.4	10	0.7	0.17	0.12	118	90	76.3	350
比較例1-3	$\text{LiMn}_{0.5}\text{Ni}_{0.5}\text{O}_2$	2.0	3	0.9	0.17	0.17	140	87	62.1	250
比較例1-4	$\text{LiMn}_{0.5}\text{Ni}_{0.5}\text{O}_2$	2.0	5	0.4	0.21	0.18	110	70	63.6	250
比較例1-5	$\text{LiMn}_{0.5}\text{Ni}_{0.5}\text{O}_2$	0.2	5	0.9	0.19	0.14	140	87	62.1	250
比較例1-6	$\text{LiMn}_{0.5}\text{Ni}_{0.5}\text{O}_2$	0.2	30	0.9	0.12	0.10	120	72	60.0	480

表2

電池	組成	正極活物質					電池性能			
		比表面積 ( $\text{g}/\text{m}^2$ )	平均粒径 ( $\mu\text{m}$ )	ピーク 強度比	半値幅 18.6°	半値幅 44.1°	1.5A放電容量 (mAh/g)	30A放電容量 (mAh/g)	高率放電性能値 (%)	サイクル 寿命
実施例2-1	$\text{LiMn}_{0.475}\text{Ni}_{0.475}\text{B}_{0.05}\text{O}_2$	0.9	9	0.9	0.16	0.10	137	89	65.0	350
実施例2-2	$\text{LiMn}_{0.475}\text{Ni}_{0.475}\text{V}_{0.05}\text{O}_2$	0.9	9	0.9	0.17	0.17	130	87	66.9	350
実施例2-3	$\text{LiMn}_{0.475}\text{Ni}_{0.475}\text{Al}_{0.05}\text{O}_2$	0.9	9	1.0	0.16	0.11	129	89	69.0	350
実施例2-4	$\text{LiMn}_{0.475}\text{Ni}_{0.475}\text{Mg}_{0.05}\text{O}_2$	0.9	9	1.1	0.16	0.12	132	89	67.4	350
実施例2-5	$\text{LiMn}_{0.475}\text{Ni}_{0.475}\text{Co}_{0.05}\text{O}_2$	0.9	9	1.0	0.16	0.14	128	88	68.8	350
実施例2-6	$\text{LiMn}_{0.475}\text{Ni}_{0.475}\text{Cr}_{0.05}\text{O}_2$	0.9	9	0.9	0.17	0.17	128	84	65.6	350
実施例2-7	$\text{LiMn}_{0.475}\text{Ni}_{0.475}\text{Ti}_{0.05}\text{O}_2$	0.9	9	0.9	0.16	0.17	129	87	67.4	350
実施例2-8	$\text{LiMn}_{0.475}\text{Ni}_{0.475}\text{Fe}_{0.05}\text{O}_2$	0.9	9	0.9	0.16	0.13	128	85	66.4	350
実施例2-9	$\text{LiMn}_{0.475}\text{Ni}_{0.475}\text{Cu}_{0.05}\text{O}_2$	0.9	9	0.9	0.16	0.14	127	83	65.4	350
実施例2-10	$\text{LiMn}_{0.475}\text{Ni}_{0.475}\text{Zn}_{0.05}\text{O}_2$	0.9	9	0.9	0.17	0.13	128	84	65.6	350
比較例2-1	$\text{LiMn}_{0.475}\text{Ni}_{0.475}\text{Mg}_{0.05}\text{O}_2$	0.2	15	1.1	0.17	0.11	95	40	42.1	300
比較例2-2	$\text{LiMn}_{0.475}\text{Ni}_{0.475}\text{Mg}_{0.05}\text{O}_2$	1.9	6	1.1	0.16	0.10	130	90	69.2	150

表3

電池	正極活物質					電池性能				
	組成	比表面積 ( $\text{g}/\text{m}^2$ )	平均粒径 ( $\mu\text{m}$ )	ピーク 強度比	半値幅 18.6°	半値幅 44.1°	1.5A放電容量 (mAh/g)	30A放電容量 (mAh/g)	高率放電性能値 (%)	サイクル 寿命
実施例3-1	$\text{LiMn}_{0.475}\text{Ni}_{0.475}\text{B}_{0.05}\text{O}_2$	1.0	9	1.0	0.15	0.12	137	89	65.0	600
実施例3-2	$\text{LiMn}_{0.475}\text{Ni}_{0.474}\text{V}_{0.05}\text{B}_{0.001}\text{O}_2$	1.0	9	1.0	0.14	0.11	130	90	69.2	550
実施例3-3	$\text{LiMn}_{0.475}\text{Ni}_{0.474}\text{Al}_{0.05}\text{B}_{0.001}\text{O}_2$	1.0	9	1.0	0.13	0.11	129	92	71.3	600
実施例3-4	$\text{LiMn}_{0.475}\text{Ni}_{0.474}\text{Mg}_{0.05}\text{B}_{0.001}\text{O}_2$	1.0	9	1.0	0.13	0.11	132	92	69.7	650
実施例3-5	$\text{LiMn}_{0.475}\text{Ni}_{0.474}\text{Co}_{0.05}\text{B}_{0.001}\text{O}_2$	1.0	9	1.0	0.13	0.11	131	93	71.0	700
実施例3-6	$\text{LiMn}_{0.475}\text{Ni}_{0.474}\text{Cr}_{0.05}\text{B}_{0.001}\text{O}_2$	1.0	9	1.0	0.14	0.11	128	87	68.0	650
実施例3-7	$\text{LiMn}_{0.475}\text{Ni}_{0.474}\text{Ti}_{0.05}\text{B}_{0.001}\text{O}_2$	1.0	9	1.0	0.16	0.14	129	90	69.8	500
実施例3-8	$\text{LiMn}_{0.475}\text{Ni}_{0.474}\text{Fe}_{0.05}\text{B}_{0.001}\text{O}_2$	1.0	9	1.0	0.16	0.14	125	86	68.8	480
実施例3-9	$\text{LiMn}_{0.475}\text{Ni}_{0.474}\text{Cu}_{0.05}\text{B}_{0.001}\text{O}_2$	1.0	9	1.0	0.15	0.13	127	85	66.9	500
実施例3-10	$\text{LiMn}_{0.475}\text{Ni}_{0.474}\text{Zn}_{0.05}\text{B}_{0.001}\text{O}_2$	1.0	10	1.0	0.16	0.15	130	93	71.5	510
比較例3-1	$\text{LiMn}_{0.475}\text{Ni}_{0.475}\text{B}_{0.05}\text{O}_2$	0.2	9	1.1	0.18	0.23	110	70	63.6	470
比較例3-2	$\text{LiMn}_{0.475}\text{Ni}_{0.475}\text{B}_{0.05}\text{O}_2$	2.4	4	1.1	0.17	0.21	132	95	72.0	200

表 4

電池	正極活物質				電池性能					
	組成	比表面積 (g/m <sup>2</sup> )	平均粒径 (μm)	ピーク 強度比	半値幅 18.6°	半値幅 44.1°	1.5A放電容量 (mAh/g)	30A放電容量 (mAh/g)	高率放電性能値 (%)	サイクル 寿命
実施例4-1	LiMn <sub>0.45</sub> Ni <sub>0.45</sub> Co <sub>0.1</sub> O <sub>2</sub>	0.9	20	1.0	0.19	0.12	160	113	70.6	700
実施例4-2	LiMn <sub>0.4</sub> Ni <sub>0.4</sub> Co <sub>0.2</sub> O <sub>2</sub>	0.9	20	1.0	0.19	0.11	165	120	72.7	750
実施例4-3	LiMn <sub>0.45</sub> Ni <sub>0.45</sub> Co <sub>0.1</sub> O <sub>2</sub>	0.3	20	1.0	0.15	0.14	160	112	70.0	600
実施例4-4	LiMn <sub>0.45</sub> Ni <sub>0.45</sub> Co <sub>0.1</sub> O <sub>2</sub>	1.5	5	1.0	0.19	0.10	160	114	71.3	700
比較例4-1	LiMn <sub>0.35</sub> Ni <sub>0.55</sub> Co <sub>0.1</sub> O <sub>2</sub>	1.0	20	1.0	0.17	0.13	160	115	71.9	400
比較例4-2	LiMn <sub>0.45</sub> Ni <sub>0.45</sub> Co <sub>0.1</sub> O <sub>2</sub>	0.3	5	1.0	0.20	0.10	160	94	58.8	300
比較例4-3	LiMn <sub>0.45</sub> Ni <sub>0.45</sub> Co <sub>0.1</sub> O <sub>2</sub>	2.0	5	0.5	0.07	0.02	160	120	75.0	350
実施例4-5	LiMn <sub>0.425</sub> Ni <sub>0.425</sub> Co <sub>0.1</sub> B <sub>0.05</sub> O <sub>2</sub>	1.0	9	1.0	0.18	0.14	157	118	75.2	700
実施例4-6	LiMn <sub>0.425</sub> Ni <sub>0.425</sub> Co <sub>0.1</sub> V <sub>0.05</sub> O <sub>2</sub>	1.0	9	0.9	0.19	0.12	150	111	74.0	600
実施例4-7	LiMn <sub>0.425</sub> Ni <sub>0.425</sub> Co <sub>0.1</sub> Al <sub>0.05</sub> O <sub>2</sub>	1.0	9	1.0	0.19	0.13	155	113	72.9	700
実施例4-8	LiMn <sub>0.425</sub> Ni <sub>0.425</sub> Co <sub>0.1</sub> Mg <sub>0.05</sub> O <sub>2</sub>	1.0	9	1.0	0.19	0.13	152	114	75.0	700
実施例4-9	LiMn <sub>0.425</sub> Ni <sub>0.425</sub> Co <sub>0.1</sub> Cr <sub>0.05</sub> O <sub>2</sub>	1.0	9	1.0	0.19	0.14	152	114	75.0	650
実施例4-10	LiMn <sub>0.425</sub> Ni <sub>0.425</sub> Co <sub>0.1</sub> Ti <sub>0.05</sub> O <sub>2</sub>	1.0	9	1.0	0.19	0.15	154	112	72.7	650
実施例4-11	LiMn <sub>0.425</sub> Ni <sub>0.425</sub> Co <sub>0.1</sub> Fe <sub>0.05</sub> O <sub>2</sub>	0.9	9	0.9	0.19	0.11	150	109	72.7	650
実施例4-12	LiMn <sub>0.425</sub> Ni <sub>0.425</sub> Co <sub>0.1</sub> Cu <sub>0.05</sub> O <sub>2</sub>	0.9	9	1.0	0.20	0.10	151	115	76.2	620
実施例4-13	LiMn <sub>0.425</sub> Ni <sub>0.425</sub> Co <sub>0.1</sub> Zn <sub>0.05</sub> O <sub>2</sub>	0.9	9	1.0	0.19	0.12	153	120	78.4	650

また、(実施例 1-1) の電池について、1.5 A (0.1 I t) で放電を行ったときの放電電圧変化を図 6 に、(実施例 1-10) の電池について、1.5 A (0.1 I t) で放電を行ったときの放電電圧変化を図 7 に、(実施例 4-1) の電池について、1.5 A (0.1 I t) で放電を行ったときの放電電圧変化を図 8 に示す。

(第一実施形態について)

空間群 R 3 / m 類似の層状構造を持つ正極活物質を用いた (実施例 1-1) ~ (実施例 1-11) の電池と、空間群 C 2 / m に属する層状構造を持つ正極活物質を用いた (比較例 1-1) の電池とを比較すると、高率放電特性が大きく改善されていることがわかる。また、空間群 R 3 / m 類似の層状構造を持つ正極活物質  $\text{LiMn}_{0.5}\text{Ni}_{0.5}\text{O}_2$  を用いた電池の中でも、(実施例 1-1) ~ (実施例 1-11) 及び (比較例 1-3) ~ (比較例 1-6) とを比較すると、比表面積の値を  $0.3 \text{ m}^2/\text{g}$  以上とすることで、高率放電特性が顕著に改善されることがわかる。一方、前記比表面積の値が  $1.5 \text{ m}^2/\text{g}$  を越えると、充放電サイクル性能が急激に低下することがわかる。このことから、 $0.3 \text{ m}^2/\text{g}$  以上  $1.5 \text{ m}^2/\text{g}$  以下の比表面積を有する  $\text{LiMn}_{0.5}\text{Ni}_{0.5}\text{O}_2$  を正極活物質に用いると、良好なサイクル寿命と高い高率放電特性を兼ね備えた二次電池が提供できる。

また、同じく  $\text{LiMn}_{0.5}\text{Ni}_{0.5}\text{O}_2$  で表される複合酸化物を用い、Cu K  $\alpha$  線を使用した粉末エックス線回折図の、 $2\theta = 18.6 \pm 1^\circ$  における回折ピークに対する  $2\theta = 44.1 \pm 1^\circ$  における回折ピークの相対強度比が異なる電池について電池性能を比べると、相対強度比が 0.6 以上となると、サイクル寿命が大きく向上することが分かる。また、前記相対強度比が 1.1 を越えると、高率放電特性値が低下する傾向となることがわかる。このことから、前記相対強度比を 0.6 以上 1.1 以下とすることにより、特に、良好なサイクル寿命と高い効率放電特性を兼ね備えた電池を提供できる。

また、 $2\theta = 18.6 \pm 1^\circ$  における回折ピークの半値幅が  $0.13^\circ$  以上であり、かつ、 $2\theta = 44.1 \pm 1^\circ$  における回折ピークの半値幅が  $0.10^\circ$  以上である場合、良好な高率放電特性が得られることがわかる。また、 $2\theta = 18$



．  $6 \pm 1^\circ$  における回折ピークの半値幅が  $0.20^\circ$  より大きく、かつ、 $2\theta = 44.1 \pm 1^\circ$  における回折ピークの半値幅が  $0.17^\circ$  より大きい場合、サイクル寿命が低下する傾向となることが分かる。このことから、 $2\theta = 18.6 \pm 1^\circ$  における回折ピークの半値幅が  $0.13 \sim 0.20^\circ$  であり、かつ、 $2\theta = 44.1 \pm 1^\circ$  における回折ピークの半値幅が  $0.10 \sim 0.17^\circ$  とすることにより、特に、良好なサイクル寿命と高い効率放電特性を兼ね備えた電池を提供できる。

なお、(比較例 1-2) の電池は、高率放電特性が比較的良好なスピネルマンガン正極の主たる活物質として用いている。この電池においては、スピネルマンガンから期待される通りの高率放電性能が得られていることから、本実施例及び比較例において、放電特性の律速が正極以外の構成要素である電解液や負極等によるものではないことが確認される。

#### (第二実施形態について)

$\text{LiMn}_{0.5}\text{Ni}_{0.5}\text{O}_2$  を構成する Mn 及び Ni の一部を異種元素で置換した(実施例 2-1)～(実施例 2-7)の電池では、類似の物性を持つ正極活物質を用いた(実施例 1-2)の電池と比べて、高率放電特性値が大きく向上することがわかる。この作用効果については必ずしも明らかではないが、Ni、Mn と異なる少量の元素による置換は、リチウムイオン移動を向上させる働きがあるものと考えられる。

また、第二実施形態において、比表面積の値が  $0.3 \text{ m}^2/\text{g}$  を下回った(比較例 2-1)の電池は、高率放電性能値が不十分であった。一方、比表面積の値が  $1.5 \text{ m}^2/\text{g}$  を越える(比較例 2-2)の電池は、充放電サイクル性能が急激に低下することがわかる。

#### (第三実施形態について)

また、(実施例 3-1)の電池は、(実施例 1-1)～(実施例 1-11)の電池に比べて、高率放電特性が高く、ホウ素による元素置換の効果が認められる。

$\text{LiMn}_{0.5}\text{Ni}_{0.5}\text{O}_2$  の Mn 及び Ni の一部を、ホウ素と、それ以外の元素とで

置換した（実施例 3-2）～（実施例 3-7）の電池では、さらに高率放電性能を改善できることがわかる。これは、Ni 及び Mn 以外の少量の異種元素による置換は、リチウムイオン移動を向上させる働きがあるものと考えられる。

また、第三実施形態において、比表面積の値が  $0.3 \text{ m}^2/\text{g}$  を下回った（比較例 3-1）の電池は、高率放電性能値が不十分であった。一方、比表面積の値が  $1.5 \text{ m}^2/\text{g}$  を越える（比較例 3-2）の電池は、充放電サイクル性能が急激に低下することがわかる。

なお、図 1 にみられるように、エックス線光電子分光法（XPS）によるエッチング時間が約 400 秒に達すると、ホウ素濃度が粒子内部と同程度にまで低減している。ここで、深さ方向のエッチング速度は  $0.07 \text{ nm (秒)}$  である。このことから、本発明の効果を発現させるために必要な正極活物質粒子の表層部の厚さは、高々  $28 \text{ nm} (= 0.028 \mu\text{m})$  あれば十分であることがわかる。正極活物質の平均粒径が  $9 \sim 10 \mu\text{m}$  の場合、前記厚さは粒子の直径の約 2% に相当する。

#### （第四実施形態について）

また、 $\text{LiMn}_{0.5}\text{Ni}_{0.5}\text{O}_2$  で表わされる複合酸化物に Co 成分を加えた  $\text{Li}[\text{Mn}_x\text{Ni}_y\text{Co}_z]\text{O}_2$  で表わされる複合酸化物を正極活物質に用いた（実施例 4-1）～（実施例 4-4）の電池では、いずれも放電容量が、（実施例 1-1）～（実施例 1-11）の電池に比べて大幅に増加した。また、結晶構造が安定になったためか、サイクル寿命も大きく向上した。

同じ組成式  $\text{LiMn}_{0.45}\text{Ni}_{0.45}\text{Co}_{0.1}\text{O}_2$  で表わされ、比表面積の異なる複合酸化物を正極活物質に用いた（実施例 4-1）、（実施例 4-3）、（実施例 4-4）、（比較例 4-2）、（比較例 4-3）について電池性能を比較すると、比表面積が  $1.5 \text{ m}^2/\text{g}$  を超えると、サイクル性能が急激に低下することがわかった。また、比表面積が  $0.3 \text{ m}^2/\text{g}$  を下回ると、高率放電性能が急激に悪くなることがわかった。このことから、複合酸化物の比表面積の値を  $0.3 \text{ m}^2/\text{g}$  以上  $1.5 \text{ m}^2/\text{g}$  以下とすることで、良好なサイクル性能と高い高率放電性能を兼ね備える非水電解質二次電池を提供できる。

Ni、Mn、Co以外の異種元素M”を組成に加えた $\text{LiMn}_{0.425}\text{Ni}_{0.425}\text{Co}_{0.1}\text{M}''_{0.05}\text{O}_2$ の組成式で表わされる複合酸化物を正極活物質に用いた（実施例4-5）～（実施例4-10）の電池では、異種元素M”を添加していない（実施例4-1）の電池と比較して高率放電性能値がいずれも向上していることがわかる。この作用効果については必ずしも明らかではないが、Ni、Mnと異なる少量の元素による置換は、リチウムイオン移動を向上させる働きがあるものと考えられる。

ところで、ホウ素を添加した実施例2-1，実施例3-1，実施例4-7の電池を解体し、電池を構成する各構成要素について元素分析を行った結果、負極表面付近からホウ素が検出された。このことから、合成時に添加したホウ素は、Mn及びNiと置換して構造を安定化させる効果よりも、むしろ、正極活物質粒子から溶出し、正極表面の状態を活性に変え、高率放電性能を向上させる効果を発現するものと考えられる。

なお、本発明の層状構造を有する活物質の場合、基本的にはLiは6aサイトに、Mn、Ni、Coは6bサイトに、そしてOは6cサイトを占有しているが、原理的には、Liが6bサイト中に拡散した形態もとらうる。その場合、Liは1価の価数であることから6bサイト中の不足する電荷は6cサイトの増減によって電荷中和される。

上記実施形態2の実施例においては、正極活物質における主構成物質に $\text{Li}[\text{Mn}_{0.475}\text{Ni}_{0.475}\text{B}_{0.05}\text{O}_2]$ 、 $\text{Li}[\text{Mn}_{0.475}\text{Ni}_{0.475}\text{V}_{0.05}\text{O}_2]$ 、 $\text{Li}[\text{Mn}_{0.475}\text{Ni}_{0.475}\text{Al}_{0.05}\text{O}_2]$ 、 $\text{Li}[\text{Mn}_{0.475}\text{Ni}_{0.475}\text{Mg}_{0.05}\text{O}_2]$ 、 $\text{Li}[\text{Mn}_{0.475}\text{Ni}_{0.475}\text{Co}_{0.05}\text{O}_2]$ 、 $\text{Li}[\text{Mn}_{0.475}\text{Ni}_{0.475}\text{Cr}_{0.05}\text{O}_2]$ 、 $\text{Li}[\text{Mn}_{0.475}\text{Ni}_{0.475}\text{Ti}_{0.05}\text{O}_2]$ 、 $\text{Li}[\text{Mn}_{0.475}\text{Ni}_{0.475}\text{Li}_{0.05}\text{O}_2]$ を用いることを記載したが、その他の異種元素Mを用いた場合についても同様な効果が得られる事が確認された。

上記実施形態3の実施例においては、正極活物質における主構成物質に $\text{Li}[\text{Mn}_{0.475}\text{Ni}_{0.475}\text{B}_{0.05}\text{O}_2]$ 、ホウ素の表面濃度が大きい $\text{Li}[\text{Mn}_{0.475}\text{Ni}_{0.475}\text{B}_{0.05}\text{O}_2]$ 、 $\text{Li}[\text{Mn}_{0.475}\text{Ni}_{0.474}\text{V}_{0.05}\text{B}_{0.001}\text{O}_2]$ 、 $\text{Li}[\text{Mn}_{0.475}\text{Ni}_{0.474}\text{V}_{0.05}\text{Al}_{0.001}\text{O}_2]$ 、 $\text{Li}[\text{Mn}_{0.475}\text{Ni}_{0.474}\text{V}_{0.05}\text{Mg}_{0.001}\text{O}_2]$ 、 $\text{Li}[\text{Mn}_{0.475}\text{Ni}_{0.474}\text{V}_{0.05}\text{Co}_{0.001}\text{O}_2]$

$O_2]$ 、 $Li [Mn_{0.475}Ni_{0.474}Cr_{0.05}B_{0.001}O_2]$ 、 $Li [Mn_{0.475}Ni_{0.474}Ti_{0.05}B_{0.001}O_2]$ 、を用いることを記載したが、その他の異種元素M'を用いた場合についても同様な効果が得られる事が確認された。

上記実施形態4の実施例においては、正極活物質における主構成物質に $Li [Mn_{0.45}Ni_{0.45}Co_{0.1}O_2]$ 、 $Li [Mn_{0.425}Ni_{0.425}Co_{0.1}B_{0.05}O_2]$ 、 $Li [Mn_{0.425}Ni_{0.425}Co_{0.1}V_{0.05}O_2]$ 、 $Li [Mn_{0.425}Ni_{0.425}Co_{0.1}Al_{0.05}O_2]$ 、 $Li [Mn_{0.425}Ni_{0.425}Co_{0.1}Mg_{0.05}O_2]$ 、 $Li [Mn_{0.425}Ni_{0.425}Co_{0.1}Cr_{0.05}O_2]$ 、 $Li [Mn_{0.425}Ni_{0.425}Co_{0.1}Ti_{0.05}O_2]$ 、 $Li [Mn_{0.425}Ni_{0.425}Co_{0.1}Li_{0.05}O_2]$ を用いることを記載したが、その他の元素を用いた場合についても同様な効果が得られる事が確認された。

ここでは、負極材料として人造黒鉛を用いた非水電解質二次電池について実施例を挙げたが、同様の効果は、その他の負極材料についても確認された。

なお、本発明は上記実施例に記載された活物質の出発原料、製造方法、正極、負極、電解質、セパレータ及び電池形状などに限定されるものではない。

#### <産業上の利用可能性>

本発明によれば、上記問題点を解決するためになされたものであって、高率充放電性能及び充放電サイクル性能に優れる高エネルギー密度の非水電解質二次電池を提供できる。

## 請 求 の 範 囲

1. Li-Mn-Ni系複合酸化物を主成分とする正極活物質であって、前記Li-Mn-Ni系複合酸化物のBET法による比表面積が $0.3 \text{ m}^2/\text{g}$ 以上 $1.5 \text{ m}^2/\text{g}$ 以下であることを特徴とする正極活物質。

2. 前記Li-Mn-Ni系複合酸化物が、 $\text{LiMn}_{0.5}\text{Ni}_{0.5}\text{O}_2$ で表される複合酸化物であることを特徴とする請求の範囲第1項に記載の正極活物質。

3. 前記Li-Mn-Ni系複合酸化物が、 $\text{LiMn}_{0.5}\text{Ni}_{0.5}\text{O}_2$ で表される複合酸化物を構成するMn及びNiの一部が異種元素で置換され、次の一般式；  
 $\text{Li}_{1-z} [\text{Mn}_{0.5-x-y}\text{Ni}_{0.5-x'-y'}\text{M}_{x+x'}\text{Li}_{y+y'}\text{O}_2]$

(但し、Mは前記異種元素；

$$x = 0.001 \sim 0.1 \quad ; \quad x' = 0.001 \sim 0.1 \quad ;$$

$$y = 0 \sim 0.1 \quad ; \quad y' = 0 \sim 0.1 \quad ;$$

$$x + x' + y + y' \leq 0.4 \quad ; \quad 0 \leq z \leq 1)$$

で示される組成の複合酸化物であることを特徴とする請求の範囲第1項に記載の正極活物質。

4. 前記Li-Mn-Ni系複合酸化物が、 $\text{LiMn}_{0.5}\text{Ni}_{0.5}\text{O}_2$ で表される複合酸化物を構成するMn及びNiの一部が異種元素で置換され、次の一般式；  
 $\text{Li}_{1-z} [\text{Mn}_{0.5-x-y}\text{Ni}_{0.5-x'-y'}\text{M}_{x+x'}\text{Li}_{y+y'}\text{O}_2]$

(但し、Mは前記異種元素；

$$x = 0.01 \sim 0.1 \quad ; \quad x' = 0.01 \sim 0.1 \quad ;$$

$$y = 0 \sim 0.1 \quad ; \quad y' = 0 \sim 0.1 \quad ;$$

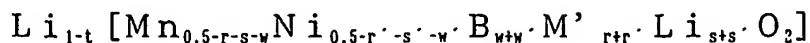
$$x + x' + y + y' \leq 0.2 \quad ; \quad 0 \leq z \leq 1)$$

で示される組成の複合酸化物であることを特徴とする請求の範囲第1項に記載の正極活物質。

5. 前記異種元素MがB, Mg, Al, Ti, V, Cr, Fe, Co, Cu及びZnから構成される群から選ばれる1種以上であることを特徴とする請求の範囲第3項または第4項に記載の正極活物質。

6. 前記Li-Mn-Ni系複合酸化物が、 $\text{LiMn}_{0.5}\text{Ni}_{0.5}\text{O}_2$ で表される

複合酸化物を構成するMn及びNiの一部が、異種元素並びにホウ素で置換され、次の一般式；



(但し、M' は前記異種元素；

$$r = 0.001 \sim 0.1 \quad ; \quad r' = 0.001 \sim 0.1 \quad ;$$

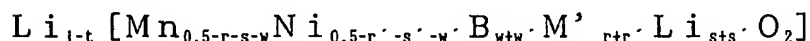
$$s = 0 \sim 0.1 \quad ; \quad s' = 0 \sim 0.1 \quad ;$$

$$r + r' + s + s' + w + w' \leq 0.4 \quad ;$$

$$w + w' = 0.0005 \sim 0.01 \quad ; \quad 0 \leq t \leq 1)$$

で示される組成の複合酸化物であることを特徴とする請求の範囲第1項に記載の正極活物質。

7. 前記Li-Mn-Ni系複合酸化物が、 $\text{LiMn}_{0.5}\text{Ni}_{0.5}\text{O}_2$ で表される複合酸化物を構成するMn及びNiの一部が、異種元素並びにホウ素で置換され、次の一般式；



(但し、M' は前記異種元素；

$$r = 0.01 \sim 0.1 \quad ; \quad r' = 0.01 \sim 0.1 \quad ;$$

$$s = 0 \sim 0.1 \quad ; \quad s' = 0 \sim 0.1 \quad ;$$

$$r + r' + s + s' + w + w' \leq 0.2 \quad ;$$

$$w + w' = 0.0005 \sim 0.01 \quad ; \quad 0 \leq t \leq 1)$$

で示される組成の複合酸化物であることを特徴とする請求の範囲第1項に記載の正極活物質。

8. 前記異種元素M' がMg, Al, Ti, V, Cr, Fe, Co, Cu及びZnから構成される群から選ばれる1種以上であることを特徴とする請求の範囲第6項または第7項に記載の正極活物質。

9. 前記Li-Mn-Ni系複合酸化物が、 $\text{Li} [\text{Mn}_c \text{Ni}_d \text{Co}_e \text{Li}_a \text{M}''_b] \text{O}_2$  (M'' はMn、Ni、Co、Li以外の元素、 $d \leq c + e + a + b$ 、 $c + d + e + a + b = 1$ 、 $0 \leq a \leq 0.05$ 、 $0 \leq b \leq 0.05$ 、 $0.2 \leq c \leq 0.5$ 、 $0.02 \leq e \leq 0.4$ ) で表される複合酸化物であることを特徴とする請求の範囲第1項に記載の正極活物質。

10. 前記M”が、B、Mg、Al、Ti、V、Cr、Fe、Cu及びZnからなる群から選ばれる少なくとも1種の元素であることを特徴とする請求の範囲第9項に記載の正極活物質。

11. 前記Li-Mn-Ni系複合酸化物が、CuK $\alpha$ 線を使用した粉末エックス線回折図の $2\theta = 18.6 \pm 1^\circ$ 、 $36.6 \pm 1^\circ$ 、 $37.8 \pm 1^\circ$ 、 $38.2 \pm 1^\circ$ 、 $44.3 \pm 1^\circ$ 、 $48.4 \pm 1^\circ$ 、 $58.4 \pm 1^\circ$ 、 $64.2 \pm 1^\circ$ 、 $64.8 \pm 1^\circ$ 、 $68.8 \pm 1^\circ$ にピークを有する層状結晶構造であることを特徴とする請求の範囲第1項～第10項のいずれかに記載の正極活物質。

12. 前記Li-Mn-Ni系複合酸化物は、CuK $\alpha$ 線を使用した粉末エックス線回折図の、 $2\theta = 18.6 \pm 1^\circ$ における回折ピークに対する $2\theta = 44.1 \pm 1^\circ$ における回折ピークの相対強度比が0.6以上1.1以下であることを特徴とする請求の範囲第1項～第11項のいずれかに記載の正極活物質。

13. 前記Li-Mn-Ni系複合酸化物は、CuK $\alpha$ 線を使用した粉末エックス線回折図の、 $2\theta = 18.6 \pm 1^\circ$ における回折ピークの半値幅が $0.13^\circ$ 以上 $0.20^\circ$ 以下であり、かつ、 $2\theta = 44.1 \pm 1^\circ$ における回折ピークの半値幅が $0.10^\circ$ 以上 $0.17^\circ$ 以下であることを特徴とする請求の範囲第1項～第12項のいずれかに記載の正極活物質。

14. 前記Li-Mn-Ni系複合酸化物の粒径が $3\mu\text{m}$ 以上 $20\mu\text{m}$ 以下である請求の範囲第1項～第13項のいずれかに記載の正極活物質。

15. 請求の範囲第1項～第14項のいずれかに記載の正極活物質を用いた非水電解質二次電池。

図 1

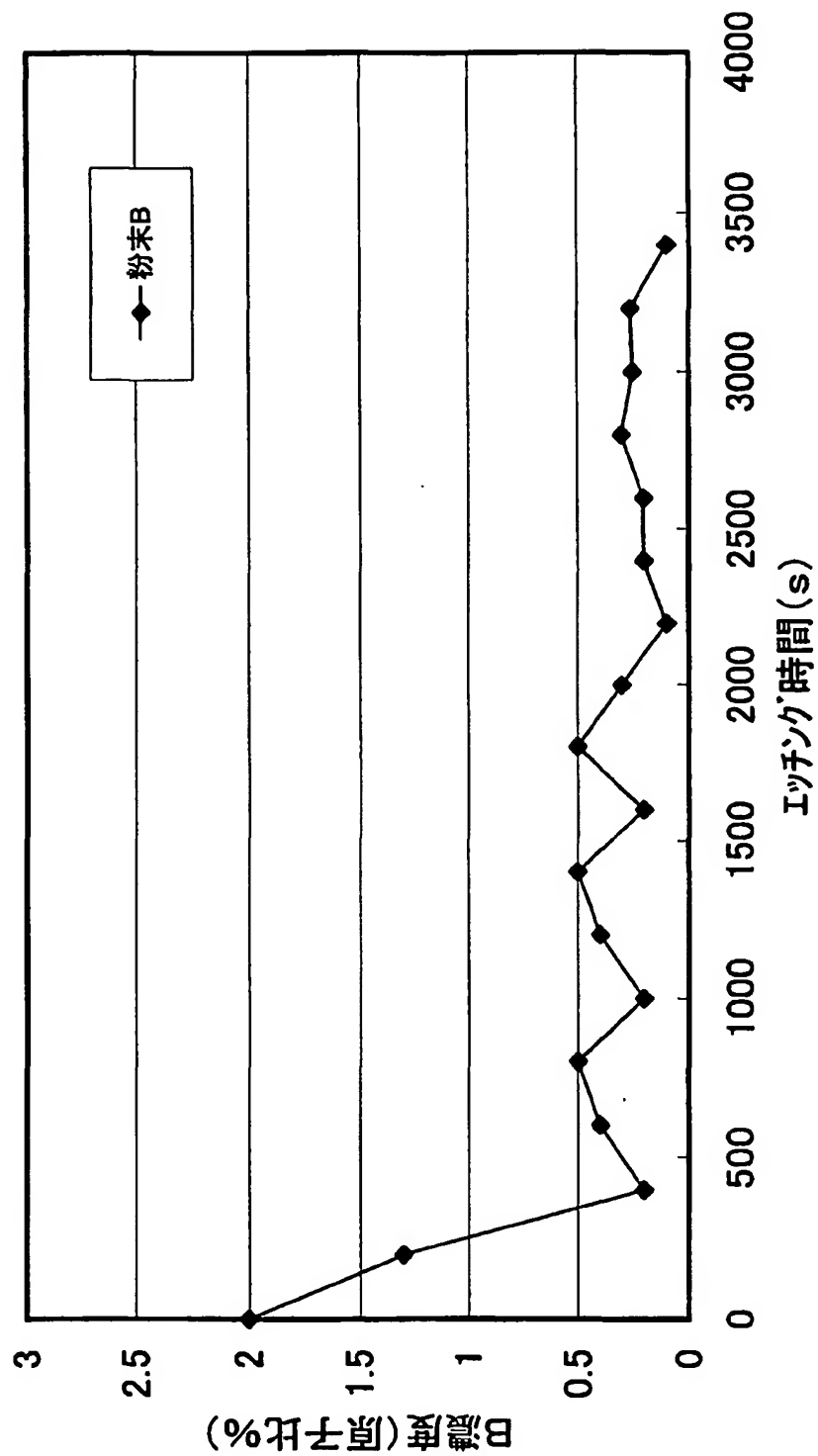




図 2

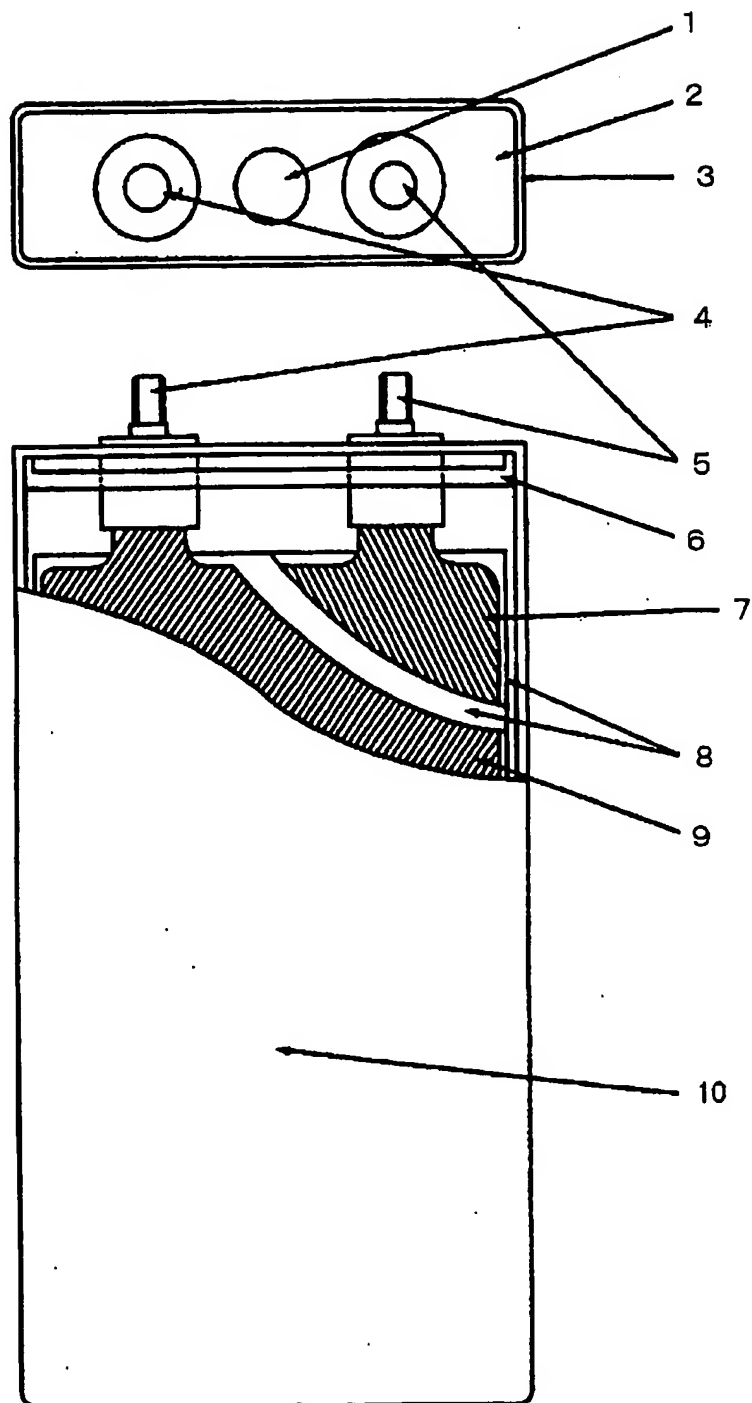


図 3

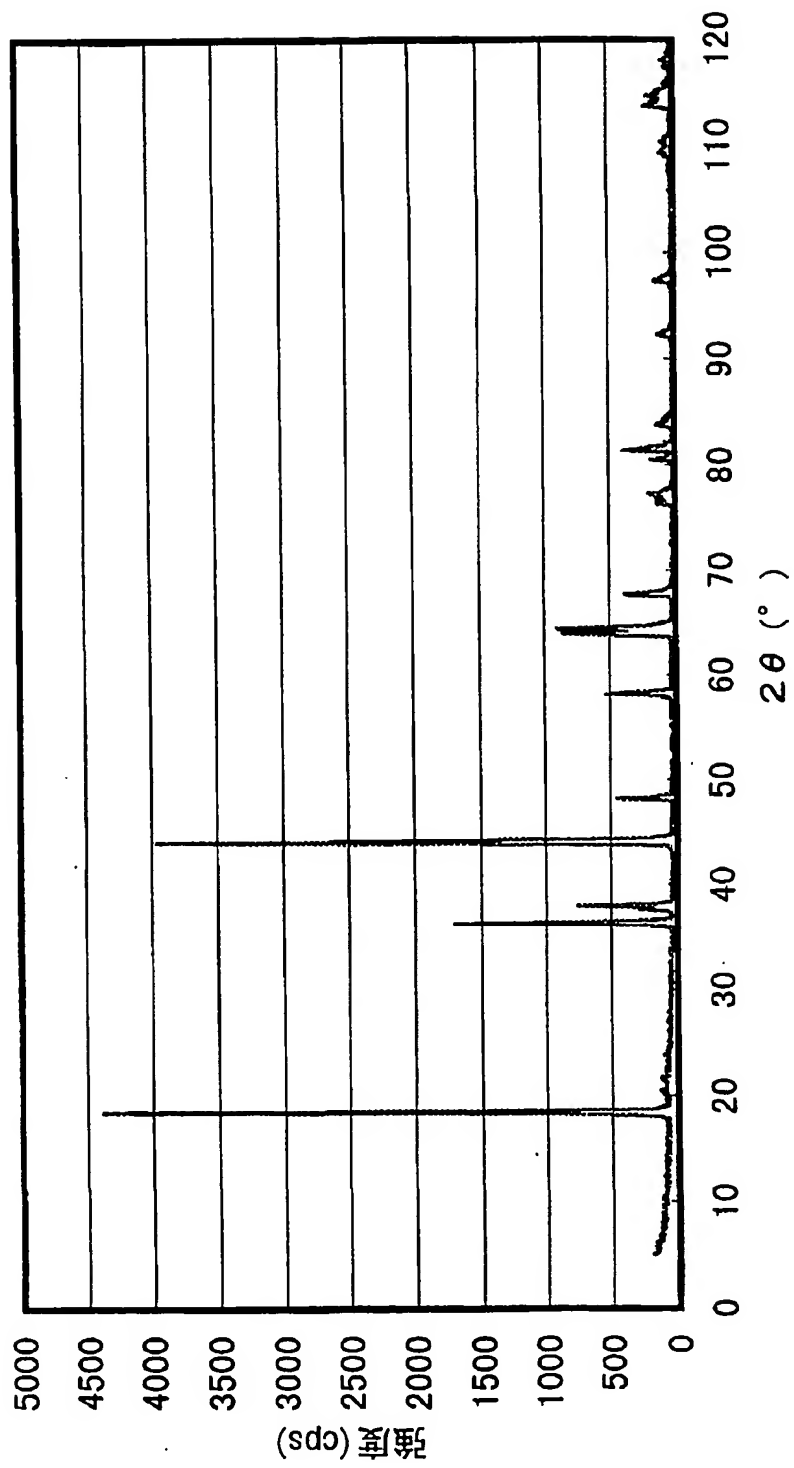


図 4

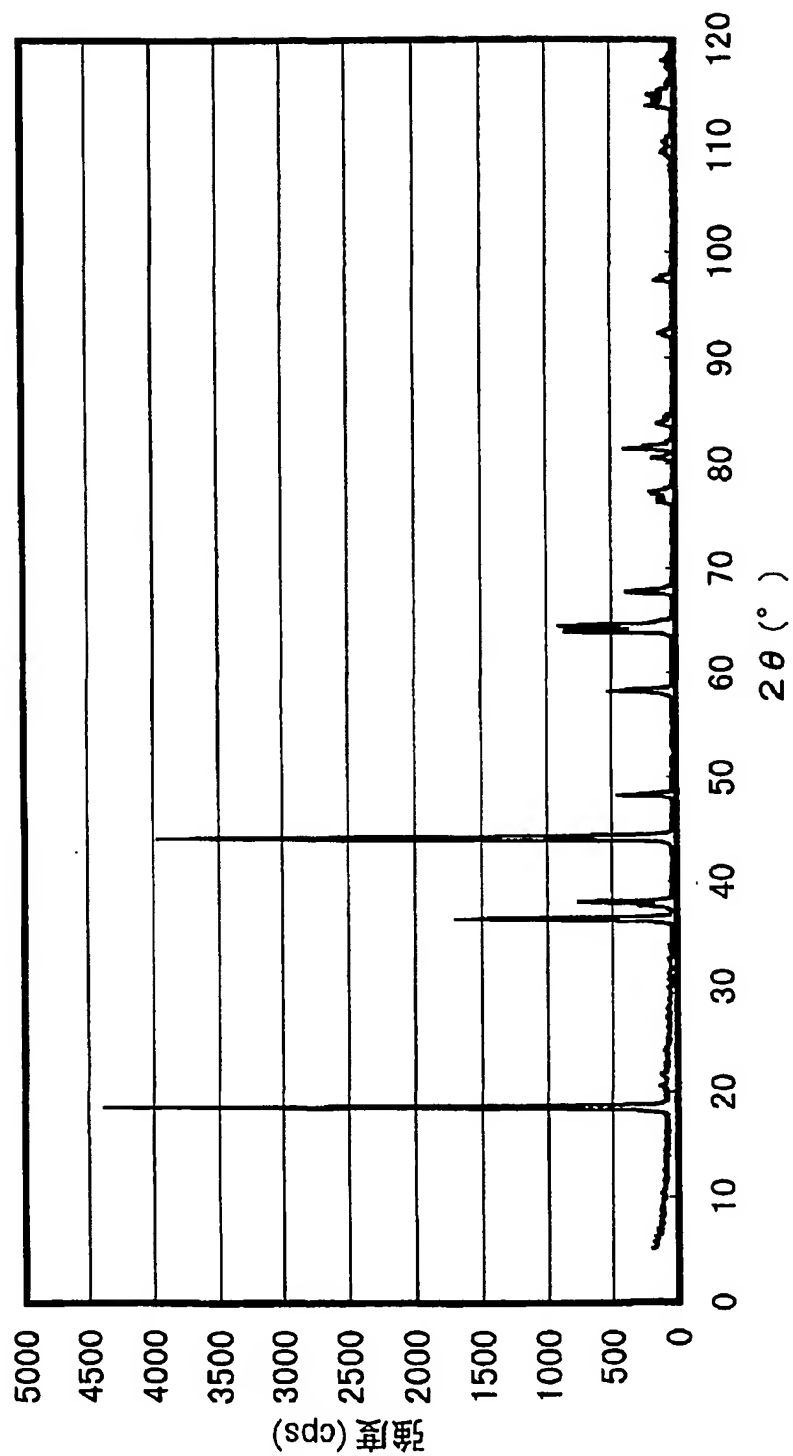


図 5

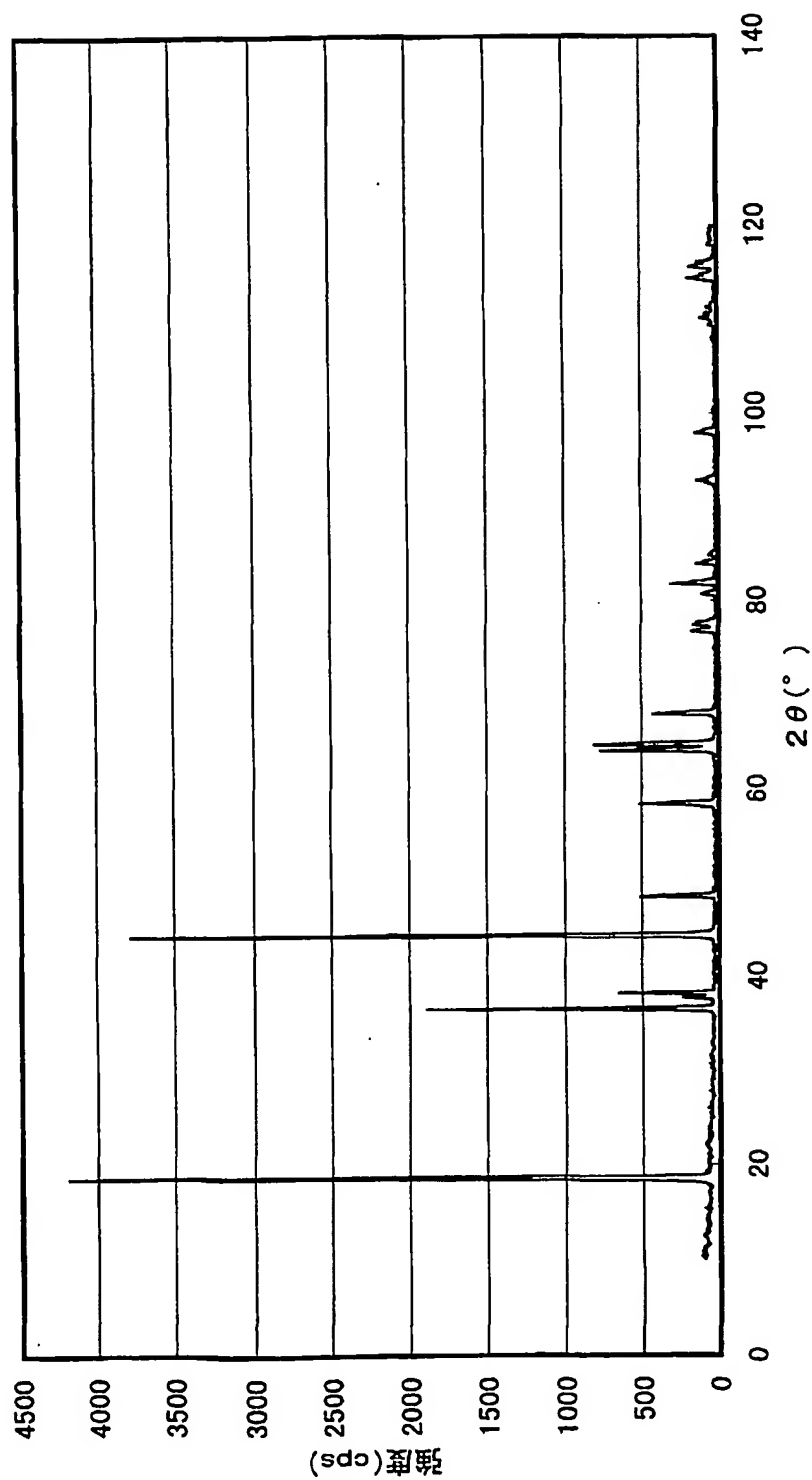


図 6

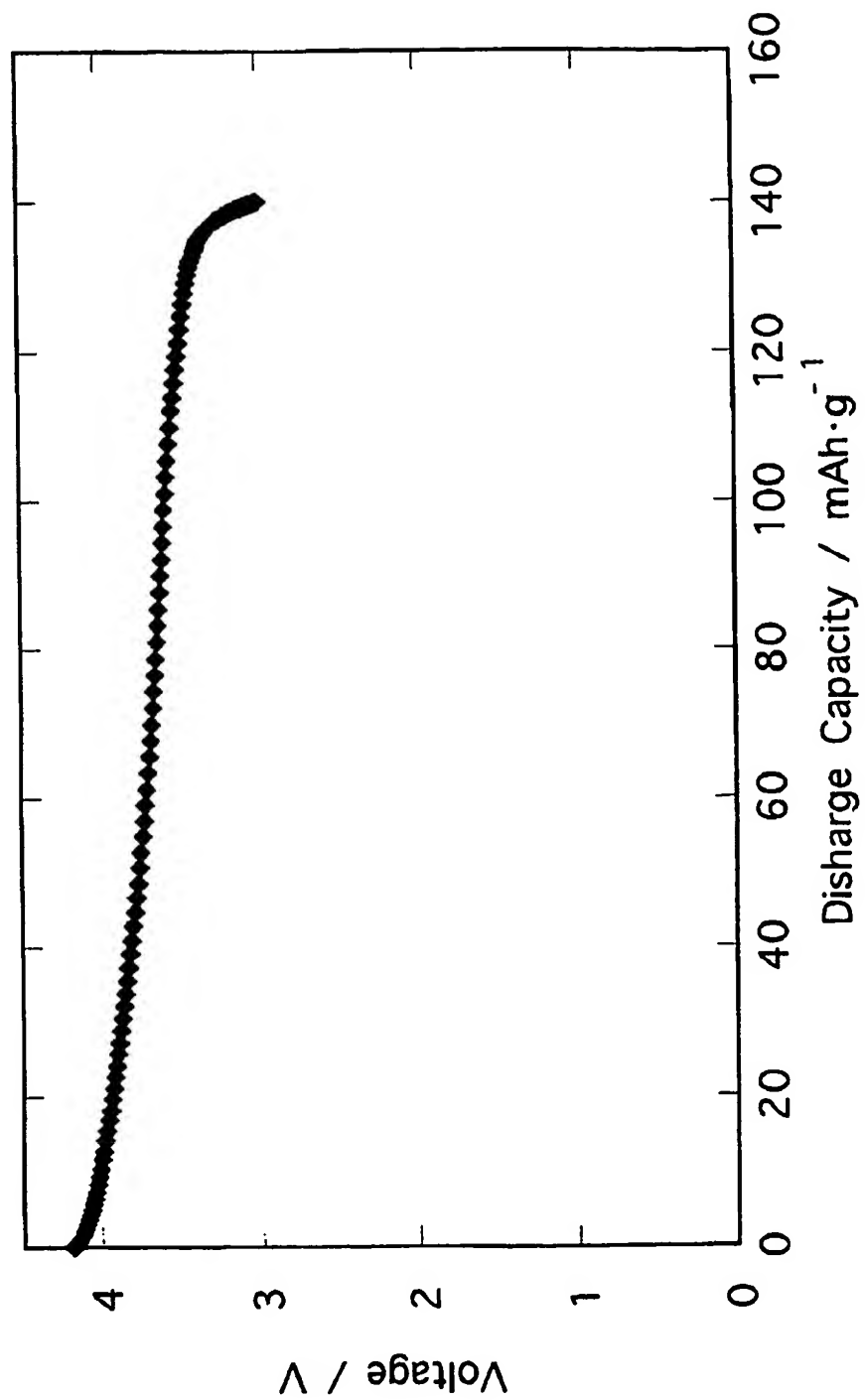


図 7

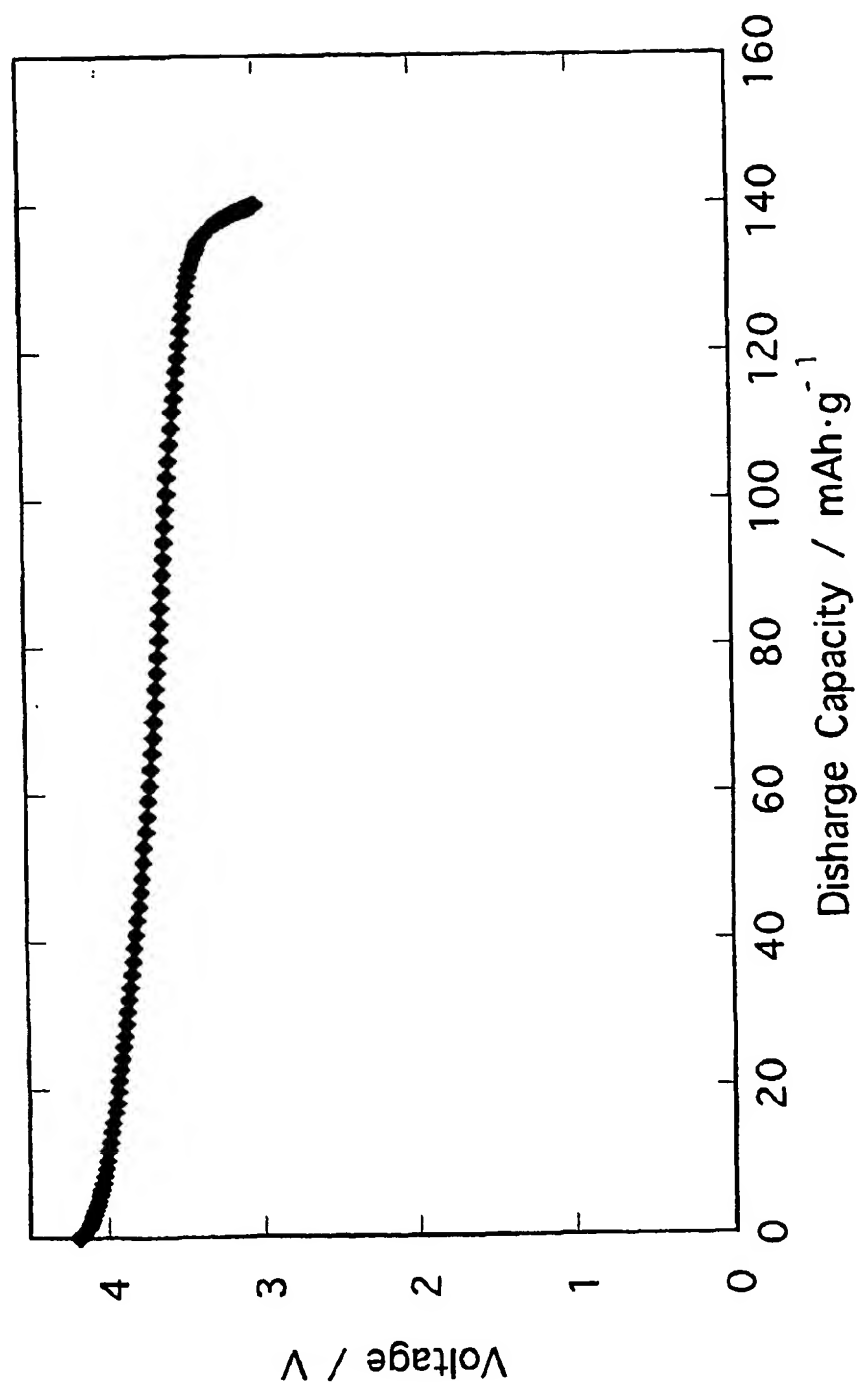
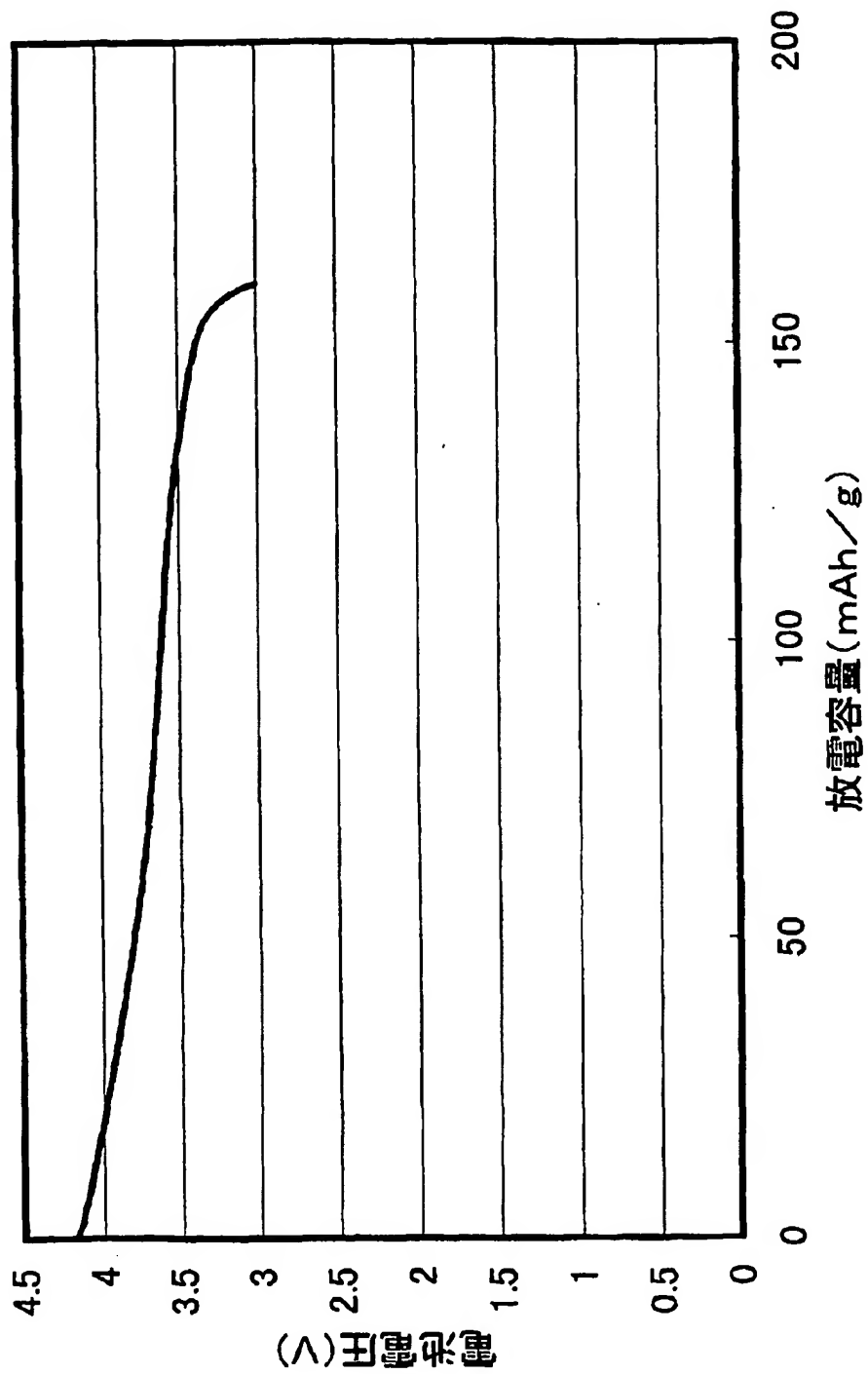


図 8



# INTERNATIONAL SEARCH REPORT

International application No.

PCT/JP02/02284

## A. CLASSIFICATION OF SUBJECT MATTER

Int.Cl.<sup>7</sup> H01M4/58, H01M4/02, H01M10/40

According to International Patent Classification (IPC) or to both national classification and IPC

## B. FIELDS SEARCHED

Minimum documentation searched (classification system followed by classification symbols)

Int.Cl.<sup>7</sup> H01M4/58, H01M4/02, H01M10/40

Documentation searched other than minimum documentation to the extent that such documents are included in the fields searched

Jitsuyo Shinan Koho	1926-1996	Toroku Jitsuyo Shinan Koho	1994-2002
Kokai Jitsuyo Shinan Koho	1971-2002	Jitsuyo Shinan Toroku Koho	1996-2002

Electronic data base consulted during the international search (name of data base and, where practicable, search terms used)

## C. DOCUMENTS CONSIDERED TO BE RELEVANT

Category*	Citation of document, with indication, where appropriate, of the relevant passages	Relevant to claim No.
X Y A	JP 2000-195516 A (Sanyo Electric Co., Ltd.), 14 July, 2000 (14.07.00), Claims 1, 3; Par. Nos. [0020], [0026] (Family: none)	1-5, 14, 15 2-12, 14, 15 13
Y	JP 05-242891 A (Sanyo Electric Co., Ltd.), 21 September, 1993 (21.09.93), Par. No. [0016]; Fig. 3 (Family: none)	9, 10
Y A	JP 09-199127 A (Matsushita Electric Industrial Co., Ltd.), 31 July, 1997 (31.07.97), Claim 1 (Family: none)	2-8, 11, 12, 14, 15 13

☒ Further documents are listed in the continuation of Box C.

☐ See patent family annex.

\* Special categories of cited documents:

"A" document defining the general state of the art which is not considered to be of particular relevance

"E" earlier document but published on or after the international filing date

"L" document which may throw doubts on priority claim(s) or which is cited to establish the publication date of another citation or other special reason (as specified)

"O" document referring to an oral disclosure, use, exhibition or other means

"P" document published prior to the international filing date but later than the priority date claimed

"T" later document published after the international filing date or priority date and not in conflict with the application but cited to understand the principle or theory underlying the invention

"X" document of particular relevance; the claimed invention cannot be considered novel or cannot be considered to involve an inventive step when the document is taken alone

"Y" document of particular relevance; the claimed invention cannot be considered to involve an inventive step when the document is combined with one or more other such documents, such combination being obvious to a person skilled in the art

"&" document member of the same patent family

Date of the actual completion of the international search

21 May, 2002 (21.05.02)

Date of mailing of the international search report

04 June, 2002 (04.06.02)

Name and mailing address of the ISA/

Japanese Patent Office

Authorized officer

Facsimile No.

Telephone No.



## INTERNATIONAL SEARCH REPORT

International application No.

PCT/JP02/02284

## C (Continuation). DOCUMENTS CONSIDERED TO BE RELEVANT

Category*	Citation of document, with indication, where appropriate, of the relevant passages	Relevant to claim No.
P, Y P, A  A	JP 2002-42813 A (Matsushita Electric Industrial Co., Ltd.), 08 February, 2002 (08.02.02), Claims 1, 3; Par. No. [0014] (Family: none)  EP 554906 A1 (Matsushita Electric Industrial Co., Ltd.), 11 August, 1993 (11.08.93), Claim 1 & US 5393622 A                      & JP 06-96768 A Claim 1	2-5, 11, 12, 14, 15 13  1-15

## A. 発明の属する分野の分類 (国際特許分類 (IPC))

Int. Cl<sup>7</sup> H01M 4/58, H01M 4/02, H01M 10/40

## B. 調査を行った分野

## 調査を行った最小限資料 (国際特許分類 (IPC))

Int. Cl<sup>7</sup> H01M 4/58, H01M 4/02, H01M 10/40

## 最小限資料以外の資料で調査を行った分野に含まれるもの

日本国実用新案公報 1926-1996年  
 日本国公開実用新案公報 1971-2002年  
 日本国登録実用新案公報 1994-2002年  
 日本国実用新案登録公報 1996-2002年

## 国際調査で使用した電子データベース (データベースの名称、調査に使用した用語)

## C. 関連すると認められる文献

引用文献の カテゴリー*	引用文献名 及び一部の箇所が関連するときは、その関連する箇所の表示	関連する 請求の範囲の番号
X Y A	JP 2000-195516 A (三洋電機株式会社), 2000. 07. 14, 請求項1, 3, 【0020】, 【0026】, (ファミリーなし)	1~5, 14, 15 2~12, 14, 15 13
Y	JP 05-242891 A (三洋電機株式会社), 1993. 09. 21, 【0016】, 図3, (ファミリーなし)	9, 10
Y A	JP 09-199127 A (松下電器産業株式会社), 1997. 07. 31, 請求項1, (ファミリーなし)	2~8, 11, 12, 14, 15 13

☒ C欄の続きにも文献が列挙されている。☐ パテントファミリーに関する別紙を参照。

## \* 引用文献のカテゴリー

「A」 特に関連のある文献ではなく、一般的技術水準を示すもの  
 「E」 国際出願日前の出願または特許であるが、国際出願日後に公表されたもの  
 「L」 優先権主張に疑義を提起する文献又は他の文献の発行日若しくは他の特別な理由を確立するために引用する文献 (理由を付す)  
 「O」 口頭による開示、使用、展示等に関する文献  
 「P」 国際出願日前で、かつ優先権の主張の基礎となる出願

## の日の後に公表された文献

「T」 国際出願日又は優先日後に公表された文献であって出願と矛盾するものではなく、発明の原理又は理論の理解のために引用するもの  
 「X」 特に関連のある文献であって、当該文献のみで発明の新規性又は進歩性がないと考えられるもの  
 「Y」 特に関連のある文献であって、当該文献と他の1以上の文献との、当業者にとって自明である組合せによって進歩性がないと考えられるもの  
 「&」 同一パテントファミリー文献

国際調査を完了した日

21. 05. 02

国際調査報告の発送日

04.06.02

国際調査機関の名称及びあて先

日本国特許庁 (ISA/J P)  
 郵便番号100-8915  
 東京都千代田区霞が関三丁目4番3号

特許庁審査官 (権限のある職員)

天野 斉

4X

3132

電話番号 03-3581-1101 内線 3477

C (続き) . . . 関連すると認められる文献		
引用文献の カテゴリー*	引用文献名 及び一部の箇所が関連するときは、その関連する箇所の表示	関連する 請求の範囲の番号
P, Y	JP 2002-42813 A (松下電器産業株式会社), 2002. 02. 08 請求項 1, 3, 【0014】, (ファミリーなし)	2~5, 11, 12,
P, A		14, 15
A		13
	EP 554906 A1 (MATSUSHITA ELECTRIC INDUSTRIAL CO., LTD.), 1993. 08. 11, 請求項 1, & US 5393622 A & JP 06-96768 A, 請求項 1	1~15

INTERNATIONAL PUBLICATION WO02/073718 A1

**POSITIVE ELECTRODE ACTIVE MATERIAL AND NONAQUEOUS ELECTROLYTE  
SECONDARY CELL COMPRISING THE SAME**

[Translated from Japanese]

[Translation No. LPX20425]

Translation Requested by: Jim McDonell 3M

Translation Provided by: Yoko and Bob Jasper  
Japanese Language Services  
16 Oakridge Drive  
White Bear Lake, MN 55110

(651) 426-3017 Fax (651) 426-8483  
e-mail: [bjasper@attbi.com](mailto:bjasper@attbi.com)

WORLD PATENT  
INTERNATIONAL AFFAIRS BUREAU  
WORLD INTELLECTUAL PROPERTY ORGANIZATION  
International Patent Publication on  
the basis of Patent Cooperation Treaty  
INTERNATIONAL PUBLICATION WO02/073718 A1

51) International Patent Classification: H 01 M 4/58, 4/02, 10/40

21) International Patent Application No.: PCT/JP02/02284

22) International Patent Application Date: March 12, 2002

43) International Patent Publication Date: September 19, 2002

30) Priority Claim No.: JP 2001-071486  
JP 2001-080430  
JP 2001-080434

Priority Claim Date: March 14, 2001  
March 21, 2001  
March 21, 2001

Priority Country: Japan JP  
Japan JP  
Japan JP

72) Inventors, and

75) Applicants (for USA alone):

Kazuya Okabe  
Ryuji Shiozaki  
Akihiro Fujii  
Akinori Itoh, and  
Hiroshi Yufu  
c/o Yuasa Corp.  
2-3-21 Kosobe-cho

Takatsuki-shi, Osaka-fu 569-1115

74) Agents:  
Teruo Naito  
Shiei Patent Office  
Arc Mori Building 29F  
1-12-32 Akasaka  
Minato-ku, Tokyo 107-6029

81) Appointed Countries (Domestic):

AE, AG, AL, AM, AT, AU, AZ, BA, BB, BG, BR, BY, BZ, CA, CH, CN, CO, CR, CU, CZ, DE, DK, DM, DZ, EC, EE, ES, FL, GB, GD, GE, GH, GM, HR, HU, ID, IL, IS, JP, KE, KG, KP, KR, KZ, LC, LK, LR, LS, LT, LU, LV, MA, MD, MG, MK, MN, MW, MX, MZ, NO, NZ, OM, PH, PL, PT, RO, RU, SD, SE, SG, SI, SK, SL, TJ, TM, TN, TR, TT, TZ, UA, UG, US, UZ, VN, YU, ZA, ZM, ZW.

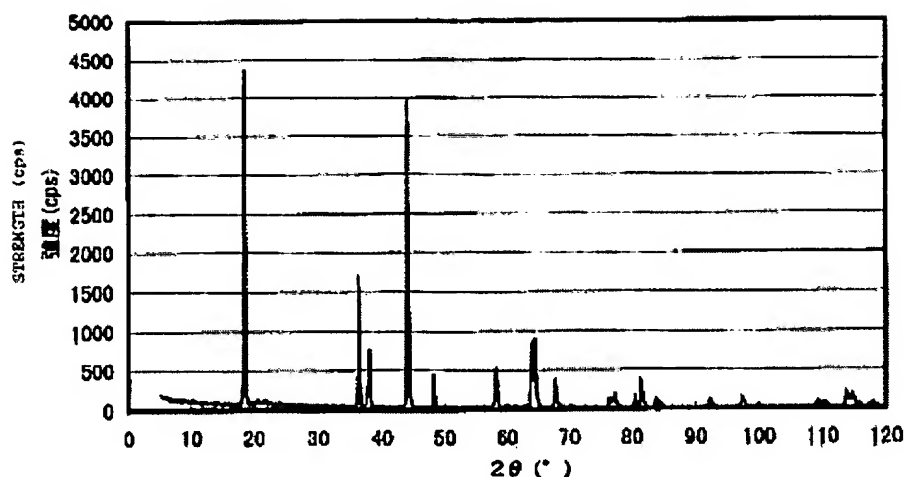
84) Appointed Countries (Wide regions): ARIPO patents (GH, GM, KE, LS, MW, MZ, SD, SL, SZ, TZ, UG, ZM, ZW), Eurasia patents (AM, AZ, BY, KG, KZ, MD, RU, TJ, TM), European Patents (AT, BE, CH, CY, DE, DK, ES, FI, FR, GB, GR, IE, IT, LU, MC, NL, PT, SE, TR), OAPI patents (BF, BJ, CF, CG, CI, CM, GA, GN, GQ, ML, MR, NE, SN, TD, TG).

Attachment International Search Report

For two letter codes and other abbreviation, see "Guide Notes for Codes and Abbreviations" listed on front of each PCT Gazette bulletin.

(54) Title: POSITIVE ELECTRODE ACTIVE MATERIAL AND NONAQUEOUS ELECTROLYTE SECONDARY CELL COMPRISING THE SAME [Seikyoku kasseibutsu oyobi koreo mochiita hisuiden'kaishitsu nijiden'chi]

(57) Abstract: [English, included] A positive electrode active material for producing a nonaqueous electrolyte secondary cell exhibiting an excellent high-rate charging/discharging performance and an excellent charging/discharging cycle performance and having a high energy density, and a nonaqueous electrolyte secondary cell exhibiting an excellent high-rate charging/discharging performance and an excellent charging/discharging cycle performance and having a high energy density. The main component of the positive electrode active material is a Li-Mn-Ni composite oxide, and the positive electrode active material is characterized in that the specific surface of the Li-Mn-Ni composite oxide measured by the BET method is  $0.3 \text{ m}^2/\text{g}$  or above and  $1.5 \text{ m}^2/\text{g}$  or below. The nonaqueous electrolyte secondary cell comprises such a positive electrode active material.



[Translator's note: vertical axis should be labeled "Intensity (cps)"]

(57) Abstract:

Production of a positive electrode active material capable of producing a nonaqueous secondary cell with high energy density exhibiting an excellent high-rate charging/discharging performance and a nonaqueous secondary cell with high energy density exhibiting an excellent high-rate charging/discharging performance and an excellent charging/discharging cycle performance.

A positive electrode active material mainly comprising a Li-Mn-Ni type composite oxide, and the positive electrode active material is characterized by the fact that the specific surface of the Li-Mn-Ni composite oxide measured by the BET method is  $0.3 \text{ m}^2/\text{g}$  or above and  $1.5 \text{ m}^2/\text{g}$  or below, and nonaqueous electrolyte secondary cell comprising the same.

[p. 1]

#### Specification

Positive electrode active material and nonaqueous secondary cell comprising the same

<Technical Field>

The present invention pertains to a positive electrode active material and a nonaqueous secondary cell comprising the same.

<Background>

Nonaqueous secondary cells such as lithium secondary cells exhibit high energy density and high voltage and are widely used as the power sources for compact portable terminals, mobile communication devices, etc. For the positive electrode active material of the lithium secondary cell, a stable crystalline structure and high electrochemical working performance are required despite repeated insertion and removal of lithium. For those with an operating voltage of around 4 V, transition metal oxides with a basic structure of a layer comprising lithium cobalt oxide, lithium nickel oxide, or lithium manganese oxide having spinel structure are known.

Currently, as positive electrode active materials for nonaqueous secondary cells with an operating voltage of around 4 V, composite oxides of lithium and a transition metal such as  $\text{LiCoO}_2$ ,  $\text{LiNiO}_2$ ,  $\text{LiMnO}_2$  and  $\text{LiMn}_2\text{O}_4$  are known. In particular, among positive electrode active materials with  $\alpha\text{-NaFeO}_2$  structure from which a high energy density can be expected, lithium cobalt composite oxide indicated by  $\text{LiCoO}_2$  is widely used for consumer lithium ion cells, but cobalt is a rare metal and the cost is high. Furthermore, lithium nickel composite oxide indicated by  $\text{LiNiO}_2$ , etc. lack stability at high temperatures, thus, safety is hard to come by and practical application is not possible. And furthermore, lithium manganese oxide having a spinel structure indicated by  $\text{LiMn}_2\text{O}_4$ , etc. is an inexpensive and safe positive electrode active material, but the energy density per unit weight is approximately 70% that of lithium cobalt composite oxide, and is used in some areas, but is not widely applied.

On the other hand, principally, high capacity can be expected from  $\text{LiMnO}_2$ , and the safety level is high; thus, it is widely studied. For the aforementioned  $\text{LiMnO}_2$ ,  $\beta\text{-NaMnO}_2$  type rhombic system layer structure having a zigzag layer structure, and  $\alpha\text{-NaFeO}_2$  type monoclinic system structure having halite layer structure are known.

[p. 2]

A higher capacity can be expected from the aforementioned  $\text{LiMnO}_2$  having rhombic system structure than that of the aforementioned  $\text{LiMn}_2\text{O}_4$ , but when charge/discharge is



repeated, slow conversion to the spinel phase occurs; thus, stability with regard to the charge/discharge cycle becomes inferior. Furthermore, a poor high efficiency charge/discharge performance in  $\text{LiMnO}_2$  having the aforementioned monoclinic system structure, and reduction in capacity that accompanies the charge/discharge cycle are reported in, for example, Chiang, Y.-M.; Sadoway, D.R.; Jang, Y.-I.; Huang, B.; Wang, H. High Capacity, Temperature-Stable Lithium Aluminium [sic] Manganese Oxide Cathodes for Rechargeable Batteries. *Electrochem. Solid-State Lett.* 2(3), 1999, 107-110.

In order to eliminate the above-mentioned problems, a technology in which the Mn in  $\text{LiMnO}_2$  is replaced with Al, Fe, Co, Ni, Mg, or Cr in an amount in the range of  $1-y$  ( $0.5 \leq y \leq 1$ ), and at the same time, a voltage of 4.0 V to 4.8 V is applied between the positive electrode and the negative electrode at a temperature of 60 to  $100^\circ\text{C}$  and the change in crystalline structure is accelerated and improvement in high efficiency charge/discharge performance is achieved is disclosed in Japanese Kokai [Unexamined] Patent Application No. 2001-23617. However, high efficiency charge/discharge performance remains insufficient despite the above-mentioned technologies.

Furthermore, the aforementioned lithium manganese oxide has many technical problems associated with it upon application as well. Poor cycle performance and storage performance, especially at high temperatures, pose problems.

Furthermore, when  $\text{LiNi}_{1-\alpha}\text{Mn}_\alpha\text{O}_2$  having the crystal structure of the space group  $R\bar{3}m$  is considered as a structure where a part of the Ni in  $\text{LiNiO}_2$  is replaced with Mn, baking at a temperature of  $800^\circ\text{C}$  or above is required to secure the replacement of the Ni site with Mn. However, Ni or Mn enters the site in the crystal where Li is normally located when the above-mentioned high temperature is used, and the crystalline structure is disturbed, and capacity or cycle performance is reduced. A technology in which 0.05 to 0.30 is used for the value of the aforementioned  $\alpha$  and baking is done at a temperature in the range of  $600^\circ\text{C}$  to  $800^\circ\text{C}$  is disclosed in Japanese Kokai [Unexamined] Patent Application No. Hei 8-171910, but the cycle

performance remains inadequate despite the aforementioned technology.

As a means to eliminate the above-mentioned problems, technology concerning the electrochemical performance of  $\text{LiMn}_a\text{Ni}_b\text{Co}_c\text{O}_2$  where a part of Ni in  $\text{LiNiO}_2$  is replaced with Mn and Co is known. For example, a report on Li composite oxide concerning a, b, c are such that  $0.02 \leq a \leq 0.5$ ,  $0.02 \leq b/(b+c) \leq 0.9$ ,  $b > 0.34$  and  $a+b+c=1$  is disclosed in Japanese Patent Application No. 3244314. However, according to the follow-up study by the present inventors, thermal stability at the time of charging remains inadequate. The reason for this is not well understood, but it is hypothesized that the method of manufacturing the Li composite oxide in the aforementioned report includes mechanical mixing of solid materials, and diffusion of the metal element is incomplete at the time of the baking process that follows and partial phase separation occurs, and as a result, thermal stability becomes inferior. Furthermore, the particles of the Li composite produced by excessive pulverization of the raw material become very fine, and when the said material is used as the positive electrode of cell, a side reaction such as oxidation decomposition of electrolyte occurs since the positive electrode comes in full contact with the electrolyte, and deterioration with time is likely to occur as well.

Furthermore, among  $\text{LiMn}_a\text{Ni}_b\text{Co}_c\text{O}_2$  compositions, a report concerning  $\text{LiCo}_{0.33}\text{Ni}_{0.33}\text{Mn}_{0.33}\text{O}_2$  composition is Yoshinari Makimura, Naoaki Yabuuchi, Tsutomu Ohzuku, Yukinori Kayama, Isao Tanaka, and Hirohiko Adachi, Lithium Insertion Material of  $\text{LiCo}_{1/3}\text{Ni}_{1/3}\text{Mn}_{1/3}\text{O}_2$  for Advanced Batteries; (II) Synthesis and Characterization as a Possible Alternative to  $\text{LiCoO}_2$ , The 42th [sic] Battery Symposium [sic] in Japan, 2118, 2119(2001). The above-mentioned Li composite oxide is produced by mixing a coprecipitate compound produced by adding an alkali to an aqueous solution of Mn, Ni, and Co with a Li compound and providing a heat treatment.

However, definition of the properties on the Li composite oxide produced is not included in the aforementioned report. The lattice volume of the above-mentioned Li composite oxide is reduced by charging and increased by discharging; thus, the trapping speed of the Li in the active

material at the time of discharging is significantly reduced in comparison to the removal speed of Li at the time of charging. Therefore, when the maximum caution is taken for the factors responsible to have a high influence on the trapping speed of Li to the positive electrode as in the contact interfacial state of the active material and electrolyte, it is not possible to produce a cell having an adequate charge/discharge performance. Thus, it is essential to define the properties of the active material that determines the above-mentioned factors upon application of the cell in which the above-mentioned active material is used as the positive electrode.

[p. 4]

It should be noted that "R3/m" is used in the present specification where the horizontal bar is to be applied above the 3 of "R3m" to indicate space group for convenience.

The present invention is to eliminate the above-mentioned existing problems, and the purpose of the present invention is to produce a positive electrode active material for producing a nonaqueous electrolyte secondary cell exhibiting excellent high-rate charging/discharging performance and an excellent charging/discharging cycle performance and having a high energy density, and a nonaqueous electrolyte secondary cell exhibiting an excellent high-rate charging/discharging performance and an excellent charging/discharging cycle performance and having a high energy density.

#### <Disclosure of the invention>

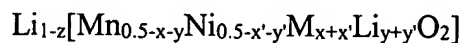
As a result of much research conducted by the present inventors in an effort to eliminate the above-mentioned existing problems, they discovered that a nonaqueous secondary cell having excellent cell performance could be produced when properties of a positive electrode active material having a specific structure were specified, and as a result, the present invention was accomplished. In other words, the technical structure and effect of the present invention are as described below provided that the assumption is included that the present invention is not limited to the correctness/incorrectness of the working mechanism.

- (1) A positive electrode active material mainly comprising a Li-Mn-Ni type composite

oxide, and the positive electrode active material is characterized by the fact that the specific surface of the Li-Mn-Ni composite oxide measured by the BET method is 0.3 m<sup>2</sup>/g or above and 1.5 m<sup>2</sup>/g or below.

(2) The positive electrode active material described in (1) above characterized by the fact that the aforementioned Li-Mn-Ni type composite oxide is the composite oxide indicated by LiMn<sub>0.5</sub>Ni<sub>0.5</sub>O<sub>2</sub>.

(3) The positive electrode active material described in (1) above characterized by the fact that a part of Mn and Ni that comprise the composite oxide indicated by LiMn<sub>0.5</sub>Ni<sub>0.5</sub>O<sub>2</sub> in the aforementioned Li-Mn-Ni type composite oxide is replaced with a dissimilar element and is a composite oxide with a composition indicated by the following general formula.



(Wherein, M is the aforementioned dissimilar element;

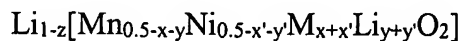
$$x=0.001 \text{ to } 0.1 \quad ; \quad x'=0.001 \text{ to } 0.1 \quad ;$$

$$y=0 \text{ to } 0.1 \quad ; \quad y'=0 \text{ to } 0.1 \quad ;$$

$$x+x'+y+y' \leq 0.4 ; \quad 0 \leq z \leq 1)$$

[p. 5]

(4) The positive electrode active material described in the (1) above characterized by the fact that a part of Mn and Ni that comprises the composite oxide indicated by LiMn<sub>0.5</sub>Ni<sub>0.5</sub>O<sub>2</sub> in the aforementioned Li-Mn-Ni type composite oxide is replaced with a dissimilar element and is a composite oxide with a composition indicated by the following general formula.



(Wherein, M is the aforementioned dissimilar element;

$$x=0.01 \text{ to } 0.1 \quad ; \quad x'=0.01 \text{ to } 0.1 \quad ;$$

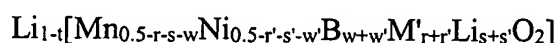
$$y=0 \text{ to } 0.1 \quad ; \quad y'=0 \text{ to } 0.1 \quad ;$$

$$x+x'+y+y' \leq 0.2 ; \quad 0 \leq z \leq 1)$$

(5) The positive electrode active material described in the aforementioned (3) or (4)

characterized by the fact that the aforementioned dissimilar element M is one or more elements selected from the group consisting of B, Mg, Al, Ti, V, Cr, Fe, Co, Cu, and Zn.

(6) The positive electrode active material described in the above-mentioned (1) characterized by the fact that a part of Mn and Ni that comprise the composite oxide indicated by  $\text{LiMn}_{0.5}\text{Ni}_{0.5}\text{O}_2$  in the aforementioned Li-Mn-Ni type composite oxide is replaced with a dissimilar element and boron and is a composite oxide with a composition indicated by the following general formula.



(Wherein, M' is the aforementioned dissimilar element;

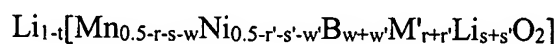
$$r=0.001 \text{ to } 0.1 \quad ; \quad r'=0.001 \text{ to } 0.1 \quad ;$$

$$s=0 \text{ to } 0.1 \quad ; \quad s'=0 \text{ to } 0.1 \quad ;$$

$$r+r'+s+s'+w+w' \leq 0.4 \quad ;$$

$$w+w'=0.0005 \text{ to } 0.01 \quad ; \quad 0 \leq t \leq 1)$$

(7) The positive electrode active material described in the (1) above characterized by the fact that a part of Mn and Ni that structures the composite oxide indicated by  $\text{LiMn}_{0.5}\text{Ni}_{0.5}\text{O}_2$  in the aforementioned Li-Mn-Ni type composite oxide is replaced with a dissimilar element and boron and is a composite oxide with the composition indicated by the following general formula.



[p. 6]

(Wherein, M' is the aforementioned dissimilar element;

$$r=0.01 \text{ to } 0.1 \quad ; \quad r'=0.01 \text{ to } 0.1 \quad ;$$

$$s=0 \text{ to } 0.1 \quad ; \quad s'=0 \text{ to } 0.1 \quad ;$$

$$r+r'+s+s'+w+w' \leq 0.2 \quad ;$$

$$w+w'=0.0005 \text{ to } 0.01 \quad ; \quad 0 \leq t \leq 1)$$

(8) The positive electrode active material described in the above-mentioned (6) or (7)

characterized by the fact that the aforementioned dissimilar element M' is one or more elements selected from the group consisting of B, Mg, Al, Ti, V, Cr, Fe, Co, Cu, and Zn.

(9) The positive electrode active material described in the (1) above characterized by the fact that the aforementioned Li-Mn-Ni type composite oxide is a composite oxide indicated by  $\text{Li}[\text{Mn}_c\text{Ni}_d\text{Co}_e\text{Li}_a\text{M}''_b]\text{O}_2$  (Wherein, M'' is an element other than Mn, Ni, Co or Li,  $d \leq c+e+a+b$ ,  $c+d+e+a+b=1$ ,  $0 \leq a \leq 0.05$ ,  $0 \leq b \leq 0.05$ ,  $0.2 \leq c \leq 0.05$ ,  $0.02 \leq e \leq 0.4$ ).

(10) The positive electrode active material described in the above-mentioned (9) characterized by the fact that the aforementioned M'' is one or more elements selected among the group consisting of B, Mg, Al, Ti, V, Cr, Fe, Co, Cu, and Zn.

(11) The positive electrode active material described in one of (1) to (10) above characterized by the fact that the aforementioned Li-Mn-Ni type composite oxide has a layer crystalline structure having peaks at  $2\theta = 18.61 \pm 1^\circ$ ,  $36.6 \pm 1^\circ$ ,  $37.8 \pm 1^\circ$ ,  $38.2 \pm 1^\circ$ ,  $44.3 \pm 1^\circ$ ,  $48.4 \pm 1^\circ$ ,  $58.4 \pm 1^\circ$ ,  $64.2 \pm 1^\circ$ ,  $64.8 \pm 1^\circ$ ,  $68.8 \pm 1^\circ$  on the X-ray diffraction chart that utilizes  $\text{CuK}\alpha$  ray.

(12) The positive electrode active material described in one of (1) to (11) above characterized by the fact that the aforementioned Li-Mn-Ni type composite oxide has a relative intensity ratio of the diffraction peak of  $2\theta = 44.1 \pm 1^\circ$  for the diffraction peak of  $2\theta = 18.6 \pm 1^\circ$  on the powder X-ray diffraction chart that utilizes  $\text{CuK}\alpha$  rays.

(13) The positive electrode active material described in one of (1) to (12) above characterized by the fact that the aforementioned Li-Mn-Ni type composite oxide has the half-bandwidth of the diffraction peak at  $2\theta = 18.6 \pm 1^\circ$  in the range of  $0.13^\circ$  to  $0.20^\circ$  and the half bandwidth of the diffraction peak at  $2\theta = 44.1 \pm 1^\circ$  in the range of  $0.10^\circ$  to  $0.17^\circ$  on the powder X-ray diffraction chart that utilizes  $\text{CuK}\alpha$  rays.

[p. 7]

(14) The positive electrode active material described in one of (1) to (13) above characterized by the fact that the particle diameter of the aforementioned Li-Mn-Ni type

composite oxide is in the range of 3  $\mu\text{m}$  to 20  $\mu\text{m}$ .

(15) The nonaqueous secondary cell that utilizes the positive electrode active material described in one of (1) to (14) above.

The present inventors placed their focus on the  $\text{LiMnO}_2$  from which high capacity can be expected, and as an element used to substitute Mn, Ni having good solubility with Mn and operating potential of around 4 V was selected. As a result, it was confirmed that the operating potential was 4.3 V to 3.0 V and good compatibility with conventional lithium ion cells was achieved in  $\text{LiMn}_{0.5}\text{Ni}_{0.5}\text{O}_2$  where the ratio of the substitution was 50% and a high-rate discharge capacity of 140 mAh/g could be achieved. However, charge/discharge cycle performance was inadequate. It was hypothesized that elution of Mn occurred from the positive electrode active material as a result of repeated charge/discharge and that an increase in electrode interfacial resistance was initiated.

Based on the above background, and as a result of much research done by the present inventors, in an effort to eliminate the above-mentioned existing problems, on the relationship between  $\text{LiMn}_{0.5}\text{Ni}_{0.5}\text{O}_2$  having different properties and compositions where a part of Ni and Mn elements that comprise  $\text{LiMn}_{0.5}\text{Ni}_{0.5}\text{O}_2$  replaced with other elements (hereinafter referred to as Li-Mn-Ni type composite oxide, at times) and the charge/discharge cycle performance, and to their surprise, they discovered that a very stable charge/discharge cycle performance could be achieved when the value of the specific surface area was specified. In other words, excellent charge/discharge cycle performance can be achieved when the value of the aforementioned specific surface area is specified at 1.5  $\text{m}^2/\text{g}$  or below.

The above-mentioned effect achieved cannot be fully explained, but it is hypothesized that the area of the positive electrode active material Li-Mn-Ni type composite oxide that comes in contact with the electrolyte is reduced as a result of reduction in the specific surface area, and oxidation decomposition of the electrolyte is controlled, and furthermore, the moisture slightly adsorbed to the surface of the grain of the aforementioned positive electrode active material is

reduced with a reduction in the specific surface area; thus, formation ratio of the hydrofluoric acid (HF) in the cell due to moisture is reduced, and decomposition reaction of Mn due to the above-mentioned acid is less likely to occur.

[p. 8]

It was further recognized that high discharge capacity could be retained even when high-rate discharge of 2 It (0.5 hr) was carried out when the value of the aforementioned specific surface area was defined at 0.3 m<sup>2</sup>/g or above.

Furthermore, when further research was conducted by the present inventors on the composition where a part of Ni and Mn among elements that comprise the LiMn<sub>0.5</sub>Ni<sub>0.5</sub>O<sub>2</sub> among Li-Mn-Ni type composite oxide was replaced with other dissimilar elements, to their surprise, a further improvement in the high-rate discharge performance was possible when the type of the aforementioned dissimilar elements was specified.

The above-mentioned effect cannot be fully explained, but the atomic radius, that is, the size of the aforementioned dissimilar element is different from the atomic radius of Mn or Ni; thus, it has an effect on the layer structure of the positive electrode active material, the mobility path of the Li ion is affected, and ion conduction is improved. Furthermore, the atomic radius, that is, the size of the aforementioned dissimilar elements other than Mn and Ni vary; thus, it seems that distortion based on expansion or contraction of the active crystal that accompanies the charge/discharge process is modified as a result of the inclusion of elements with different size.

It is further hypothesized that the close relationship of surface composition is based on the fact that the exchange of the Li ion is achieved at the boundary between the positive electrode active material particle and the electrolyte.

Furthermore, when a further study of the baking conditions, type, and composition of dissimilar metal elements other than Li, Mn, and Ni added at the time of synthesis of LiMn<sub>0.5</sub>Ni<sub>0.5</sub>O<sub>2</sub> was carried out, it was discovered that the structure of the crystal produced varied widely and a further increase in the charge/discharge cycle performance was made possible



depending on the type of crystal. In specific terms, it was confirmed that an excellent cycle performance could be achieved when the Li-Mn-Ni type composite oxide has a layer crystal structure having peaks at  $2\theta = 18.6\pm 1^\circ, 36.6\pm 1^\circ, 37.8\pm 1^\circ, 38.2\pm 1^\circ, 44.3\pm 1^\circ, 48.4\pm 1^\circ, 58.4\pm 1^\circ, 64.2\pm 1^\circ, 64.8\pm 1^\circ, 68.8\pm 1^\circ$  on the powder X-ray diffraction chart that utilizes  $\text{CuK}\alpha$  ray.

[p. 9]

The above-mentioned effect achieved cannot be fully explained, but it seems that distortion is insignificant and the crystal structure itself is stable in crystals having the aforementioned powder X-ray diffraction pattern. Furthermore, it seems that the structure can be further stabilized, and extraction of lithium from the aforementioned crystalline structure can be promoted at a lower potential and as a result, an increase in the charge/discharge capacity is achieved when Co is added.

Furthermore, the crystalline structure varies widely even when the same component is used when the baking temperature is from  $850^\circ\text{C}$  to  $1000^\circ\text{C}$ , and the shape of the change in potential at the time of charge/discharge varies widely as well. In particular, the high-rate discharge performance is influenced by a slight change in the temperature and baking time at the time of the aforementioned baking.

Based on the above-mentioned background, the present inventors believe that the crystalline structure is influenced by the baking conditions, and placed their focus on the relative intensity ratio of the diffraction peak of  $2\theta=44.1\pm 1^\circ$  for the diffraction peak of  $2\theta=18.6\pm 1^\circ$  on the powder X-ray diffraction chart that utilizes  $\text{CuK}\alpha$  rays for the powder produced after baking, and to their surprise, they discovered that an obvious increase in the high-rate discharge performance was observed when a lithium- manganese-nickel composite oxide having the aforementioned relative intensity of 1.1 or below was used.

The above-mentioned effect cannot be fully explained, but it seems that shifting of the lithium ion inside the solid material is facilitated when the aforementioned relative intensity is 1.1 or below.

However, when the aforementioned relative intensity is 0.6 or below, shifting of the lithium ion inside the solid material is inhibited due to slow crystal growth and charge/discharge cycle performance is reduced. Therefore, when a positive electrode active material having the aforementioned relative intensity in the range of 0.6 to 1.1 is used, production of a nonaqueous secondary cell having excellent high-rate discharge performance and excellent charge/discharge cycle performance is made possible.

Furthermore, it seems that the half bandwidth at  $2\theta=18.6\pm1^\circ$  and  $2\theta=44.1\pm1^\circ$  reflects the growth and crystal diameter of the positive electrode active material used for the cell of the present invention, and that the higher the half bandwidth, the lower the crystal diameter; but, to their surprise, it was confirmed that exceptionally good high-rate discharge performance and charge/discharge cycle performance was achieved when the half bandwidth of the diffraction peak at  $2\theta=18.6\pm1^\circ$  is in the range of  $0.13^\circ$  to  $0.20^\circ$  and the half bandwidth of the diffraction peak at  $2\theta=44.1\pm1^\circ$  is in a  $0.10^\circ$  to  $0.17^\circ$ .

[p. 10]

The above-mentioned effect cannot be fully explained, but it seems that shifting of the Li ion inside the solid material is facilitated when the half bandwidth of the diffraction peak at  $2\theta=18.6\pm1^\circ$  is  $0.20^\circ$  or below and at the same time, the half band width of the diffraction peak at  $2\theta=44.1\pm1^\circ$  is  $0.17^\circ$  or below, and improvement in high-rate discharge performance is made possible, but charge/discharge cycle performance is reduced due to the reduced stability of the crystal. Thus, an appropriate shifting of Li ion in the crystal and an adequate crystal stability can be achieved and excellent high-rate discharge performance and charge/discharge cycle performance can be achieved when the half bandwidth of the diffraction peak at  $2\theta=18.6\pm1^\circ$  is  $0.13^\circ$  or above and at the same time, the half band width of the diffraction peak at  $2\theta=44.1\pm1^\circ$  is  $0.10^\circ$  or above.

<Brief description of figures>

Fig. 1 shows the analysis results for the positive electrode active material used in the

present invention based on the X-ray photoelectric spectral (XPS). Fig. 2 is a partial cross-section view of the cells of the working examples and comparative examples. Fig. 3 is an X-ray analysis chart of the positive electrode active material of Working Example 1-1. Fig. 4 is the X-ray analysis chart of the positive electrode active material of Working Example 1-10. Fig. 5 is the X-ray analysis chart of the positive electrode active material of Working Example 4-1. Fig. 6 is the discharge performance of the cell of Working Example 1-10. And Fig. 8 is the discharge performance of the cell of Working Example 4-1.

In the figures, 1 is a safety valve, 2 is the lid, 3 is the laser weld zone, 4 is the negative electrode terminal, 5 is the positive electrode terminal, 6 is a gasket, 7 is the positive electrode plate, 8 is the separator, 9 is the negative electrode plate, and 10 is the cell jar.

<Desirable embodiment of the invention>

Embodiments of the present invention are shown below, but the present invention is not limited to these embodiments.

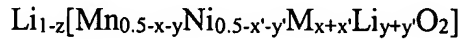
The positive electrode active material of concern in the present invention is a positive electrode active material mainly comprising an Li-Mn-Ni type composite oxide and is characterized by the fact that the specific surface of the aforementioned Li-Mn-Ni composite oxide measured by the BET method (hereinafter referred to as specific surface area, at times) is  $0.3 \text{ m}^2/\text{g}$  or above and  $1.5 \text{ m}^2/\text{g}$  or below. As described above, when the specific surface area is  $1.5 \text{ m}^2/\text{g}$  or below, a nonaqueous secondary cell (hereinafter referred to as cell, at times) having an excellent charge/discharge cycle performance can be produced, and when the specific surface area is  $0.3 \text{ m}^2/\text{g}$  or above, a cell having an excellent high-rate charge/discharge performance can be produced.

[p. 11]

A desirable embodiment of the Li-Mn-Ni type composite oxide of the present invention is explained below. However, the Li-Mn-Ni type composite oxide is not limited to the embodiment shown below.

The first form of the first embodiment of the Li-Mn-Ni type composite oxide is a composite oxide indicated by  $\text{LiMn}_{0.5}\text{Ni}_{0.5}\text{O}_2$ .

The second form of the first embodiment of Li-Mn-Ni type composite oxide is a composite oxide having a composition in which a part of Mn and Ni that comprise the composite oxide indicated by  $\text{LiMn}_{0.5}\text{Ni}_{0.5}\text{O}_2$  is substituted with a dissimilar element and is indicated by the following general formula:



(Wherein, M is the aforementioned dissimilar element,

$$x = 0.001 \text{ to } 0.1 \quad ; \quad x' = 0.001 \text{ to } 0.1 \quad ;$$

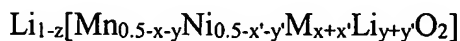
$$y = 0 \text{ to } 0.1 \quad ; \quad y' = 0 \text{ to } 0.1 \quad ;$$

$$x + x' + y + y' \leq 0.4 \quad ; \quad 0 \leq z \leq 1$$

When  $x+x'+y+y' \leq 0.4$ , the crystal structure of the composite oxide remains stable despite repeated charge/discharge and excellent charge/discharge cycle performance can be achieved.

The second embodiment of Li-Mn-Ni type composite oxide is a composite oxide having a composition in which a part of Mn and Ni that comprises the composite oxide indicated by  $\text{LiMn}_{0.5}\text{Ni}_{0.5}\text{O}_2$  is replaced with a dissimilar element and is indicated by the following general formula:

[p. 12]



(Wherein, M is the aforementioned dissimilar element,

$$x = 0.01 \text{ to } 0.1 \quad ; \quad x' = 0.01 \text{ to } 0.1 \quad ;$$

$$y = 0 \text{ to } 0.1 \quad ; \quad y' = 0 \text{ to } 0.1 \quad ;$$

$$x + x' + y + y' \leq 0.2 \quad ; \quad 0 \leq z \leq 1$$

When  $x+x'+y+y' \leq 0.2$ , the crystal structure of the composite oxide remains stable despite repeated charge/discharge and excellent charge/discharge cycle performance can be achieved.

It is desirable when the above-mentioned dissimilar element M is an element other than Mn, Ni or Li and can be substituted with Mn. For example, B, Be, V, C, Si, P, Sc, Cu, Zn, Ga, Ge, As, Se, Sr, Mo, Pd, Ag, Cd, In, Sn, Sb, Te, Ba, Ta, W, Pb, Bi, Co, Fe, Cr, Ni, Ti, Zr, Nb, Y, Al, Na, K, Mg, Ca, Cs, La, Ce, Nd, Sm, Eu, Tb, etc. can be mentioned.

It is further desirable when one of B, Mg, Al, Ti, V, Cr, Fe, Co, Cu, or Zn is used for an obvious high-rate discharge performance.

In this case, the x and y that show the substitution ratio of Mn are such that  $0 < x + y \leq 0.2$ , and x' and y' that show the substitution ratio of Ni are such that  $0 < x' + y' \leq 0.2$ . The reason is that the amount of effective lithium decreases when the substitution amount of Mn, x+y, and the substitution amount of Ni, x'+y', are increased.

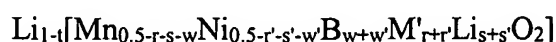
z represents the amount of lithium used, and the greater the amount of dissimilar element for Mn and Ni, the smaller the ratio.

In this case, the lithium portion indicated by  $Li_{y+y'}$  shows the composition ratio in the aforementioned formula, and does not show the arrangement state of the lithium element in the basic skeleton of  $LiMn_{0.5}Ni_{0.5}O_2$ , or does not show whether it is substituted with a part of the element that comprises the aforementioned basic skeleton.

[p. 13]

The higher the amount of the dissimilar element for Mn and Ni, the higher the high-rate discharge performance at  $0 < x' + y' \leq 0.2$  and  $0 < x + y \leq 0.2$ , and it is desirable when x and x' are at least 0.001 and at least 0.01, respectively.

The first form of the third embodiment of the Li-Mn-Ni type composite oxide is a composite oxide having a composition in which a part of Mn and Ni that comprise the composite oxide indicated by  $LiMn_{0.5}Ni_{0.5}O_2$  is substituted with a dissimilar element and boron and is indicated by the following general formula:

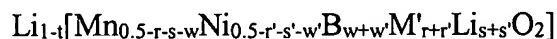


(Wherein, M' is the aforementioned dissimilar element;

$$\begin{aligned} r &= 0.001 \text{ to } 0.1 & ; & & r' &= 0.001 \text{ to } 0.1 & ; \\ s &= 0 \text{ to } 0.1 & ; & & s' &= 0 \text{ to } 0.1 & ; \\ r+r'+s+s'+w+w' &\leq 0.4 & ; & & & & \\ w+w' &= 0.0005 \text{ to } 0.01 & ; & & 0 \leq t \leq 1 & ) \end{aligned}$$

When  $r+r'+s+s'+w+w' \leq 0.4$ , the crystal structure of the composite oxide remains stable despite repeated charge/discharge, and excellent charge/discharge cycle performance can be achieved.

The second form of the third embodiment of the Li-Mn-Ni type composite oxide is a composite oxide having a composition in which a part of Mn and Ni that comprise the composite oxide indicated by  $\text{LiMn}_{0.5}\text{Ni}_{0.5}\text{O}_2$  is replaced with a dissimilar element and boron and is indicated by the following general formula:



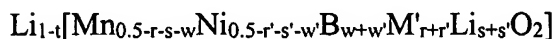
(Wherein, M' is the aforementioned dissimilar element;

$$\begin{aligned} r &= 0.01 \text{ to } 0.1 & ; & & r' &= 0.01 \text{ to } 0.1 & ; \\ s &= 0 \text{ to } 0.1 & ; & & s' &= 0 \text{ to } 0.1 & ; \\ r+r'+s+s'+w+w' &\leq 0.2 & ; & & & & \\ w+w' &= 0.0005 \text{ to } 0.01 & ; & & 0 \leq t \leq 1 & ) \end{aligned}$$

[p. 14]

When  $r+r'+s+s'+w+w' \leq 0.2$ , and the crystal structure of the composite oxide remains stable despite repeated charge/discharge, and excellent charge/discharge cycle performance can be achieved.

Furthermore, in the present specification, the composition of the positive electrode active material containing boron is shown as a dissimilar element where boron is substituted as in the case of



but it is known that the aforementioned boron undergoes dissolving by charge/discharge of the cell and is deposited onto the negative electrode. It seems that an active surface is formed on the surface of the crystal particle used as the above-mentioned positive electrode active material when elution of the boron occurs inside the cell where the positive electrode active material itself that utilizes boron as a dissimilar element is used, and as a result, the high-rate discharge performance is improved.

As a means to determine the elemental structure of the particle surface, a method in which measurement were made by X-ray photoelectric spectral analysis (XPS) as etching of the particle is being done can be mentioned. As an example, the change in the concentration of B when etching of the surface of the particle is carried out at a rate of 0.07 nm per second is shown (see Fig. 1 for reference). As shown, in the case of the particle of the sample shown by the black squares, the majority of B is collected at 400 seconds from the surface, that is, approximately 28  $\mu\text{m}$ .

It is desirable for the dissimilar element M' to be an element other than Mn, Ni, or Li and can be substituted for Mn. For example, Be, V, C, Si, P, Sc, Cu, Zn, Ga, Ge, As, Se, Sr, Mo, Pd, Ag, Cd, In, Sn, Sb, Te, Ba, Ta, W, Pb, Bi, Co, Fe, Cr, Ni, Ti, Zr, Nb, Y, Al, Na, K, Mg, Ca, Cs, La, Ce, Nd, Sm, Eu, Tb, etc. can be mentioned.

It is further desirable when one of Mg, Al, Ti, V, Cr, Fe, Co, Cu, or Zn is used for an obvious high-rate discharge performance.

In this case, r, s and w that indicate the degree of substitution of Mn are such that  $0 < r+s+w \leq 0.2$ , and r', s' and w' that indicate the degree of substitution of Ni are such that  $0 < r'+s'+w' \leq 0.2$ .

The reason is that when the degree of substitution of Mn  $0 < r+s+w$  and the degree of substitution of Ni  $0 < r'+s'+w'$  are increased, the available amount of lithium is reduced.

Furthermore,  $t$  represents the amount of lithium available, and the higher the amount of the dissimilar elements for Mn and Ni, the lower the above-mentioned amount.

The greater the amount of the dissimilar elements for Mn and Ni, the higher the degree of increase in high-rate discharge performance when  $0 < r'+s'+w' \leq 0.2$  and  $0 < r+s+w \leq 0.2$ , and it is desirable when  $r$  and  $r'$  are at least 0.001, and at least 0.01 is further desirable.

Furthermore, for the method used to replace a part of the aforementioned Mn and Ni with lithium or a dissimilar element in the second embodiment and the third embodiment of the Li-Mn-Ni type composite oxide, a method in which the substituted element is added to the baking raw material of the active material or a method in which baking is performed for  $\text{LiMn}_{0.5}\text{Ni}_{0.5}\text{O}_2$ , then substitution is performed with the dissimilar element using a method such as an ion-exchange method, etc. can be mentioned, but it is not limited to the above-mentioned methods.

The fourth embodiment of the Li-Mn-Ni type composite oxide is a composite oxide indicated by  $\text{Li}[\text{Mn}_c\text{Ni}_d\text{Co}_e\text{Li}_2\text{M}^a\text{b}]\text{O}_2$  (Wherein,  $\text{M}^a$  is an element other than Mn, Ni, Co and Li,  $d \leq c+e+a+b$ ,  $c+d+e+a+b=1$ ,  $0 \leq a \leq 0.05$ ,  $0 \leq b \leq 0.05$ ,  $0.2 \leq c \leq 0.5$ ,  $0.02 \leq e \leq 0.4$ ). When  $c$  is 0.2 or below, the cycle performance is likely to be inadequate; on the other hand, when  $c$  exceeds 0.5, not only is the cycle performance likely to be inadequate, but also impurities such as  $\text{Li}_2\text{MnO}_3$  are likely to form stably inside the raw material during the course of baking, starting from a relatively low temperature, and is not desirable. When  $e$  exceeds 0.4, thermal stability at the time of charging is likely to be poor. When  $a$  exceeds 0.05, discharge capacity is likely to be reduced.

Furthermore, when a study was conducted as the composition ratio of the structural elements was intentionally changed for an improvement in the high-rate charge/discharge performance, to their surprise, a further improvement in the high-rate discharge performance was



possible when a specific dissimilar element was added.

[p. 16]

It is desirable for the dissimilar element M" to be an element other than Mn, Ni, or Li and can be substituted with Mn. For example, B, Be, V, C, Si, P, Sc, Cu, Zn, Ga, Ge, As, Se, Sr, Mo, Pd, Ag, Cd, In, Sn, Sb, Te, Ba, Ta, W, Pb, Bi, Fe, Cr, Ni, Ti, Zr, Nb, Y, Al, Na, K, Mg, Ca, Cs, La, Ce, Nd, Sm, Eu, Tb, etc. can be mentioned.

It is further desirable when one of B, Mg, Al, Ti, V, Cr, Fe, Co, Cu, or Zn is used for obvious high-rate discharge performance.

The above-mentioned effect achieved cannot be fully explained, but the size of the aforementioned dissimilar element is different from the size of the aforementioned Mn element or Ni element, dissimilar element, is different from the atomic radius of Mn; thus, an influence is placed upon the layer structure of the positive electrode active material, the traveling path of Li ion is influenced, and ion conduction is improved.

Furthermore, the atomic radius, namely, the size, of the aforementioned dissimilar elements other than Mn and Ni vary; thus, it seems that distortion based on expansion and contraction of the active crystal that accompanies charge/discharge is modified as a result of elements with different sizes included.

Furthermore, as a means to include the aforementioned dissimilar elements in the aforementioned composite oxide in the fourth embodiment of the Li-Mn-Ni type composite oxide, a method in which the substituted element is added to the baking raw material ahead of time or a method in which baking is performed; then, substitution with the dissimilar element is achieved using a method such as an ion-exchange method, etc. can be mentioned, but it is not limited to the above-mentioned methods.

Each embodiment of the Li-Mn-Ni type composite oxide is shown absorbed, and the Li-Mn-Ni type composite oxide has peaks at  $2\theta=18.6\pm1^\circ$ ,  $36.6\pm1^\circ$ ,  $37.8\pm1^\circ$ ,  $38.2\pm1^\circ$ ,  $44.3\pm1^\circ$ ,  $48.4\pm1^\circ$ ,  $58.4\pm1^\circ$ ,  $64.2\pm1^\circ$ ,  $64.8\pm1^\circ$ ,  $68.8\pm1^\circ$  on the powder X-ray diffraction chart that utilizes

CuK $\alpha$  ray, and good cycle performance can be achieved.

[p. 17]

Furthermore, as described above, it is desirable for the Li-Mn-Ni type composite oxide to have diffraction peaks at  $2\theta=18.6\pm1^\circ$  and at  $2\theta=44.1\pm1^\circ$ , to have the relative intensity ratio of the diffraction peak of  $2\theta=44.1\pm1^\circ$  for the diffraction peak of  $2\theta=18.6\pm1^\circ$  in the range of 0.6 to 1.1, and the half bandwidth of the diffraction peak at  $2\theta=18.6\pm1^\circ$  is in the range of  $0.13^\circ$  to  $0.20^\circ$ , and the half bandwidth of the diffraction peak at  $2\theta=44.1\pm1^\circ$  is in the range of  $0.10^\circ$  to  $0.17^\circ$ .

Furthermore, the lower the particle diameter of the Li-Mn-Ni type composite oxide, the higher the specific surface area and better the output characteristics, but in order to prevent reduction in other properties, especially, storage stability, or taking coatability at the time of production of the electrode into account, it is desirable when the mean particle diameter ( $D_{50}$ ) is in the range of 3  $\mu\text{m}$  to 30  $\mu\text{m}$ , especially, in the range of 5  $\mu\text{m}$  to 20  $\mu\text{m}$ . When the above-mentioned range is used, the effect on the storage stability and charge/discharge cycle performance of the cell is insignificant, and it is not especially limited. It should be noted that the aforementioned particle diameter is not the particle diameter of the primary particle but the particle diameter of the secondary particle. Furthermore, the mean particle diameter of the positive electrode active material used in working examples shown below is in the range of 9 to 20  $\mu\text{m}$  in all cases.

A suitable method of manufacturing the Li-Mn-Ni type composite oxide is shown below.

It is desirable for the Li-Mn-Ni type composite oxide to have a heat history where baking is done at a temperature of  $900^\circ\text{C}$  or above. In specific terms, it is desirable when baking is done "for a Li-Mn-Ni type composite oxide precursor containing at least an Li component, Mn component, and Ni component" at a temperature of  $900^\circ\text{C}$  or above to produce a Li-Mn-Ni type composite oxide. In this case, baking temperature in the range of  $900^\circ\text{C}$  to  $1100^\circ\text{C}$  is desirable, and in the range of  $950^\circ\text{C}$  to  $1025^\circ\text{C}$  is further desirable.

When the baking temperature is 900°C or below, it is difficult to form the specific surface area of the Li-Mn-Ni type composite oxide at 1.5 m<sup>2</sup>/g or below, and a cell with an poor cycle performance is likely to be produced.

On the other hand, when the baking temperature used exceeds 1100°C, the composite oxide with the target composition is less likely to be produced as a result of evaporation of Li, or cell performance is likely to become inferior due to increased density of the particle. When the above-mentioned temperature exceeds 1100°C, an increase in the primary particle growth rate occurs, and the size of the crystal particles of the composite oxide are likely to be increased, and furthermore, localized absence of Li increases and structural instability results.

[p. 18]

It is desirable when the baking time used is in the range of 3 hours to 50 hours. When the baking time exceeds 50 hours, the specific surface area of the Li-Mn-Ni type composite oxide is less likely to become 0.3 m<sup>2</sup>/g or greater, and a cell with an inadequate high-rate charge/discharge performance is likely to be produced. On the other hand, when the baking time is 3 hours or less, the specific surface area of the Li-Mn-Ni type composite oxide is less likely to become 1.5 m<sup>2</sup>/g or less, and a cell with a poor cycle performance is likely to be produced.

A suitable baking temperature range and suitable baking time are described above, and the conditions are appropriately selected so that the specific surface area of the composite oxide specified in the present invention can be achieved.

Production of Li-Mn-Ni type composite oxide precursor is done via "a method in which an alkali compound is added to an aqueous solution produced by dissolving a manganese (Mn) compound and a nickel (Ni) compound in water, or an aqueous solution produced by dissolving an Mn compound, a Ni compound and a compound containing a dissimilar element (a compound containing the aforementioned dissimilar elements M, M' or M" and is hereinafter referred to as [M] compound at times) in water, and deposition of Mn-Ni composite coprecipitate or Mn-Ni-[M] composite coprecipitate is achieved".

In this case, for the Ni compound, nickel hydroxide, nickel carbonate, nickel sulfate, nickel nitrate, etc., and for Mn compound, manganese oxide, manganese carbonate, manganese sulfate, manganese nitrate, etc. can be mentioned.

For the [M] compound, boric acid, etc. can be used when the dissimilar element is B; vanadium oxide, etc. can be used when the dissimilar element is V; aluminum nitrate, etc. can be used when the dissimilar element is Al; magnesium nitrate, etc. can be used when the dissimilar element is Mg; cobalt hydroxide, cobalt carbonate, cobalt oxide, cobalt sulfate, cobalt nitrate, etc. can be used when the dissimilar element is Co; chromium nitrate, etc. can be used when the dissimilar element is Cr; titanium oxide, etc. can be used when the dissimilar element is Ti; iron sulfate, iron nitrate, etc. can be used when the dissimilar element is Fe; copper sulfate and copper nitrate can be used when the dissimilar element is Cu; and zinc sulfate and zinc nitrate, etc. can be used when the dissimilar element is Zn.

For the alkali compound, ammonium hydroxide, sodium hydroxide, etc. can be mentioned. Furthermore, it is desirable when the alkali compound is used in the form of an aqueous solution.

[p. 19]

When baking is done for a mixture of the Mn-Ni composite coprecipitate or Mn-Ni-[M] composite coprecipitate (hereinafter referred to as "composite coprecipitate" at times) produced as described above and a lithium compound and used as an Li-Mn-Ni type composite oxide precursor according to the above-mentioned baking conditions, production of Li-Mn-Ni type composite oxide can be efficiently achieved.

In this case, for the Li-Mn-Ni type composite oxide precursor, a mixture produced by evaporating water from the aqueous solution of the composite coprecipitate and lithium compound and drying can be used effectively.

For the Li compound, lithium hydroxide, lithium carbonate, etc. can be mentioned.

In addition to the aforementioned main ingredients of the Li-Mn-Ni type composite

oxide, other compounds may be mixed and used in the positive electrode active material of the present invention, and, for example, high cycle performance can be achieved when one or more of the other transition metal oxides containing lithium, etc. is used.

For examples of other transition metal oxide containing lithium, compound indicated by general formula  $\text{Li}_x\text{MX}_2$ ,  $\text{Li}_x\text{MN}_y\text{X}_2$  (wherein, M and N are metals of groups I to III, X is oxygen or a calcogen compound such as sulfur), and for example,  $\text{Li}_y\text{Co}_{1-x}\text{M}_x\text{O}_2$ ,  $\text{Li}_y\text{Mn}_{2-x}\text{M}_x\text{O}_4$  (M is a metal of groups I to III, for example, one or more elements selected from the group consisting of Li, Ca, Cr, Ni, Fe and Co), etc. can be mentioned. As for the value of x that indicates the degree of substitution of the dissimilar element in the aforementioned transition metal oxide containing lithium, the maximum substitution ratio may be used, but from the standpoint of discharge capacity,  $0 \leq x \leq 1$  is suitable. Furthermore, the maximum ratio can be used for the value of y that indicates amount of lithium, but from the standpoint of discharge capacity,  $0 \leq y \leq 1$  is suitable, but it is not especially limited.

Furthermore, for other compounds, metal compounds such as lithium-cobalt composite oxide and lithium-manganese composite oxide represented by metal compound of group I such as CuO,  $\text{Cu}_2\text{O}$ ,  $\text{Ag}_2\text{O}$ , CuS, and  $\text{CuSO}_4$ , metal compound of group IV such as  $\text{TiS}_2$ ,  $\text{SiO}_2$ , and SnO, metal compound of group V such as  $\text{V}_2\text{O}_5$ ,  $\text{V}_6\text{O}_{12}$ ,  $\text{VO}_x$ ,  $\text{Nb}_2\text{O}_5$ ,  $\text{Bi}_2\text{O}_3$ , and  $\text{Sb}_2\text{O}_3$ , metal compound of group VI such as  $\text{CrO}_3$ ,  $\text{Cr}_2\text{O}_3$ ,  $\text{MoO}_3$ ,  $\text{MoS}_2$ ,  $\text{WO}_3$  and  $\text{SeO}_2$ , metal compound of group VII such as  $\text{MnO}_2$ , and  $\text{Mn}_2\text{O}_3$ , and metal compound of group VIII such as  $\text{Fe}_2\text{O}_3$ , FeO,  $\text{Fe}_3\text{O}_4$ ,  $\text{Ni}_2\text{O}_3$ , NiO,  $\text{CoO}_3$ , CoO, and furthermore, electrically conductive polymer compounds such as disulfide, polypyrrole, polyaniline, polyparaphenylene, and polyacetylene, carbaceous material having pseudo-graphite structure, etc. can be mentioned, but it is not limited to the above-mentioned examples.

[p. 20]

When the aforementioned other compounds are used in combination with the above-mentioned Li-Mn-Ni type composite oxide as a positive electrode active material, the amount of

the other compounds is not especially limited as long as the effect of the present invention is not inhibited, and in general, the amount of the other components is in the range of 1 wt% to 50 wt%, preferably, 5 wt% to 30 wt%, for the total amount of the positive electrode active material.

The nonaqueous secondary cell of the present invention is explained in detail below. The nonaqueous secondary cell (hereinafter referred to as cell, as well) of the present invention is a cell that utilizes the positive electrode active material of the present invention, and in general, comprises the positive electrode mainly consisting of the positive electrode active material of the present invention, negative electrode mainly consisting of the negative material, and a nonaqueous electrolyte in which an electrolytic salt is included in a nonaqueous solvent, and in general, a separator is provided between the positive electrode and negative electrode.

In this case, nonaqueous electrolytes commonly used for lithium cells, etc. may be used. For the nonaqueous solvent, cyclic carbonates such as propylene carbonate, ethylene carbonate, butylene carbonate, chloroethylene carbonate, and vinylene carbonate; cyclic esters such as  $\gamma$ -butyrolactone, and  $\gamma$ -valerolactone, chain carbonates such as dimethyl carbonate, diethyl carbonate and ethyl methyl carbonate; chain esters such as methyl formate, methyl acetate, and methyl butyrate, ethers such as 1,3-dioxane, 1,4-dioxane, 1,2-dimethoxy ethane, 1,4-dibutoxy ethane, and methyl diglyme; nitriles such as acetonitrile and benzonitrile; dioxolane and derivatives of the same; ethylene sulfide, sulfolane, sultone and derivatives of the same, and mixtures of the same, etc. can be mentioned, but it is not especially limited.

[p. 21]

For electrolytic salts, inorganic ionic salts containing one of lithium (Li), sodium (Na) or potassium (K) such as  $\text{LiClO}_4$ ,  $\text{LiBF}_4$ ,  $\text{LiAsF}_6$ ,  $\text{LiPF}_6$ ,  $\text{LiSCN}$ ,  $\text{LiBr}$ ,  $\text{LiI}$ ,  $\text{Li}_2\text{SO}_4$ ,  $\text{Li}_2\text{B}_{10}\text{Cl}_{10}$ ,  $\text{NaClO}_4$ ,  $\text{NaI}$ ,  $\text{NaSCN}$ ,  $\text{NaBr}$ ,  $\text{KClO}_4$ ,  $\text{KSCN}$ , organic ionic salts such as  $\text{LiCF}_3\text{SO}_3$ ,  $\text{LiN}(\text{CF}_3\text{SO}_2)_2$ ,  $\text{LiN}(\text{C}_2\text{F}_5\text{SO}_2)_2$ ,  $\text{LiN}(\text{CF}_3\text{SO}_2)(\text{C}_4\text{F}_9\text{SO}_2)$ ,  $\text{LiC}(\text{CF}_3\text{SO}_2)_3$ ,  $\text{LiC}(\text{C}_2\text{F}_5\text{SO}_2)_3$ ,  $(\text{CH}_3)_4\text{NBF}_4$ ,  $(\text{CH}_3)_4\text{NBr}$ ,  $(\text{C}_2\text{H}_5)_4\text{NClO}_4$ ,  $(\text{C}_2\text{H}_5)_4\text{NI}$ ,  $(\text{C}_3\text{H}_7)_4\text{NBr}$ ,  $(n\text{-C}_4\text{H}_9\text{NClO}_4)$ ,  $(n\text{-C}_4\text{H}_9)_4\text{NI}$ ,  $(\text{C}_2\text{H}_5)_4\text{N-maleate}$ ,  $(\text{C}_2\text{H}_5)_4\text{N-benzoate}$ ,  $(\text{C}_2\text{H}_5)_4\text{N-phthalate}$  [sic], lithium stearyl sulfonate, lithium

octyl sulfonate, and lithium dodecyl benzene sulfonate, etc. can be mentioned, and furthermore, one type or two or more different types of the above-mentioned ionic compounds may be mixed and used in combination in this case as well.

Furthermore, the viscosity of the nonaqueous electrolyte can be further reduced when a lithium salt containing perfluoroalkyl group such as  $\text{LiBF}_4$  and  $\text{LiN}(\text{C}_2\text{F}_5\text{SO}_2)_2$  is used in combination; thus, low temperature characteristics can be further enhanced.

The concentration of the electrolytic salt in the nonaqueous electrolyte is preferably in the range of 0.1 mol/l to 5 mol/l for production of a cell having high cell performance, and in the range of 1 mol/l to 2.5 mol/l is further desirable.

The electrode structured of the Li-Mn-Ni type composite oxide of the present invention is used as the positive electrode and an electrode structured consisting of graphite is used as the negative electrode in the cell of the present invention.

Production of the positive electrode is achieved as mixing is performed for the composite oxide of the present invention with an electrically conductive material, a binder, and optional filler to form a positive electrode agent, and coating or depositing the positive electrode agent produced onto a foil or lath board used as a collector and heating at a temperature of approximately 50°C to 250°C for 2 hours.

For the negative electrode material, in addition to lithium metal and lithium alloys (alloys containing lithium metals such as lithium-aluminum, lithium-lead, lithium-tin, lithium aluminum-tin, lithium-gallium and wood alloy), alloys capable of occlusion and releasing lithium, carbon materials (for example, graphite, hard carbon, low temperature baked carbon, amorphous carbonate, etc.), etc. can be mentioned. Among those listed above, graphite has an operating potential very close to that of metal lithium; thus, autodischarge can be reduced when a lithium salt is used as an electrolytic salt, and reduction in irreversible capacity at the time of charge/discharge is made possible; thus, it is desirable when used as a negative electrode material.

For example, synthetic graphites and natural graphites can be used effectively. Furthermore, a graphite of which the surface of the negative electrode active material particle is modified with an amorphous carbon is desirable since gas formation at the time of charge/discharge is insignificant.

Analysis result based on Ex-ray analysis, etc. of graphite that can be used effectively in the present invention is shown below.

Lattice spacing (d002): 0.333 to 0.350 nm

Crystal size in a-axis direction La: 20 nm or greater

Crystal size in c-axis direction Lc: 20 nm or greater

True density: 2.00 to 2.25 g/cm<sup>3</sup>

Furthermore, metal oxides such as tin oxide and silicon oxide, phosphorus, boron, amorphous carbon, etc. may be added to graphite and modifications can be done as well. When a modification is carried out for the surface of the graphite, decomposition of electrolyte is controlled and cell performance is increased. Furthermore, lithium metals and alloys containing lithium metals such as lithium-aluminum, lithium-lead, lithium-tin, lithium aluminum-tin, lithium-gallium and wood-alloy may be used in combination with graphite, or an electrochemical reduction may be performed ahead of time so as to include lithium in the graphite, etc. may be used as the negative electrode material as well.

It is desirable for the positive electrode active material fine particle and negative electrode material fine particle to have a mean particle size of 100  $\mu\text{m}$  or below. It is further desirable when the size of the positive electrode active material fine particle is 10  $\mu\text{m}$  or below from the standpoint of increase in the high output performance of the nonaqueous secondary cell. In order to produce fine particles with a specific shape, pulverizers and classifiers are used. For example, mortars, ball mills, sand mills, vibrating ball mills, planetary ball mills, jet mills, counter jet



mills, swivel current jet mills, sieves, etc. are used. In this case, the wet pulverization method, where water or an organic solvent such as hexane is used, may be used. Furthermore, the classification method is not especially limited, and sieves and pneumatic classifiers may be used for wet method or dry method, as needed.

[p. 23]

The positive electrode active material and negative electrode materials used as the primary structural components of positive electrode and negative electrode are explained in detail above, and in addition to the aforementioned primary structural components, electrically conductive materials, binders, thickeners, fillers, etc. may be further included in the aforementioned positive electrode and negative electrode.

The electrically conductive materials used in this case is not especially limited as long as the cell performance is not adversely influenced, and in general, electrically conductive materials such as natural graphites (flaky graphite, scale graphite, earthy graphite, etc.), synthetic graphites, carbon blacks, acetylene blacks, kitchen blacks, carbon whiskers, carbon fibers, metal (copper, nickel, aluminum, silver, gold, etc.) powders, metal fibers, and electrically conductive ceramic materials may be used independently or in combination.

Among electrically conductive materials listed above, acetylene black is further desirable from the standpoint of electron conductivity and coatability. The amount of the electrically conductive material used in this case is preferably in the range of 0.1 wt% to 50 wt%, and in the range of 0.5 wt% to 30 wt% is further desirable. When acetylene black is pulverized to form a super-fine particle of 0.1 to 0.5  $\mu\text{m}$  and used, the amount of carbon required can be reduced. The mixing method used in this case is physical mixing, and uniform mixing is desirable. In this case, wet or dry mixing can be done by using a powder mixer such as V-type mixer, S-type mixer, ball mill, or planetary ball mill.

For the aforementioned binder, in general, thermoplastic resins such as polytetrafluoroethylene (PTFE), polyvinylidene fluoride (PVDF), polyethylene and

polypropylene, or polymers with rubber elasticity such as ethylene-propylene-diene terpolymer (EPDM), sulfonated EPDM, styrene butadiene rubber (SBR), and fluoro rubbers may be used independently or in combination. The amount of binder added is in the range of 1 to 50 wt%, preferably, 2 to 30 wt%, for the total weight of the positive electrode or negative electrode.

[p. 24]

In general, for the above-mentioned thickeners, polysaccharides such as carboxy methyl cellulose and methyl cellulose may be used independently or in combination. In this case, it is desirable when deactivation, for example, methylation, is performed for the functional group for the thickener having a functional group that forms a reaction with lithium as in the case of polysaccharides. The amount of thickener added is in the range of 0.5 to 10 wt%, preferably, 1 to 2 wt%, for the total weight of the positive electrode or negative electrode.

The filler used in this case is not especially limited as long as the cell performance is adversely influenced. In general, olefin type polymers such as polypropylene and polyethylene, amorphous silica, alumina, zeolite, glass, carbon, etc. are used. The amount of the filler added is 30 wt% or less for the total weight of the positive electrode or negative electrode.

Production of the positive electrode or negative electrode is carried out as an optional electrically conductive material or binder is added to the aforementioned positive electrode active material or positive electrode, mixing is performed with an organic solvent such as N-methylpyrrolidone and toluene, coating the solution produced onto the collector described below and drying the solution. For the coating method used in this case, it is not especially limited and coating can be achieved to form a desired thickness and form using a coating method such as applicator roll coating method, screen coating method, doctor blade coating method, spin coating method, or bar coating method.

For the collector, an electron conductive material with an absence of adverse influence on the cell performance may be used. For example, as a collector for the positive electrode, in addition to materials such as aluminum, titanium, stainless steel, nickel, baked carbon,

conductive polymer, and conductive glass, an aluminum or a copper with the surface treated with a carbon, nickel, titanium or silver for an increase in adhesion, conductivity, and oxidation resistance may be used. As a collector for the negative electrode, in addition to materials such as copper, nickel, iron, stainless steel, aluminum, baked carbon, conductive polymer, conductive glass, and Al-Cd alloy, copper with the surface treated with a carbon, nickel, titanium, or silver for increased adhesion, conductivity, and reduction in resistance may be used. Furthermore, oxidation treatment may be carried out for the surface of the above-mentioned materials as well.

[p. 25]

For the shape of the collector, in addition to foils, films, sheets, nets, punched or expanded materials, lath materials, porous materials, foams, and fibers, etc. may be used. The thickness is not especially limited, and a thickness in the range of 1 to 500  $\mu\text{m}$  is used. Among the above-mentioned collectors, an aluminum foil having high oxidation resistance is desirable for the positive electrode, and an inexpensive copper foil, nickel foil, iron foil and alloy foil containing the same having reduction resistance and electron conductivity are desirable for the negative electrode. Furthermore, a foil with a surface roughness of at least 0.2  $\mu\text{m Ra}$  is desirable, and in this case, high adhesion between the composite coprecipitate or negative electrode and collector can be achieved. Thus, it is desirable when an electrolytic foil having the above-mentioned rough surface is used. In particular, a treated electrolytic foil is further desirable. When both surfaces of the above-mentioned foil are to be coated, it is desirable when each surface roughness of the foil is the same or nearly the same.

It is desirable when a porous film, non-woven fabric, etc. having excellent high-rate discharge performance is used for the separator independently or in combination. For the material that structures the separator, polyolefin type resins such as polyethylene and polypropylene, polyester type resins such as polyethylene terephthalate and polybutylene terephthalate, polyvinylidene fluoride, vinylidene fluoride-hexafluoropropylene copolymer, vinylidene fluoride-perfluorovinyl ether copolymer, vinylidene fluoride-tetrafluoroethylene

copolymer, vinylidene fluoride-trifluoroethylene copolymer, vinylidene fluoride- fluoroethylene copolymer, vinylidene fluoride-hexafluoroacetone copolymer, vinylidene fluoride-ethylene copolymer, vinylidene fluoride-propylene copolymer, vinylidene fluoride-trifluoropropylene copolymer, vinylidene fluoride-tetrafluoroethylene-hexafluoropropylene copolymer, vinylidene fluoride-ethylene-tetrafluoroethylene copolymer, etc. can be mentioned.

From the standpoint of strength, it is desirable when the porosity of the separator is 98 vol% or below. Furthermore, from the standpoint of charge/discharge performance, at least 20 vol% of porosity is desirable.

Furthermore, a polymer gel comprising a polymer such as acrylonitrile, ethylene oxide, propylene oxide, methyl methacrylate, vinyl acetate, vinyl pyrrolidone and polyvinylidene fluoride, and electrolyte may be used as well.

[p. 26]

When the nonaqueous secondary cell of the present invention is used in the form of a gel as described above, it is effective to prevent leakage.

Furthermore, it is desirable when the above-mentioned porous film, non-woven fabric, etc. is used in combination with a polymer gel for the separator since liquid retention of the electrolyte can be improved. In other words, when a polymer having affinity with the solvent is formed on the surface and walls of the micropores of a polyethylene microporous film to form a film with a thickness of several microns or below, and electrolyte is retained inside the aforementioned micropores of the above-mentioned film and production of the aforementioned polymer gel having affinity with solvent can be achieved.

For the aforementioned polymer having affinity with solvent, in addition to polyvinylidene fluoride, acrylate monomers having an ethylene oxide group or ester group, polymers crosslinked with an epoxy monomer or monomers having an isocyanate group, etc. can be mentioned. Crosslinking reaction may be carried out for the above-mentioned monomers by heat-treatment or ultraviolet ray (UV) in the presence of a radical initiator, or by an activated

beam such as an electron beam (EB).

In order to increase the strength and to control properties, modifiers may be included in the aforementioned polymer having affinity with solvent in an amount that does not interfere with the crosslinking property. For examples of the aforementioned modifiers, inorganic fillers [metal oxides such as silicon oxide, titanium oxide, aluminum oxide, magnesium oxide, zirconium oxide, zinc oxide, and iron oxide, metal carbonates such as calcium carbonate and magnesium carbonate], polymers [polyvinylidene fluoride, vinylidene fluoride/hexafluoropropylene copolymer, poly acrylonitrile, polymethyl methacrylate, etc.] etc. can be mentioned. In general, the amount of the aforementioned modifiers added is 50 wt% or below, preferably, 20 wt% or below, for the crosslinking monomer.

For the aforementioned acrylate monomer, unsaturated monomers of bifunctional or higher can be mentioned, and in specific terms, bifunctional (meth)acrylates {ethylene glycol di(meth)acrylate, propylene glycol di(meth)acrylate, adipic acid-dineopentyl glycol ester di(meth)acrylate, polyethylene glycol di(meth)acrylate with polymerization of 2 or higher, polypropylene di(meth)acrylate with polymerization of 2 or higher, di(meth)acrylate of polyoxy ethylene-polyoxy propylene copolymer, butane diol di(meth)acrylate, hexamethylene glycol di(meth)acrylate, etc.},

[p. 27]

trifunctional (meth)acrylates {trimethylol propane tri(meth)acrylate, glycerol tri(meth)acrylate, tri(meth)acrylate of ethylene oxide adduct of glycerol, tri(meth)acrylate of propylene oxide adduct of glycerol, ethylene oxide of glycerol, tri(meth)acrylate of propylene oxide adduct, etc.}, tetrafunctional or higher (meth)acrylates {pentaerythritol tetra (meth)acrylate, diglycerol hexa (meth)acrylate, etc.} can be mentioned. Furthermore, one type or two or more different types of the above-mentioned monomers may be mixed and used in combination in this case.

For the purpose of adjustment of properties, etc., monofunctional monomers may be

added to the aforementioned acrylate monomers. For examples of the aforementioned monofunctional monomers, unsaturated carboxylic acids {acrylic acid, methacrylic acid, crotonic acid, cinnamic acid, vinyl benzoic acid, maleic acid, fumaric acid, itaconic acid, citraconic acid, mesaconic acid, methylene malonic acid, aconitic acid, etc.}, unsaturated sulfonic acids {styrene sulfonate, acrylamide-2-methyl propane sulfonic acid, etc.} or salts of the same (Li salt, Na salt, K salt, ammonium salt, tetraalkyl ammonium salt, etc.), furthermore, a partially esterified above-mentioned unsaturated carboxylic acids with an aliphatic or alicyclic alcohols with C1 to C18, alkylene (C2 to C4) glycol, polyalkylene (C2 to C4) glycol, etc. (methyl maleate, monohydroxy ethyl maleate, etc.) and a partially amidated acids with ammonia, primary or secondary amine (maleic acid monoamide, N-methyl maleic acid monoamide, N,N-diethyl maleic acid monoamide, etc.), (meth)acrylates [esters of C1 to C18 aliphatic alcohols (methyl, ethyl, propyl, butyl, 2-ethyl hexyl, stearyl, etc.) and (meth)acrylic acid, esters of alkylene (C2 to C4) glycol (ethylene glycol, propylene glycol, 1,4-butane diol, etc.) and polyalkylene glycol (C2 to C4) glycol (polyethylene glycol, polypropylene glycol) and (meth)acrylic acid]; (meth)acrylamide or N-substituted (meth)acrylamide [(meth)acrylamide, N-methyl (meth)acrylamide, N-methylol (meth)acrylamide, etc.]; vinyl ester or allyl ester [vinyl acetate, allyl acetate, etc.];

[p. 28]

vinyl ether or allyl ether [butyl vinyl ether, dodecyl allyl ether etc.]; unsaturated nitrile compounds [(meth) acrylonitrile, croton nitrile, etc.]; unsaturated alcohols [(meth)allyl alcohol, etc.]; unsaturated amines [(meth)allyl amine, dimethyl aminoethyl (meth)acrylate, diethyl aminoethyl (meth)acrylate, etc.]; monomer containing heterocycles [N-vinyl pyrrolidone, vinyl pyridine, etc.]; olefin type aliphatic hydrocarbons [ethylene, propylene, butylene, isobutylene, pentene, (C6 to C50)  $\alpha$ -olefin, etc.]; olefin type alicyclic hydrocarbons [cyclopentene, cyclohexene, cycloheptene, norbornane, etc.]; olefin type aromatic hydrocarbons [styrene,  $\alpha$ -methyl styrene, stilbene, etc.]; unsaturated imides [maleimide, etc.]; monomers containing halogens [vinyl chloride, vinylidene chloride, vinylidene fluoride, hexafluoropropylene, etc.], etc.

can be mentioned.

For examples of the above-mentioned epoxy monomers, glycidyl ethers {bisphenol A diglycidyl ether, bisphenol F diglycidyl ether, brominated bisphenol A diglycidyl ether, phenol novolak glycidyl ether, diglycidyl ether, cresol novolak glycidyl ether, etc.}, glycol esters {hexahydrophthalic acid glycidyl ester, dimer acid glycidyl ester, etc.}, glycidyl amines {triglycidyl isocyanurate, tetraglycidyl diaminophenyl methane, etc.}, linear aliphatic epoxides {epoxidated polybutadiene, epoxidated soybean oil, etc.}, alicyclic epoxides {3,4-epoxy-6-methyl cyclohexyl methyl carboxylate, 3,4-epoxy-cyclohexyl methyl carboxylate, etc.}, etc. can be mentioned. The above-mentioned epoxy resins may be used alone or a hardener may be added and curing carried out.

For examples of the aforementioned curing agents, aliphatic polyamines {diethylene triamine, triethylene tetramine, 3,9-(3-aminopropyl)-2,4,8,10-tetraoxaspiro[5,5]undecane, etc.}, aromatic polyamines {metaxylene diamine, diaminophenyl methane, etc.}, polyamides {dimer acid polyamide, etc.}, acid anhydrides {phthalic anhydride, tetrahydromethyl phthalic anhydride, hexahydrophthalic anhydride, trimellitic anhydride, etc.}, phenols {phenol novolak resin, etc.}, polymercaptan {polysulfide, etc.}, tertiary amines {tris(dimethyl aminomethyl) phenol, 2-ethyl-4-methyl imidazole, etc.}, Lewis acid composite complex {trifluoroboron-ethyl amine complex}, etc. can be mentioned.

[p. 29]

For monomers having the aforementioned isocyanate groups, toluene diisocyanate, diphenyl methane diisocyanate, 1,6-hexamethylene diisocyanate, 2,2,4-(2,2,4)-trimethyl-hexamethylene diisocyanate, p-phenylene diisocyanate, 4,4'-dicyclohexyl methane diisocyanate, 3,3'-dimethyl diphenyl-4,4'-diisocyanate, dianicidine diisocyanate, m-xylene diisocyanate, trimethyl xylene diisocyanate, isophorone diisocyanate, 1,5-naphthalene diisocyanate, trans-1,4-cyclohexyl diisocyanate, lysin diisocyanate, etc. can be mentioned.

In crosslinking of the aforementioned isocyanate groups, compounds having active

hydrogen, for example, polyols and polyamines [bifunctional compounds {water, ethylene glycol, propylene glycol, diethylene glycol, dipropylene glycol, etc.}, trifunctional compounds {glycerol, trimethylol propane, 1,2,6-hexane triol, triethanol amine, etc.}, tetrafunctional compounds {pentaerythritol, ethylene diamine, tolylene diamine, diphenyl methane diamine, tetramethylol cyclohexane, methyl glucoxide, etc.}, pentafunctional compounds {2,2,6,6-tetrakis(hydroxy methyl) cyclohexanol, diethylene triamine, etc.}, hexafunctional compounds {sorbitol, mannitol, dulcitol, etc.}, octafunctional compounds {succrose, etc.}] and polyether polyols {propylene oxide of the aforementioned polyol or polyamine and/or ethylene oxide adduct}, polyester polyol [a condensate of the aforementioned polyol and polybasic acid {adipic acid, o,m,p-phthalic acid, succinic acid, azelaic acid, sebacic acid, ricinoleic acid}, polycaprolactone polyol {poly-epsilon-caprolactone, etc.}, polycondensate of hydroxy carboxylic acid, etc.], etc. may be used in combination.

[p. 30]

Upon performing the above-mentioned crosslinking reaction, a catalyst may be used in combination. For examples of catalysts used in this case, organic tin compounds, trialkyl phosphines, amines, amines [monoamines {N,N-dimethyl cyclohexylamine, triethyl amine, etc.}, cyclic monoamines {pyridine, N-methyl morpholine, etc.}, diamines {N,N,N',N'-tetramethyl ethylene diamine, N,N,N',N'-tetramethyl-1,3-butane diamine, etc.}, triamines {N,N,N',N'-pentamethyl diethylene triamine, etc.}, hexamines {N,N,N',N'-tetra(3-dimethyl aminopropyl)-methane diamine, etc.}, cyclic polyamines {diazabicyclooctane (DABCO), N,N'-dimethyl piperadine, 1,2-dimethyl imidazole, 1,8-diazabicyclo(5,4,0)undecene-7 (DBU), etc.}, and salts of the same] can be mentioned.

Production of the nonaqueous secondary cell concerning the present invention can be achieved when an electrolyte is injected before or after laminating a separator, positive electrode and negative electrode and sealing with a sheath material. Furthermore, in a nonaqueous secondary cell consisting of wrapping a generating component in which the positive electrode



and negative electrode are laminated with the separator in between, it is desirable to inject the electrolyte to the generating component before and after wrapping. As for the injection method used in this case, injection can be performed under ambient pressure, or vacuum impregnation method or pressure impregnation method may be used as well.

For the material used for the sheath of the nonaqueous secondary cell, a nickel-plated iron, stainless steel, aluminum, metal resin composite film, etc. can be mentioned. For example, a metal resin composite film where a metal foil is sandwiched with resin films is desirable. For specific examples of the aforementioned metal foils, foils without pinholes, for example, aluminum, iron, nickel, copper, stainless steel, titanium, gold, and silver, can be used, and a light-weight and low-cost aluminum foil is further desirable in this case. Furthermore, for the resin film used for outside the cell, a resin film having high puncture resistance such as polyethylene terephthalate film and nylon film is desirable, and for the resin film used inside the cell, a thermally-fusible film having high solvent resistance such as polyethylene film and nylon film is desirable.

The structure of the nonaqueous secondary cell is not especially limited, and a coin cell or button cell having a positive electrode, negative electrode and single layer or multilayer separator, furthermore, cylinder cell, square cell, flat cell having a positive electrode, negative electrode and single layer or multilayer separator, etc. can be mentioned.

[p. 31]

#### <Working examples>

In the following, the present invention is explained further in specific terms with working examples and comparative examples below, but the present invention is not limited to working examples shown below.

#### [First embodiment]

##### (Working Example 1-1)

A sodium hydroxide solution was added to an aqueous solution containing manganese

nitrate and nickel nitrate at an atomic ratio for Mn:Ni of 1:1 and coprecipitation was performed; then, heating was provided to 150°C and sequentially, drying was performed to produce a manganese-nickel coprecipitate compound. The aforementioned manganese-nickel coprecipitate compound was added to a lithium hydroxide solution, stirring was provided; then, evaporation of the solvent was carried out to dry, and baking was done for 12 hours at a temperature of 1000°C in an oxygen atmosphere, and finally, classification of the particles was carried out to produce a powder of  $D_{50}=9\text{ }\mu\text{m}$ . The specific surface area of the particles based on the BET method was  $1.0\text{ m}^2/\text{g}$ .

The measurement results of X-ray analysis of the above-mentioned powder by  $\text{CuK}\alpha$  ray indicated diffraction peaks at around  $2\theta=18.58$  degrees, 36.38 degrees, 37.68 degrees, 38.02 degrees, 44.10 degrees, 48.24 degrees, 58.22 degrees, 63.92 degrees, 64.10 degrees, 64.4 degrees, 67.68 degrees, and a monolayer having high crystallinity that appears to be a layer structure belonging to the spatial group R3/m was synthesized. The X-ray analysis chart of the aforementioned powder is indicated by Fig. 3. As a result of the elemental analysis, the composition of the aforementioned powder was  $\text{LiMn}_{0.5}\text{Ni}_{0.5}\text{O}_2$ . The powder produced above was defined as Powder A.

The aforementioned Powder A was used as the positive electrode active material, and production of a square nonaqueous secondary cell having a capacity of approximately 15 Ah indicated by Fig. 2 was carried out as shown below.

Mixing was done for Powder A used as the positive electrode active material, acetylene black used as an electrically conductive material, and polyvinylidene fluoride (PVDF) used as a binder at a weight ratio of 85:10:5, N-methyl pyrrolidone was added as a solvent, and kneading and dispersing were carried out to produce a positive electrode coating composition. In this case, a solution with a solid component of the aforementioned polyvinylidene fluoride dispersed in it was used and weight conversion was done for the solid component. The aforementioned positive electrode coating composition was coated onto both surfaces of an aluminum foil collector with a

thickness of 20  $\mu\text{m}$  and an adjustment was made to achieve an overall thickness of 230  $\mu\text{m}$ , and production of a positive electrode sheet having a capacity of 6.3  $\text{mAh}/\text{cm}^2$  was achieved. The aforementioned positive electrode sheet was cut to a width of 61 mm and height of 107 mm, and an aluminum lead sheet with a thickness of 20  $\mu\text{m}$  and width of 10 mm was attached to the end of the sheet to form positive electrode plate 7.

[p. 32]

Furthermore, a synthetic graphite (particle diameter 6  $\mu\text{m}$ ) was used as a negative electrode material, 10 wt% of polyvinylidene fluoride (PVDF) was added to the aforementioned negative electrode material as a binder, N-methylpyrrolidone was added as a solvent, and kneading and dispersing were done to produce a negative electrode coating composition. In this case, a solution dispersed with a solid component of the aforementioned polyvinylidene fluoride was used and the weight conversion was carried out for the solid component. The aforementioned negative electrode coating composition was coated onto both surfaces of a copper foil collector with a thickness of 10  $\mu\text{m}$  and an adjustment was made to achieve an overall thickness of 180  $\mu\text{m}$ , and production of a negative electrode sheet having a capacity of 7  $\text{mAh}/\text{cm}^2$  was achieved. The aforementioned negative electrode sheet was cut to form the width of 65 mm and height of 111 mm, and a copper lead sheet with a thickness of 10  $\mu\text{m}$  and width of 10 mm was attached to the end of the sheet to form negative electrode plate 9.

Vacuum drying was carried out for the aforementioned positive electrode plate 7 and negative electrode plate 9 for 12 hours at a temperature of 150°C. Furthermore, the aforementioned positive electrode plate was inserted into a case with a width of 65 mm and height of 111 mm made of a polyethylene microporous film and used as separator 8, and the positive electrode plate 7 with separator 8 and negative electrode plate 9 were alternately laminated to form a laminate consisting of 40 positive electrode plates 7 with separators 8 and 41 negative electrode plates 9.

The aforementioned electrode laminate was wrapped with an insulating film made of a

polyethylene resin, and stored in a square battery jar 10 made of aluminum, the lead plate of positive electrode plate 7 and negative electrode plate 9 are connected with bolts to positive electrode terminal 5 and negative electrode terminal 4, respectively, attached to cover 2 made of aluminum and having safety valve 1. In this case, gasket 6 made of a polypropylene resin was used and terminals 4 and 5 are insulated from the aforementioned cover 2.

Furthermore, welding was performed for the aforementioned cover 2 and battery jar 10 with laser weld 3, 65 g of electrolyte produced by dissolving 1 mol/l of  $\text{LiPF}_6$  in a 1:1 volume ratio mixed solvent of ethylene carbonate and diethylene carbonate was poured into the aforementioned battery jar 10, and sealing was performed, then, constant-current and constant-voltage charging was done at a temperature of  $25^\circ\text{C}$  under 1.5A, 4.2V for 15 hours, and then, constant-current discharge was carried out under 1.5A and at a final voltage of 3V. In this manner, a square lithium cell with a width of 70 mm, height of 130 mm (height with terminal of 136 mm) and depth of 22 mm. The cell produced was defined as the cell of Working Example 1-1.

[p. 33]

(Working Example 1-2)

A sodium hydroxide solution was added to an aqueous solution containing manganese nitrate and nickel nitrate at an atomic ratio of Mn:Ni of 1:1 and coprecipitation was performed, then, heating was provided to  $150^\circ\text{C}$  and sequentially, drying was done to produce a manganese-nickel coprecipitate compound. The aforementioned manganese-nickel coprecipitate compound was added to lithium hydroxide solution, and stirring was performed, then, evaporation of the solvent was done to dry, and baking was done for 12 hours at a temperature of  $1000^\circ\text{C}$  in an oxygen atmosphere, and finally, classification of the particle was carried out to produce a powder of  $D_{50}=20\text{ }\mu\text{m}$ . The specific surface area of the particles based on the BET method was  $1.0\text{ m}^2/\text{g}$ .

The measurement results of X-ray analysis of the above-mentioned powder by  $\text{CuK}\alpha$  ray indicated formation of a monolayer having high crystallinity that appears to be a layer structure

similar to that of the above-mentioned powder A. The results of the elemental analysis indicated that the composition of the aforementioned powder was  $\text{LiMn}_{0.5}\text{Ni}_{0.5}\text{O}_2$ . The powder produced above was used as the positive electrode active material and production of a square lithium cell having a capacity of approximately 15 Ah indicated by Fig. 2 was done as in (Working Example 1-1). The cell produced was defined as the cell of Working Example 1-2.

(Working Example 1-3)

A sodium hydroxide solution was added to an aqueous solution containing manganese nitrate and nickel nitrate at an atomic ratio of Mn:Ni of 1:1 and coprecipitation was performed; then, heating was provided to 150°C and sequentially, drying was done to produce a manganese-nickel coprecipitate compound. The aforementioned manganese-nickel coprecipitate compound was added to a lithium hydroxide solution, stirring was provided; then, evaporation of the solvent was done to dry, and baking was done for 12 hours at a temperature of 1030°C in an oxygen atmosphere, and finally, classification of the particles was done to produce a powder of  $D_{50}=20\text{ }\mu\text{m}$ . The specific surface area of the particle based on the BET method was  $0.9\text{ m}^2/\text{g}$ .

The measurement results of X-ray analysis of the above-mentioned powder by  $\text{CuK}\alpha$  ray indicated formation of a monolayer having high crystallinity that appears to be a layer structure similar to that of the above-mentioned powder A. The results of the elemental analysis indicated that the composition of the aforementioned powder was  $\text{LiMn}_{0.5}\text{Ni}_{0.5}\text{O}_2$ . The powder produced above was used as the positive electrode active material and production of a square lithium cell having a capacity of approximately 15 Ah indicated by Fig. 2 was done as in (Working Example 1-1). The cell produced was defined as the cell of Working Example 1-3.

[p. 34]

(Working Example 1-4)

A sodium hydroxide solution was added to an aqueous solution containing manganese nitrate and nickel nitrate at an atomic ratio of Mn:Ni of 1:1 and coprecipitation was performed; then, heating was provided to 150°C and sequentially, drying was done to produce a manganese-

nickel coprecipitate compound. The aforementioned manganese-nickel coprecipitate compound was added to lithium hydroxide solution, stirring was provided; then, evaporation of the solvent was done to dry, and baking was done for 12 hours at a temperature of 1060°C in an oxygen atmosphere, and finally, classification of the particles was carried out to produce a powder of  $D_{50}=20\text{ }\mu\text{m}$ . The specific surface area of the particles based on the BET method was  $0.9\text{ m}^2/\text{g}$ .

The measurement results of X-ray analysis of the above-mentioned powder by  $\text{CuK}\alpha$  ray indicated formation of a monolayer having high crystallinity that appears to be a layer structure similar to that of the above-mentioned powder A. The results of elemental analysis indicated that the composition of the aforementioned powder was  $\text{LiMn}_{0.5}\text{Ni}_{0.5}\text{O}_2$ . The powder produced above was used as the positive electrode active material and production of a square lithium cell having a capacity of approximately 15 Ah indicated by Fig. 2 was done as in (Working Example 1-1). The cell produced was defined as the cell of Working Example 1-4.

(Working Example 1-5)

A sodium hydroxide solution was added to an aqueous solution containing manganese nitrate and nickel nitrate at an atomic ratio of Mn:Ni of 1:1 and coprecipitation was performed; then, heating was provided to 150°C and sequentially, drying was done to produce a manganese-nickel coprecipitate compound. The aforementioned manganese-nickel coprecipitate compound was added to lithium hydroxide solution, stirring was provided; then, evaporation of the solvent was done to dry, and baking was done for 12 hours at a temperature of 1000°C in an oxygen atmosphere, and finally, classification of the particles was carried out to produce a powder of  $D_{50}=20\text{ }\mu\text{m}$ . The specific surface area of the particles based on the BET method was  $0.9\text{ m}^2/\text{g}$ .

The measurement results of X-ray analysis of the above-mentioned powder by  $\text{CuK}\alpha$  ray indicated formation of a monolayer having high crystallinity that appears to be the layer structure similar to that of the above-mentioned powder A. The results of elemental analysis indicated that the composition of the aforementioned powder was  $\text{LiMn}_{0.5}\text{Ni}_{0.5}\text{O}_2$ . The powder produced above was used as the positive electrode active material and production of a square lithium cell having

a capacity of approximately 15 Ah indicated by Fig. 2 was done as in (Working Example 1-1).

The cell produced was defined as the cell of Working Example 1-5.

(Working Example 1-6)

A sodium hydroxide solution was added to an aqueous solution containing manganese nitrate and nickel nitrate at an atomic ratio of Mn:Ni of 1:1 and coprecipitation was performed; then, heating was provided to 150°C and sequentially, drying was done to produce a manganese-nickel coprecipitate compound. The aforementioned manganese-nickel coprecipitate compound was added to lithium hydroxide solution, stirring was provided; then, evaporation of the solvent was done to dry, and baking was done for 12 hours at a temperature of 950°C in an oxygen atmosphere, and finally, classification of the particles was carried out to produce a powder of  $D_{50}=20\text{ }\mu\text{m}$ . The specific surface area of the particles based on the BET method was  $0.9\text{ m}^2/\text{g}$ .

[p. 35]

The measurement results of X-ray analysis of the above-mentioned powder by  $\text{CuK}\alpha$  ray indicated formation of a monolayer having high crystallinity that appears to be a layer structure similar to that of the above-mentioned powder A. The results of the elemental analysis indicated that the composition of the aforementioned powder was  $\text{LiMn}_{0.5}\text{Ni}_{0.5}\text{O}_2$ . The powder produced above was used as the positive electrode active material and production of a square lithium cell having a capacity of approximately 15 Ah indicated by Fig. 2 was done as in (Working Example 1-1). The cell produced was defined as the cell of Working Example 1-6.

(Working Example 1-7)

A sodium hydroxide solution was added to an aqueous solution containing manganese nitrate and nickel nitrate at an atomic ratio of Mn:Ni of 1:1 and coprecipitation was performed; then, heating was provided to 150°C and sequentially, drying was performed to produce a manganese-nickel coprecipitate compound. The aforementioned manganese-nickel coprecipitate compound was added to lithium hydroxide solution, stirring was provided; then, evaporation of

the solvent was done to dry, and baking was done for 12 hours at a temperature of 960°C in an oxygen atmosphere, and finally, classification of the particles was carried out to produce a powder of  $D_{50}=20\text{ }\mu\text{m}$ . The specific surface area of the particles based on the BET method was  $0.9\text{ m}^2/\text{g}$ .

The measurement results of X-ray analysis of the above-mentioned powder by  $\text{CuK}\alpha$  ray indicated formation of a monolayer having high crystallinity that appears to be a layer structure similar to that of the above-mentioned powder A. The results of elemental analysis indicated that the composition of the aforementioned powder was  $\text{LiMn}_{0.5}\text{Ni}_{0.5}\text{O}_2$ . The powder produced above was used as the positive electrode active material and production of a square lithium cell having a capacity of approximately 15 Ah indicated by Fig. 2 was done as in (Working Example 1-1). The cell produced was defined as the cell of Working Example 1-7.

(Working Example 1-8)

A sodium hydroxide solution was added to an aqueous solution containing manganese nitrate and nickel nitrate at an atomic ratio of Mn:Ni of 1:1 and coprecipitation was performed; then, heating was provided to 150°C and sequentially, drying was performed to produce a manganese-nickel coprecipitate compound. The aforementioned manganese-nickel coprecipitate compound was added to lithium hydroxide solution, stirring was provided; then, evaporation of the solvent was done to dry, and baking was done for 12 hours at a temperature of 980°C in an oxygen atmosphere, and finally, classification of the particles was carried out to produce a powder of  $D_{50}=20\text{ }\mu\text{m}$ . The specific surface area of the particles based on the BET method was  $0.9\text{ m}^2/\text{g}$ .

The measurement results of X-ray analysis of the above-mentioned powder by  $\text{CuK}\alpha$  ray indicated formation of a monolayer having high crystallinity that appears to be a layer structure similar to that of the above-mentioned powder A. The results of the elemental analysis indicated that the composition of the aforementioned powder was  $\text{LiMn}_{0.5}\text{Ni}_{0.5}\text{O}_2$ . The powder produced above was used as the positive electrode active material and production of a square lithium cell



having a capacity of approximately 15 Ah indicated by Fig. 2 was done as in (Working Example 1-1). The cell produced was defined as the cell of Working Example 1-8.

[p. 36]

(Working Example 1-9)

A sodium hydroxide solution was added to an aqueous solution containing manganese nitrate and nickel nitrate at an atomic ratio of Mn:Ni of 1:1 and coprecipitation was performed; then, heating was performed to 150°C and sequentially, drying was done to produce a manganese-nickel coprecipitate compound. The aforementioned manganese-nickel coprecipitate compound was added to lithium hydroxide solution, stirring was provided; then, evaporation of the solvent was done to dry, and baking was done for 5 hours at a temperature of 1000°C in an oxygen atmosphere, and finally, classification of the particles was carried out to produce a powder of  $D_{50}=20\text{ }\mu\text{m}$ . The specific surface area of the particle based on the BET method was  $0.3\text{ m}^2/\text{g}$ .

The measurement result of the X-ray analysis of the above-mentioned powder by  $\text{CuK}\alpha$  ray indicated formation of a monolayer having high crystallinity that appears to be the layer structure similar to that of the above-mentioned powder A. The results of the elemental analysis indicated that the composition of the aforementioned powder was  $\text{LiMn}_{0.5}\text{Ni}_{0.5}\text{O}_2$ . The powder produced above was used as the positive electrode active material and production of a square lithium cell having a capacity of approximately 15 Ah indicated by Fig. 2 was done as in (Working Example 1-1). The cell produced was defined as the cell of Working Example 1-9.

(Working Example 1-10)

A sodium hydroxide solution was added to an aqueous solution containing manganese nitrate and nickel nitrate at an atomic ratio of Mn:Ni of 1:1 and coprecipitation was performed; then, heating was provided to 150°C and sequentially, drying was done to produce a manganese-nickel coprecipitate compound. The aforementioned manganese-nickel coprecipitate compound was added to lithium hydroxide solution, stirring was provided; then, evaporation of the solvent

was done to dry, and baking was done for 5 hours at a temperature of 1000°C in an oxygen atmosphere, and finally, classification of the particles was carried out to produce a powder of  $D_{50}=20\text{ }\mu\text{m}$ . The specific surface area of the particles based on the BET method was  $0.3\text{ m}^2/\text{g}$ .

The measurement results of X-ray analysis of the above-mentioned powder by  $\text{CuK}\alpha$  ray indicated formation of a monolayer having high crystallinity that appears to be the layer structure similar to that of the above-mentioned powder A. The X-ray diffraction chart of the aforementioned powder is indicated by Fig. 4. The results of elemental analysis indicated that the composition of the aforementioned powder was  $\text{LiMn}_{0.5}\text{Ni}_{0.5}\text{O}_2$ . The powder produced above was used as the positive electrode active material and production of a square lithium cell having a capacity of approximately 15 Ah indicated by Fig. 2 was done as in (Working Example 1-1). The cell produced was defined as the cell of Working Example 1-10.

[p. 37]

(Working Example 1-11)

A sodium hydroxide solution was added to an aqueous solution containing manganese nitrate and nickel nitrate at an atomic ratio of Mn:Ni of 1:1 and coprecipitation was performed; then, heating was provided to 150°C and sequentially, drying was done to produce a manganese-nickel coprecipitate compound. The aforementioned manganese-nickel coprecipitate compound was added to lithium hydroxide solution, stirring was provided; then, evaporation of the solvent was done to dry, and baking was done for 20 hours at a temperature of 1000°C in an oxygen atmosphere, and finally, classification of the particles was carried out to produce a powder of  $D_{50}=5\text{ }\mu\text{m}$ . The specific surface area of the particles based on the BET method was  $1.5\text{ m}^2/\text{g}$ .

The measurement results of X-ray analysis of the above-mentioned powder by  $\text{CuK}\alpha$  ray indicated formation of a monolayer having high crystallinity that appears to be the layer structure similar to that of the above-mentioned powder A. The X-ray diffraction chart of the aforementioned powder is indicated by Fig. 4. The result of the elemental analysis indicated that the composition of the aforementioned powder was  $\text{LiMn}_{0.5}\text{Ni}_{0.5}\text{O}_2$ . The powder produced above

was used as the positive electrode active material and production of a square lithium cell having a capacity of approximately 15 Ah indicated by Fig. 2 was done as in (Working Example 1-1). The cell produced was defined as the cell of Working Example 1-11.

(Comparative Example 1-1)

A sodium hydroxide solution was added to an aqueous solution containing manganese nitrate and nickel nitrate at an atomic ratio of Mn:Ni of 1.9:0.1 and coprecipitation was performed; then, heating was provided to 150°C and sequentially, drying was done to produce a manganese-nickel coprecipitate compound. The aforementioned manganese-nickel coprecipitate compound was added to lithium hydroxide solution, stirring was provided; then, evaporation of the solvent was done to dry, and baking was done for 3 hours at a temperature of 950°C in an oxygen atmosphere, and finally, classification of the particles was carried out to produce a powder of  $D_{50}=20\text{ }\mu\text{m}$ . The specific surface area of the particles based on the BET method was  $0.6\text{ m}^2/\text{g}$ .

Based on the results of X-ray analysis of the above-mentioned powder by  $\text{CuK}\alpha$  ray, diffraction peaks were observed at  $2\theta$  18 degrees, 37 degrees, 39 degrees, 45 degrees, 61 degrees, 65 degrees and 67 degrees, and synthesis of layer-structured halite that belongs to special group C3/m was confirmed. The results of elemental analysis indicated that the composition of the aforementioned powder was  $\text{LiMn}_{0.95}\text{Ni}_{0.05}\text{O}_2$ . The powder produced above was used as the positive electrode active material and production of a square lithium cell having a capacity of approximately 15 Ah indicated by Fig. 2 was done as in (Working Example 1-1). The cell produced was defined as the cell of Comparative Example 1-1.

[p. 38]

(Comparative Example 1-2)

A sodium hydroxide solution was added to an aqueous solution containing manganese nitrate and precipitation was performed; then, heating was provided to 150°C and sequentially, drying was done to produce a manganese compound. The aforementioned manganese compound

was added to lithium hydroxide solution, stirring was provided; then, evaporation of the solvent was done to dry, and baking was done for 3 hours at a temperature of 850°C in an oxygen atmosphere, and finally, classification of the particles was carried out to produce a powder of  $D_{50}=10\text{ }\mu\text{m}$ . The specific surface area of the particles based on the BET method was  $0.4\text{ m}^2/\text{g}$ . The measurement results of X-ray analysis of the above-mentioned powder by  $\text{CuK}\alpha$  ray indicated formation of a crystal having a spinel structure. The results of elemental analysis indicated that the composition of the aforementioned powder was  $\text{LiMn}_{1.05}\text{Ni}_{1.95}\text{O}_4$ . The powder produced above was used as the positive electrode active material and production of a square lithium cell having a capacity of approximately 15 Ah indicated by Fig. 2 was done as in (Working Example 1-1). The cell produced was defined as the cell of Comparative Example 1-2.

(Comparative Example 1-3)

A sodium hydroxide solution was added to an aqueous solution containing manganese nitrate and nickel nitrate at an atomic ratio of Mn:Ni of 1:1 and coprecipitation was performed; then, heating was provided to 150°C and sequentially, drying was done to produce a manganese-nickel coprecipitate compound. The aforementioned manganese-nickel coprecipitate compound was added to lithium hydroxide solution, stirring was provided; then, evaporation of the solvent was done to dry, and baking was done for 3 hours at a temperature of 1000°C in an oxygen atmosphere, and finally, classification of the particles was carried out to produce a powder of  $D_{50}=3\text{ }\mu\text{m}$ . The specific surface area of the particles based on the BET method was  $2.0\text{ m}^2/\text{g}$ .

The measurement results of X-ray analysis of the above-mentioned powder by  $\text{CuK}\alpha$  ray indicated formation of a monolayer having high crystallinity that appears to be the layer structure similar to that of the above-mentioned powder A. The results of the elemental analysis indicated that the composition of the aforementioned powder was  $\text{LiMn}_{0.5}\text{Ni}_{0.5}\text{O}_2$ . The powder produced above was used as the positive electrode active material and production of a square lithium cell having a capacity of approximately 15 Ah indicated by Fig. 2 was done as in (Working Example 1-1). The cell produced was defined as the cell of Comparative Example 1-3.

## (Comparative Example 1-4)

A sodium hydroxide solution was added to an aqueous solution containing manganese nitrate and nickel nitrate at an atomic ratio of Mn:Ni of 1:1 and coprecipitation was performed; then, heating was provided to 150°C and sequentially, drying was done to produce a manganese-nickel coprecipitate compound. The aforementioned manganese-nickel coprecipitate compound was added to lithium hydroxide solution, stirring was provided; then, evaporation of the solvent was done to dry, and baking was done for 15 hours at a temperature of 800°C in an oxygen atmosphere, and finally, classification of the particles was carried out to produce a powder of  $D_{50}=5\text{ }\mu\text{m}$ . The specific surface area of the particles based on the BET method was  $2.0\text{ m}^2/\text{g}$ .

The measurement results of X-ray analysis of the above-mentioned powder by  $\text{CuK}\alpha$  ray indicated formation of a monolayer having high crystallinity that appears to be the layer structure similar to that of the above-mentioned powder A. The results of elemental analysis indicated that the composition of the aforementioned powder was  $\text{LiMn}_{0.5}\text{Ni}_{0.5}\text{O}_2$ . The powder produced above was used as the positive electrode active material and production of a square lithium cell having a capacity of approximately 15 Ah indicated by Fig. 2 was done as in (Working Example 1-1). The cell produced was defined as the cell of Comparative Example 1-4.

## (Comparative Example 1-5)

A sodium hydroxide solution was added to an aqueous solution containing manganese nitrate and nickel nitrate at an atomic ratio of Mn:Ni of 1:1 and coprecipitation was performed; then, heating was provided to 150°C and sequentially, drying was done to produce a manganese-nickel coprecipitate compound. The aforementioned manganese-nickel coprecipitate compound was added to lithium hydroxide solution, stirring was provided; then, evaporation of the solvent was done to dry, and baking was done for 24 hours at a temperature of 1000°C in an oxygen atmosphere, and finally, classification of the particles was carried out to produce a powder of  $D_{50}=5\text{ }\mu\text{m}$ . The specific surface area of the particles based on the BET method was  $0.2\text{ m}^2/\text{g}$ .

The measurement results of X-ray analysis of the above-mentioned powder by  $\text{CuK}\alpha$  ray indicated formation of a monolayer having high crystallinity that appears to be a layer structure similar to that of the above-mentioned powder A. The results of the elemental analysis indicated that the composition of the aforementioned powder was  $\text{LiMn}_{0.5}\text{Ni}_{0.5}\text{O}_2$ . The powder produced above was used as the positive electrode active material and production of a square lithium cell having a capacity of approximately 15 Ah indicated by Fig. 2 was done as in (Working Example 1-1). The cell produced was defined as the cell of Comparative Example 1-5.

[p. 40]

## (Comparative Example 1-6)

A sodium hydroxide solution was added to an aqueous solution containing manganese nitrate and nickel nitrate at an atomic ratio of Mn:Ni of 1:1 and coprecipitation was performed; then, heating was provided to 150°C and sequentially, drying was done to produce a manganese-nickel coprecipitate compound. The aforementioned manganese-nickel coprecipitate compound was added to lithium hydroxide solution, stirring was provided; then, evaporation of the solvent was done to dry, and baking was done for 24 hours at a temperature of 1100°C in an oxygen atmosphere, and finally, classification of the particles was carried out to produce a powder of  $D_{50}=30\text{ }\mu\text{m}$ . The specific surface area of the particles based on the BET method was  $0.2\text{ m}^2/\text{g}$ .

The measurement results of X-ray analysis of the above-mentioned powder by  $\text{CuK}\alpha$  ray indicated formation of a monolayer having high crystallinity that appears to be the layer structure similar to that of the above-mentioned powder A. The results of elemental analysis indicated that the composition of the aforementioned powder was  $\text{LiMn}_{0.5}\text{Ni}_{0.5}\text{O}_2$ . The powder produced above was used as the positive electrode active material and production of a square lithium cell having a capacity of approximately 15 Ah indicated by Fig. 2 was done as in (Working Example 1-1). The cell produced was defined as the cell of Comparative Example 1-6.

[Second embodiment]

## (Working Example 2-1)

A sodium hydroxide solution was added to an aqueous solution containing manganese nitrate and nickel nitrate at an atomic ratio of Mn:Ni of 0.95:0.95 and coprecipitation was performed; then, heating was provided to 150°C and sequentially, drying was done to produce a manganese-nickel coprecipitate compound. Furthermore, the aforementioned manganese-nickel coprecipitate compound and boric acid were added to lithium hydroxide solution at an elemental ratio of Li:Mn:Ni:B of 2:0.95:0.95:0.10, and baking was done for 12 hours at a temperature of 1000°C in an oxygen atmosphere, and finally, classification of the particles was carried out to produce a powder of  $D_{50}=9\text{ }\mu\text{m}$ . The specific surface area of the particles based on the BET method was  $0.9\text{ m}^2/\text{g}$ . The measurement results of X-ray analysis of the above-mentioned powder by  $\text{CuK}\alpha$  ray indicated formation of a monolayer having high crystallinity that appears to be the layer structure similar to that of the above-mentioned powder A. The results of elemental analysis indicated that the composition of the aforementioned powder was  $\text{LiMn}_{0.475}\text{Ni}_{0.475}\text{B}_{0.05}\text{O}_2$ . The powder produced above was used as the positive electrode active material and production of a square lithium cell having a capacity of approximately 15 Ah indicated by Fig. 2 was done as in (Working Example 1-1). The cell produced was defined as the cell of Working Example 2-1.

(Working Example 2-2)

A sodium hydroxide solution was added to an aqueous solution containing manganese nitrate, nickel nitrate and vanadium oxide at an atomic ratio of Mn:Ni:V of 0.95:0.95:0.1 and coprecipitation was performed; then, heating was provided to 150°C and sequentially, drying was done to produce a manganese-nickel-vanadium coprecipitate compound.

[p. 41]

Furthermore, the aforementioned manganese-nickel-vanadium coprecipitate compound was added to lithium hydroxide solution, then, evaporation of the solvent was done to dry, and baking was done for 12 hours at a temperature of 1000°C in an oxygen atmosphere, and finally, classification of the particles was carried out to produce a powder of  $D_{50}=9\text{ }\mu\text{m}$ . The specific

surface area of the particles based on the BET method was  $0.9 \text{ m}^2/\text{g}$ . The measurement results of X-ray analysis of the above-mentioned powder by  $\text{CuK}\alpha$  ray indicated formation of a monolayer having high crystallinity that appears to be the layer structure similar to that of the above-mentioned powder A. The results of elemental analysis indicated that the composition of the aforementioned powder was  $\text{LiMn}_{0.475}\text{Ni}_{0.475}\text{V}_{0.05}\text{O}_2$ . The powder produced above was used as the positive electrode active material and production of a square lithium cell having a capacity of approximately 15 Ah indicated by Fig. 2 was done as in (Working Example 1-1). The cell produced was defined as the cell of Working Example 2-2.

(Working Example 2-3)

A sodium hydroxide solution was added to an aqueous solution containing manganese nitrate, nickel nitrate and aluminum nitrate at an atomic ratio of Mn:Ni:Al of 0.95:0.95:0.1 and coprecipitation was performed; then, heating was provided to  $150^\circ\text{C}$  and sequentially, drying was done to produce a manganese-nickel-aluminum coprecipitate compound. Furthermore, the aforementioned manganese-nickel-aluminum coprecipitate compound was added to lithium hydroxide solution; then, evaporation of the solvent was done to dry, and baking was done for 12 hours at a temperature of  $1000^\circ\text{C}$  in an oxygen atmosphere, and finally, classification of the particles was carried out to produce a powder of  $D_{50}=9 \text{ }\mu\text{m}$ . The specific surface area of the particles based on the BET method was  $0.9 \text{ m}^2/\text{g}$ . The measurement results of X-ray analysis of the above-mentioned powder by  $\text{CuK}\alpha$  ray indicated formation of a monolayer having high crystallinity that appears to be the layer structure similar to that of the above-mentioned powder A. The results of elemental analysis indicated that the composition of the aforementioned powder was  $\text{LiMn}_{0.475}\text{Ni}_{0.475}\text{Al}_{0.05}\text{O}_2$ . The powder produced above was used as the positive electrode active material and production of a square lithium cell having a capacity of approximately 15 Ah indicated by Fig. 2 was done as in (Working Example 1-1). The cell produced was defined as the cell of Working Example 2-3.

(Working Example 2-4)



A sodium hydroxide solution was added to an aqueous solution containing manganese nitrate, nickel nitrate and magnesium nitrate at an atomic ratio of Mn:Ni:Mg of 0.95:0.95:0.1 and coprecipitation was performed; then, heating was provided to 150°C and sequentially, drying was done to produce a manganese-nickel-magnesium coprecipitate compound. Furthermore, the aforementioned manganese-nickel-magnesium coprecipitate compound was added to lithium hydroxide solution; then, evaporation of the solvent was done to dry, and baking was done for 12 hours at a temperature of 1000°C in an oxygen atmosphere, and finally, classification of the particles was carried out to produce a powder of  $D_{50}=9\text{ }\mu\text{m}$ . The specific surface area of the particles based on the BET method was  $0.9\text{ m}^2/\text{g}$ .

[p. 42]

The measurement results of X-ray analysis of the above-mentioned powder by  $\text{CuK}\alpha$  ray indicated formation of a monolayer having high crystallinity that appears to be the layer structure similar to that of the above-mentioned powder A. The results of elemental analysis indicated that the composition of the aforementioned powder was  $\text{LiMn}_{0.475}\text{Ni}_{0.475}\text{Mg}_{0.05}\text{O}_2$ . The powder produced above was used as the positive electrode active material and production of a square lithium cell having a capacity of approximately 15 Ah indicated by Fig. 2 was done as in (Working Example 1-1). The cell produced was defined as the cell of Working Example 2-4.

(Working Example 2-5)

A sodium hydroxide solution was added to an aqueous solution containing manganese nitrate, nickel nitrate and cobalt nitrate at an atomic ratio of Mn:Ni:Co of 0.95:0.95:0.1 and coprecipitation was performed; then, heating was provided to 150°C and sequentially, drying was done to produce a manganese-nickel-cobalt coprecipitate compound. Furthermore, the aforementioned manganese-nickel-cobalt coprecipitate compound was added to lithium hydroxide solution; then, evaporation of the solvent was done to dry, and baking was done for 12 hours at a temperature of 1000°C in an oxygen atmosphere, and finally, classification of the particles was carried out to produce a powder of  $D_{50}=9\text{ }\mu\text{m}$ . The specific surface area of the

particles based on the BET method was  $0.9 \text{ m}^2/\text{g}$ . The measurement results of X-ray analysis of the above-mentioned powder by  $\text{CuK}\alpha$  ray indicated formation of a monolayer having high crystallinity that appears to be the layer structure similar to that of the above-mentioned powder A. The results of elemental analysis indicated that the composition of the aforementioned powder was  $\text{LiMn}_{0.475}\text{Ni}_{0.475}\text{Co}_{0.05}\text{O}_2$ . The powder produced above was used as the positive electrode active material and production of a square lithium cell having a capacity of approximately 15 Ah indicated by Fig. 2 was done as in (Working Example 1-1). The cell produced was defined as the cell of Working Example 2-5.

(Working Example 2-6)

A sodium hydroxide solution was added to an aqueous solution containing manganese nitrate, nickel nitrate and chromium nitrate at an atomic ratio of Mn:Ni:Cr of 0.95:0.95:0.1 and coprecipitation was performed; then, heating was provided to  $150^\circ\text{C}$  and sequentially, drying was done to produce a manganese-nickel-chromium coprecipitate compound. Furthermore, the aforementioned manganese-nickel-magnesium coprecipitate compound was added to lithium hydroxide solution; then, evaporation of the solvent was done to dry, and baking was done for 12 hours at a temperature of  $1000^\circ\text{C}$  in an oxygen atmosphere, and finally, classification of the particles was carried out to produce a powder of  $D_{50}=9 \text{ }\mu\text{m}$ . The specific surface area of the particles based on the BET method was  $0.9 \text{ m}^2/\text{g}$ .

[p. 43]

The measurement results of X-ray analysis of the above-mentioned powder by  $\text{CuK}\alpha$  ray indicated formation of a monolayer having high crystallinity that appears to be the layer structure similar to that of the above-mentioned powder A. The results of elemental analysis indicated that the composition of the aforementioned powder was  $\text{LiMn}_{0.475}\text{Ni}_{0.475}\text{Cr}_{0.05}\text{O}_2$ . The powder produced above was used as the positive electrode active material and production of a square lithium cell having a capacity of approximately 15 Ah indicated by Fig. 2 was done as in (Working Example 1-1). The cell produced was defined as the cell of Working Example 2-6.

## (Working Example 2-7)

A sodium hydroxide solution was added to an aqueous solution containing manganese nitrate, nickel nitrate, and titanium oxide at an atomic ratio of Mn:Ni:Ti of 0.95:0.95:0.1 and coprecipitation was performed; then, heating was provided to 150°C and sequentially, drying was done to produce a manganese-nickel-titanium coprecipitate compound. Furthermore, the aforementioned manganese-nickel-titanium coprecipitate compound was added to lithium hydroxide solution; then, evaporation of the solvent was done to dry, and baking was done for 12 hours at a temperature of 1000°C in an oxygen atmosphere, and finally, classification of the particles was carried out to produce a powder of  $D_{50}=9\text{ }\mu\text{m}$ . The specific surface area of the particles based on the BET method was  $0.9\text{ m}^2/\text{g}$ . The measurement results of X-ray analysis of the above-mentioned powder by  $\text{CuK}\alpha$  ray indicated formation of a monolayer having high crystallinity that appears to be the layer structure similar to that of the above-mentioned powder A. The results of elemental analysis indicated that the composition of the aforementioned powder was  $\text{LiMn}_{0.475}\text{Ni}_{0.475}\text{Ti}_{0.05}\text{O}_2$ . The powder produced above was used as the positive electrode active material and production of a square lithium cell having a capacity of approximately 15 Ah indicated by Fig. 2 was done as in (Working Example 1-1). The cell produced was defined as the cell of Working Example 2-7.

## (Working Example 2-8)

A sodium hydroxide solution was added to an aqueous solution containing manganese nitrate, nickel nitrate and iron sulfate at an atomic ratio of Mn:Ni:Fe of 0.95:0.95:0.1 and coprecipitation was performed; then, heating was provided to 150°C and sequentially, drying was done to produce a manganese-nickel-iron coprecipitate compound. Furthermore, the aforementioned manganese-nickel-iron coprecipitate compound was added to lithium hydroxide solution, stirring was provided; then, evaporation of the solvent was done to dry, and baking was done for 12 hours at a temperature of 1000°C in an oxygen atmosphere, and finally, classification of the particles was carried out to produce a powder of  $D_{50}=9\text{ }\mu\text{m}$ . The specific surface area of

the particles based on the BET method was  $0.9 \text{ m}^2/\text{g}$ .

[p. 44]

The measurement results of X-ray analysis of the above-mentioned powder by  $\text{CuK}\alpha$  ray indicated formation of a monolayer having high crystallinity that appears to be the layer structure similar to that of the above-mentioned powder A. The results of elemental analysis indicated that the composition of the aforementioned powder was  $\text{LiMn}_{0.475}\text{Ni}_{0.475}\text{Fe}_{0.05}\text{O}_2$ . The powder produced above was used as the positive electrode active material and production of a square lithium cell having a capacity of approximately 15 Ah indicated by Fig. 2 was done as in (Working Example 1-1). The cell produced was defined as the cell of Working Example 2-8.

(Working Example 2-9)

A sodium hydroxide solution was added to an aqueous solution containing manganese nitrate, nickel nitrate and copper sulfate at an atomic ratio of Mn:Ni:Cu of 0.95:0.95:0.1 and coprecipitation was performed; then, heating was provided to  $150^\circ\text{C}$  and sequentially, drying was done to produce a manganese-nickel-copper coprecipitate compound. Furthermore, the aforementioned manganese-nickel-copper coprecipitate compound was added to lithium hydroxide solution, stirring was provided; then, evaporation of the solvent was done to dry, and baking was done for 12 hours at a temperature of  $1000^\circ\text{C}$  in an oxygen atmosphere, and finally, classification of the particles was carried out to produce a powder of  $D_{50}=9 \text{ }\mu\text{m}$ . The specific surface area of the particles based on the BET method was  $0.9 \text{ m}^2/\text{g}$ . The measurement results of X-ray analysis of the above-mentioned powder by  $\text{CuK}\alpha$  ray indicated formation of a monolayer having high crystallinity that appears to be the layer structure similar to that of the above-mentioned powder A. The results of elemental analysis indicated that the composition of the aforementioned powder was  $\text{LiMn}_{0.475}\text{Ni}_{0.475}\text{Cu}_{0.05}\text{O}_2$ . The powder produced above was used as the positive electrode active material and production of a square lithium cell having a capacity of approximately 15 Ah indicated by Fig. 2 was done as in (Working Example 1-1). The cell produced was defined as the cell of Working Example 2-9.

## (Working Example 2-10)

A sodium hydroxide solution was added to an aqueous solution containing manganese nitrate, nickel nitrate and zinc sulfate at an atomic ratio of Mn:Ni:Zn of 0.95:0.95:0.1 and coprecipitation was performed; then, heating was provided to 150°C and sequentially, drying was done to produce a manganese-nickel-zinc coprecipitate compound. Furthermore, the aforementioned manganese-nickel-zinc coprecipitate compound was added to lithium hydroxide solution, stirring was provided; then, evaporation of the solvent was done to dry, and baking was done for 12 hours at a temperature of 1000°C in an oxygen atmosphere, and finally, classification of the particles was carried out to produce a powder of  $D_{50}=9\text{ }\mu\text{m}$ . The specific surface area of the particles based on the BET method was  $0.9\text{ m}^2/\text{g}$ . The measurement results of X-ray analysis of the above-mentioned powder by  $\text{CuK}\alpha$  ray indicated formation of a monolayer having high crystallinity that appears to be the layer structure similar to that of the above-mentioned powder A.

[p. 45]

The results of elemental analysis indicated that the composition of the aforementioned powder was  $\text{LiMn}_{0.475}\text{Ni}_{0.475}\text{Zn}_{0.05}\text{O}_2$ . The powder produced above was used as the positive electrode active material and production of a square lithium cell having a capacity of approximately 15 Ah indicated by Fig. 2 was done as in (Working Example 1-1). The cell produced was defined as the cell of Working Example 2-10.

## (Comparative Example 2-1)

A sodium hydroxide solution was added to an aqueous solution containing manganese nitrate, nickel nitrate and magnesium nitrate at an atomic ratio of Mn:Ni:Mg of 0.95:0.95:0.1 and coprecipitation was performed; then, heating was provided to 150°C and sequentially, drying was done to produce a manganese-nickel-magnesium coprecipitate compound. Furthermore, the aforementioned manganese-nickel-magnesium coprecipitate compound was added to lithium hydroxide solution, stirring was provided; then, evaporation of the solvent was done to dry, and

baking was done for 12 hours at a temperature of 1000°C in an oxygen atmosphere, and finally, classification of the particles was carried out to produce a powder of  $D_{50}=15\text{ }\mu\text{m}$ . The specific surface area of the particles based on the BET method was  $0.2\text{ m}^2/\text{g}$ . The measurement results of X-ray analysis of the above-mentioned powder by  $\text{CuK}\alpha$  ray indicated formation of a monolayer having high crystallinity that appears to be the layer structure similar to that of the above-mentioned powder A. The results of elemental analysis indicated that the composition of the aforementioned powder was  $\text{LiMn}_{0.475}\text{Ni}_{0.475}\text{Mg}_{0.05}\text{O}_2$ . The powder produced above was used as the positive electrode active material and production of a square lithium cell having a capacity of approximately 15 Ah indicated by Fig. 2 was done as in (Working Example 1-1). The cell produced was defined as the cell of Comparative Example 2-1.

(Comparative Example 2-2)

A sodium hydroxide solution was added to an aqueous solution containing manganese nitrate, nickel nitrate and magnesium nitrate at an atomic ratio of Mn:Ni:Mg of 0.95:0.95:0.1 and coprecipitation was performed; then, heating was provided to 150°C and sequentially, drying was done to produce a manganese-nickel-magnesium coprecipitate compound. Furthermore, the aforementioned manganese-nickel-magnesium coprecipitate compound was added to lithium hydroxide solution, stirring was provided; then, evaporation of the solvent was done to dry, and baking was done for 12 hours at a temperature of 1000°C in an oxygen atmosphere, and finally, classification of the particles was carried out to produce a powder of  $D_{50}=6\text{ }\mu\text{m}$ . The specific surface area of the particles based on the BET method was  $1.9\text{ m}^2/\text{g}$ . The measurement results of X-ray analysis of the above-mentioned powder by  $\text{CuK}\alpha$  ray indicated formation of a monolayer having high crystallinity that appears to be the layer structure similar to that of the above-mentioned powder A.

[p. 46]

The results of elemental analysis indicated that the composition of the aforementioned powder was  $\text{LiMn}_{0.475}\text{Ni}_{0.475}\text{Mg}_{0.05}\text{O}_2$ . The powder produced above was used as the positive electrode

active material and production of a square lithium cell having a capacity of approximately 15 Ah indicated by Fig. 2 was done as in (Working Example 1-1). The cell produced was defined as the cell of Comparative Example 2-2.

[Third embodiment]

(Working Example 3-1)

A sodium hydroxide solution was added to an aqueous solution containing manganese nitrate and nickel nitrate at an atomic ratio of Mn:Ni of 0.95:0.95 and coprecipitation was performed; then, heating was provided to 150°C and subsequently, drying was performed to produce a manganese-nickel coprecipitate compound. Furthermore, the aforementioned manganese-nickel coprecipitate compound and boric acid were added to lithium hydroxide solution at an elemental ratio Li:Mn:Ni:B of 2.00:0.95:0.95:0.1; then, baking was done for 12 hours at a temperature of 1000°C in an oxygen atmosphere, and finally, classification of the particles was carried out to produce a powder of  $D_{50}=9\text{ }\mu\text{m}$ . The specific surface area of the particles based on the BET method was  $1.0\text{ m}^2/\text{g}$ . The measurement results of X-ray analysis of the above-mentioned powder by  $\text{CuK}\alpha$  ray indicated formation of a monolayer having high crystallinity that appears to be a layer structure similar to that of the above-mentioned powder A. The above-mentioned powder produced was defined as powder B. The results of elemental analysis indicated that the composition of the aforementioned powder was  $\text{LiMn}_{0.475}\text{Ni}_{0.475}\text{B}_{0.05}\text{O}_2$ .

Segregation of the B (boron) on the surface was observed when an analysis was made in the depth direction (see Fig. 1 for reference). The powder B produced above was used as the positive electrode active material and production of a square lithium cell having a capacity of approximately 15 Ah indicated by Fig. 2 was done as in (Working Example 1-1). The cell produced was defined as the cell of Comparative Example 3-1.

(Working Example 3-2)

A sodium hydroxide solution was added to an aqueous solution containing manganese

nitrate, nickel nitrate, and vanadium oxide at an atomic ratio of Mn:Ni:V of 0.95:0.948:0.1 and coprecipitation was performed; then, heating was provided to 150°C and subsequently, drying was done to produce a manganese-nickel-vanadium coprecipitate compound. Furthermore, the aforementioned manganese-nickel-vanadium coprecipitate compound and boric acid were added to lithium hydroxide solution to form an elemental ratio of Li:Mn:Ni:V:B of 2:0.95:0.948:0.1:0.002, and baking was done for 12 hours at a temperature of 1000°C in an oxygen atmosphere, and finally, classification of the particles was carried out to produce a powder of  $D_{50}=9\text{ }\mu\text{m}$ .

[p. 47]

The specific surface area of the particles based on the BET method was  $1.0\text{ m}^2/\text{g}$ . The measurement results of X-ray analysis of the above-mentioned powder by  $\text{CuK}\alpha$  ray indicated formation of a monolayer having high crystallinity that appears to be a layer structure similar to that of the above-mentioned powder A. The results of elemental analysis indicated that the composition of the aforementioned powder was  $\text{LiMn}_{0.475}\text{Ni}_{0.474}\text{V}_{0.05}\text{B}_{0.001}\text{O}_2$ .

The powder produced above was used as the positive electrode active material and production of a square lithium cell having a capacity of approximately 15 Ah indicated by Fig. 2 was done as in (Working Example 1-1). The cell produced was defined as the cell of Working Example 3-2.

(Working Example 3-3)

A sodium hydroxide solution was added to an aqueous solution containing manganese nitrate, nickel nitrate, and aluminum nitrate at an atomic ratio of Mn:Ni:Al of 0.95:0.948:0.1 and coprecipitation was performed; then, heating was provided to 150°C and subsequently, drying was done to produce a manganese-nickel- aluminum coprecipitate compound. Furthermore, the aforementioned manganese-nickel-aluminum coprecipitate compound and boric acid were added to lithium hydroxide solution to form an elemental ratio of Li:Mn:Ni:Al:B of 2:0.95:0.948:0.1:0.002, and baking was done for 12 hours at a temperature of 1000°C in an



oxygen atmosphere, and finally, classification of the particles was carried out to produce a powder of  $D_{50}=9\text{ }\mu\text{m}$ . The specific surface area of the particles based on the BET method was  $1.0\text{ m}^2/\text{g}$ . The measurement results of X-ray analysis of the above-mentioned powder by  $\text{CuK}\alpha$  ray indicated formation of a monolayer having high crystallinity that appears to be a layer structure similar to that of the above-mentioned powder A. The results of elemental analysis indicated that the composition of the aforementioned powder was  $\text{LiMn}_{0.475}\text{Ni}_{0.474}\text{Al}_{0.05}\text{B}_{0.001}\text{O}_2$ .

The powder produced above was used as the positive electrode active material and production of a square lithium cell having a capacity of approximately 15 Ah indicated by Fig. 2 was done as in (Working Example 1-1). The cell produced was defined as the cell of Working Example 3-3.

(Working Example 3-4)

A sodium hydroxide solution was added to an aqueous solution containing manganese nitrate, nickel nitrate and magnesium nitrate at an atomic ratio of Mn:Ni:Mg of 0.95:0.948:0.1 and coprecipitation was performed; then, heating was provided to  $150^\circ\text{C}$  and subsequently, drying was done to produce a manganese-nickel-magnesium coprecipitate compound.

[p. 48]

Furthermore, the aforementioned manganese-nickel-magnesium coprecipitate compound and boric acid were added to lithium hydroxide solution to form an elemental ratio of Li:Mn:Ni:Mg:B of 2:0.95:0.948:0.1:0.002, and baking was done for 12 hours at a temperature of  $1000^\circ\text{C}$  in an oxygen atmosphere, and finally, classification of the particles was carried out to produce a powder of  $D_{50}=9\text{ }\mu\text{m}$ . The specific surface area of the particles based on the BET method was  $1.0\text{ m}^2/\text{g}$ . The measurement results of X-ray analysis of the above-mentioned powder by  $\text{CuK}\alpha$  ray indicated formation of a monolayer having high crystallinity that appears to be a layer structure similar to that of the above-mentioned powder A. The results of elemental analysis indicated that the composition of the aforementioned powder was  $\text{LiMn}_{0.475}\text{Ni}_{0.474}\text{Mg}_{0.05}\text{B}_{0.001}\text{O}_2$ .

The powder produced above was used as the positive electrode active material and production of a square lithium cell having a capacity of approximately 15 Ah indicated by Fig. 2 was done as in (Working Example 1-1). The cell produced was defined as the cell of Working Example 3-4.

(Working Example 3-5)

A sodium hydroxide solution was added to an aqueous solution containing manganese nitrate, nickel nitrate and cobalt nitrate at an atomic ratio of Mn:Ni:Co of 0.95:0.948:0.1 and coprecipitation was performed; then, heating was provided to 150°C and subsequently, drying was done to produce a manganese-nickel-cobalt coprecipitate compound. Furthermore, the aforementioned manganese-nickel-cobalt coprecipitate compound and boric acid were added to lithium hydroxide solution to form an elemental ratio of Li:Mn:Ni:Co:B of 2:0.95:0.948:0.1:0.002, and baking was done for 12 hours at a temperature of 1000°C in an oxygen atmosphere, and finally, classification of the particles was carried out to produce a powder of  $D_{50}=9\text{ }\mu\text{m}$ . The specific surface area of the particles based on the BET method was  $1.0\text{ m}^2/\text{g}$ . The measurement results of X-ray analysis of the above-mentioned powder by  $\text{CuK}\alpha$  ray indicated formation of a monolayer having high crystallinity that appears to be a layer structure similar to that of the above-mentioned powder A. The results of elemental analysis indicated that the composition of the aforementioned powder was  $\text{LiMn}_{0.475}\text{Ni}_{0.474}\text{Co}_{0.05}\text{B}_{0.001}\text{O}_2$ .

The powder produced above was used as the positive electrode active material and production of a square lithium cell having a capacity of approximately 15 Ah indicated by Fig. 2 was done as in (Working Example 1-1). The cell produced was defined as the cell of Working Example 3-5.

[p. 49]

(Working Example 3-6)

A sodium hydroxide solution was added to an aqueous solution containing manganese

nitrate, nickel nitrate and chromium nitrate at an atomic ratio of Mn:Ni:Cr of 0.95:0.948:0.1 and coprecipitation was performed; then, heating was provided to 150°C and subsequently, drying was done to produce a manganese-nickel-vanadium coprecipitate compound. Furthermore, the aforementioned manganese-nickel-chromium coprecipitate compound and boric acid were added to lithium hydroxide solution to form an elemental ratio of Li:Mn:Ni:Cr:B of 2:0.95:0.948:0.1:0.002, and baking was done for 12 hours at a temperature of 1000°C in an oxygen atmosphere, and finally, classification of the particles was carried out to produce a powder of  $D_{50}=9\text{ }\mu\text{m}$ . The specific surface area of the particles based on the BET method was  $1.0\text{ m}^2/\text{g}$ . The measurement results of X-ray analysis of the above-mentioned powder by  $\text{CuK}\alpha$  ray indicated formation of a monolayer having high crystallinity that appears to be a layer structure similar to that of the above-mentioned powder A. The results of elemental analysis indicated that the composition of the aforementioned powder was  $\text{LiMn}_{0.475}\text{Ni}_{0.474}\text{Cr}_{0.05}\text{B}_{0.001}\text{O}_2$ .

The powder produced above was used as the positive electrode active material and production of a square lithium cell having a capacity of approximately 15 Ah indicated by Fig. 2 was done as in (Working Example 1-1). The cell produced was defined as the cell of Working Example 3-6.

(Working Example 3-7)

A sodium hydroxide solution was added to an aqueous solution containing manganese nitrate, nickel nitrate, and titanium oxide at an atomic ratio of Mn:Ni:V of 0.95:0.948:0.1 and coprecipitation was performed; then, heating was provided to 150°C and subsequently, drying was done to produce a manganese-nickel- titanium coprecipitate compound. Furthermore, the aforementioned manganese-nickel-titanium coprecipitate compound and boric acid were added to lithium hydroxide solution to form an elemental ratio of Li:Mn:Ni:Ti:B of 2:0.95:0.948:0.1:0.002, and baking was done for 12 hours at a temperature of 1000°C in an oxygen atmosphere, and finally, classification of the particles was carried out to produce a powder of  $D_{50}=9\text{ }\mu\text{m}$ . The specific surface area of the particles based on the BET method was

1.0 m<sup>2</sup>/g. The measurement results of X-ray analysis of the above-mentioned powder by CuK $\alpha$  ray indicated formation of a monolayer having high crystallinity that appears to be a layer structure similar to that of the above-mentioned powder A. The results of elemental analysis indicated that the composition of the aforementioned powder was LiMn<sub>0.475</sub>Ni<sub>0.474</sub>Ti<sub>0.05</sub>B<sub>0.001</sub>O<sub>2</sub>.

The powder produced above was used as the positive electrode active material and production of a square lithium cell having a capacity of approximately 15 Ah indicated by Fig. 2 was done as in (Working Example 1-1). The cell produced was defined as the cell of Working Example 3-7.

[p. 50]

(Working Example 3-8)

A sodium hydroxide solution was added to an aqueous solution containing manganese nitrate, nickel nitrate, and iron sulfate at an atomic ratio of Mn:Ni:Fe of 0.95:0.948:0.1 and coprecipitation was performed; then, heating was provided to 150°C and subsequently, drying was done to produce a manganese-nickel-iron coprecipitate compound. Furthermore, the aforementioned manganese-nickel-iron coprecipitate compound and boric acid were added to lithium hydroxide solution to form an elemental ratio of Li:Mn:Ni:Fe:B of 2:0.95:0.948:0.1:0.002, and baking was done for 12 hours at a temperature of 1000°C in an oxygen atmosphere, and finally, classification of the particles was carried out to produce a powder of D<sub>50</sub>=9  $\mu$ m. The specific surface area of the particles based on the BET method was 1.0 m<sup>2</sup>/g. The measurement results of X-ray analysis of the above-mentioned powder by CuK $\alpha$  ray indicated formation of a monolayer having high crystallinity that appears to be a layer structure similar to that of the above-mentioned powder A. The results of elemental analysis indicated that the composition of the aforementioned powder was LiMn<sub>0.475</sub>Ni<sub>0.474</sub>Fe<sub>0.05</sub>B<sub>0.001</sub>O<sub>2</sub>.

The powder produced above was used as the positive electrode active material and production of a square lithium cell having a capacity of approximately 15 Ah indicated by Fig. 2

was done as in (Working Example 1-1). The cell produced was defined as the cell of Working Example 3-8.

(Working Example 3-9)

A sodium hydroxide solution was added to an aqueous solution containing manganese nitrate, nickel nitrate and copper sulfate at an atomic ratio of Mn:Ni:Cu of 0.95:0.948:0.1 and coprecipitation was performed; then, heating was provided to 150°C and subsequently, drying was done to produce a manganese-nickel-copper coprecipitate compound. Furthermore, the aforementioned manganese-nickel-copper coprecipitate compound and boric acid were added to lithium hydroxide solution to form an elemental ratio of Li:Mn:Ni:Cu:B of 2:0.95:0.948:0.1:0.002, and baking was done for 12 hours at a temperature of 1000°C in an oxygen atmosphere, and finally, classification of the particles was carried out to produce a powder of  $D_{50}=9\text{ }\mu\text{m}$ . The specific surface area of the particles based on the BET method was  $1.0\text{ m}^2/\text{g}$ . The measurement results of X-ray analysis of the above-mentioned powder by  $\text{CuK}\alpha$  ray indicated formation of a monolayer having high crystallinity that appears to be a layer structure similar to that of the above-mentioned powder A. The results of elemental analysis indicated that the composition of the aforementioned powder was  $\text{LiMn}_{0.475}\text{Ni}_{0.474}\text{Cu}_{0.05}\text{B}_{0.001}\text{O}_2$ .

[p. 51]

The powder produced above was used as the positive electrode active material and production of a square lithium cell having a capacity of approximately 15 Ah indicated by Fig. 2 was done as in (Working Example 1-1). The cell produced was defined as the cell of Working Example 3-9.

(Working Example 3-10)

A sodium hydroxide solution was added to an aqueous solution containing manganese nitrate, nickel nitrate, and zinc sulfate at an atomic ratio of Mn:Ni:Zn of 0.95:0.948:0.1 and coprecipitation was performed; then, heating was provided to 150°C and subsequently, drying

was done to produce a manganese-nickel-zinc coprecipitate compound. Furthermore, the aforementioned manganese-nickel-zinc coprecipitate compound and boric acid were added to lithium hydroxide solution to form an elemental ratio of Li:Mn:Ni:Zn:B of 2:0.95:0.948:0.1:0.002, and baking was done for 12 hours at a temperature of 1000°C in an oxygen atmosphere, and finally, classification of the particles was carried out to produce a powder of  $D_{50}=10\text{ }\mu\text{m}$ . The specific surface area of the particles based on the BET method was  $1.0\text{ m}^2/\text{g}$ . The measurement results of X-ray analysis of the above-mentioned powder by  $\text{CuK}\alpha$  ray indicated formation of a monolayer having high crystallinity that appears to be a layer structure similar to that of the above-mentioned powder A. The results of elemental analysis indicated that the composition of the aforementioned powder was  $\text{LiMn}_{0.475}\text{Ni}_{0.474}\text{Zn}_{0.05}\text{B}_{0.001}\text{O}_2$ .

The powder produced above was used as the positive electrode active material and production of a square lithium cell having a capacity of approximately 15 Ah indicated by Fig. 2 was done as in (Working Example 1-1). The cell produced was defined as the cell of Working Example 3-10.

(Comparative Example 3-1)

A sodium hydroxide solution was added to an aqueous solution containing manganese nitrate and nickel nitrate at an atomic ratio of Mn:Ni of 0.95:0.95 and coprecipitation was performed; then, heating was provided to 150°C and subsequently, drying was done to produce a manganese-nickel coprecipitate compound. Furthermore, the aforementioned manganese-nickel coprecipitate compound and boric acid were added to lithium hydroxide solution to form an elemental ratio of Li:Mn:Ni:B of 2.00:0.95:0.95:0.1, and baking was done for 12 hours at a temperature of 1000°C in an oxygen atmosphere, and finally, classification of the particles was carried out to produce a powder of  $D_{50}=9\text{ }\mu\text{m}$ . The specific surface area of the particles based on the BET method was  $0.2\text{ m}^2/\text{g}$ .

[p. 52]

The measurement results of X-ray analysis of the above-mentioned powder by  $\text{CuK}\alpha$  ray indicated formation of a monolayer having high crystallinity that appears to be a layer structure similar to that of the above-mentioned powder A. The results of elemental analysis indicated that the composition of the aforementioned powder was  $\text{LiMn}_{0.475}\text{Ni}_{0.475}\text{B}_{0.05}\text{O}_2$ .

The powder produced above was used as the positive electrode active material and production of a square lithium cell having a capacity of approximately 15 Ah indicated by Fig. 2 was done as in (Working Example 1-1). The cell produced was defined as the cell of Comparative Example 3-1.

(Comparative Example 3-2)

A sodium hydroxide solution was added to an aqueous solution containing manganese nitrate and nickel nitrate at an atomic ratio of Mn:Ni of 0.95:0.95 and coprecipitation was performed; then, heating was provided to 150°C and subsequently, drying was done to produce a manganese-nickel coprecipitate compound. Furthermore, the aforementioned manganese-nickel coprecipitate compound and boric acid were added to lithium hydroxide solution to form an elemental ratio of Li:Mn:Ni:B of 2.00:0.95:0.95:0.1, and baking was done for 12 hours at a temperature of 1000°C in an oxygen atmosphere, and finally, classification of the particles was carried out to produce a powder of  $D_{50}=4\text{ }\mu\text{m}$ . The specific surface area of the particles based on the BET method was  $2.4\text{ m}^2/\text{g}$ .

The measurement results of X-ray analysis of the above-mentioned powder by  $\text{CuK}\alpha$  ray indicated formation of a monolayer having high crystallinity that appears to be a layer structure similar to that of the above-mentioned powder A. The results of elemental analysis indicated that the composition of the aforementioned powder was  $\text{LiMn}_{0.475}\text{Ni}_{0.475}\text{B}_{0.05}\text{O}_2$ .

The powder produced above was used as the positive electrode active material and production of a square lithium cell having a capacity of approximately 15 Ah indicated by Fig. 2 was done as in (Working Example 1-1). The cell produced was defined as the cell of Comparative Example 3-2.

[Fourth embodiment]

(Working Example 4-1)

A sodium hydroxide solution was added to an aqueous solution containing manganese nitrate, nickel nitrate and cobalt nitrate at an atomic ratio of Mn:Ni:Co of 9:9:2 and coprecipitation was performed; then, heating was provided to 150°C and subsequently, drying was done to produce a manganese-nickel-cobalt coprecipitate compound. The aforementioned manganese-nickel-cobalt coprecipitate compound was added to lithium hydroxide solution, stirring was performed; then, evaporation of the solvent was done to dry, and baking was done for 12 hours at a temperature of 1000°C in an oxygen atmosphere, and finally, classification of the particles was carried out to produce a powder of  $D_{50}=20\text{ }\mu\text{m}$ . The specific surface area of the particles based on the BET method was  $0.9\text{ m}^2/\text{g}$ .

[p. 53]

Based on the results of X-ray analysis of the above-mentioned powder by  $\text{CuK}\alpha$  ray, diffraction peaks were observed at  $2\theta$  18.56 degrees, 36.56 degrees, 38.24 degrees, 44.32 degrees, 48.4 degrees, 58.4 degrees, 64.16 degrees, 64.8 degrees, and 68.8 degrees, and a monolayer having high crystallinity that appears to be a layer structure that belongs to spatial group R3m was synthesized. The X-ray diffraction chart of the aforementioned powder is indicated by Fig. 5. The results of elemental analysis indicated that the composition of the aforementioned powder was  $\text{LiMn}_{0.45}\text{Ni}_{0.45}\text{Co}_{0.1}\text{O}_2$ . The above-mentioned powder produced was defined as powder D.

The powder produced above was used as the positive electrode active material and production of a square lithium cell having a capacity of approximately 15 Ah indicated by Fig. 2 was done as in (Working Example 1-1). The cell produced was defined as the cell of Working Example 4-1.

(Working Example 4-2)



A sodium hydroxide solution was added to an aqueous solution containing manganese nitrate, nickel nitrate and cobalt nitrate at an atomic ratio of Mn:Ni:Co of 2:2:1 and coprecipitation was performed; then, heating was provided to 150°C and subsequently, drying was done to produce a manganese-nickel-cobalt coprecipitate compound. Furthermore, the aforementioned manganese-nickel-cobalt coprecipitate compound was added to lithium hydroxide solution and baking was done for 12 hours at a temperature of 1000°C in an oxygen atmosphere, and finally, classification of the particles was carried out to produce a powder of  $D_{50}=20\text{ }\mu\text{m}$ . The specific surface area of the particles based on the BET method was  $0.9\text{ m}^2/\text{g}$ .

The measurement results of X-ray analysis of the above-mentioned powder by  $\text{CuK}\alpha$  ray indicated formation of a monolayer having high crystallinity that appears to be a layer structure similar to that of the above-mentioned powder D. The results of elemental analysis indicated that the composition of the aforementioned powder was  $\text{LiMn}_{0.4}\text{Ni}_{0.4}\text{Co}_{0.2}\text{O}_2$ . The powder produced above was used as the positive electrode active material and production of a square lithium cell having a capacity of approximately 15 Ah indicated by Fig. 2 was done as in (Working Example 1-1). The cell produced was defined as the cell of Working Example 4-2.

[p. 54]

## (Working Example 4-3)

A sodium hydroxide solution was added to an aqueous solution containing manganese nitrate, nickel nitrate, and cobalt nitrate at an atomic ratio of Mn:Ni:Co of 9:9:2 and coprecipitation was performed; then, heating was provided to 150°C and subsequently, drying was done to produce a manganese-nickel-cobalt coprecipitate compound. Furthermore, the aforementioned manganese-nickel-cobalt coprecipitate compound was added to lithium hydroxide solution and baking was done for 5 hours at a temperature of 1000°C in an oxygen atmosphere, and finally, classification of the particles was carried out to produce a powder of  $D_{50}=20\text{ }\mu\text{m}$ . The specific surface area of the particles based on the BET method was  $0.3\text{ m}^2/\text{g}$ .

The measurement results of X-ray analysis of the above-mentioned powder by  $\text{CuK}\alpha$  ray

indicated formation of a monolayer having high crystallinity that appears to be a layer structure similar to that of the above-mentioned powder D. The results of elemental analysis indicated that the composition of the aforementioned powder was  $\text{LiMn}_{0.45}\text{Ni}_{0.45}\text{Co}_{0.1}\text{O}_2$ . The powder produced above was used as the positive electrode active material and production of a square lithium cell having a capacity of approximately 15 Ah indicated by Fig. 2 was done as in (Working Example 1-1). The cell produced was defined as the cell of Working Example 4-3.

(Working Example 4-4)

A sodium hydroxide solution was added to an aqueous solution containing manganese nitrate, nickel nitrate and cobalt nitrate at an atomic ratio of Mn:Ni:Co of 9:9:2 and coprecipitation was performed; then, heating was provided to 150°C and subsequently, drying was done to produce a manganese-nickel-cobalt coprecipitate compound. Furthermore, the aforementioned manganese-nickel-cobalt coprecipitate compound was added to lithium hydroxide solution and baking was done for 20 hours at a temperature of 1000°C in an oxygen atmosphere, and finally, classification of the particles was carried out to produce a powder of  $D_{50}=5\text{ }\mu\text{m}$ . The specific surface area of the particles based on the BET method was  $1.5\text{ m}^2/\text{g}$ .

The measurement results of X-ray analysis of the above-mentioned powder by  $\text{CuK}\alpha$  ray indicated formation of a monolayer having high crystallinity that appears to be a layer structure similar to that of the above-mentioned powder D. The results of elemental analysis indicated that the composition of the aforementioned powder was  $\text{LiMn}_{0.45}\text{Ni}_{0.45}\text{Co}_{0.1}\text{O}_2$ . The powder produced above was used as the positive electrode active material and production of a square lithium cell having a capacity of approximately 15 Ah indicated by Fig. 2 was done as in (Working Example 1-1). The cell produced was defined as the cell of Working Example 4-4.

(Working Example 4-5)

A sodium hydroxide solution was added to an aqueous solution containing manganese nitrate, nickel nitrate and cobalt nitrate at an atomic ratio of Mn:Ni:Co of 17:17:4 and coprecipitation was performed; then, heating was provided to 150°C and subsequently, drying

was done to produce a manganese-nickel-cobalt coprecipitate compound.

[p. 55]

Furthermore, the aforementioned coprecipitate compound and boric acid were added to lithium hydroxide solution to form an elemental ratio of Li:Mn:Ni:Co:B of 2:0.85:0.85:0.2:0.1 and baking was done for 12 hours at a temperature of 1000°C in an oxygen atmosphere, and finally, classification of the particles was carried out to produce a powder of  $D_{50}=9\text{ }\mu\text{m}$ . The specific surface area of the particles based on the BET method was  $1.0\text{ m}^2/\text{g}$ .

The measurement results of X-ray analysis of the above-mentioned powder by  $\text{CuK}\alpha$  ray indicated formation of a monolayer having high crystallinity that appears to be a layer structure similar to that of the above-mentioned powder D. The results of elemental analysis indicated that the composition of the aforementioned powder was  $\text{LiMn}_{0.425}\text{Ni}_{0.425}\text{Co}_{0.1}\text{B}_{0.05}\text{O}_2$ . The powder produced above was used as the positive electrode active material and production of a square lithium cell having a capacity of approximately 15 Ah indicated by Fig. 2 was done as in (Working Example 1-1). The cell produced was defined as the cell of Working Example 4-5.

(Working Example 4-6)

A sodium hydroxide solution was added to an aqueous solution containing manganese nitrate, nickel nitrate, cobalt nitrate and vanadium oxide at an atomic ratio of Mn:Ni:Co:V of 17:17:4:2 and coprecipitation was performed; then, heating was provided to 150°C and subsequently, drying was done to produce a manganese-nickel-cobalt-vanadium coprecipitate compound. Furthermore, the aforementioned coprecipitate compound was added to lithium hydroxide solution and baking was done for 12 hours at a temperature of 1000°C in an oxygen atmosphere, and finally, classification of the particles was carried out to produce a powder of  $D_{50}=9\text{ }\mu\text{m}$ . The specific surface area of the particles based on the BET method was  $1.0\text{ m}^2/\text{g}$ .

The measurement results of X-ray analysis of the above-mentioned powder by  $\text{CuK}\alpha$  ray indicated formation of a monolayer having high crystallinity that appears to be a layer structure similar to that of the above-mentioned powder D. The results of elemental analysis indicated that

the composition of the aforementioned powder was  $\text{LiMn}_{0.425}\text{Ni}_{0.425}\text{Co}_{0.1}\text{V}_{0.05}\text{O}_2$ . The powder produced above was used as the positive electrode active material and production of a square lithium cell having a capacity of approximately 15 Ah indicated by Fig. 2 was done as in (Working Example 1-1). The cell produced was defined as the cell of Working Example 4-6.

(Working Example 4-7)

A sodium hydroxide solution was added to an aqueous solution containing manganese nitrate, nickel nitrate, cobalt nitrate and aluminum nitrate at an atomic ratio of Mn:Ni:Co:Al of 17:17:4:2 and coprecipitation was performed; then, heating was provided to 150°C and subsequently, drying was done to produce a manganese-nickel-cobalt-aluminum coprecipitate compound. Furthermore, the aforementioned coprecipitate compound was added to lithium hydroxide solution and baking was done for 12 hours at a temperature of 1000°C in an oxygen atmosphere, and finally, classification of the particles was carried out to produce a powder of  $D_{50}=9\text{ }\mu\text{m}$ . The specific surface area of the particles based on the BET method was  $1.0\text{ m}^2/\text{g}$ .

The measurement results of X-ray analysis of the above-mentioned powder by  $\text{CuK}\alpha$  ray indicated formation of a monolayer having high crystallinity that appears to be a layer structure similar to that of the above-mentioned powder D. The results of elemental analysis indicated that the composition of the aforementioned powder was  $\text{LiMn}_{0.425}\text{Ni}_{0.425}\text{Co}_{0.1}\text{Al}_{0.05}\text{O}_2$ . The powder produced above was used as the positive electrode active material and production of a square lithium cell having a capacity of approximately 15 Ah indicated by Fig. 2 was done as in (Working Example 1-1). The cell produced was defined as the cell of Working Example 4-7.

(Working Example 4-8)

A sodium hydroxide solution was added to an aqueous solution containing manganese nitrate, nickel nitrate, cobalt nitrate and magnesium nitrate at an atomic ratio of Mn:Ni:Co:Mg of 17:17:4:2 and coprecipitation was performed; then, heating was provided to 150°C and subsequently, drying was done to produce a manganese-nickel-cobalt-magnesium coprecipitate compound. Furthermore, the aforementioned coprecipitate compound was added to lithium

hydroxide solution and baking was done for 12 hours at a temperature of 1000°C in an oxygen atmosphere, and finally, classification of the particles was carried out to produce a powder of  $D_{50}=9\text{ }\mu\text{m}$ . The specific surface area of the particles based on the BET method was  $1.0\text{ m}^2/\text{g}$ .

The measurement results of X-ray analysis of the above-mentioned powder by  $\text{CuK}\alpha$  ray indicated formation of a monolayer having high crystallinity that appears to be a layer structure similar to that of the above-mentioned powder D. The results of elemental analysis indicated that the composition of the aforementioned powder was  $\text{LiMn}_{0.425}\text{Ni}_{0.425}\text{Co}_{0.1}\text{Mg}_{0.05}\text{O}_2$ . The powder produced above was used as the positive electrode active material and production of a square lithium cell having a capacity of approximately 15 Ah indicated by Fig. 2 was done as in (Working Example 1-1). The cell produced was defined as the cell of Working Example 4-8.

[p. 57]

(Working Example 4-9)

A sodium hydroxide solution was added to an aqueous solution containing manganese nitrate, nickel nitrate, cobalt nitrate, and chromium nitrate at an atomic ratio of Mn:Ni:Co:Cr of 17:17:4:2 and coprecipitation was performed; then, heating was provided to 150°C and subsequently, drying was done to produce a manganese-nickel-cobalt-chromium coprecipitate compound. Furthermore, the aforementioned coprecipitate compound was added to lithium hydroxide solution and baking was done for 12 hours at a temperature of 1000°C in an oxygen atmosphere, and finally, classification of the particles was carried out to produce a powder of  $D_{50}=9\text{ }\mu\text{m}$ . The specific surface area of the particles based on the BET method was  $1.0\text{ m}^2/\text{g}$ .

The measurement results of X-ray analysis of the above-mentioned powder by  $\text{CuK}\alpha$  ray indicated formation of a monolayer having high crystallinity that appears to be a layer structure similar to that of the above-mentioned powder D. The results of elemental analysis indicated that the composition of the aforementioned powder was  $\text{LiMn}_{0.425}\text{Ni}_{0.425}\text{Co}_{0.1}\text{Cr}_{0.05}\text{O}_2$ . The powder produced above was used as the positive electrode active material and production of a square lithium cell having a capacity of approximately 15 Ah indicated by Fig. 2 was done as in

(Working Example 1-1). The cell produced was defined as the cell of Working Example 4-9.

(Working Example 4-10)

A sodium hydroxide solution was added to an aqueous solution containing manganese nitrate, nickel nitrate, cobalt nitrate and titanium oxide at an atomic ratio of Mn:Ni:Co:Ti of 17:17:4:2 and coprecipitation was performed; then, heating was provided to 150°C and subsequently, drying was done to produce a manganese-nickel-cobalt- titanium coprecipitate compound. Furthermore, the aforementioned coprecipitate compound was added to lithium hydroxide solution and baking was done for 12 hours at a temperature of 1000°C in an oxygen atmosphere, and finally, classification of the particles was carried out to produce a powder of  $D_{50}=9\text{ }\mu\text{m}$ . The specific surface area of the particles based on the BET method was  $1.0\text{ m}^2/\text{g}$ .

The measurement results of X-ray analysis of the above-mentioned powder by  $\text{CuK}\alpha$  ray indicated formation of a monolayer having high crystallinity that appears to be a layer structure similar to that of the above-mentioned powder D. The results of elemental analysis indicated that the composition of the aforementioned powder was  $\text{LiMn}_{0.425}\text{Ni}_{0.425}\text{Co}_{0.1}\text{Ti}_{0.05}\text{O}_2$ . The powder produced above was used as the positive electrode active material and production of a square lithium cell having a capacity of approximately 15 Ah indicated by Fig. 2 was done as in (Working Example 1-1). The cell produced was defined as the cell of Working Example 4-10.

[p. 58]

(Working Example 4-11)

A sodium hydroxide solution was added to an aqueous solution containing manganese nitrate, nickel nitrate, cobalt nitrate and iron sulfate at an atomic ratio of Mn:Ni:Co:Fe of 17:17:4:2 and coprecipitation was performed; then, heating was provided to 150°C and subsequently, drying was done to produce a manganese-nickel-cobalt-iron coprecipitate compound. Furthermore, the aforementioned coprecipitate compound was added to lithium hydroxide solution and baking was done for 12 hours at a temperature of 1000°C in an oxygen atmosphere, and finally, classification of the particles was carried out to produce a powder of

$D_{50}=9\text{ }\mu\text{m}$ . The specific surface area of the particles based on the BET method was  $0.9\text{ m}^2/\text{g}$ .

The measurement results of X-ray analysis of the above-mentioned powder by  $\text{CuK}\alpha$  ray indicated formation of a monolayer having high crystallinity that appears to be a layer structure similar to that of the above-mentioned powder D. The results of elemental analysis indicated that the composition of the aforementioned powder was  $\text{LiMn}_{0.425}\text{Ni}_{0.425}\text{Co}_{0.1}\text{Fe}_{0.05}\text{O}_2$ . The powder produced above was used as the positive electrode active material and production of a square lithium cell having a capacity of approximately 15 Ah indicated by Fig. 2 was done as in (Working Example 1-1). The cell produced was defined as the cell of Working Example 4-11.

(Working Example 4-12)

A sodium hydroxide solution was added to an aqueous solution containing manganese nitrate, nickel nitrate, cobalt nitrate, and copper sulfate at an atomic ratio of Mn:Ni:Co:Cu of 17:17:4:2 and coprecipitation was performed; then, heating was provided to  $150^\circ\text{C}$  and subsequently, drying was done to produce a manganese-nickel-cobalt-copper coprecipitate compound. Furthermore, the aforementioned coprecipitate compound was added to lithium hydroxide solution and baking was done for 12 hours at a temperature of  $1000^\circ\text{C}$  in an oxygen atmosphere, and finally, classification of the particles was carried out to produce a powder of  $D_{50}=9\text{ }\mu\text{m}$ . The specific surface area of the particles based on the BET method was  $0.9\text{ m}^2/\text{g}$ .

The measurement results of X-ray analysis of the above-mentioned powder by  $\text{CuK}\alpha$  ray indicated formation of a monolayer having high crystallinity that appears to be a layer structure similar to that of the above-mentioned powder D. The results of elemental analysis indicated that the composition of the aforementioned powder was  $\text{LiMn}_{0.425}\text{Ni}_{0.425}\text{Co}_{0.1}\text{Cu}_{0.05}\text{O}_2$ . The powder produced above was used as the positive electrode active material and production of a square lithium cell having a capacity of approximately 15 Ah indicated by Fig. 2 was done as in (Working Example 1-1). The cell produced was defined as the cell of Working Example 4-12.

[p. 59]

(Working Example 4-13)

A sodium hydroxide solution was added to an aqueous solution containing manganese nitrate, nickel nitrate, cobalt nitrate, and zinc sulfate at an atomic ratio of Mn:Ni:Co:Zn of 17:17:4:2 and coprecipitation was performed; then, heating was provided to 150°C and subsequently, drying was done to produce a manganese-nickel-cobalt-zinc coprecipitate compound. Furthermore, the aforementioned coprecipitate compound was added to lithium hydroxide solution and baking was done for 12 hours at a temperature of 1000°C in an oxygen atmosphere, and finally, classification of the particles was carried out to produce a powder of  $D_{50}=9\text{ }\mu\text{m}$ . The specific surface area of the particles based on the BET method was  $0.9\text{ m}^2/\text{g}$ .

The measurement results of X-ray analysis of the above-mentioned powder by  $\text{CuK}\alpha$  ray indicated formation of a monolayer having high crystallinity that appears to be a layer structure similar to that of the above-mentioned powder D. The results of elemental analysis indicated that the composition of the aforementioned powder was  $\text{LiMn}_{0.425}\text{Ni}_{0.425}\text{Co}_{0.1}\text{Zn}_{0.05}\text{O}_2$ . The powder produced above was used as the positive electrode active material and production of a square lithium cell having a capacity of approximately 15 Ah indicated by Fig. 2 was done as in (Working Example 1-1). The cell produced was defined as the cell of Working Example 4-13.

(Comparative Example 4-1)

A sodium hydroxide solution was added to an aqueous solution containing manganese nitrate, nickel nitrate and cobalt nitrate at an atomic ratio of Mn:Ni:Co of 7:11:2 and coprecipitation was performed; then, heating was provided to 150°C and subsequently, drying was done to produce a manganese-nickel-cobalt coprecipitate compound. Furthermore, the aforementioned coprecipitate compound was added to lithium hydroxide solution and baking was done for 12 hours at a temperature of 1000°C in an oxygen atmosphere, and finally, classification of the particles was carried out to produce a powder of  $D_{50}=20\text{ }\mu\text{m}$ . The specific surface area of the particles based on the BET method was  $20\text{ m}^2/\text{g}$ .

The measurement results of X-ray analysis of the above-mentioned powder by  $\text{CuK}\alpha$  ray indicated formation of a monolayer having high crystallinity that appears to be a layer structure



similar to that of the above-mentioned powder D. The results of elemental analysis indicated that the composition of the aforementioned powder was  $\text{LiMn}_{0.35}\text{Ni}_{0.55}\text{Co}_{0.1}\text{O}_2$ . The powder produced above was used as the positive electrode active material and production of a square lithium cell having a capacity of approximately 15 Ah indicated by Fig. 2 was done as in (Working Example 1-1). The cell produced was defined as the cell of Comparative Example 4-1.

[p. 60]

(Comparative Example 4-2)

A sodium hydroxide solution was added to an aqueous solution containing manganese nitrate, nickel nitrate and cobalt nitrate at an atomic ratio of Mn:Ni:Co of 9:9:2 and coprecipitation was performed; then, heating was provided to 150°C and subsequently, drying was done to produce a manganese-nickel-cobalt coprecipitate compound. Furthermore, the aforementioned coprecipitate compound was added to lithium hydroxide solution and baking was done for 24 hours at a temperature of 1000°C in an oxygen atmosphere, and finally, classification of the particles was carried out to produce a powder of  $D_{50}=5\text{ }\mu\text{m}$ . The specific surface area of the particles based on the BET method was  $0.3\text{ m}^2/\text{g}$ .

The measurement results of X-ray analysis of the above-mentioned powder by  $\text{CuK}\alpha$  ray indicated formation of a monolayer having high crystallinity that appears to be a layer structure similar to that of the above-mentioned powder D. The results of elemental analysis indicated that the composition of the aforementioned powder was  $\text{LiMn}_{0.45}\text{Ni}_{0.45}\text{Co}_{0.1}\text{O}_2$ . The powder produced above was used as the positive electrode active material and production of a square lithium cell having a capacity of approximately 15 Ah indicated by Fig. 2 was done as in (Working Example 1-1). The cell produced was defined as the cell of Comparative Example 4-2.

(Comparative Example 4-3)

A sodium hydroxide solution was added to an aqueous solution containing manganese nitrate, nickel nitrate, and cobalt nitrate at an atomic ratio of Mn:Ni:Co of 9:9:2 and coprecipitation was performed; then, heating was provided to 150°C and subsequently, drying

was done to produce a manganese-nickel-cobalt coprecipitate compound. Furthermore, the aforementioned coprecipitate compound was added to lithium hydroxide solution and baking was done for 3 hours at a temperature of 1000°C in an oxygen atmosphere, and finally, classification of the particles was carried out to produce a powder of  $D_{50}=5\text{ }\mu\text{m}$ . The specific surface area of the particles based on the BET method was  $2.0\text{ m}^2/\text{g}$ .

The measurement results of X-ray analysis of the above-mentioned powder by  $\text{CuK}\alpha$  ray indicated formation of a monolayer having high crystallinity that appears to be a layer structure similar to that of the above-mentioned powder D. The results of elemental analysis indicated that the composition of the aforementioned powder was  $\text{LiMn}_{0.45}\text{Ni}_{0.45}\text{Co}_{0.1}\text{O}_2$ . The powder produced above was used as the positive electrode active material and production of a square lithium cell having a capacity of approximately 15 Ah indicated by Fig. 2 was done as in (Working Example 1-1). The cell produced was defined as the cell of Comparative Example 4-3.

[p. 61]

(Cell performance test)

A High-rate discharge performance test was performed for the above-mentioned cells of the present invention and cells of comparisons at a temperature of 25°C, and subsequently, charge/discharge cycle performance was tested as well.

As for the condition used for the high-rate discharge performance test, charging was performed at constant-current 7.5 A (0.5It), 4.3 V, and 3 hrs, and discharging was done at constant-current 1.5 A (0.1It), 3.0 V (2It), end voltage of 3.0V.

For the condition used for the charge/discharge cycle test, charging was done at constant-current 7.5 A (0.5It), 4.3 V, and 3 hrs, and discharging was done at constant-current 7.5 A (0.5It) and end voltage of 3.0V. 10 minutes dead time mode was provided after charging and discharging.

In the high-rate discharge performance test, the ratio of the discharge capacity when discharging is done at 1.5 A for the discharge capacity when discharging is done at 30 A is

defined as high-rate discharge performance (%). In the charge/discharge cycle performance test, the number of cycles where the discharge capacity is reduced to 80% of the initial discharge capacity is defined as the cycle life. The results of the above-mentioned performance tests are indicated by Table I to Table IV below. In the Tables, "half bandwidth  $18.6^\circ$ " means the half bandwidth of the diffraction peak at  $2\theta=18.6\pm1^\circ$ , and "half bandwidth  $44.1^\circ$ " means the half bandwidth of the diffraction peak at  $2\theta=44.1\pm1^\circ$ , and furthermore, "peak intensity ratio" means the relative peak intensity ratio at the diffraction peak at  $2\theta=44.1\pm1^\circ$  for the diffraction peak at  $2\theta=18.6\pm1^\circ$ .

Table I

Cell	Positive electrode active material						Cell performance			
	Composition	Specific surface area (g/m <sup>2</sup> )	Mean particle diameter (μm)	Peak intensity ratio	Half BW* 18.6°	Half BW* 44.1°	1.5 A discharge capacity (mAh/g)	30 A discharge capacity (mAh/g)	High-rate discharge perf. (%)	Cycle life
Work. Ex. 1-1	LiMn <sub>0.5</sub> Ni <sub>0.5</sub> O <sub>2</sub>	1.5	9	1.0	0.17	0.15	140	85	60.7	500
Work. Ex. 1-2	LiMn <sub>0.5</sub> Ni <sub>0.5</sub> O <sub>2</sub>	0.9	20	0.9	0.17	0.14	140	85	60.7	500
Work. Ex. 1-3	LiMn <sub>0.5</sub> Ni <sub>0.5</sub> O <sub>2</sub>	2.0	20	0.6	0.20	0.17	150	92	61.3	350
Work. Ex. 1-4	LiMn <sub>0.5</sub> Ni <sub>0.5</sub> O <sub>2</sub>	0.9	20	0.6	0.17	0.15	150	93	62.0	450
Work. Ex. 1-5	LiMn <sub>0.5</sub> Ni <sub>0.5</sub> O <sub>2</sub>	0.9	20	1.1	0.17	0.12	118	81	60.0	480
Work. Ex. 1-6	LiMn <sub>0.5</sub> Ni <sub>0.5</sub> O <sub>2</sub>	0.9	20	1.1	0.13	0.12	135	78	57.8	520
Work. Ex. 1-7	LiMn <sub>0.5</sub> Ni <sub>0.5</sub> O <sub>2</sub>	1.5	20	1.2	0.17	0.12	130	65	50.0	550
Work. Ex. 1-8	LiMn <sub>0.5</sub> Ni <sub>0.5</sub> O <sub>2</sub>	0.9	20	1.0	0.12	0.10	137	62	45.3	500
Work. Ex. 1-9	LiMn <sub>0.5</sub> Ni <sub>0.5</sub> O <sub>2</sub>	0.3	20	0.9	0.18	0.15	140	84	60.0	510
Work. Ex. 1-10	LiMn <sub>0.5</sub> Ni <sub>0.5</sub> O <sub>2</sub>	0.3	9	0.9	0.17	0.15	140	84	60.0	510
Work. Ex. 1-11	LiMn <sub>0.5</sub> Ni <sub>0.5</sub> O <sub>2</sub>	1.5	5	0.9	0.17	0.15	140	85	60.7	470
Comp. Ex. 1-1	LiMn <sub>0.95</sub> Ni <sub>0.05</sub> O <sub>2</sub>	0.9	20	0.6	0.20	0.12	150	50	31.3	300
Comp. Ex. 1-2	Li <sub>1.05</sub> Mn <sub>1.95</sub> O <sub>4</sub>	0.4	10	0.7	0.17	0.12	118	90	76.3	350
Comp. Ex. 1-3	LiMn <sub>0.5</sub> Ni <sub>0.5</sub> O <sub>2</sub>	2.0	3	0.9	0.17	0.17	140	87	62.1	250
Comp. Ex. 1-4	LiMn <sub>0.5</sub> Ni <sub>0.5</sub> O <sub>2</sub>	2.0	5	0.4	0.21	0.18	110	70	63.6	250
Comp. Ex. 1-5	LiMn <sub>0.5</sub> Ni <sub>0.5</sub> O <sub>2</sub>	0.2	5	0.9	0.19	0.18	140	87	62.1	250
Comp. Ex. 1-6	LiMn <sub>0.5</sub> Ni <sub>0.5</sub> O <sub>2</sub>	0.2	30	0.9	0.12	0.10	120	72	60.0	480

Table II

Cell	Positive electrode active material						Cell performance			
	Composition	Specific surface area (g/m <sup>2</sup> )	Mean particle diameter (μm)	Peak intensity ratio	Half BW* 18.6°	Half BW* 44.1°	1.5 A discharge capacity (mAh/g)	30 A discharge capacity (mAh/g)	High-rate discharge perf. (%)	Cycle life
Work. Ex. 2-1	LiMn <sub>0.475</sub> Ni <sub>0.475</sub> Bo <sub>0.05</sub> O <sub>2</sub>	0.9	9	0.9	0.16	0.16	137	89	65.0	350
Work. Ex. 2-2	LiMn <sub>0.475</sub> Ni <sub>0.475</sub> Vo <sub>0.05</sub> O <sub>2</sub>	0.9	9	0.9	0.17	0.17	130	87	66.9	350
Work. Ex. 2-3	LiMn <sub>0.475</sub> Ni <sub>0.475</sub> Al <sub>0.05</sub> O <sub>2</sub>	0.9	9	1.0	0.16	0.11	128	89	69.0	350
Work. Ex. 2-4	LiMn <sub>0.475</sub> Ni <sub>0.475</sub> Mg <sub>0.05</sub> O <sub>2</sub>	0.9	9	1.0	0.16	0.17	132	89	67.4	350
Work. Ex. 2-5	LiMn <sub>0.475</sub> Ni <sub>0.475</sub> Co <sub>0.05</sub> O <sub>2</sub>	0.9	9	1.0	0.14	0.14	128	88	68.8	350
Work. Ex. 2-6	LiMn <sub>0.475</sub> Ni <sub>0.475</sub> Cr <sub>0.05</sub> O <sub>2</sub>	0.9	9	0.9	0.17	0.17	128	84	65.6	350
Work. Ex. 2-7	LiMn <sub>0.475</sub> Ni <sub>0.475</sub> Ti <sub>0.05</sub> O <sub>2</sub>	0.9	9	0.9	0.16	0.17	129	87	67.4	350
Work. Ex. 2-8	LiMn <sub>0.475</sub> Ni <sub>0.475</sub> Fe <sub>0.05</sub> O <sub>2</sub>	0.9	9	0.9	0.16	0.13	128	85	66.4	350
Work. Ex. 2-9	LiMn <sub>0.475</sub> Ni <sub>0.475</sub> Cu <sub>0.05</sub> O <sub>2</sub>	0.9	9	0.9	0.16	0.14	127	83	65.4	350
Work. Ex. 2-10	LiMn <sub>0.475</sub> Ni <sub>0.475</sub> Zn <sub>0.05</sub> O <sub>2</sub>	0.9	9	0.9	0.17	0.13	128	84	65.6	350
Comp. Ex. 2-1	LiMn <sub>0.475</sub> Ni <sub>0.475</sub> Mg <sub>0.05</sub> O <sub>2</sub>	0.2	15	1.1	0.17	0.17	95	40	42.1	300
Comp. Ex. 2-2	LiMn <sub>0.475</sub> Ni <sub>0.475</sub> Mg <sub>0.05</sub> O <sub>2</sub>	1.9	6	1.1	0.16	0.16	130	90	69.2	150

\*BW = Bandwidth

Table III

Cell	Positive electrode active material						Cell performance			
	Composition	Specific surface area (g/m <sup>2</sup> )	Mean particle diameter (μm)	Peak intensity ratio	Half BW* 18.6°	Half BW* 44.1°	1.5 A discharge capacity (mAh/g)	30 A discharge capacity (mAh/g)	High-rate discharge perf. (%)	Cycle life
Work. Ex. 3-1	LiMn <sub>0.475</sub> Ni <sub>0.475</sub> B <sub>0.05</sub> O <sub>2</sub>	1.0	9	1.0	0.15	0.12	137	89	65.0	600
Work. Ex. 3-2	LiMn <sub>0.475</sub> Ni <sub>0.474</sub> V <sub>0.05</sub> B <sub>0.001</sub> O <sub>2</sub>	1.0	9	1.0	0.14	0.11	130	90	69.2	550
Work. Ex. 3-3	LiMn <sub>0.475</sub> Ni <sub>0.474</sub> Al <sub>0.05</sub> B <sub>0.001</sub> O <sub>2</sub>	1.0	9	1.0	0.13	0.11	129	92	71.3	600
Work. Ex. 3-4	LiMn <sub>0.475</sub> Ni <sub>0.474</sub> Mg <sub>0.05</sub> B <sub>0.001</sub> O <sub>2</sub>	1.0	9	1.0	0.13	0.13	132	92	69.7	650
Work. Ex. 3-5	LiMn <sub>0.475</sub> Ni <sub>0.474</sub> Co <sub>0.05</sub> B <sub>0.001</sub> O <sub>2</sub>	1.0	9	1.0	0.13	0.11	131	90	71.0	700
Work. Ex. 3-6	LiMn <sub>0.475</sub> Ni <sub>0.474</sub> Cr <sub>0.05</sub> B <sub>0.001</sub> O <sub>2</sub>	1.0	9	1.0	0.14	0.11	128	87	68.0	650
Work. Ex. 3-7	LiMn <sub>0.475</sub> Ni <sub>0.474</sub> Ti <sub>0.05</sub> B <sub>0.001</sub> O <sub>2</sub>	1.0	9	1.0	0.16	0.14	129	90	69.8	500
Work. Ex. 3-8	LiMn <sub>0.475</sub> Ni <sub>0.474</sub> Fe <sub>0.05</sub> B <sub>0.001</sub> O <sub>2</sub>	1.0	9	1.0	0.16	0.14	125	86	68.8	480
Work. Ex. 3-9	LiMn <sub>0.475</sub> Ni <sub>0.474</sub> Cu <sub>0.05</sub> B <sub>0.001</sub> O <sub>2</sub>	1.0	9	1.0	0.15	0.13	127	90	66.9	500
Work. Ex. 3-10	LiMn <sub>0.475</sub> Ni <sub>0.474</sub> Zn <sub>0.05</sub> B <sub>0.001</sub> O <sub>2</sub>	1.0	10	1.0	0.16	0.15	130	90	71.5	510
Comp. Ex. 3-1	LiMn <sub>0.475</sub> Ni <sub>0.475</sub> B <sub>0.05</sub> O <sub>2</sub>	0.2	9	1.1	0.15	0.23	110	70	63.6	470
Comp. Ex. 3-2	LiMn <sub>0.475</sub> Ni <sub>0.475</sub> B <sub>0.05</sub> O <sub>2</sub>	2.4	4	1.1	0.17	0.21	132	90	72.0	200

\*BW = Bandwidth

[p. 65] BW\* = Bandwidth

Table IV

Cell	Positive electrode active material					Cell performance				
	Composition	Specific surface area (g/m <sup>2</sup> )	Mean particle diameter (μm)	Peak intensity ratio	Half BW* 18.6°	Half BW* 44.1°	1.5 A discharge capacity (mAh/g)	30 A discharge capacity (mAh/g)	High-rate discharge perf. (%)	Cycle life
Work. Ex. 4-1	LiMn <sub>0.45</sub> Ni <sub>0.45</sub> Co <sub>0.1</sub> O <sub>2</sub>	0.9	20	1.0	0.19	0.12	160	113	70.0	700
Work. Ex. 4-2	LiMn <sub>0.4</sub> Ni <sub>0.4</sub> Co <sub>0.2</sub> O <sub>2</sub>	0.9	20	1.0	0.19	0.11	165	120	72.7	750
Work. Ex. 4-3	LiMn <sub>0.45</sub> Ni <sub>0.45</sub> Co <sub>0.1</sub> O <sub>2</sub>	0.3	20	1.0	0.15	0.14	160	112	70.0	600
Work. Ex. 4-4	LiMn <sub>0.45</sub> Ni <sub>0.45</sub> Co <sub>0.1</sub> O <sub>2</sub>	1.0	5	1.0	0.19	0.10	160	112	71.3	700
Comp. Ex. 4-1	LiMn <sub>0.35</sub> Ni <sub>0.55</sub> Co <sub>0.1</sub> O <sub>2</sub>	1.0	20	1.0	0.18	0.13	160	115	75.9	400
Comp. Ex. 4-2	LiMn <sub>0.45</sub> Ni <sub>0.45</sub> Co <sub>0.1</sub> O <sub>2</sub>	0.3	5	1.0	0.20	0.10	160	94	58.8	300
Comp. Ex. 4-3	LiMn <sub>0.45</sub> Ni <sub>0.45</sub> Co <sub>0.1</sub> O <sub>2</sub>	2.0	5	0.5	0.07	0.02	160	120	75.0	350
Work. Ex. 4-5	LiMn <sub>0.425</sub> Ni <sub>0.425</sub> Co <sub>0.1</sub> B <sub>0.05</sub> O <sub>2</sub>	1.0	9	1.0	0.18	0.14	157	118	75.2	700
Work. Ex. 4-6	LiMn <sub>0.425</sub> Ni <sub>0.425</sub> Co <sub>0.1</sub> V <sub>0.05</sub> O <sub>2</sub>	1.0	9	0.9	0.19	0.02	150	111	78.4	600
Work. Ex. 4-7	LiMn <sub>0.425</sub> Ni <sub>0.425</sub> Co <sub>0.1</sub> Al <sub>0.05</sub> O <sub>2</sub>	1.0	9	1.0	0.15	0.13	155	113	70.9	700
Work. Ex. 4-8	LiMn <sub>0.425</sub> Ni <sub>0.425</sub> Co <sub>0.1</sub> Mg <sub>0.05</sub> O <sub>2</sub>	1.0	9	1.0	0.19	0.13	152	114	75.0	700
Work. Ex. 4-9	LiMn <sub>0.425</sub> Ni <sub>0.425</sub> Co <sub>0.1</sub> Cr <sub>0.05</sub> O <sub>2</sub>	1.0	9	1.0	0.19	0.14	152	114	70.0	650
Work. Ex. 4-10	LiMn <sub>0.425</sub> Ni <sub>0.425</sub> Co <sub>0.1</sub> Ti <sub>0.05</sub> O <sub>2</sub>	1.0	9	1.0	0.19	0.15	154	112	72.7	650
Work. Ex. 4-11	LiMn <sub>0.425</sub> Ni <sub>0.425</sub> Co <sub>0.1</sub> Fe <sub>0.05</sub> O <sub>2</sub>	0.3	9	0.9	0.19	0.11	150	105	72.7	650
Work. Ex. 4-12	LiMn <sub>0.425</sub> Ni <sub>0.425</sub> Co <sub>0.1</sub> Cu <sub>0.05</sub> O <sub>2</sub>	0.3	9	1.0	0.20	0.10	151	115	76.2	620
Work. Ex. 4-13	LiMn <sub>0.425</sub> Ni <sub>0.425</sub> Co <sub>0.1</sub> Zn <sub>0.05</sub> O <sub>2</sub>	0.3	9	1.0	0.19	0.12	153	120	78.4	650

Furthermore, the change in the discharge voltage of the cell of (Working Example 1-1) when discharging is done at 1.5 A (0.1It) is indicated by Fig. 6, the change in the discharge voltage of the cell of (Working Example 1-10) when discharging is done at 1.5 A (0.1It) is indicated by Fig. 7, and the change in the discharge voltage of the cell of (Working Example 4-1) when discharging is done at 1.5 A (0.1It) is indicated by Fig. 8, respectively.

(Regarding the first embodiment)

When comparison is made between the cells of (Working Example 1-1) to (Working Example 1-11) that utilize the positive electrode active material having the layer structure belonging to spatial group R3/m and the cell of (Comparative Example 1-1) that utilizes the positive electrode active material having the layer structure belonging to spatial group C2/m, a significant increase in the high-rate discharge performance is observed. Furthermore, when comparison is made among cells that utilize a positive electrode active material  $\text{LiMn}_{0.5}\text{Ni}_{0.5}\text{O}_2$  having a layer similar to the space group R3/m of (Working Example 1-1) to (Working Example 1-11) and (Comparative Example 1-3) to (Comparative Example 1-6), an obvious improvement in the high-rate discharge performance is observed when the value of the specific surface area is at least  $0.3 \text{ m}^2/\text{g}$ . On the other hand, a sharp decrease in the charge/discharge cycle is observed when the value of the aforementioned specific surface area exceeds  $1.5 \text{ m}^2/\text{g}$ . Therefore, when an  $\text{LiMn}_{0.5}\text{Ni}_{0.5}\text{O}_2$  having a specific surface area in the range of  $0.3 \text{ m}^2/\text{g}$  to  $1.5 \text{ m}^2/\text{g}$  is used as a positive electrode active material, production of a secondary cell having excellent cycle performance and high-rate discharge performance is made possible.

Furthermore, when a composite oxide indicated by  $\text{LiMn}_{0.5}\text{Ni}_{0.5}\text{O}_2$  is used and a comparison is made on cell performance of cells having different relative intensity ratios of the diffraction peak at  $2\theta=44.1\pm1^\circ$  for the diffraction peak of  $2\theta=18.6\pm1^\circ$  on the powder X-ray diffraction chart that utilizes  $\text{CuK}\alpha$  ray, a significant increase in the cycle life is observed when the relative intensity ratio exceeds 0.6. Furthermore, reduction in the high-rate discharge



performance is observed when the aforementioned relative intensity ratio exceeds 1.1. Thus, when the aforementioned relative intensity ratio is between 0.6 to 1.1, production of cells with excellent cycle life and high-rate discharge performance is made possible.

Furthermore, when the half bandwidth is  $0.13^\circ$  or above at  $2\theta=18.6\pm1^\circ$  and the half bandwidth is  $0.10^\circ$  or above at  $2\theta=44.1\pm1^\circ$ , excellent high-rate discharge performance can be achieved.

[p. 67]

Furthermore, when the half bandwidth is  $0.20^\circ$  or above at  $2\theta=18.6\pm1^\circ$  and at the same time, the half bandwidth is  $0.17^\circ$  or above at  $2\theta=44.1\pm1^\circ$ , reduction in cycle life is observed. Thus, production of a cell having an excellent cycle life and high-rate discharge performance is made possible when the half bandwidth is in the range of  $0.13$  to  $0.20^\circ$  at  $2\theta=18.6\pm1^\circ$  and at the same time, the half bandwidth is  $0.10$  to  $0.17^\circ$  at  $2\theta=44.1\pm1^\circ$ .

It should be noted that the cell of (Comparative Example 1-2) having a relatively good high-rate discharge performance utilizes spinel manganese as the active material of positive electrode. In the above-mentioned cell, the expected high-rate discharge performance is achieved by spinel manganese, which indicates that the rate-determining factor of the discharge performance is not based on electrolyte or negative electrode, which are the structural elements other than positive electrode in the working examples and comparative examples.

(Regarding the second embodiment)

When the cells of (Working Example 2-1) to (Working Example 2-7) in which a part of the Mn and Ni that comprise the  $\text{LiMn}_{0.5}\text{Ni}_{0.5}\text{O}_2$  is replaced with a dissimilar element, a significant increase in the value of the high-rate discharge performance is observed in comparison to the cell made of a positive electrode active material having similar properties. The above-mentioned effect achieved is not well understood, but it seems that increase in shifting of the lithium ion occurs when some of the Ni and Mn is replaced with a small amount of another element.

Furthermore, the value of the high-rate discharge performance is insufficient in a cell where the value of the specific surface area is less than  $0.3 \text{ m}^2/\text{g}$  (Comparative Example 2-1) in the second embodiment. On the other hand, in a cell where the value of specific surface area exceeds  $1.5 \text{ m}^2/\text{g}$  (comparative Example 2-2), a sharp decrease in the charge/discharge cycle is observed.

(Regarding the third embodiment)

Furthermore, compared with cells of (Working Example 1-1) to (Working Example 1-11), the high-rate discharge performance is high in the cell of (Working Example 3-1) and the effect achieved through substitution of boron is observed.

[p. 68]

In cells of (Working Example 3-2) to (Working Example 3-7) in which a part of the Mn and Ni in  $\text{LiMn}_{0.5}\text{Ni}_{0.5}\text{O}_2$  is replaced with boron and other elements, a further improvement in the high-rate discharge performance is observed. It is hypothesized that an increase in shifting of the lithium ion occurs when the Ni and Mn are replaced with a small amount of other elements.

Furthermore, the value of the high-rate discharge performance is insufficient in a cell where the value of the specific surface area is less than  $0.3 \text{ m}^2/\text{g}$  (comparative Example 3-1) in the third embodiment. On the other hand, in a cell where the value of specific surface area exceeds  $1.5 \text{ m}^2/\text{g}$  (Comparative Example 3-2), a sharp decrease in the charge/discharge cycle is observed.

Furthermore, as indicated by Fig. 1, when the etching time based on the X-ray photoelectron spectra method (XPS) is approximately 400 seconds, the concentration of the boron is reduced to approximately the same as inside the particle. In this case, the etching rate in the depth direction is  $0.07 \text{ nm (sec)}$ . This indicates that the thickness of the surface layer of the positive electrode active material particle required to achieved the effect of the present invention is  $28 \text{ nm}$  ( $=0.028 \text{ }\mu\text{m}$ ) at most. When the mean particle diameter of the positive electrode active material is  $9$  to  $10 \text{ }\mu\text{m}$ , the aforementioned thickness corresponds to approximately 2% of the

diameter.

(Regarding the fourth embodiment)

Furthermore, in cells where the composite oxide indicated by  $\text{Li}[\text{Mn}_x\text{Ni}_y\text{Co}_z]\text{O}_2$  where a Co component is added to a composite oxide indicated by  $\text{LiMn}_{0.5}\text{Ni}_{0.5}\text{O}_2$  (Working Example 4-1) to (Working Example 4-4), a significant increase in discharge capacity is observed in comparison to the cells of (Working Example 1-1) to (Working Example 1-11). Furthermore, possibly due to stable crystal structure, a significant increase in cycle life is observed.

When comparison is made for the cell performance among composite oxides in which the same structural formula of  $\text{LiMn}_{0.45}\text{Ni}_{0.45}\text{Co}_{0.1}\text{O}_2$  is used as positive electrode active material but the specific surface area is different (Working Example 4-1), (Working Example 4-3), (Working Example 4-4), (Comparative Example 4-2) and (Comparative Example 4-3), a sharp decrease in cycle performance is observed when the specific surface area exceeds  $1.5 \text{ m}^2/\text{g}$ . Furthermore, a sharp decrease in high-rate discharge performance is observed when the specific surface area becomes less than  $0.3 \text{ m}^2/\text{g}$ . Thus, a nonaqueous secondary cell equipped with excellent cycle performance and excellent high-rate discharge performance can be produced when the value of the specific surface area of the composite oxide is in the range of  $0.3 \text{ m}^2/\text{g}$  to  $1.5 \text{ m}^2/\text{g}$ .

[p. 69]

An increased value of the high-rate discharge performance is observed in cells in which the composite oxide indicated by the structural formula of  $\text{LiMn}_{0.425}\text{Ni}_{0.425}\text{Co}_{0.1}\text{M}_{0.05}\text{O}_2$  where a dissimilar element M" is added to Ni, Mn, and Co is used as a positive electrode active material (Working Example 4-5) to (Working Example 4-10) in comparison to the cell without a dissimilar element M" (Working Example 4-1). The above-mentioned effect achieved is not well understood, but it seems that increase in shifting of the lithium ion occurs when the Ni and Mn are replaced with a small amount of other elements.

Furthermore, when disassembly is performed for the cells of Working Example 2-1, Working Example 3-1, and Working Example 4-7 with boron added and an elemental analysis

was performed for each structural element that comprises the cell, boron was detected at near the surface of the negative electrode. Based on the result obtained, it is hypothesized that the boron added at the time of synthesis leaks out of the positive electrode active material particle and activates the condition on the surface of the positive electrode and increases the high-rate discharge performance rather than stabilizing the structure upon replacing Mn and Ni.

Furthermore, in the case of the active material that comprises the layer structure of the present invention, basically, the 6a site is occupied with Li, and the 6b is occupied with Mn, Ni, and Co, and the 6c site is occupied with O, but it is possible for the Li to be dispersed in the 6b site as well. In this case, Li has a monovalent valence; thus, the charge deficiency at 6b site can be increased and neutralized with an increase or a decrease of the 6c site.

In the above-mentioned Working Examples of the second embodiment, it is stated that  $\text{Li}[\text{Mn}_{0.475}\text{Ni}_{0.475}\text{B}_{0.05}\text{O}_2]$ ,  $\text{Li}[\text{Mn}_{0.475}\text{Ni}_{0.475}\text{V}_{0.05}\text{O}_2]$ ,  $\text{Li}[\text{Mn}_{0.475}\text{Ni}_{0.475}\text{Al}_{0.05}\text{O}_2]$ ,  $\text{Li}[\text{Mn}_{0.475}\text{Ni}_{0.475}\text{Mg}_{0.05}\text{O}_2]$ ,  $\text{Li}[\text{Mn}_{0.475}\text{Ni}_{0.475}\text{Co}_{0.05}\text{O}_2]$ ,  $\text{Li}[\text{Mn}_{0.475}\text{Ni}_{0.475}\text{Cr}_{0.05}\text{O}_2]$ ,  $\text{Li}[\text{Mn}_{0.475}\text{Ni}_{0.475}\text{Ti}_{0.05}\text{O}_2]$ ,  $\text{Li}[\text{Mn}_{0.475}\text{Ni}_{0.475}\text{Li}_{0.05}\text{O}_2]$  [sic], are used as the main structural components of the positive electrode active material, but a similar effect can be achieved when other dissimilar elements M are used as well.

In the above-mentioned working examples of the third embodiment, it is stated to use  $\text{Li}[\text{Mn}_{0.475}\text{Ni}_{0.475}\text{B}_{0.05}\text{O}_2]$ ,  $\text{Li}[\text{Mn}_{0.475}\text{Ni}_{0.475}\text{B}_{0.05}\text{O}_2]$  [sic, repeated],  $\text{Li}[\text{Mn}_{0.475}\text{Ni}_{0.474}\text{V}_{0.05}\text{B}_{0.001}\text{O}_2]$ ,  $\text{Li}[\text{Mn}_{0.475}\text{Ni}_{0.474}\text{V}_{0.05}\text{Al}_{0.001}\text{O}_2]$ ,  $\text{Li}[\text{Mn}_{0.475}\text{Ni}_{0.474}\text{V}_{0.05}\text{Mg}_{0.001}\text{O}_2]$ ,  $\text{Li}[\text{Mn}_{0.475}\text{Ni}_{0.474}\text{V}_{0.05}\text{Co}_{0.001}\text{O}_2]$ ,  $\text{Li}[\text{Mn}_{0.475}\text{Ni}_{0.474}\text{Cr}_{0.05}\text{B}_{0.001}\text{O}_2]$ ,  $\text{Li}[\text{Mn}_{0.475}\text{Ni}_{0.474}\text{Ti}_{0.05}\text{B}_{0.001}\text{O}_2]$ , having a high surface concentration of Boron as the main structural components of the positive electrode active material, but a similar effect can be achieved when other dissimilar elements M' are used as well.

[p. 70]

In the above-mentioned Working Examples of the fourth embodiment, it is stated that

Li[Mn<sub>0.45</sub>Ni<sub>0.45</sub>Co<sub>0.01</sub>O<sub>2</sub>], Li[Mn<sub>0.425</sub>Ni<sub>0.425</sub>Co<sub>0.1</sub>B<sub>0.05</sub>O<sub>2</sub>], Li[Mn<sub>0.425</sub>Ni<sub>0.425</sub>Co<sub>0.1</sub>V<sub>0.05</sub>O<sub>2</sub>],  
 Li[Mn<sub>0.425</sub>Ni<sub>0.425</sub>Co<sub>0.1</sub>Al<sub>0.05</sub>O<sub>2</sub>], Li[Mn<sub>0.425</sub>Ni<sub>0.425</sub>Co<sub>0.1</sub>Mg<sub>0.05</sub>O<sub>2</sub>], Li[Mn<sub>0.425</sub>Ni<sub>0.425</sub>Co<sub>0.1</sub>Cr<sub>0.05</sub>O<sub>2</sub>],  
 Li[Mn<sub>0.425</sub>Ni<sub>0.425</sub>Co<sub>0.1</sub>Ti<sub>0.05</sub>O<sub>2</sub>], Li[Mn<sub>0.425</sub>Ni<sub>0.425</sub>Co<sub>0.1</sub>Li<sub>0.05</sub>O<sub>2</sub>],

are used as the main structural components of the positive electrode active material, but a similar effect can be achieved when other dissimilar elements are used as well.

In this case, working examples are explained with a nonaqueous secondary cells that utilize a synthetic graphite as the negative electrode material, and the same good effect was achieved with other negative electrode materials as well.

Furthermore, the present invention is not limited to the above-mentioned starting raw material activated material, manufacturing method, positive electrode, negative electrode, electrolyte, separator, shape of the cell, etc.

#### <Field of industrial application>

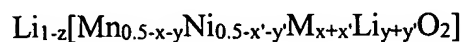
The present invention is to eliminate the above-mentioned existing problems, and production of a secondary cell with high energy density exhibiting an excellent high-rate charging/discharging performance and high charging/discharging cycle performance is made possible.

[p. 71]

#### Claims of Invention

1. A positive electrode active material mainly comprising a Li-Mn-Ni type composite oxide, and the positive electrode active material is characterized by the fact that the specific surface of the Li-Mn-Ni composite oxide measured by the BET method is 0.3 m<sup>2</sup>/g or above and 1.5 m<sup>2</sup>/g or below.
2. The positive electrode active material described in Claim 1 above characterized by the fact that the aforementioned Li-Mn-Ni type composite oxide is the composite oxide indicated by LiMn<sub>0.5</sub>Ni<sub>0.5</sub>O<sub>2</sub>.
3. The positive electrode active material described in 1 above characterized by the fact

that a part of Mn and Ni that comprise the composite oxide indicated by  $\text{LiMn}_{0.5}\text{Ni}_{0.5}\text{O}_2$  in the aforementioned Li-Mn-Ni type composite oxide is replaced with a dissimilar element and is a composite oxide with a composition indicated by the following general formula.



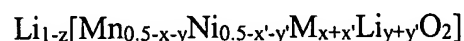
(Wherein, M is the aforementioned dissimilar element;

$$x=0.001 \text{ to } 0.1 \quad ; \quad x'=0.001 \text{ to } 0.1 \quad ;$$

$$y=0 \text{ to } 0.1 \quad ; \quad y'=0 \text{ to } 0.1 \quad ;$$

$$x+x'+y+y' \leq 0.4 ; \quad 0 \leq z \leq 1)$$

4. The positive electrode active material described in the Claim 1 above characterized by the fact that a part of Mn and Ni that comprises the composite oxide indicated by  $\text{LiMn}_{0.5}\text{Ni}_{0.5}\text{O}_2$  in the aforementioned Li-Mn-Ni type composite oxide is replaced with a dissimilar element and is a composite oxide with a composition indicated by the following general formula.



(Wherein, M is the aforementioned dissimilar element;

$$x=0.01 \text{ to } 0.1 \quad ; \quad x'=0.01 \text{ to } 0.1 \quad ;$$

$$y=0 \text{ to } 0.1 \quad ; \quad y'=0 \text{ to } 0.1 \quad ;$$

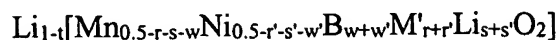
$$x+x'+y+y' \leq 0.2 ; \quad 0 \leq z \leq 1)$$

5. The positive electrode active material described in the aforementioned Claim 3 or Claim 4 characterized by the fact that the aforementioned dissimilar element M is one or more elements selected from the group consisting of B, Mg, Al, Ti, V, Cr, Fe, Co, Cu, and Zn.

[p. 72]

6. The positive electrode active material described in Claim 1 above characterized by the fact that a part of Mn and Ni that comprise the composite oxide indicated by  $\text{LiMn}_{0.5}\text{Ni}_{0.5}\text{O}_2$  in the aforementioned Li-Mn-Ni type composite oxide is replaced with a dissimilar element and

boron and is a composite oxide with a composition indicated by the following general formula.



(Wherein, M' is the aforementioned dissimilar element;

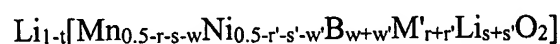
$$r=0.001 \text{ to } 0.1 \quad ; \quad r'=0.001 \text{ to } 0.1 ;$$

$$s=0 \text{ to } 0.1 \quad ; \quad s'=0 \text{ to } 0.1 \quad ;$$

$$r+r'+s+s'+w+w' \leq 0.4 \quad ;$$

$$w+w'=0.0005 \text{ to } 0.01 \quad ; \quad 0 \leq t \leq 1)$$

7. The positive electrode active material described in Claim 1 above characterized by the fact that a part of Mn and Ni that structures the composite oxide indicated by  $\text{LiMn}_{0.5}\text{Ni}_{0.5}\text{O}_2$  in the aforementioned Li-Mn-Ni type composite oxide is replaced with a dissimilar element and boron and is a composite oxide with the composition indicated by the following general formula.



(Wherein, M' is the aforementioned dissimilar element;

$$r=0.01 \text{ to } 0.1 \quad ; \quad r'=0.01 \text{ to } 0.1 \quad ;$$

$$s=0 \text{ to } 0.1 \quad ; \quad s'=0 \text{ to } 0.1 \quad ;$$

$$r+r'+s+s'+w+w' \leq 0.2 \quad ;$$

$$w+w'=0.0005 \text{ to } 0.01 \quad ; \quad 0 \leq t \leq 1)$$

8. The positive electrode active material described in Claim 6 or Claim 7 above characterized by the fact that the aforementioned dissimilar element M' is one or more elements selected from the group consisting of B, Mg, Al, Ti, V, Cr, Fe, Co, Cu, and Zn.

9. The positive electrode active material described in the Claim 1 above characterized by the fact that the aforementioned Li-Mn-Ni type composite oxide is a composite oxide indicated by  $\text{Li}[\text{Mn}_c\text{Ni}_d\text{Co}_e\text{Li}_a\text{M}''_b]\text{O}_2$  (Wherein, M'' is an element other than Mn, Ni, Co or Li,  $d \leq c+e+a+b$ ,  $c+d+e+a+b=1$ ,  $0 \leq a \leq 0.05$ ,  $0 \leq b \leq 0.05$ ,  $0.2 \leq c \leq 0.05$ ,  $0.02 \leq e \leq 0.4$ ).

[p. 73]

10. The positive electrode active material described in the Claim 9 above characterized by

the fact that the aforementioned M" is one or more elements selected among the group consisting of B, Mg, Al, Ti, V, Cr, Fe, Co, Cu, and Zn.

11. The positive electrode active material described in one of Claim 1 to Claim 10 above characterized by the fact that the aforementioned Li-Mn-Ni type composite oxide has a layer crystalline structure having peaks at  $2\theta = 18.6 \pm 1^\circ$ ,  $36.6 \pm 1^\circ$ ,  $37.8 \pm 1^\circ$ ,  $38.2 \pm 1^\circ$ ,  $44.3 \pm 1^\circ$ ,  $48.4 \pm 1^\circ$ ,  $58.4 \pm 1^\circ$ ,  $64.2 \pm 1^\circ$ ,  $64.8 \pm 1^\circ$ ,  $68.8 \pm 1^\circ$  on the X-ray diffraction chart that utilizes CuK $\alpha$  ray.

12. The positive electrode active material described in one of Claim 1 to Claim 11 above characterized by the fact that the aforementioned Li-Mn-Ni type composite oxide has a relative intensity ratio of the diffraction peak of  $2\theta = 44.1 \pm 1^\circ$  for the diffraction peak of  $2\theta = 18.6 \pm 1^\circ$  on the powder X-ray diffraction chart that utilizes CuK $\alpha$  rays.

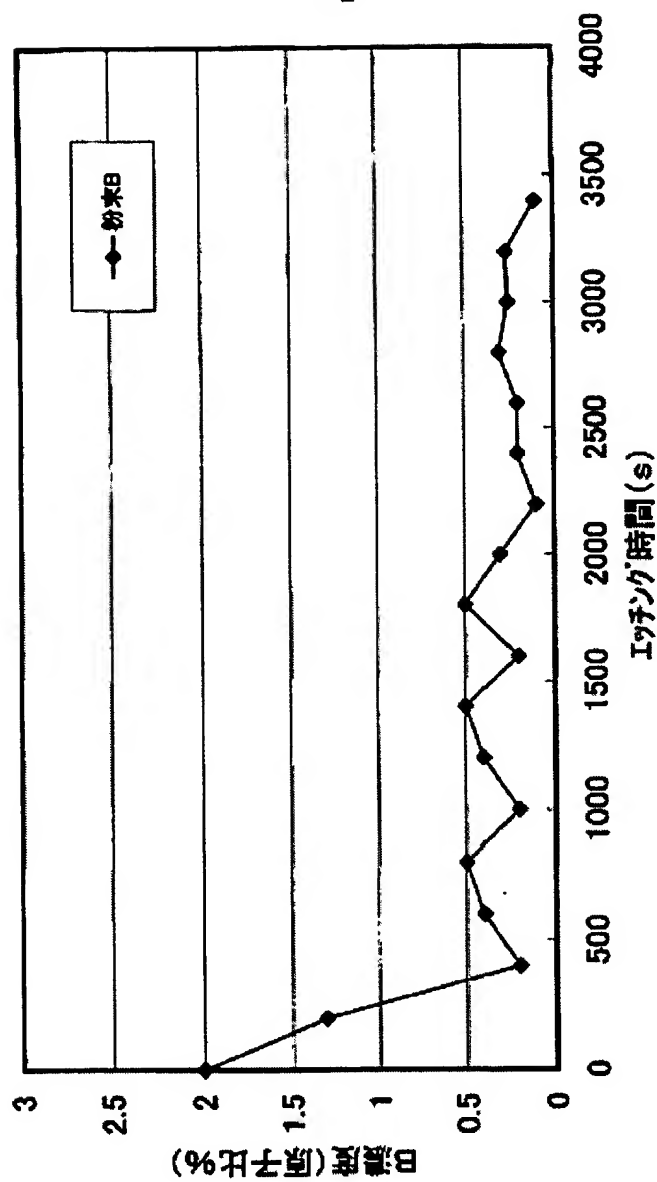
13. The positive electrode active material described in one of Claim 1 to Claim 12 above characterized by the fact that the aforementioned Li-Mn-Ni type composite oxide has the half-bandwidth of the diffraction peak at  $2\theta = 18.6 \pm 1^\circ$  in the range of  $0.13^\circ$  to  $0.20^\circ$  and the half bandwidth of the diffraction peak at  $2\theta = 44.1 \pm 1^\circ$  in the range of  $0.10^\circ$  to  $0.17^\circ$  on the powder X-ray diffraction chart that utilizes CuK $\alpha$  rays.

14. The positive electrode active material described in one of Claim 1 to Claim 13 above characterized by the fact that the particle diameter of the aforementioned Li-Mn-Ni type composite oxide is in the range of  $3 \mu\text{m}$  to  $20 \mu\text{m}$ .

15. The nonaqueous secondary cell that utilizes the positive electrode active material described in one of Claim 1 to Claim 14 above.



Fig. 1



B Concentration (atomic %)

Horizontal axis: Etching time (s)

Solid diamonds: Powder B

Fig. 2

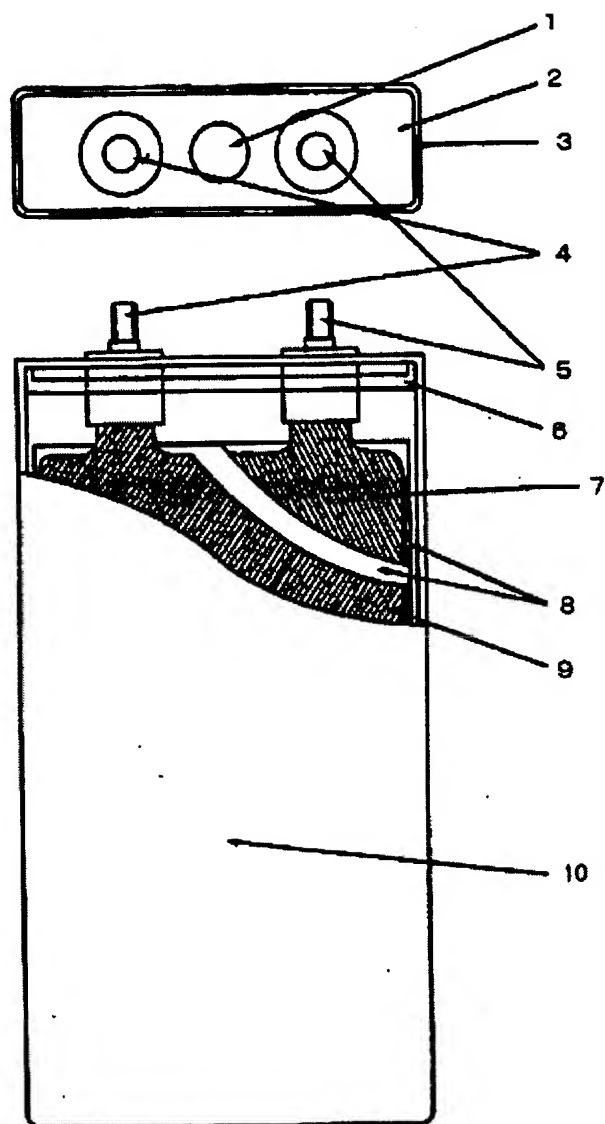
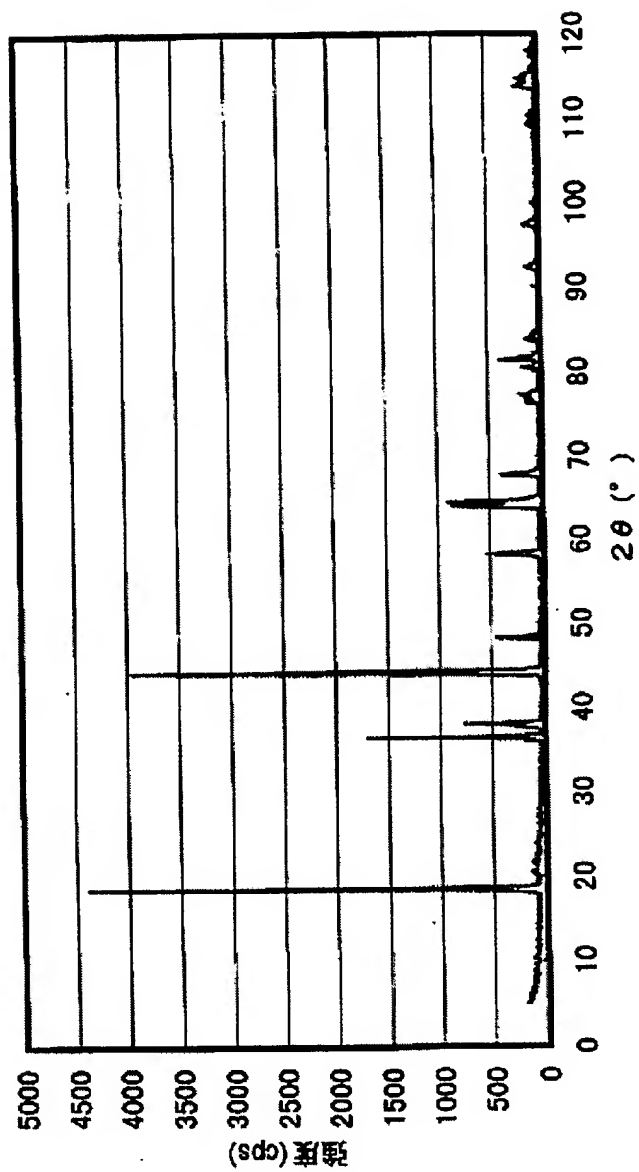
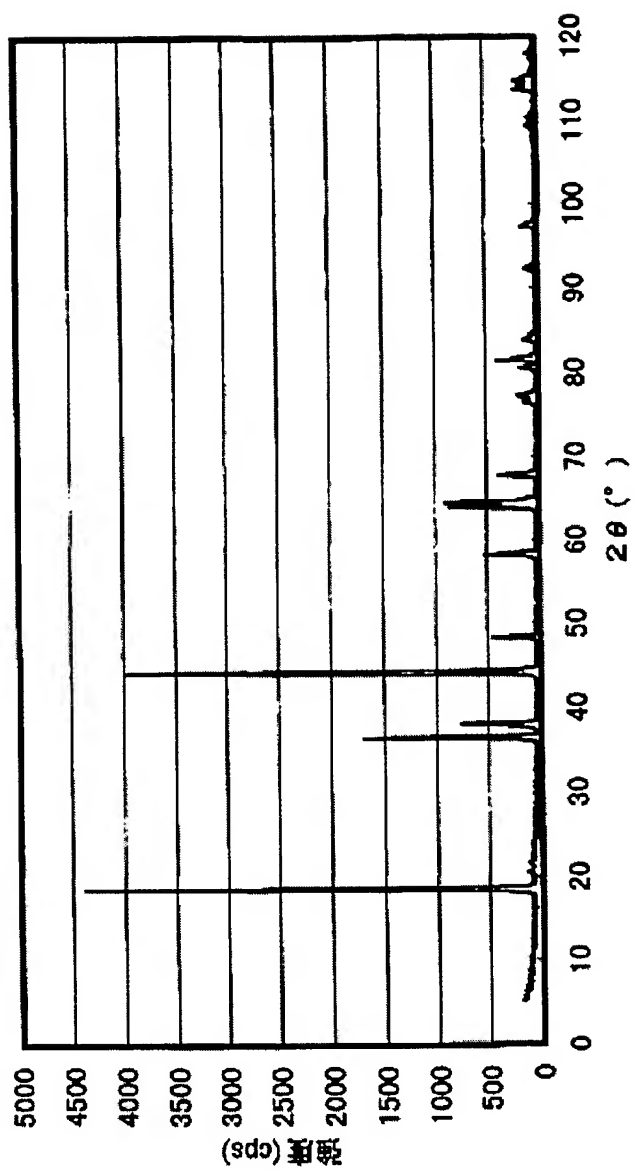


Fig. 3



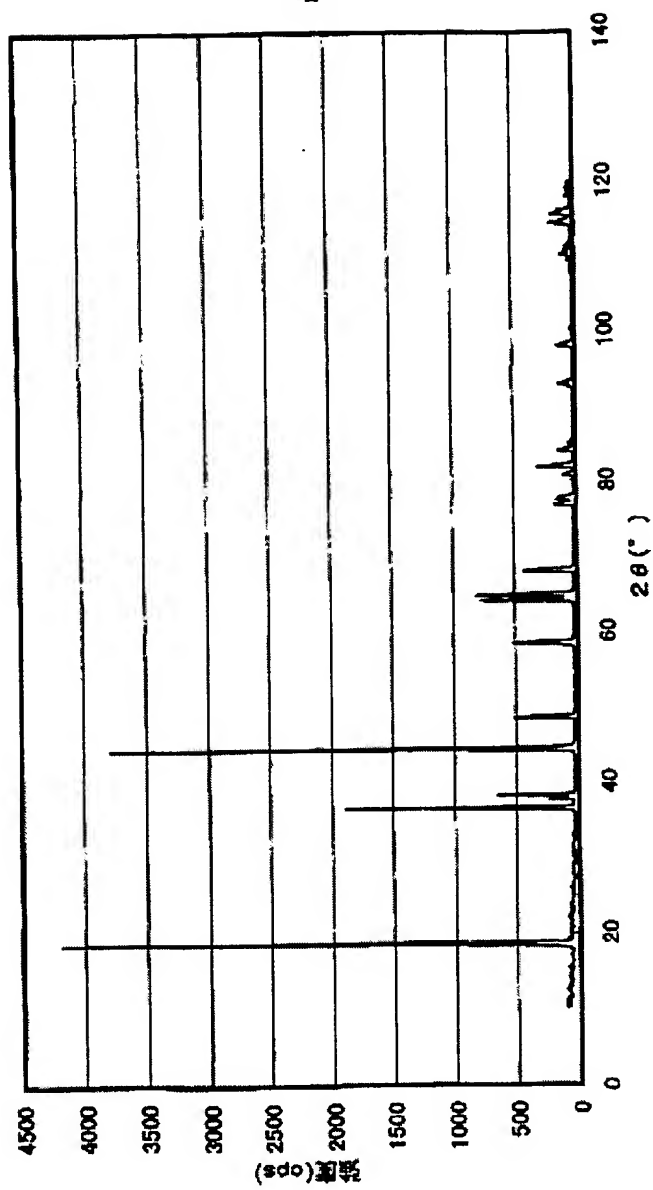
Intensity (cps)

Fig. 4



Intensity (cps)

Fig. 5



Intensity (cps)

Fig. 6

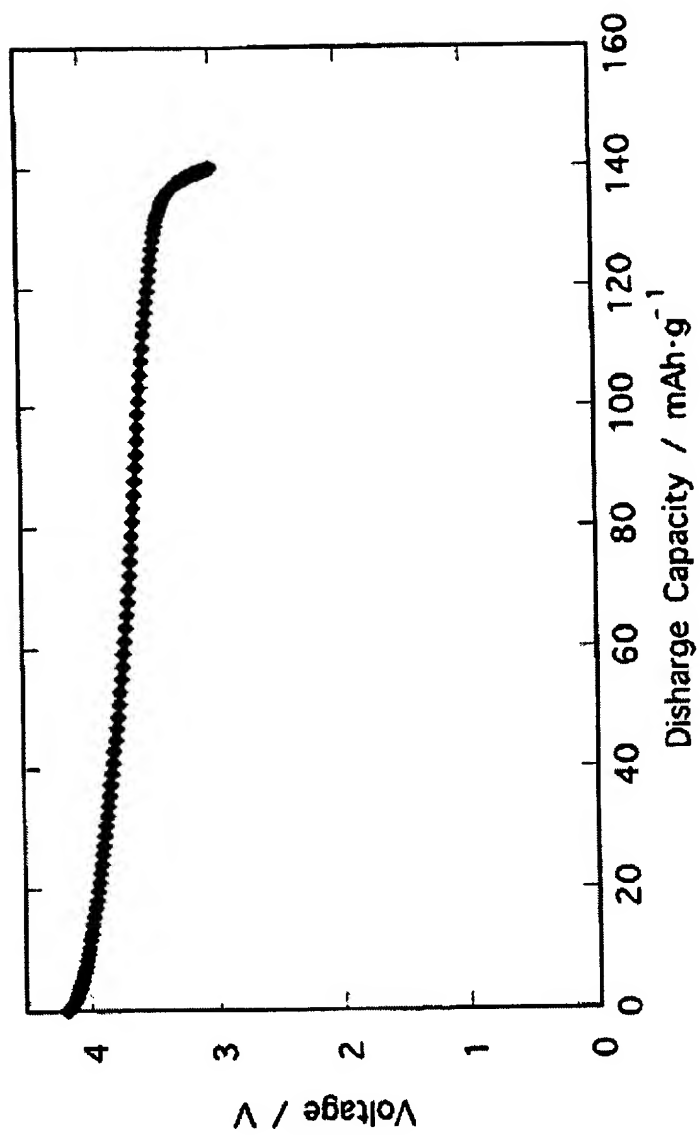


Fig. 7

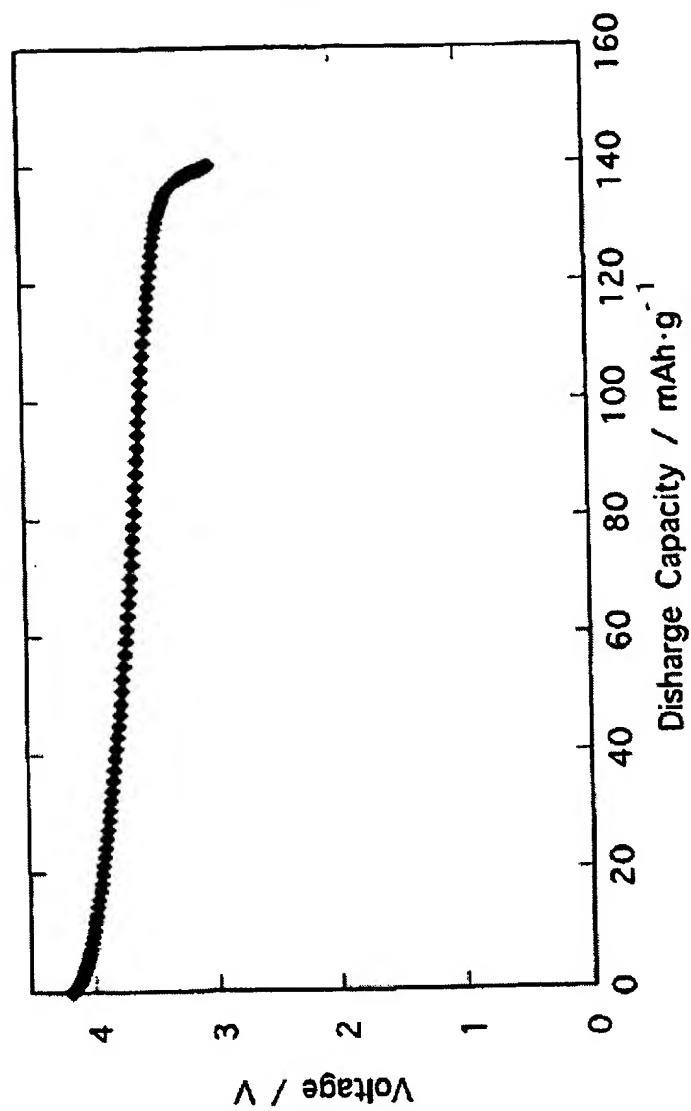
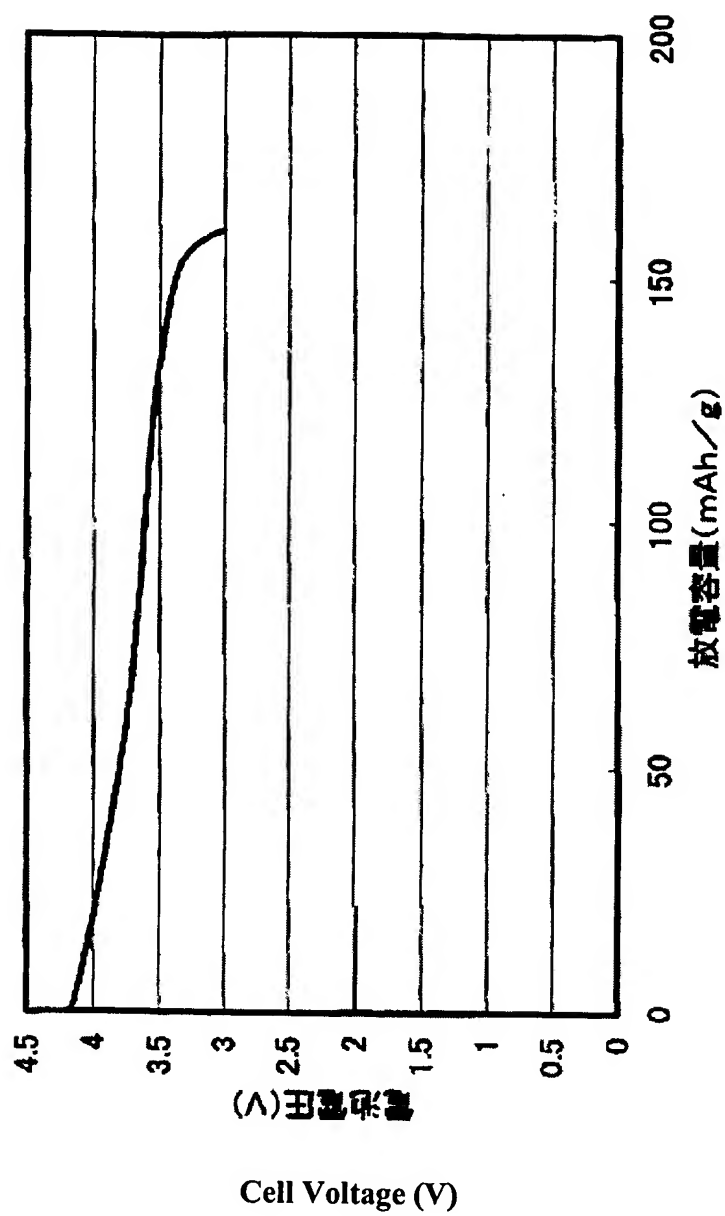


Fig. 8



Horizontal axis: Charge capacity (mAh/g)



**This Page is Inserted by IFW Indexing and Scanning  
Operations and is not part of the Official Record**

**BEST AVAILABLE IMAGES**

Defective images within this document are accurate representations of the original documents submitted by the applicant.

Defects in the images include but are not limited to the items checked:

- ☐ BLACK BORDERS
- ☐ IMAGE CUT OFF AT TOP, BOTTOM OR SIDES
- ☐ FADED TEXT OR DRAWING
- ☐ BLURRED OR ILLEGIBLE TEXT OR DRAWING
- ☐ SKEWED/SLANTED IMAGES
- ☒ COLOR OR BLACK AND WHITE PHOTOGRAPHS
- ☒ GRAY SCALE DOCUMENTS
- ☐ LINES OR MARKS ON ORIGINAL DOCUMENT
- ☐ REFERENCE(S) OR EXHIBIT(S) SUBMITTED ARE POOR QUALITY
- ☐ OTHER: \_\_\_\_\_

**IMAGES ARE BEST AVAILABLE COPY.**

**As rescanning these documents will not correct the image problems checked, please do not report these problems to the IFW Image Problem Mailbox.**